

ESB Incorporated  
The Carl F. Norberg Research Center  
Yardley, Pennsylvania  
The Exide Missile and Electronics Division  
Raleigh, North Carolina

HEAT STERILIZABLE,  
IMPACT RESISTANT CELL  
DEVELOPMENT

JET PROPULSION LABORATORY  
CONTRACT NO. 951296

INTERIM SUMMARY REPORT  
SEPTEMBER 24, 1965 TO SEPTEMBER 30, 1967

"This work was performed for the Jet Propulsion Laboratory, California Institute of Technology, sponsored by the National Aeronautics and Space Administration under Contract NAS7-100."

Edited by G. W. Bodamer Approved by R. A. Schaefer / G. W. B.  
G. W. BODAMER R. A. SCHAEFER  
Program Director Director of Research

## NOTICE

This report was prepared as an account of Government - sponsored work. Neither the United States, nor the National Aeronautics and Space Administration (NASA), nor any person acting on behalf of NASA:

- (a) Makes warranty or representation, expressed or implied with respect to the accuracy, completeness, or usefulness of the information contained in this report, or that the use of any information, apparatus, method, or process disclosed in this report may not infringe privately-owned rights; or
- (b) Assumes any liabilities with respect to the use of, or for damages resulting from the use of any information, apparatus, method, or process disclosed in this report.

As used above, "person acting on behalf of NASA" includes any employee or contractor of NASA, or employee of such contractor, to the extent that such employees or contractor of NASA, or employee of such contractor prepares, disseminates, or provides access to, any information pursuant to his employment with such contractor.

Requests for copies of this report should be referred to:

National Aeronautics and Space Administration  
Office of Scientific and Technical Information  
Washington 25, D. C.

Attention: AFSS-A

JPL CONTRACT 951296

HEAT STERILIZABLE, HIGH IMPACT RESISTANT  
CELL DEVELOPMENT

INTERIM SUMMARY REPORT  
SEPTEMBER 24, 1965 TO SEPTEMBER 30, 1967

ABSTRACT

Contract 951296 between the Jet Propulsion Laboratory (JPL) and ESB Incorporated called for research and development of a high energy density cell capable of heat sterilization in the unformed condition, formation, decontamination with ethylene oxide, survival of launching vibration, survival of high impact shock upon landing on a distant planet, and thereafter delivery of four complete electrical discharge cycles. Governing specifications were GMP-50437-DSN-A, GMP-50198-ETS-A, XSO-30275-TST-A, 3025 B including Amendments 1, 2, and 3, 20016 C, and NASA NPC-200-3.

Research on the electrochemical system (principally silver-zinc) and on the plastic case and cover as well as on sealing techniques was carried out by the ESB Research Center at Yardley, Penna., development of a vibration and shock resistant cell assembly was conducted by ESB Exide Missile and Electronics Division, Raleigh, N. C., and shock testing was performed by JPL, Pasadena, California.

The present report reviews and summarizes all of the work during the first two years of this contract. Since additional tasks have been added during the course of the investigation, this is not truly a final report, and some studies are expected to continue for a considerable time to come.

The salient features revealed during the first two years are as follows. Standard ESB silver electrodes resist heat sterilization and give rated electrical capacity, but require strong internal metal supports to survive high impact shock. Zinc electrodes must not contain mercury oxide, since the solubility of the latter in KOH at sterilization temperatures permits it to migrate to the silver electrode, amalgamate with it and decrease its capacity. A useful substitute for mercury oxide has been found to be Compound 323-43. Zinc electrodes also need reinforcement with strong metal supports.

Three separators - RAI-110, RAI-116, and SWRI-GX - are not adversely affected by heat sterilization when wet with concentrated KOH. RAI-110 has given cells with the longest cycle life. However, only a single batch of RAI-110, represented by 250 ft. in four different rolls, was available for testing. SWRI-GX, which has not yet been studied as extensively, has better uniformity of properties. Kendall Mills' EM476 is a satisfactory absorber.

ABSTRACT (continued)

The electrolyte should be 35 to 45% KOH saturated with zincate ion.

Filled polyphenylene oxides are good case materials from the standpoint of resistance to sterilization, decontamination, and severe shock, and for their ability to be sealed with epoxy adhesives.

Sealed, sterilized cells often show unexpectedly high pressures during formation, and nearly always show considerably diminished capacities. Further work must be concentrated on solving these two very important problems.

Cell designs have been evolving slowly toward greater shock resistance, but present capability is less than half of the specified requirements. The use of stronger internal metal supports in the electrodes is expected to improve this property very greatly.



## TABLE OF CONTENTS

Abstract . . . . .	i
I. GENERAL REQUIREMENTS OF THE SYSTEM . . . . .	1
A. Resistance to Heat Sterilization . . . . .	1
B. Non-Magnetic Materials . . . . .	1
C. Pressure Tests . . . . .	1
D. Resistance to High Impact . . . . .	2
II. DIVISION OF WORK . . . . .	2
A. ESB Research Center . . . . .	2
B. ESB Exide Missile and Electronics Division . . . . .	3
C. Jet Propulsion Laboratory . . . . .	3
III. ELECTROCHEMISTRY. . . . .	3
A. Cell Components . . . . .	3
1. General Methods . . . . .	4
a. Sterilization . . . . .	4
b. Electrodes - Fabrication and Use . . . . .	5
2. Electrode Study . . . . .	7
a. The Cadmium Electrode . . . . .	7
b. The Silver Electrode . . . . .	10
c. The Zinc Electrode . . . . .	17
3. Electrolyte Properties . . . . .	19
a. Vapor Pressure . . . . .	21
b. Conductivity . . . . .	23
c. Solubility of ZnO in KOH . . . . .	23

## TABLE OF CONTENTS

d.	Solubility of AgO ( $\text{Ag}_2\text{O}$ ) in KOH . . . . .	.34
e.	Cell Performance as a Function of Electrolyte Composition . . . . .	.35
4.	Separators . . . . .	.40
a.	Separator Screening Tests . . . . .	.49
b.	Testing of SWRI-GX in AgO-Cd Cells during Float, and on Charged Stand . . . . .	.49
5.	Absorbers . . . . .	.56
a.	Commercial Materials . . . . .	.57
b.	Grafted Absorbers . . . . .	.64
6.	Effects of PPO and Epoxy Resin Ag-Zn Cells . . . . .	.66
B.	Cell Study. . . . .	.71
1.	Cycle Life of Unsealed Three-Plate Silver-Zinc Cells . . . . .	.71
2.	Performance of Sealed Cells . . . . .	.73
a.	Cell Packs Sterilized Then Sealed . . . . .	.73
b.	Cells Sealed in PPO Cases Prior to Sterilization . . . . .	.77
c.	Gas Generation in Sealed Cells . . . . .	.80
IV.	CASE MATERIALS AND SEALING TECHNIQUES . . . . .	.92
A.	Material Qualifying Studies . . . . .	.92
1.	Stability under Sterilization Conditions . . . . .	.92
2.	Stability under Decontamination Procedures . . . . .	.95
B.	Molded Cell Cases and Covers . . . . .	.96

## TABLE OF CONTENTS

C. Cell Case Seals . . . . .	.103
1. Heat Sealing. . . . .	.108
a. Hot Gas Welded Polysulfone Cases. . . . .	.108
b. Sterilization of Polysulfone Cases . . . . .	.108
c. Heat Sealing of PPO 531-801 . . . . .	.109
d. Hot Gas Welding of PPO 541-801 . . . . .	.109
e. Hot Gas Welding of PPO 681-111 . . . . .	.109
f. Sterilization of Hot Gas Welded JPL Cases in PPO 541-801 . . . . .	.110
g. Sterilization of Welded PPO 681-111 JPL Cases . . . . .	.110
2. Solvent Sealing. . . . .	.111
a. Crazing of Polysulfone . . . . .	.111
b. Solvent Seals on PPO 531-801 . . . . .	.111
c. Pressure Tests and Sterilization of Solvent Sealed PPO 531-801 Cases . . . . .	.111
d. Solvent Seals on PPO 681-111 . . . . .	.112
3. Adhesive Seals . . . . .	.112
a. Adhesive Seals on PPO 531-801 . . . . .	.112
b. Sterilization of Adhesive Epocast 221 on PPO 531-801 . . . . .	.112
c. Solvent Loss and Cure Rates for Epoxy Resin DEN438-EK85. . . . .	.112
d. Sterilization of Epoxy-Sealed PPO 531-801 Cases (1-062). . . . .	.113
e. Epoxy Seals on PPO 531-801 JPL Cases . . . . .	.113

## TABLE OF CONTENTS

f.	PPO 531-801 Cases and PPO 541-801 Covers. . . . .	116
g.	Adhesive Seal on JPL Cases in PPO 541-801 . . . . .	116
4.	Ultrasonic Sealing . . . . .	122
V.	FABRICATION AND TESTING OF CELLS . . . . .	122
A.	Twenty-Five Ampere-Hour Sealed Cell . . . . .	122
1.	Objectives . . . . .	122
2.	Cell Components Stress Analysis under Shock . . . . .	122
3.	First Generation Cells - Model 325 Family. . . . .	123
a.	Structural Design Features. . . . .	123
b.	Materials and Process Development. . . . .	128
c.	Stress Analysis of Model 325 Plate Structures . . . . .	129
d.	Shock Tests of Model 325 Cells . . . . .	129
(1)	Shock Test Method. . . . .	129
(2)	Relative Damage and Failure Mechanisms . . . . .	132
e.	Electrical Characteristics of Model 325 Type A, B, and C Cells . . . . .	137
(1)	Cycle Test Results . . . . .	137
(2)	Charged Stand Tests . . . . .	137
4.	Second Generation Cells - Model 334 Design . . . . .	143
a.	Objectives . . . . .	143
b.	Cell Design and Process Development . . . . .	143
c.	Heat Sterilization Tests . . . . .	147
d.	Shock Tests at JPL and Failure Modes. . . . .	147

## TABLE OF CONTENTS

5.	Third Generation Cells - Model 343 -	
	Metal Supports . . . . .	154
	a. Design Development . . . . .	154
	b. Heat Sterilization . . . . .	159
	c. Shock Tests at JPL . . . . .	159
	d. Shock Damage - Individual Cells . . . . .	164
	e. Discussion of Shock Damage . . . . .	166
B.	7.5 Amp-Hr Design Parameter Cell Tests . . . . .	166
C.	Heat Sterilizable-High Impact 5.0 AH Cell . . . . .	175
	1. Objectives . . . . .	175
	2. Cell Design and Prototype Fabrication . . . . .	175
VI.	CONCLUSIONS . . . . .	179
VII.	FUTURE WORK . . . . .	181

## LIST OF TABLES

Table I	Electrode Composition . . . . .	5
Table II	Silver Electrode Efficiency for Ag Limiting Ag-Cd Cells . . . . .	10
Table III	Effect of Sterilization of Silver Electrodes in the Presence of Other Cell Components . . .	12
Table IV	Effect of HgO Concentration in ZnO Electrodes in Sterilized Ag Limiting Cells with 40% KOH .	14
Table V	Effect of Additives on Ag Limiting Ag-Zn Cells . . .	15
Table VI	X-Ray Study of Electrodes . . . . .	16
Table VII	Tafel and Gassing Data . . . . .	18
Table VIII	Volume of Gas (ml) from Couples in 40% KOH at a Given Time . . . . .	20
Table IX	Vapor Pressure of Aqueous KOH . . . . .	21
Table X	Solubility of ZnO in KOH at 25°C . . . . .	27
Table XI	Solubility of ZnO in KOH at Elevated Temperatures . . . . .	32
Table XII	Ag-Zn Cell Capacities as a Function of Electrolyte Composition . . . . .	37
Table XIII	Ag-Cd Cell Capacities as a Function of Electrolyte Composition . . . . .	39
Table XIV	Specific Resistance of Clear and Brown Areas in RAI-116 . . . . .	40
Table XV	Dimensional Changes in RAI Separators Due to Sterilization . . . . .	42
Table XVI	Electrolyte Retention Before and After Sterilization . . . . .	41
Table XVII	Ion Exchange Capacity of RAI Separators, . . . . .	43

## LIST OF TABLES

Table XVIII	Electrical Resistance of RAI-116 Before and After Sterilization. . . . .	.44
Table XIX	Electrical Resistance of RAI-110 Before and After Sterilization. . . . .	.45
Table XX	Electrical Resistance of SWRI-GX Before and After Sterilization. . . . .	.46
Table XXI	Capacity of Cells with RAI-116 and RAI-110 during Four Cycles . . . . .	.48
Table XXII	Silver Content of RAI-116 Layers After Four Cycles . . . . .	.48
Table XXIII	Summary of RAI-116 Membrane Evaluation Data . . . . .	.50
Table XXIV	Acceptance Test Results SWRI-GX Separator Material . . . . .	.51
Table XXV	Constructional Details Three Plate Silver Cadmium Cells . . . . .	.54
Table XXVI	Absorber Composition and Stability . . . . .	.58
Table XXVII	Specific Resistance of EM476 and Glass Fiber Absorbers . . . . .	.59
Table XXVIII	Energy Utilization of Cells with Asbestos Absorber. . . . .	.60
Table XXIX	Absorber Wicking Tests on EM476 and SM 134.5. . . . .	.62
Table XXX	Capacity Test for Absorber Wicking Ability. . . . .	.63
Table XXXI	Wicking Action in 40% KOH of Grafted Absorbers . . . . .	.65
Table XXXII	Electrolyte Retention and Wicking Ability vs. Capacity . . . . .	.65
Table XXXIII	Effect of PPO and Epoxy Resin on Cell Performance - Test A . . . . .	.67

## LIST OF TABLES

Table XXXIV	Effect of PPO + Epoxy on Cell Performance - Test B. . . . .	.68
Table XXXV	Effect of Epoxy on Cell Performance - Test C. . . . .	.70
Table XXXVI	Cycling of Unsealed Three-Plate Silver-Zinc Cells Capacity in Amp-Hours . . . . .	.72
Table XXXVII	Discharge Capacities of Twenty Cells Sealed After Sterilization . . . . .	.75
Table XXXVIII	Capacity Retention After Stand at 160°F . . . . .	.78
Table XXXIX	Cycle Tests - Cells Sealed Before Sterilization . . . . .	.81
Table XL	Internal Pressure as a Function of Cell Pack Tightness . . . . .	.83
Table XLI	Cycle and Pressure Data - Positive Wrapped Cells . . . . .	.85
Table XLII	Pressures and Voltages of Positive- Wrapped Sealed Ag-Zn Cells . . . . .	.86
Table XLIII	Pressure Data on Ag-Zn Cells Floating at Constant Potential - No Teflon in Negative . . . . .	.88
Table XLIV	Pressure Data on Ag-Zn Cells Floating at Constant Potential 2% Teflon in Negative . . . . .	.89
Table XLV	Pressure (psig) and Discharge Capacity (amp-hr) of 7-Plate Sterilized Then Sealed Ag-Zn Cells . . . . .	.90
Table XLVI	Mechanical Properties of PS P-1700 and PPO 531-801 and 681-111; Determined at 72°F Using ASTM D638 Molded Tensile Bars . . . . .	.93
Table XLVII	Properties of Polyphenylene Oxides . . . . .	.94



## TABLE OF CONTENTS

Table XLVIII	Stability of P-1700 and PPO 531-801, 533-111, 541-801, and 681-111 Under Sterilized Conditions . . . . .	95 a
Table XLIX	Stability of PPO 531-801 and PS P-1700 in Ethylene Oxide. . . . .	97
Table L	Molding Conditions for JPL Cell Case Assemblies with Silver Terminals . . . . .	107
Table LI	Epoxy Seals on JPL Cases in PPO 531-801 . . . . .	115
Table LII	Adhesive Seal on JPL Cases in PPO 531-801. . . . .	117
Table LIII	Adhesive Seal on JPL Cases in PPO 531-801. . . . .	118
Table LIV	Adhesive Seals on JPL Cases in PPO 531-801 . . . . .	119
Table LV	Adhesive Seal on JPL Case in PPO 541-801 . . . . .	120
Table LVI	Adhesive Seals on JPL Cases in PPO 541-801 with Terminal 1-096 . . . . .	121
Table LVII	Weight Analysis of Model 325 Cells Types A, B, and C. . . . .	124
Table LVIII	Stresses at 5,000 g for Selected Points on Model 325 Cell Pack . . . . .	130
Table LIX	Model 325 Sealed Ag-Zn Cell Impact Shock Levels . . . . .	131
Table LX	Loaded Voltages of Type "A" Cells Before and After Single Shocks . . . . .	133
Table LXI	Loaded Voltages of Type "B" Cells Before and After Single Shocks . . . . .	134
Table LXII	Loaded Voltages of Type "C" Cells Before and After Single Shocks . . . . .	135
Table LXIII	Comparison of Impact Damage Model 325 Type A, B, and C Cells . . . . .	136
Table LXIV	Discharge Capacity and Energy of Model 325 Cells Types A, B, and C . . . . .	141

## TABLE OF CONTENTS

Table LXV	Wet Charged Stand Capacity Losses of Model 325 Cells During 30 Days at 49°C . . .	.142
Table LXVI	Model 334 Cell Design . . . . .	.144
Table LXVII	Model 334 Control Cell Cycling Tests . . . . .	.148
Table LXVIII	Electrical Tests on Model 334 Cells Before and After Heat Sterilization . . . . .	.149
Table LXIX	Shock Data for Model 334 Cells . . . . .	.151
Table LXX	Decrease in Cell Voltages from High Impact . . . . .	.152
Table LXXI	Model 343 25 AH Heat Sterilizable High Impact Cell Design . . . . .	.156
Table LXXII	Formation Charge Acceptance Model 343 Cells . . . . .	.160
Table LXXIII	Shock Environment Data on Model 343 Cells (Non-Sterilized) . . . . .	.161
Table LXXIV	Decrease in Cell Voltage from High Impact on Model 343 Cells . . . . .	.162
Table LXXV	7.5 AH Cell Design Sets . . . . .	.168
Table LXXVI	Effect of Cell Pack Design on Sealed 7.5 AH Cell Performance . . . . .	.169
Table LXXVII	Capacity Energy Stand Loss, 7.5 AH Cells . . . . .	.173
Table LXXVIII	Model 344 5 AH High Rate Heat Sterilizable, High Impact Cell Design . . . . .	.177

## LIST OF FIGURES

Figure 1	Othmer Type Plot: Vapor Pressure of KOH Solutions . . . . .	.22
Figure 2	Conductivity of KOH Solutions . . . . .	.24
Figure 3	Conductivity of KOH-ZnO Solutions . . . . .	.25
Figure 4	Dissolution of ZnO in KOH at 145°C . . . . .	.26
Figure 5	Dissolution of ZnO into 40% KOH at 25°C . . . . .	.28
Figure 6	Solubility of ZnO in KOH as a Function of KOH Concentration and Temperature . . . . .	.30
Figure 7	Schematic of Solubility Apparatus . . . . .	.31
Figure 8	Solubility of ZnO in KOH at Elevated Temperatures . . . . .	.33
Figure 9	Electrical Resistance of RAI-116 as a Function of Number of Layers . . . . .	.47
Figure 10	Separator Test Program Schedule. . . . .	.53
Figure 11	Container 1-062. . . . .	.98
Figure 12	Cover 1-070 . . . . .	.99
Figure 13	Terminal 1-069. . . . .	.100
Figure 14	Container 1-074 Rev. "A" . . . . .	.101
Figure 15	Cover 1-089 . . . . .	.102
Figure 16	JPL Case . . . . .	.104
Figure 17	JPL Cover . . . . .	.105
Figure 18	Insert for Cell Cover JPL Case Assembly . . . . .	.106
Figure 19	Model 325-X Cell Assembly . . . . .	.125
Figure 20	Model 325-X Negative Plate Grid Assembly . . . . .	.126
Figure 21	Model 325-X Positive Plate Assembly . . . . .	.127

## LIST OF FIGURES

Figure 22	Voltage Characteristics Model 325 Type "A" Cells . . . . .	138
Figure 23	Voltage Characteristics Model 325 Type "B" Cells . . . . .	139
Figure 24	Voltage Characteristics Model 325 Type "C" Cells . . . . .	140
Figure 25	Assembly Sketch of Epoxy-Sealed Model 334 . . . . .	145
Figure 26	Structural Design of Positive Plate for Model 334 . . . . .	146
Figure 27	Decrease in Cell Voltage During High Impact Tests . . . . .	153
Figure 28	Assembly Sketch of Model 343 Cell . . . . .	157
Figure 29	Cell Voltage Drop After High Impact Shocks on Model 343 Cells . . . . .	163
Figure 30	Shock Level and Cell Voltage Traces Model 343 Cells . . . . .	165
Figure 31	Plate, Damage, Cell S/N 4, -Y Velocity Vector, 23K "g". follows page	165
Figure 32	Plate Damage, Cell S/N 6, +Y Velocity Vector, 14K "g". " "	165
Figure 33	Plate Damage, Cell S/N 5, +Y Velocity Vector, 7K "g". " "	165
Figure 34	Voltage Characteristics Various Cell Pack Designs . . . . .	170
Figure 35	Formation Charge Acceptance 7.5 AH Cell Tests. . .	172
Figure 36	Cell Pressure, 7.5 AH Cell Tests . . . . .	174
Figure 37	Assembly Sketch of Proposed 5 AH Cell. . . . .	176
Figure 38	5 AH Cell Plate Support Structure for 10,000 "g" Impacts . . . . .	178

## I. GENERAL REQUIREMENTS OF THE SYSTEM

The present contract, JPL 951296, covers the study, design, development fabrication and testing of nominal 50 AH sealed silver-zinc and silver-cadmium cells with an energy density of at least 25 WH per pound and meeting JPL Specification GMP-50437-DSN-C. Primarily, this specification covers a heat sterilizable, high impact resistant battery capable of withstanding nine months of interplanetary environment, planet entry and landing before delivering its rated capacity. To prevent planet contamination the battery must be sterile at spacecraft launch. A further requirement is that the battery should be constructed of non-magnetic materials.

### A. Resistance to Heat Sterilization

Throughout most of this work temperatures for sterilization were 125, 135, and 145°C. Preliminary testing was done at 145°C, the most severe condition. This specification called for raising the temperature of the sterilization chamber at a rate not exceeding 30°C/hr until 145°C was reached. The chamber was to be maintained at this temperature for 36 hours and then returned to ambient at a rate not exceeding 30°C/hr. After a stand of not longer than three hours the procedure was to be repeated for a total of three cycles.

The most recent specification (C modification) decreased the 145°C requirement. Testing at 135°C is for type approval, demonstrating satisfactory design, whereas 125°C testing is for flight acceptance, demonstrating that the hardware is ready for flight. At the 135°C sterilization temperature, the heating rate is 19°C/hr. The chamber is held at this temperature for 64 hours and then cooled to room temperature at the same rate at which it was heated. Two such cycles are now required. For preliminary testing one 120 hour cycle may be used.

### B. Non-Magnetic Materials

The magnetic requirements are such that no magnetic materials shall be used. The total field magnitudes of the battery should be less than one gamma at six times its average dimension measured along three natural rectilinear axes. This requirement obviates the usual addition of nickel powder to cadmium electrodes to the detriment of their capacity. It also limits the choice of grid materials that might be used to strengthen either silver, zinc, or cadmium electrodes against shock. Good design is required to limit the magnitude of the field caused by current loops to five gamma when measured as described above.

### C. Pressure Tests

A further requirement, since the cells are to be sealed, is that the cases withstand not only the pressure and temperature of sterilization but also

gas pressure which may build up during flight. Cases and their seals must withstand 65 psig at the sterilization temperature and 90 psig at room temperature. The leak rate must be less than  $10^{-6}$  ml/sec at a helium pressure of 10 psig. In addition other applicable tests and requirements as given in JPL specification GMP-50437-DSN also apply to insure that the case material is strong enough to withstand the shock of a hard landing and is compatible with other requirements of the system.

#### D. Resistance to High Impact

Sealed cells fabricated under this contract must be designed to survive shock-landing. To test various reinforced electrode designs and configurations, sealed cells incorporating these modifications were to be subjected to various shock or impact tests. Five cells were to be tested at a shock level of 5,000 g peak from a velocity of  $110 \pm 20$  feet per second. In this test each of the five cells was to be tested in one of the non-identical directions of the three orthogonal axes. The results were to be analyzed so as to improve future designs.

Another requirement was an identical test as described above but at a shock level of 10,000 g peak from a velocity of  $180 \pm 20$  feet per second.

## II. DIVISION OF WORK

The research and development involved in this investigation was quite diverse and extensive and was divided among the Carl F. Norberg Research Center and the Exide Missile and Electronics Division of ESB Incorporated, and the Jet Propulsion Laboratory to take full advantage of each group's special disciplines. The project was divided into several tasks such as: ESB personnel resident at JPL, electrochemistry, cell case development, cell fabrication and testing, quality assurance, and documentation. The responsibility for, and the overall control of, the project resided with the Program Director and the Director of Research at the ESB Research Center.

#### A. ESB Research Center

Work at the Research Center was concentrated on a study of the silver-zinc cell and its parameters so as to be able to fabricate an optimized cell which would go through heat sterilization without a loss of capacity. Implied here were studies of electrolyte, electrodes, separators and absorbers as well as cell case material, sealing methods, and terminal contacts. Sealing methods included hot gas welding as well as the use of adhesives. The compatibility of all materials with the electrochemical system was mandatory. Information on plastics, sealing methods, and electrochemical systems which completed sterilization unimpaired was passed on to application engineers.

## B. Exide Missile and Electronics Division

This division of ESB (hereafter referred to as EMED) has been particularly concerned with the impact shock requirements of the individual cell. Their goals have included an analysis of cell components for design values involved in high level shock survival, development and fabrication of 50 AH sealed cells capable of surviving high level shock and using heat sterilizable components where possible in the early stages of the work, testing cells at the Jet Propulsion Lab facilities at 5,000 and 10,000 g impacts, and eventual development of cells which will resist both heat sterilization and high impact.

## C. Jet Propulsion Laboratory

JPL made available its environmental test facilities and supervisory and technical personnel to conduct shock and vibration tests on EMED experimental cells. EMED supplied an engineer to observe the tests, record data, and evaluate the results in terms of any cell design changes which might be required.

## III. ELECTROCHEMISTRY

This portion of the project included performing studies to characterize cell components and applying the knowledge gained to construct cells capable of being sterilized without undue loss of capacity and without excessive pressure build-up during formation. In general, voltage characteristics, electrical capacity, and pressure development in test cells through four cycles were used to characterize the systems. In addition the study of some of these cells was continued several months while they were left on stand or float.

### A. Cell Components

The various parts of the cell were studied individually from the standpoint of their effect on the electrochemical system. These included electrodes, electrolyte, separators, absorbers, case material and sealants. In addition to electrochemical measurements, chemical, optical and x-ray diffraction methods were used where necessary. Separators and absorbers were also studied physically to determine the change in dimensions as a result of sterilization. Case materials and sealants were studied for their effect on the electrochemical system only after materials were found which met the other requirements as given under section IV. CASE MATERIALS AND SEALING TECHNIQUES.

The goal to be achieved by this work was a minimum of 25 watt-hr per pound in the final battery design. Although this appears to be a modest requirement the structural design problems to meet the high shock requirements places a premium on high performance electrodes.

The greater inherent capacity and voltage of zinc over cadmium would permit a higher percentage of the total weight to be utilized in the structural design of the battery and still meet the overall desired performance if zinc were employed. In addition cadmium electrodes required nickel powder to develop their maximum capacity. Because of the non-magnetic requirement, this addition was not possible, and the substitution of silver powder was only partially satisfactory. Thus, the cadmium electrode was considered a back-up electrode and only a minimum amount of work was performed on it.

## 1. General Methods

There were two techniques which became quite standardized in this investigation. One was the method of sterilization and the other was the preparation and use of electrodes. Under Electrodes - Fabrication and Use there are included construction details for three plate cells which were used quite extensively in studying electrode properties. Sterilization of the electrodes was not performed in accordance with the specification but rather by a modified procedure which facilitated the research. It is, therefore, described in some detail. Methods developed for a specific purpose are described in those sections where they were employed.

### a. Sterilization

The sterilization procedure is described in specification GMP-50437-DSN-C. However, for facilitating the early experimental work a different method was employed, and the specification method was reserved for sealed cells. This experimental procedure consisted of heating the sterilization bombs in an oil bath rather than in an air oven so that any leaks could be readily detected as bubbles in the oil bath. Another advantage was that the cell pressure gauges would be unheated without having to modify an oven.

The three oil baths used were Blue M, Model MOD-1115A which operate in the temperature range of 0-180°C. They maintained temperature at  $\pm 0.5^\circ\text{C}$ . The "oil" used was Blue M High Temperature Ucon Fluid as recommended by the manufacturer. At the highest temperature used, 145°C, it did not fume or have objectionable odors. Also, it was water soluble. Each bath held six bombs.

The bombs evolved from iron pipe with plastic liners to nickel pipe with sheet nickel cell cases to fit. The most satisfactory arrangement consisted of 2 1/2" nickel pipe nipples 8" long and nickel pipe couplings. Both items were cut in half and a 1/4" thick, round nickel plate heliarc welded to all cut surfaces making two bombs. This made a shorter bomb with a flat base which proved to be cheaper than 4" pipe nipples with two end caps each.



The gauges were 3" dial, ammonia gauges with a range 0-100 psig. These were connected to the cap through 1/4" stainless steel fittings and tubing. Also incorporated were SS safety valves and a loop in the SS tubing to control heat conducted to the gauge. In use the parts were assembled using Teflon pipe tape which helped to seal and prevented galling.

Sterilization was accomplished by placing either cell parts (electrodes, separators, absorbers, or other test materials) or cell packs, exclusive of the plastic case, in flat nickel cases two of which fitted each bomb. Electrolyte was added to both the nickel cases and externally to the cases to provide the water vapor atmosphere without affecting the limited electrolyte in the cell packs. Sterilization temperatures specified were 125, 135, and 145°C. Most of our work on electrodes was done at 145°C on the hypothesis that if a cell could be made to withstand this temperature, testing at lower temperatures would be minimized. However, after most of our electrode studies were completed, the specification was changed to include only 125 and 135°C. At 145°C the time of sterilization was three exposures of 36 hours each. In order to simplify the experimental work one exposure of approximately 112 hours was used. At 135°C sterilization time was two exposures of 64 hours each. Again we used about 112 hours for convenience in experimental work. Later tests were run on sterilized cells sealed in the chosen case material and performed in accordance with the specification.

#### b. Electrodes - Fabrication and Use

All electrodes used in this investigation were 1.75 inches x 1.88 inches. Whenever possible standard production plates made by ESB-EMED were employed. These had the composition and properties shown in Table I.

TABLE I  
Electrode Composition

<u>Electrode</u>	<u>Additive</u>	<u>Binder</u>	<u>Theoretical Electrode Capacity, amp-hr</u>
Silver (100%)	-	-	3.2
Zinc (91% ZnO)	7% HgO	2% Teflon	3.2
Zinc (98% ZnO)	-	2% Teflon	3.4
Cadmium (93% CdO)	5% Ag	2% Teflon	2.4

When necessary, negatives containing special additives were made at ESB-Research using the same dimensions. In all cases, the electrodes were pressed onto 2/0 expanded silver grid. They were made and sterilized in the unformed condition.

The negative electrodes were contained in non-woven polypropylene retainers 3 mils thick, designated Kendall Mills EM 476. The silver electrode was enclosed in a tent-shaped piece of Kendall EM 476 absorber cut somewhat larger than the plate to allow for shrinkage. Negative electrodes, including their retainers, were encased in four layers of RAI separator, either 110 or 116 except where designated. The separator was wrapped over a form 1/16 inch larger on all sides than the electrode to allow for shrinkage. A U-fold was used, and, with the usual three-plate cells, positive limiting cells contained a silver electrode between the arms of the U. In negative limiting cells, silver electrodes were placed on either side of one negative electrode contained in one arm of the U. The empty arm of the U came up out of the way along one side of the cell case.

Since the sterilizable plastic case had not yet been developed (this work was proceeding simultaneously), the cell packs were placed in nickel cases to be sterilized in the presence of 40% KOH. After sterilization, they were transferred to polystyrene cases and shimmed to essentially zero clearance using various thicknesses of sheet polypropylene to take up the extra space in the oversized cases. A strip of polymethyl methacrylate plastic with a 1/4 inch hole to contain a Hg-HgO reference electrode was cemented to the case adjacent to the edges of the electrodes. A communicating hole connected the bottom of the reference chamber to the bottom of the case.

In general, unless otherwise stated, the electrolyte was 40% KOH made by diluting "Baker Analyzed" Reagent 45% solution KOH. During the early phase of the work the cells were open and in the flooded condition. They were charged at constant current using 35 ma (5.3 ma/in<sup>2</sup> for silver limiting cells) for formation on the first cycle. In subsequent cycles the current was raised to 100 ma. The cells were generally overcharged by approximately 10% to insure that silver limiting cells were also silver limiting on discharge. Some cells were monitored with automatic equipment which could be set to cut-off the charge when the reference to a particular electrode voltage indicated gassing of that electrode.

Discharges were forced with constant current equipment to facilitate capacity calculations. The discharge rate was usually 600 ma which is at the three to four hour rate for the experimental cells. Again reference electrode potentials were used to determine end of discharge or to determine which electrode had failed. Automatic equipment which monitored each cell once every 20 minutes could lead to a maximum error of 0.2 amp-hr. Supplemented with visual observations cell capacities were determined on the automatic equipment within 0.1 amp-hr which is +5% error or less for those cells with capacities large enough to be of particular interest. The error for single cell discharges is  $\pm 0.01$  amp-hr.

In the last phase of this work cells were sealed and were either made of cell packs which were sterilized and sealed or, after sterilizable cases became available, were sealed and sterilized.

## 2. Electrode Study

Both cadmium and zinc electrodes were studied with silver antipodes to determine their ability to go through sterilization without undue loss of capacity or other unwanted effects. The structure of silver and zinc electrodes was studied by means of x-ray diffraction to show differences due to sterilization, charge and discharge. Some studies were also conducted with dummy nickel antipodes to further isolate the test electrode, and zinc electrodes were particularly studied in reference to gas formation.

### a. The Cadmium Electrode

The cadmium electrode was studied to determine the effect of sterilization on the capacity of this electrode in the uncharged, charged and discharged state. Standard ESB cadmium oxide electrodes of the composition given in Table I were used in this investigation. In the following single electrode experiments constant potential charging was used with the current limited to 200 ma and the voltage to 1.72 volts. Instead of constructing cells, the plates were charged and discharged between sheet nickel dummies contained in polyethylene cups filled with 40% KOH. The containers were closed with a polyethylene bag held in place with a rubber band to minimize carbonate formation. Discharge was at 600 ma using a constant current device. A recorder with a cut-off stopped the discharge when the voltage across the cell reached -1.0 volts. This also stopped a minute timer which displayed the ampere-hour capacity after the decimal point was adjusted. While all single electrodes were run in this manner, open silver-cadmium cells were charged using constant current and overcharged about 10%.

#### (1) Unsterilized CdO Electrodes

To establish a base line for comparison of possible capacity changes attributable to sterilization, the capacities of several standard ESB electrodes were run in the as-received condition. Discharges of one electrode, 323-20, were followed through four cycles to establish the approximate change of capacity with cycles. The results obtained on this cell follow:

<u>Cycle</u>	<u>Capacity amp-hr</u>	<u>Capacity amp-hr/g CdO</u>	<u>% Faradaic Efficiency</u>
1	1.30	0.237	56.5
2	1.22	0.223	53.1
3	1.11	0.203	48.3
4	1.11	0.203	48.3

First cycle discharge for electrodes 323-12 and 323-24 were 0.232 and 0.226 amp-hr/g CdO respectively. These tests establish a range so that the effects of sterilization on charged or uncharged electrodes can be determined.

### (2) Sterilization of Charged Cd Electrodes

Electrodes 323-12 and 323-20, which had been run through one cycle to establish their capacity, were recharged and sterilized at 145°C for 112 hours to determine the effect of sterilization. When the electrodes were discharged it was found that very little capacity remained. Presumably the cadmium was oxidized by the oxygen in the air sealed in the bomb even though the electrode was covered with 40% KOH to minimize this. A typical charge remaining after sterilization was 0.055 amp-hr/g CdO. When the electrode was recharged overnight using a constant potential charger, the following discharge was also 0.055 amp-hr/g showing permanent damage. To determine if the polypropylene retainer on the electrode was responsible for the damage, electrode 323-21 was charged and sterilized under KOH without its wrap on the bottom of a nickel bomb. Electrode 323-22 was similarly treated except it was rewrapped in RAI separator to prevent metal to metal contact between the charged electrode and the nickel bomb. Both electrodes exhibited essentially the same capacity, 0.040 amp-hr/g. This did not improve with recharge and it was concluded that charged sterilized electrodes were permanently damaged.

### (3) Sterilization of Uncharged CdO Electrodes

Another series of experiments was run to determine the effect of sterilization on the capacity of uncharged CdO electrodes. Electrode 323-22B was given the usual sterilization in 40% KOH. It would not accept a charge. The initial low current of 60 ma dropped off quickly. The voltage of the constant potential charger was then raised from 1.72 to see what voltage was required to cause 200 ma to flow; it proved to be about two volts. The voltage was then lowered to 1.72 v where 180 ma now flowed. In the morning the electrode was still accepting 80 ma. It was left on charge another day after which period the charging current had dropped to 4 ma. On discharge 1.88 amp-hr or 0.343 amp-hr/g was obtained for a Faradaic efficiency of 81.7%.

From this experiment it was concluded that sterilization was beneficial to the capacity of a CdO electrode but that sterilization had somehow introduced a high resistance path in the electrode. Once that was overcome the electrode accepted charge. This experiment also explained why the sterilized charge electrodes would not recover on subsequent cycles. They were charged at 1.72 v with a constant potential charger. If constant current charging had been used, whatever voltage was required would have developed across the cell to charge it.

A retest of the beneficial effects of sterilization on a CdO electrode, 323-25, showed an initial Faradaic efficiency of 68.5% on the first cycle which fell off to 50.5% on the fourth discharge.

#### (4) Sterilization of Discharged Cd Electrodes

The effects of sterilization on a cadmium electrode which had been cycled once and then sterilized in the discharged condition was determined. Due to sterilization the utilization dropped from 0.202 amp-hr/g to 0.132 amp-hr/g CdO. On recharge the capacity was only 0.119 amp-hr/g showing permanent damage. The beneficial effect of sterilization on fresh CdO was not observed.

#### (5) Silver-Cadmium Cells

After working with single cadmium electrodes, a few experiments were run in cells to test the earlier results using silver antipodes, separators, controlled spacing, and controlled electrolyte. As far as passing sterilization is concerned, the best state for the cadmium electrode to be in had been found to be as the uncharged electrode. Thus, a new CdO electrode, 323-27, was sterilized and placed between two silver electrodes which had been wrapped in four layers of RAI-116 separator in a U-fold to make a cadmium limiting cell. The electrode pack was placed in a polystyrene case and about 8 ml of 40% KOH was added. After soaking about six hours it was formed overnight using constant current at 100 ma. The first discharge yielded 0.254 amp-hr/g CdO or a Faradaic efficiency of 60.5%. By the fourth cycle the utilization was 0.218 amp-hr/g or 51.5% efficient.

This result, 0.254 amp-hr/g CdO, is slightly better than the range 0.226-0.237 amp-hr/g CdO established for first cycle unsterilized electrodes. It shows that sterilized CdO electrodes will perform well in cells.

To determine whether or not the silver electrode would be affected by cadmium ions during sterilization several silver limiting silver-cadmium cells were constructed as three plate cells. The cell packs of cells 3 and 4 were sterilized whereas those of cells 5 and 6 were not. The first cycle results are given in Table II.

TABLE II  
Silver Electrode Efficiency for Ag  
Limiting Ag-Cd Cells,  
Cycle #1

<u>Cell</u> <sup>1</sup>		<u>Input amp - hr</u>	<u>Input Theor.</u>	<u>Discharge amp-hr</u>	<u>Discharge D/C<sup>2</sup></u>	<u>Efficiency D/T<sup>3</sup></u>
321-19	No. 3 S	2.29	71%	2.17	94%	67%
	No. 4 S	2.76	85	2.5	90	78
	Av.		78		92	73
	No. 5 U	2.37	74	2.25	95	70
	No. 6 U	2.43	75	2.37	97	73
	Av.		75		96	72

1 Letter after cell no. refers to sterilized or unsterilized.

2 D/C = Discharge/Charge

3 D/T = Discharge/Theoretical

In Table II it is shown that the sterilization of silver electrodes in the presence of CdO electrodes is without effect on cell capacity.

From this study the following conclusions concerning cadmium electrodes may be drawn:

- (1) In all states of charge or discharge investigated, sterilization interferes with charge acceptance.
- (2) Poor charge acceptance after sterilization can be overcome at least in the case of sterilized uncharged electrodes by either increasing the charging voltage temporarily or by using constant current equipment.
- (3) Sterilization is beneficial to the potential capacity of uncharged CdO electrodes.
- (4) The capacity of silver electrodes is not lessened when the electrodes are sterilized in the presence of CdO.

#### b. The Silver Electrode

The capacity of silver limiting silver-zinc cells made with standard ESB silver and ZnO + 7% HgO electrodes is 2.25 amp-hr with a Faradaic efficiency of 69% for the silver electrode (average of four cells on the first

cycle). However, if the cell packs are sterilized at 145°C, the capacity drops to 1.0 amp-hr with an efficiency of 31%. To determine the cause for this, cell parts were sterilized alone and in combination with other parts. These were assembled into cells and the capacities determined as shown in Table III. It will be noted that the average discharge capacity of these cells over four cycles is 2.3 amp-hr in all but two combinations. The average capacity is 1.8 amp-hr when the silver electrode is sterilized in the presence of its absorber and 1.5 amp-hr, when it is sterilized with a ZnO electrode containing 7% HgO. Since the presence of Kendall EM 476 absorber on a silver electrode in a sterilized Ag-Cd cell does not detract from its capacity, it was concluded that the main loss in capacity due to sterilization comes from the ZnO-HgO electrodes. Further, since the combination, sterilized Ag-ZnO without HgO, gave normal capacity, the loss must be due to HgO.

As an additional check to determine if this poor performance was due to some damage to the cathode, a silver electrode, 316-48-1, was sterilized in 40% KOH-7.5% ZnO-52.5% H<sub>2</sub>O without absorber or separator but sandwiched between two ZnO electrodes containing 7% HgO. After sterilization for 112 hours at 145°C, a cell was made using only the silver electrode, fresh Kendall EM 476 absorber, four layers of RAI-116 separator, 40% KOH, and two CdO antipodes. This cell, which contained no intentionally introduced mercury, performed poorly. Its capacity on the first cycle was only 1.5 amp-hr. whereas the capacity of sterilized silver limiting Ag-Cd cells is of the order of 2.4 amp-hr. It would seem that the mere presence of HgO in the sterilization bomb with the silver electrode was enough to drop its capacity to 62% of the expected value, and that the damage is entirely in the silver electrode. This phenomenon has become known as the "mercury effect".

Further substantiation of this effect has been obtained from experiments where silver electrodes were sterilized in 100 ml 40% KOH containing 5 g HgO. The electrodes were inspected using a binocular microscope at 60 magnification. Bright spots which may have been silver amalgam were observed. Electrodes with the wrap retained showed more bright spots and some bright loose material in the wrap itself. When these electrodes were charged and discharged against nickel dummies, the electrode with the wrap retained showed the greatest damage with a capacity of only 0.86 amp-hr. The electrode sterilized in the presence of HgO without a wrap had a capacity of 1.40 amp-hr whereas the control sterilized with no HgO or wrap had a capacity of 2.60 amp-hr.

Mercury is used in the zinc electrode to raise the hydrogen overvoltage and, thereby, to control gassing of sealed cells on stand or float. If it could be replaced with something else, which would raise the overvoltage equally well without affecting the silver electrode, a heat sterilizable Ag-Zn cell would be practical.

TABLE III  
Effect of Sterilization of Silver Electrodes in the Presence of Other  
Cell Components  
Ampere-Hours

Cell No.	Cycle Variable	1		2		3		4		Ave. Disc.	Cap.
		Input	Output	Input	Output	Input	Output	Input	Output		
316-20-2	unsteril. control	2.0	1.9	-	2.4	1.5	2.3	2.0	2.6	2.3	
316-20-4	ditto	2.0	1.9	-	2.3	1.8	2.3	2.0	2.6	2.3	
316-36-1	Ag steril. alone	3.5	2.4	-	2.4	2.0	2.0	-	-	2.3	
316-36-2	ditto	3.5	2.4	-	2.4	2.0	2.0	-	-	2.3	
316-20-1	Ag+ EM 476 steril.	2.0	1.9	-	2.0	2.0	2.0	1.5	1.4	1.8	
316-20-3	ditto	2.0	2.1	-	1.9	2.0	1.7	1.5	1.4	1.8	
316-39-5	Ag with ZnO + HgO steril.	1.5	1.4	1.7	1.7	<2	1.6	<2	1.4	1.5	
316-36-3	Ag with ZnO steril.	3.5	2.4	-	2.4	2.0	2.0	-	-	2.3	



Another solution might be to lower the amount of HgO in the electrode. If a concentration of HgO could be found which would be effective in suppressing gassing and yet not adversely affect cell capacity, the problem of making a heat sterilizable Ag-Zn cell would be solved. Table IV gives the discharge data of sterilized Ag limiting cells through three cycles as a function of the percent of HgO. Even as little as 2% HgO has a considerable effect on cell capacity. However, gassing protection is not adequate as will be shown later.

The other possibility, that of replacing the HgO with something else, was considered. One compound which is known to raise the hydrogen overvoltage is PbO. Other compounds are 323-43 and 321-51. Table V shows the effect of these additives on cell capacity after sterilization. In all cases cell capacities are virtually unaffected by the additives used. Cell no. 5, one of the cells containing 3% PbO, did, however, develop a high resistance short which cut the capacity on the third and fourth cycles. Gassing studies on electrodes containing these additives to determine if they are equivalent to those containing HgO are reported later.

X-ray diffraction was used to determine changes which took place in silver and zinc electrodes before and after sterilization, charge and discharge. Experimental conditions and results appear in Table VI. In general, the results were as expected in the unsterilized set with Ag going to AgO and ZnO + 7% HgO going to the metals on charge. However, the sterilized cells gave patterns which show the probable mechanism by which Hg damages an electrode during sterilization.

In the past without the benefit of this data it has been observed that sterilized cells containing ZnO electrodes with HgO accepted a charge immediately, i.e. came up to the Zn potential without pausing for any length of time to reduce HgO to Hg at a lower voltage. Reference to Table VI, cell JV-6 shows only a trace of HgO in the negative electrode. Presumably upon sterilization HgO by some mechanism is reduced to Hg which being liquid has no well defined crystal pattern. The fact that mercury metal is present in the normal amount is shown in cell JV-5 where it has been picked up in the charged negative electrode as a zinc amalgam.

During sterilization some mercury finds its way to the silver electrode. In cell JV-6, sterilized and unformed, the silver electrode pattern shows no HgO whereas in a charged cell, JV-5, it does. The conclusion is that the mercury must be present in the liquid form on the silver electrode of JV-6. X-ray diffraction peaks of silver in the sterilized silver electrodes were shifted from  $0.2^\circ$  to  $0.4^\circ$  to the higher  $2\theta$  angles. This is true only on the surface of the sterilized electrodes and not on the interior portion. This is probably indicative of the amalgam. When this electrode is charged the mercury goes to HgO whereas the silver goes to AgO as may be seen in cell JV-5.

TABLE IV  
Effect of HgO Concentration in ZnO Electrodes in  
Sterilized Ag Limiting Cells with 40% KOH

Cell	% HgO	Cycle #1			Cycle #2			Cycle #3		
		amp- hr.	Midvolt	watt- hr.	amp- hr.	Midvolt	watt- hr.	amp- hr.	Midvolt	watt- hr.
82	0	2.46	1.37	3.37	2.08	1.37	2.85	2.01	1.37	2.75
83	"	2.39	1.40	3.35	2.05	1.39	2.85	1.82	1.40	2.55
84	"	2.40	1.39	3.33	2.05	1.38	2.83	1.99	1.40	2.79
85	2	1.44	1.40	2.01	-	-	-	-	-	-
86	"	1.36	1.42	1.93	1.51	1.42	2.15	1.38	1.46	2.02
87	"	1.34	1.43	1.92	-	-	-	1.35	1.45	1.96
88	4	1.62	1.44	2.34	1.59	1.45	2.30	0.90	1.46	1.31
89	"	1.21	1.45	1.76	1.35	1.47	1.98	1.58	1.46	2.31
90	"	1.22	1.41	1.75	0.94	1.47	1.38	1.21	1.47	1.78
91	7	1.15	1.40	1.60	>.25	-	-	.30	-	-
92	"	1.28	1.35	1.73	1.01	1.38	1.39	.30	-	-

TABLE V  
Effect of Additives on Ag Limiting Ag-Zn Cells \*

Cell	Additive	Cycle #1		Cycle #2		Cycle #3		Cycle #4	
		Discharge (amp-hr.)	% Theo- retical	Discharge (amp-hr)	% Theo- retical	Discharge (amp-hr.)	% Theo- retical	Discharge (amp-hr.)	% Theo- retical
16	2% 321-51	2.4	75	2.4	74	2.4	75	2.3	72
17	ditto	2.3	71	2.2	68	2.3	72	2.3	72
Ave.			73		71		74		72
18	7% 323-43	2.4	75	2.2	70	2.3	73	2.4	75
19	ditto	2.6	80	2.4	73	2.4	76	2.5	77
Ave.			78		72		75		76
5	3% PbO	2.6	83	2.5	79	1.9	58	1.0	30
6	ditto	2.6	83	2.4	75	2.5	79	2.37	74
Ave.			83		77		-		-
7	ditto	2.5	80	2.5	79	2.5	77	2.2	69
8	ditto	2.5	80	2.4	77	2.5	77	2.5	72
Ave.			80		78		77		71
2	3% 323-43	2.6	82	2.3	73	2.5	78	2.4	74
	2% 321-51								
3	2% 323-43	2.6	80	2.3	73	2.5	78	2.4	74
	2% 321-51								

\* Cell packs were sterilized at 145°C for 112 hours.

TABLE VI  
X-Ray Study of Electrodes

<u>Cell No.</u>	<u>Sterilized</u>	<u>State</u>	<u>Electrode</u>	<u>Compounds Present in Decreasing Order of X-Ray Intensity</u>
JV-1	No	Unformed	Pos. Neg.	Ag, Trace ZnO ZnO, HgO
JV-2	No	Charged	Pos. Neg.	AgO, Ag ZnO, Zn, ZnHg Trace
JV-3	No	Chg-Dischg	Pos. Neg.	Ag, small amount Ag <sub>2</sub> O ZnO, trace Zn, trace ZnHg
JV-4	Yes	Chg-Dischg	Pos. Neg.	Ag, Trace HgO, Trace Ag <sub>2</sub> O ZnO
JV-5	Yes	Charged	Pos. Neg.	AgO, HgO, Ag, Trace ZnO ZnO, Zn, ZnHg
JV-6	Yes	Unformed	Pos. Neg.	Ag ZnO, Trace HgO

NOTE: (1) Patterns for all negative electrodes contained small unidentified peaks as did the charged, charged-discharged positives in the sterilized set.

(2) Cell conditions for above electrodes where applicable are:

Silver limiting positives  
Negatives-ZnO with 7% HgO  
Wrap - Polypropylene  
Separator - Four layers RAI-116  
Electrolyte - 40% KOH  
Sterilization - 112 hrs. at 145°C  
Charged at 35 ma for 91.4 hrs.  
Discharged at 600 ma until pos. vs. ref. V = -0.100

The conclusion is that in damaged silver electrodes the metallic mercury covers the surface of the silver electrodes including the pores. Charging causes the mercury to convert to HgO before the silver is oxidized thus plugging the pore structure to an extent dependent upon the amount of mercury damage. This limits the amount of silver available for charge.

### c. The Zinc Electrode

While zinc as an anode material has a capacity 57% greater than cadmium oxide and a voltage about 0.4 volts higher than cadmium, it has several deficiencies which limit its usefulness in space applications. Principal among these in the present case is its tendency to produce hydrogen gas on formation and stand. Thus, most of our work was concentrated on this aspect. The zinc electrode was studied both by itself and as part of a sealed cell. This section is limited to a study of the electrode out of the cell.

#### (1) Gassing of Zinc Electrodes

Zinc electrodes tend to self-discharge on standing. Counteracting this to some extent are two factors. First, zinc possesses a high hydrogen over-voltage which makes it difficult for hydrogen to discharge on its surface, and second, zincate ion in KOH rapidly approaches saturation which decreases the zinc potential so that self-discharge is lessened. The addition of materials such as mercury which also have a higher hydrogen over-voltage than zinc further improves the wet-stand characteristics of the zinc electrode.

In the past sealed cells have been made with electrodes composed of ZnO containing 7% HgO. The amount of hydrogen evolved in these cells is low enough to diffuse through the plastic cases without excessive pressure build-up. Electrodes of this composition were, therefore, considered standard for these studies.

Since ZnO electrodes containing 7% HgO cause a loss of capacity in sterilized Ag-Zn cells, other additives were investigated. Among the additives tried were lower percentages of HgO, various percentages of PbO and compounds 323-43 and 321-51.

Two tests were used to study gassing characteristics of the several electrode mixes. The first simply measured the volume of gas produced when half sized strips of the various electrodes, in the charged condition, were placed in inverted burets containing 40% KOH-7.5% ZnO. This test has the disadvantage of requiring a long stand time before significant data can be obtained upon which to draw valid conclusions. A second test, which is very rapid and the results from which are related to gassing characteristics of the electrodes, is derived from Tafel studies. The underlying principle is that an additive prevents gassing of zinc by raising the hydrogen overvoltage

of the electrode so that hydrogen ions can not be discharged on the surface. By measuring the half cell potential of the negative electrode at various current densities using a reference electrode enclosed in a Luggin capillary, the relative effectiveness of various additives in decreasing gassing is obtained. A plot of these voltages against the logarithm of the current yields straight lines. The values of A and B determined by the method of least squares for an equation similar to that of Tafel ( $V = A + B \log_{10} i$ ) are given in Table VII. In this equation V is the voltage of the electrode vs. a Hg-HgO reference electrode and i is the current in milliamperes.

Gassing results, also given in Table VII, show one ml of gas per month for the standard 7% HgO additive whereas 7% additive 323-43 produced two ml in the same time. In general, the small (approximately 4 ml or less) amounts of gas evolved in 30 days were probably within the experimental accuracy of the method. The principal error in this procedure was occasional small leaks around the stop-cock at the top of the buret in which the gas is collected. Such leaks admitted air and led to slightly higher gas volumes than might actually be evolved from the electrode.

TABLE VII  
Tafel and Gassing Data

<u>Additive</u>	<u>A</u>	<u>B</u>	<u>ml of gas/30 days</u> Exp.
3% 323-43 ) 2% 321-51 )	1.5278	0.1140	4.4
4% 323-43	1.5222	0.1061	4.0
7% 323-43	1.5194	0.1005	2.0
7% HgO	1.5238	0.1062	1.0
1% 321-51	1.4381	0.1264	15.2
2% "	1.4468	0.1126	12.4
3% "	1.4375	0.1330	11.0
6% "	1.4329	0.1411	6.4
No Additive	1.3919	0.1156	103

## (2) The Couple Effect

It was suggested that a large part of the gas build-up during the formation of a Ag-ZnO cell might be due to the couple formed between the zinc nega-

tive and its silver grid as demonstrated by Snyder and Lander\*. Usually HgO is added to the zinc mix and the mercury produced during formation gives protection against the phenomenon. However, with the present cells in which Compound 323-43 is used, it was proposed that the zinc might charge before the additive becomes effective, and this might lead to the observed gas pressure. To test this hypothesis and evaluate grid materials a number of experiments were carried out using regular gassing tubes. Various pieces of other metals were fastened to zinc sheets 1 inch by 1 inch square, and these combinations were placed in gassing tubes in 40% KOH. The data are shown in Table VIII. Amalgamations, when used, were carried out in 0.3% HgCl<sub>2</sub> solution or electrolytically from a solution of potassium mercuric iodide.

The data indicate that using bare Ag as a grid in the presence of zinc would produce about 8 times as much gas as when the Ag grid was amalgamated. Moreover, amalgamated zinc in the presence of pure silver produces very little gas. As might be expected, the best results were obtained when both the zinc and the silver were amalgamated. For the metals tested, the order of protection appears to be Cu > Pb ≈ In > beryllium copper > Cd ≈ Ag > Ni.

From this work on the zinc electrode it is concluded that: (1) additive 323-43 is about as effective as HgO in suppressing gas from a zinc electrode during stand, (2) amalgamation of the silver grid is the most effective way of suppressing hydrogen from the couple effect if this causes gas in sealed cells.

### 3. Electrolyte Properties

Fundamental physical chemistry studies on the electrolyte system KOH-ZnO included measurement of vapor pressure, electrical conductivity, and solubility of ZnO in KOH. The effect of AgO (Ag<sub>2</sub>O) on the electrolyte was also considered and is discussed in this section. In general, reagent grade ZnO powder was dissolved in KOH solutions of various concentrations to make electrolyte for these measurements. Analysis for ZnO content was made by titrating Zn<sup>++</sup> with 0.1M EDTA to the xylenol orange endpoint at pH 5.0-5.5, and for KOH by titrating K<sup>+</sup> with sodium tetraphenylborate solution using amperometric endpoint detection. Limits of experimental error were ±0.05% ZnO and ± 0.25% KOH.

---

\* R. N. Snyder and J. J. Lander, Rate of Hydrogen Evolution of Zinc Electrodes in Alkaline Solutions, *Electrochemical Technology*, 3, 161 (1965).

TABLE VIII

Volume of Gas (ml) from Couples in 40% KOH at a  
Given Time

Electrode	5 hrs.			24 hrs.			48 hrs.			168 hrs.			400 hrs.		
	1*	2*	3*	1	2	3	1	2	3	1	2	3	1	2	3
Zn + Ag wire	0.3	0.3	0.4	2.7	4.0	3.3	2.7	4.0	3.3	3.5	5.3	4.2			
Zn + Cd	0.8	0.6		2.9	2.6		3.4	3.4							
Zn + Ni	5.6	3.0		8.5	4.3		9.5	4.6							
Zn + Be - Cu	1.0	1.4		1.7	2.3		2.0	2.6							
Zn + In	0.3	0.5		1.0	1.7		1.4	2.3							
Zn + Pb	0	0		1.8	1.4		2.5	1.8							
Zn + Cu	-			-			0.6	0.7		0.5	0.7		1.1	1.8	
Zn-Hg+Ag-Hg	-			-			0	0		0	0		0	0	
Zn + Ag - Hg	-			-			0.4	-		0.6	-		0.8	-	
Zn-Hg + Ag	-			-			0	0.2		0.1	0.3		0.3	0.5	

\* Replicates



### a. Vapor Pressure

Vapor pressures of KOH solutions during sterilization were measured by means of the ammonia gauge of the nickel bomb assembly already described. Initial experiments were run to show that aqueous KOH directly in contact with nickel yielded the same pressure as when contained in a Teflon or polypropylene container. Pressures of electrolyte in the sealed bombs were read directly in psig and corrected for increase of air pressure with temperature, for expansion of electrolyte, and for loss of water vapor from the solution. Vapor pressures of pure solutions as a function of concentration and temperature over the ranges 30-45% KOH and 100-145°C are given in Table IX.

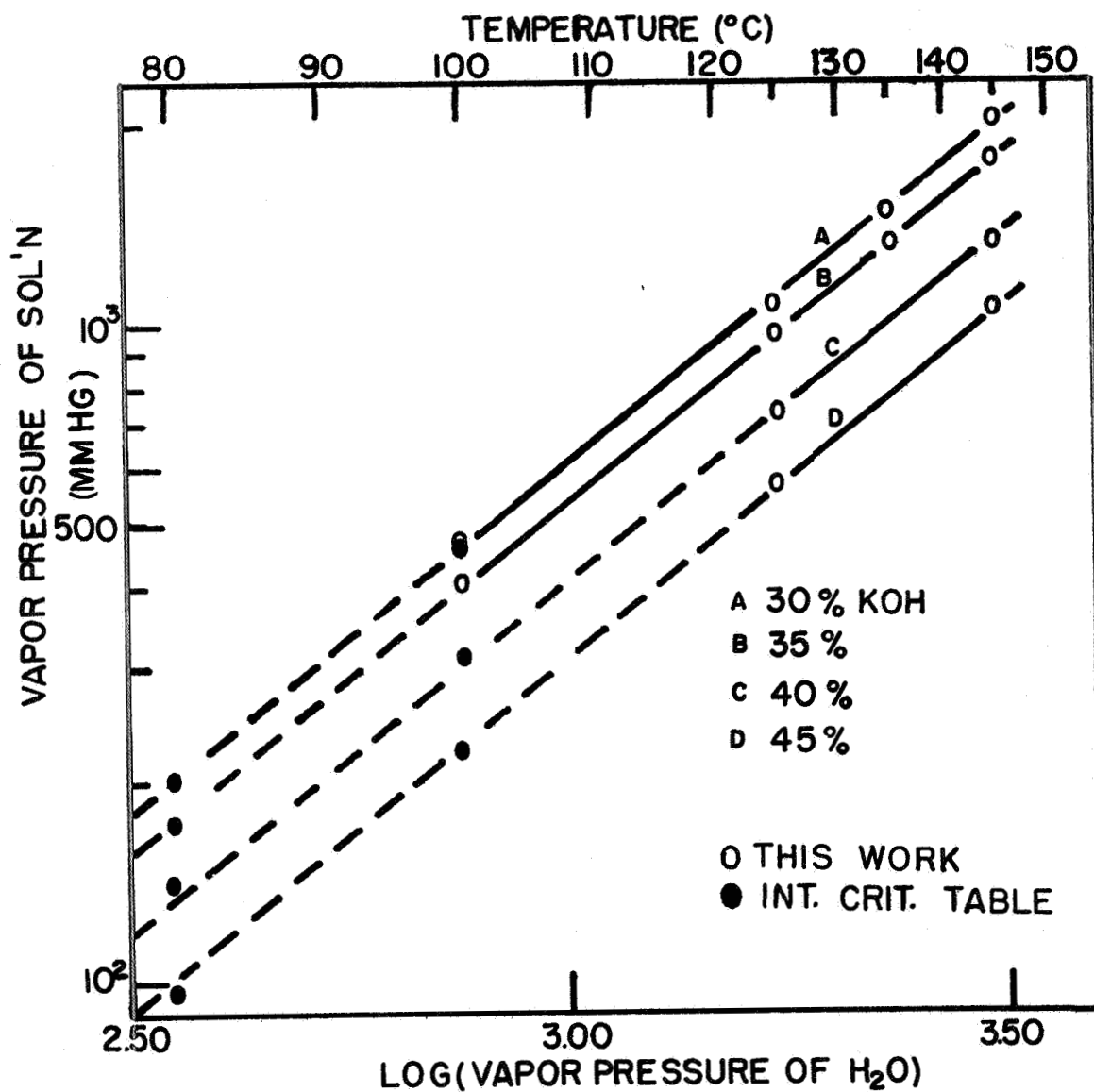
TABLE IX  
Vapor Pressure of Aqueous KOH  
(mm Hg)

<u>% KOH}</u>	<u>30</u>	<u>35</u>	<u>40</u>	<u>45</u>
<u>T(°C)</u>				
145	2010	1760	1330	1050
135	1470	1310	-	-
125	1080	960	725	570
100	470	410	-	-

Figure 1 is an Othmer-type plot (D. F. Othmer and R. Gilmont, Kirk-Othmer Encyclopedia of Chemical Technology, Vol. 14, page 611, 1st Edition) of the data, including values for 100°C and below from the International Critical tables for comparison. The extrapolation indicates that the Othmer treatment of vapor pressure data for this system is valid up to and including the highest sterilization temperature.

Experiments with KOH-ZnO solutions yielded no consistent pattern of vapor pressure vs. ZnO concentration at sterilization temperatures. Within limits of experimental error ( $\pm 1^\circ\text{C}$ ;  $\pm 0.25\%$  KOH;  $\pm 15\text{mm Hg}$ ) there was no effect of ZnO dissolution on the vapor pressures of the KOH solutions. Similarly, the presence of other cell components such as silver or silver oxide, separator or absorber material, etc., had no effect on vapor pressure. Hence, the Othmer Plot given can be used for readily determining vapor pressure in a practical sealed cell under any conditions in the range 80-145°C and 30-45% KOH.

FIG.1  
 OTHMER TYPE PLOT: VAPOR PRESSURE  
 OF KOH SOLUTIONS



## b. Conductivity

Electrical conductivities of aqueous KOH and KOH-ZnO solutions were measured using a 50 ml conductivity cell and a Wayne-Kerr Universal Bridge with low impedance adaptor. The cell was immersed in a temperature-controlled water bath until the resistance reading for a given electrolyte at a given temperature became constant. Calibration and cell-constant determination were periodically checked using a 1 demal\* KCl standard solution. Conductivities of pure KOH solutions at three temperatures are plotted in Figure 2, which includes data for 25°C from Klochko and Godneva (Russ. J. Inorg. Chem., Vol. IV, #9, 1959). Figure 3 gives data on KOH-ZnO conductivities for the same temperatures. Each line of Figure 3 begins with the conductivity of pure KOH of a given concentration; the conductivity then decreases slightly with increasing addition of ZnO (expressed as final wt. % ZnO in the given initial KOH solution). A large number of data points were determined for 40% KOH at 25°C to indicate the experimental accuracy of the measurements. Conductivity points are included for ZnO-saturated solutions at 25°C from the data of Dirkse (J. Electrochem. Soc. 106, 154 (1959)).

Heat sterilization of electrolytes with other components of the electrochemical (Ag-Zn) system had little or no effect on conductivity. Also, conductivities of electrolyte samples from typical test cells (subjected to various sterilization treatments and cycling programs) were in agreement with those predicted by Figure 3 for pure solutions of the same KOH-ZnO composition. Hence the electrolyte conductivity in an actual cell may be considered to be determined by the ZnO-KOH composition alone.

## c. Solubility of ZnO in KOH

### (1) Rate of Dissolution

Preliminary experiments for determining the rate of ZnO dissolution in KOH at sterilization temperatures were run in the sealed nickel bombs, or in similar bombs of stainless steel with Teflon inserts which permitted use of magnetic stirring. In Figure 4 is plotted the dissolution of ZnO into aqueous KOH at 145°C as a function of time. For each run of this experiment, sufficient ZnO powder was added to 100 ml of a given KOH concentration to yield 8% ZnO in the final solution if all were to dissolve. No stirring was employed; samples for analysis were siphoned from the supernatant solution after the bombs were allowed to cool to room temperature. Solution of ZnO in the electrolyte under these conditions increased with time and with KOH concentration. In similar experiments with stirring

---

\* A demal solution is used in conductivity work and is a solution containing one gram mole of salt per cubic decimeter of solution at 0°C.

FIG. 2  
CONDUCTIVITY OF KOH SOLUTIONS

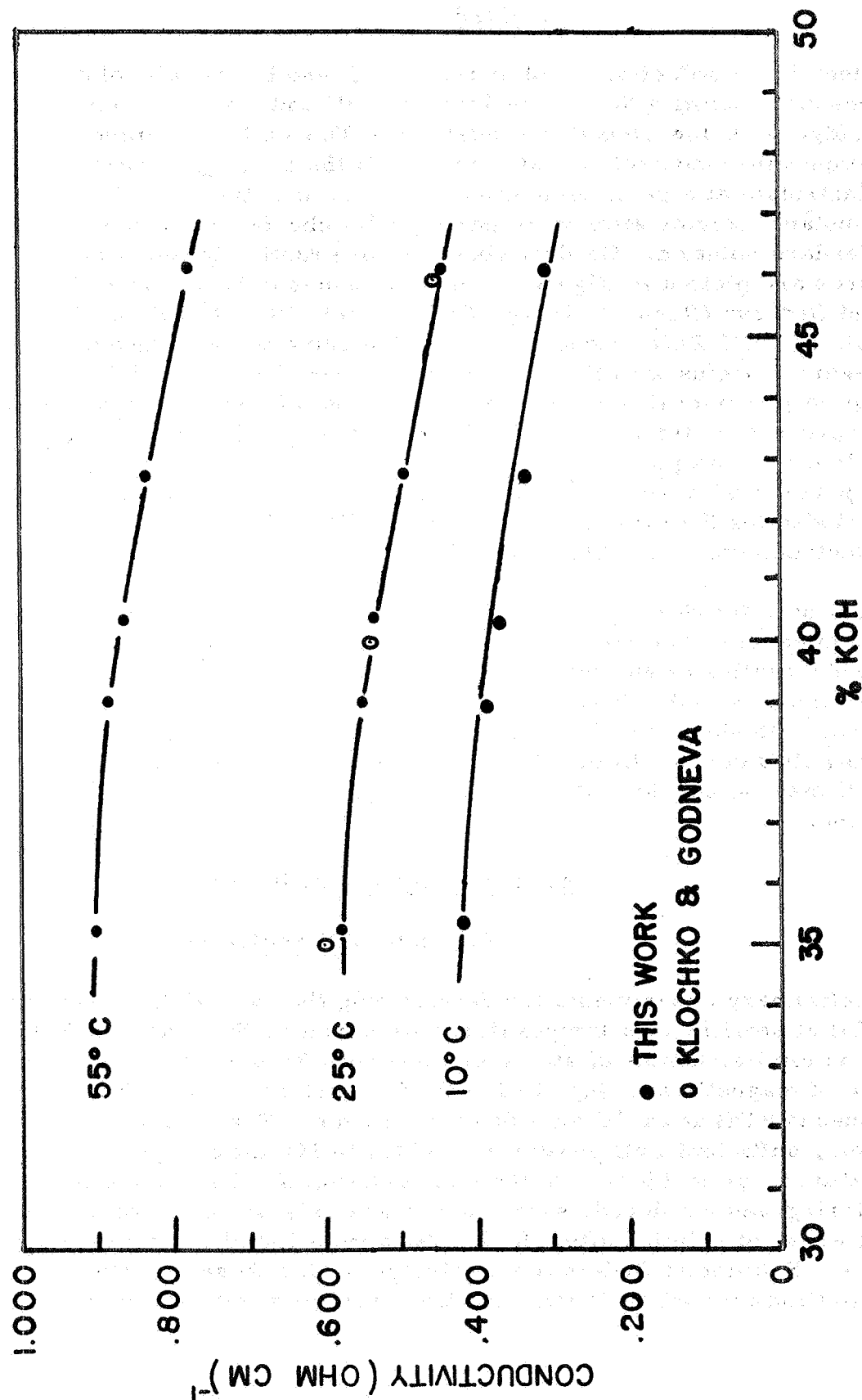


FIG. 3  
CONDUCTIVITY OF KOH-ZnO SOLUTIONS

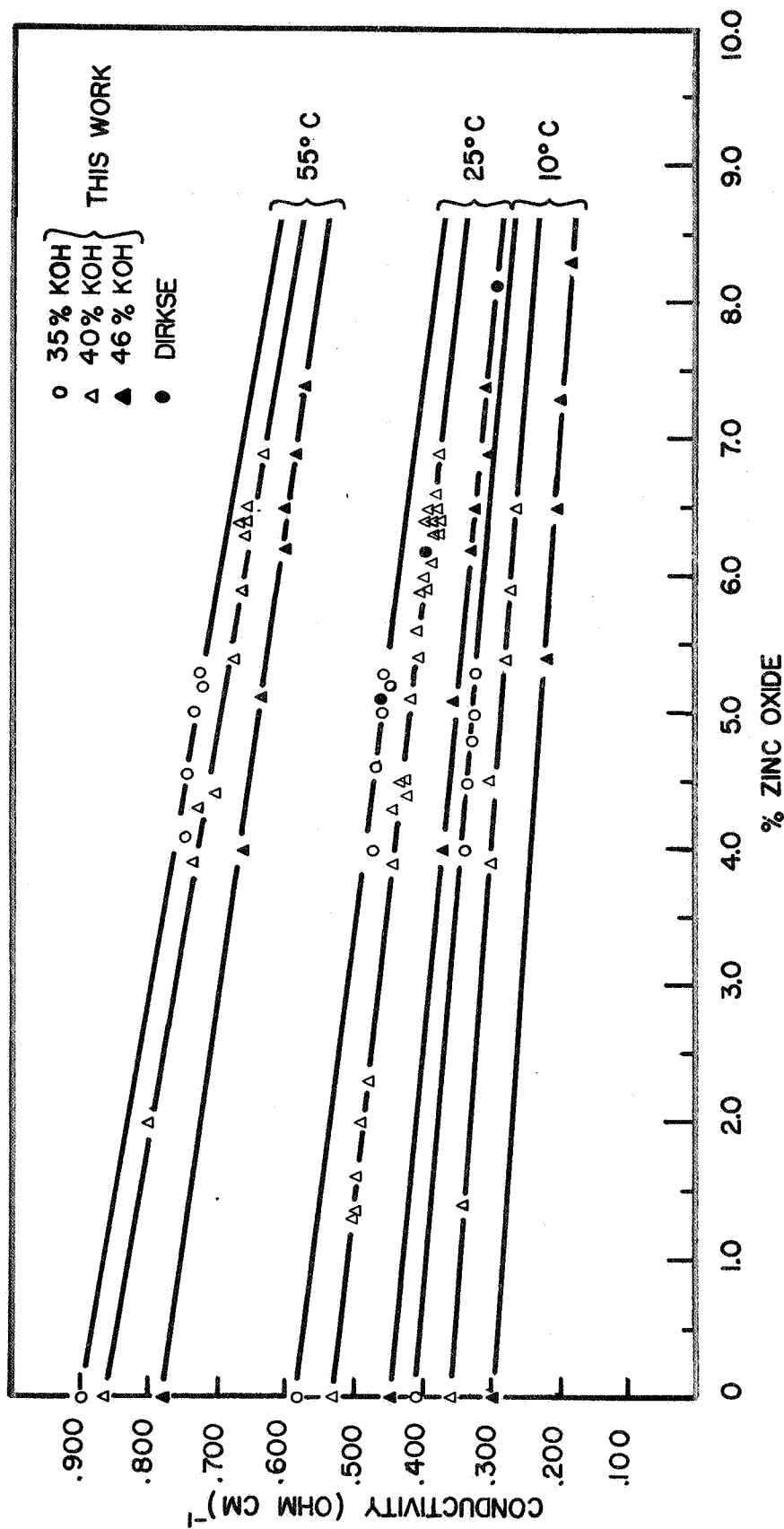
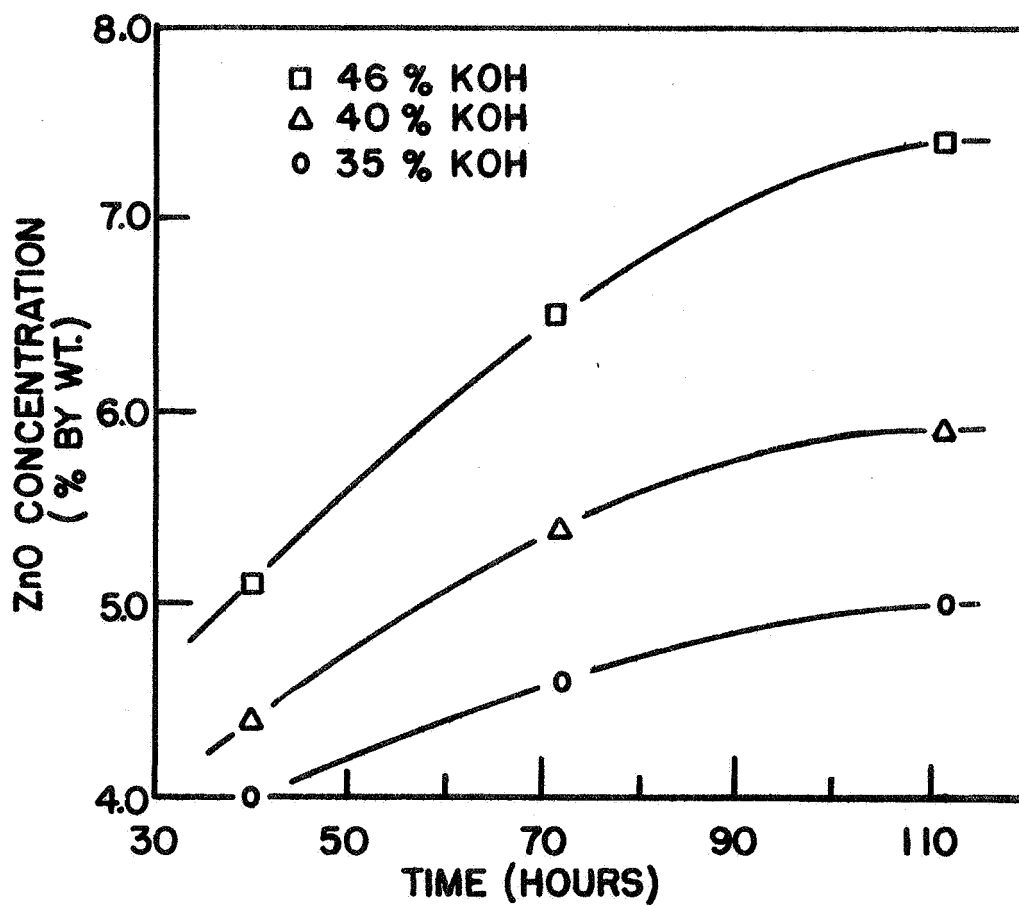


FIG. 4  
DISSOLUTION OF ZnO IN KOH AT 145° C



during the heating period, however, the time dependence was not present and all solutions appeared to be saturated with ZnO at room temperature even after short heating times. Furthermore, even when samples were unstirred during sterilization, simply mixing the electrolyte and excess ZnO present and then centrifuging yielded the same saturation values as though the KOH-ZnO system had been stirred for the whole time. These room temperature solubility values, which agreed with those obtained by dissolution of excess ZnO in KOH at 25°C with stirring, are given in Table X.

TABLE X  
Solubility of ZnO in KOH at 25°C

<u>Initial % KOH</u>	<u>Final % ZnO</u>
46	8.3
40	6.5
35	5.2

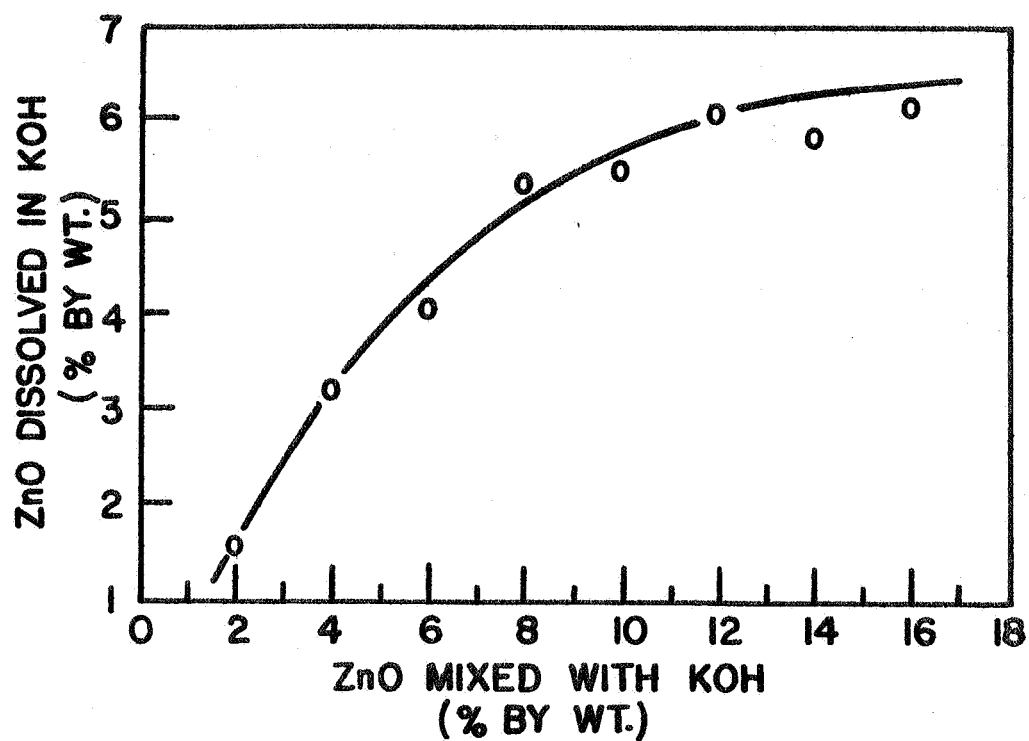
The above experiments indicated that the rate of ZnO dissolution in KOH is rapid when stirring is employed, but is strongly time dependent in unstirred systems in which diffusion of the soluble species away from the solid-electrolyte interface is a significant factor. A further experiment was devised to confirm this point. Eight 75 ml samples of 40% KOH, containing varying quantities of ZnO powder, were shaken for one minute each at 25°C and then immediately centrifuged and the solutions analyzed. The results are plotted in Figure 5, in which "ZnO mixed with KOH" signifies sufficient ZnO to yield the final % ZnO indicated if all were to dissolve. The actual amount of ZnO dissolved for a given amount present increases linearly at low ZnO and levels off with increasing excess ZnO as saturation is approached.

In many of the dissolution rate experiments colloidal dispersion accompanied solution of ZnO, as indicated by Tyndall effect observations. It was determined by centrifuging and by comparing analyses of clear saturated solutions with those of saturated solutions having heavy Tyndall effects that the amount of ZnO in colloidal form was very small and could be neglected in comparison to the amount in solution.

The following conclusions were reached as a result of the dissolution rate experiments:

FIG. 5

DISSOLUTION OF ZnO INTO 40% KOH AT 25° C





1. Solution of ZnO powder in KOH is rapid when stirring or mixing is used.
2. Solution may be slow in unstirred solution due to (a) small quantity of ZnO surface exposed to electrolyte, and (b) limited diffusion of dissolved species away from the solid-liquid interface.
3. The diffusion-limiting nature of the dissolution of ZnO in aqueous KOH, and the resulting stratification effect in unstirred electrolyte, is more pronounced the higher the KOH concentration.
4. Colloidal dispersion may occur when excess ZnO is present; however, the quantity in colloidal form is small compared to that in solution.

## (2) Solubility of ZnO

Initial experiments for determining equilibrium solubilities were run for the range 10-95°C. Excess ZnO was added to solutions saturated at room temperature in stoppered flasks. These were immersed in a water-bath at the desired temperature and agitated for two days or longer, then allowed to settle until no Tyndall effect was observable in the supernatant solution. Samples of the solution were then siphoned for analysis. Results indicated little or no variation of ZnO solubility with temperature, i. e. the quantity of ZnO dissolved in each KOH concentration was the same over the entire temperature range as listed in Table X. To check this further, a plot of literature data (listed as % Zn vs. % K in the equilibrium saturated solutions by T. P. Dirkse, J. Electrochem. Soc. 106, 154) was made as shown in Figure 6. The solid line is drawn for the 25°C data; ZnO solubility increases with KOH concentration along this smooth curve up to about 36% K (corresponding to about 52% KOH), then decreases rapidly with increasing KOH concentration above this point. The data for other temperatures fall along this curve, but the "critical region" of KOH concentration differs for each temperature, as indicated by the broken lines in Figure 6. For the range of KOH concentration of interest in the present studies, viz. 35-45% initial KOH (or about 23-30% K in the final saturated solution), Figure 6 suggests that ZnO solubility is temperature independent or very nearly so for all temperatures above 0°C.

In order to ascertain whether the temperature invariance of ZnO solubility in aqueous KOH extends up to sterilization temperatures, a special solubility apparatus was constructed as illustrated in Figure 7. It consisted of two sealed stainless steel bombs with Teflon liners, connected by a nickel siphon tube for isolating and transferring a small sample of saturated solution. Valves and fittings were monel, and gaskets were Teflon. For a

FIG. 6

SOLUBILITY OF  $ZnO$  IN  $KOH$  AS A FUNCTION OF  
KOH CONCENTRATION AND TEMPERATURE

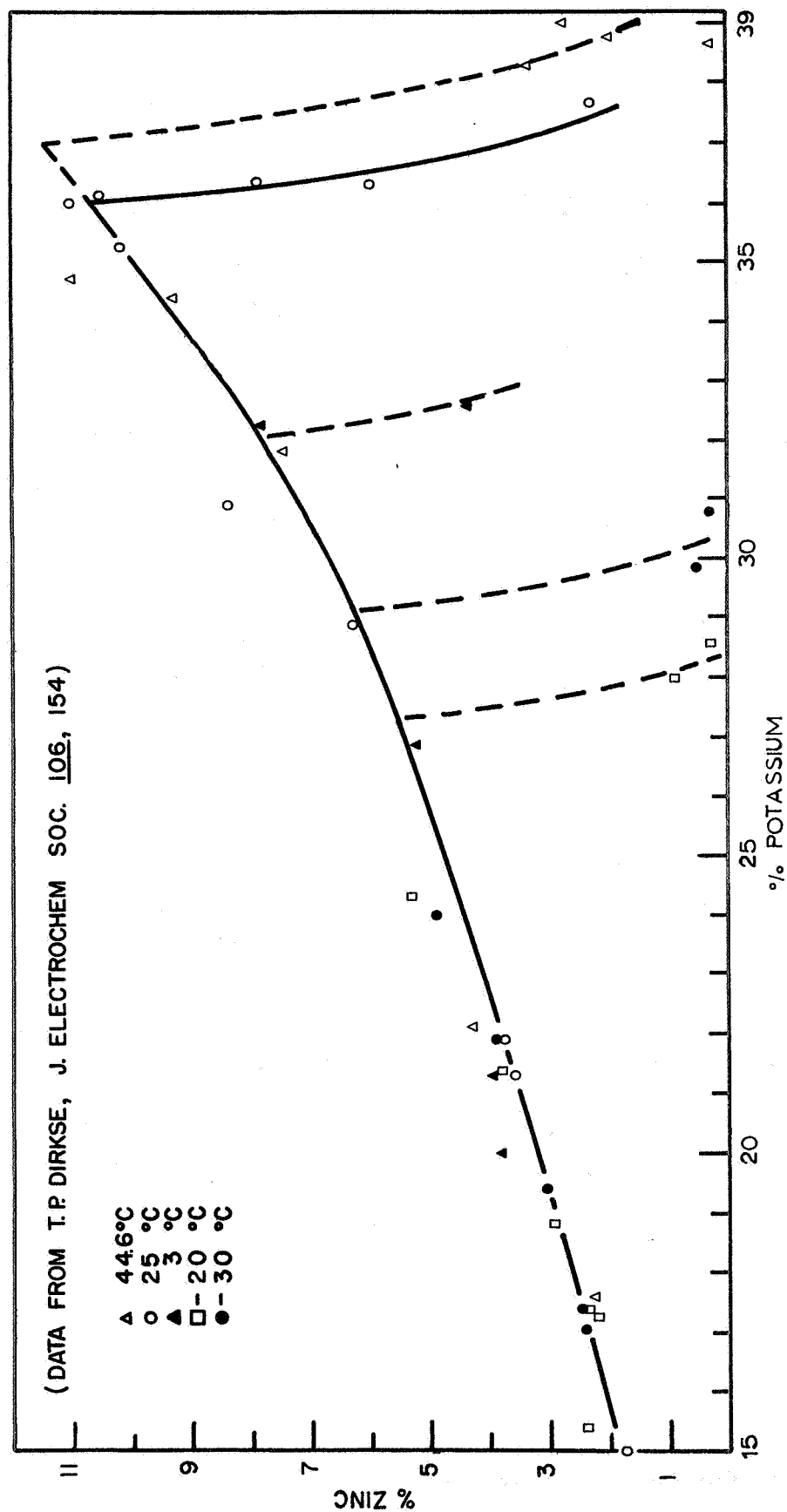
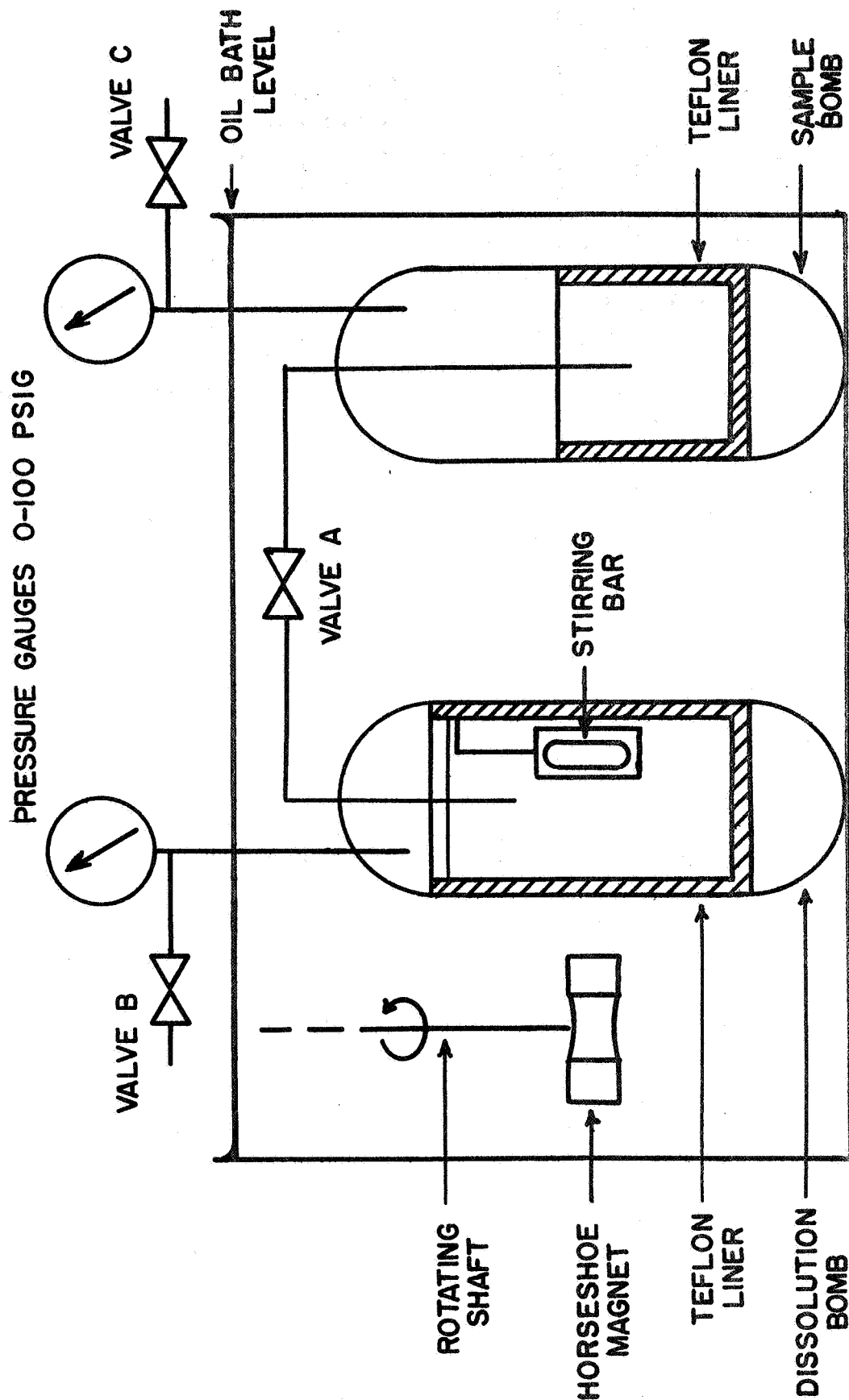


FIG. 7

SCHEMATIC OF SOLUBILITY APPARATUS



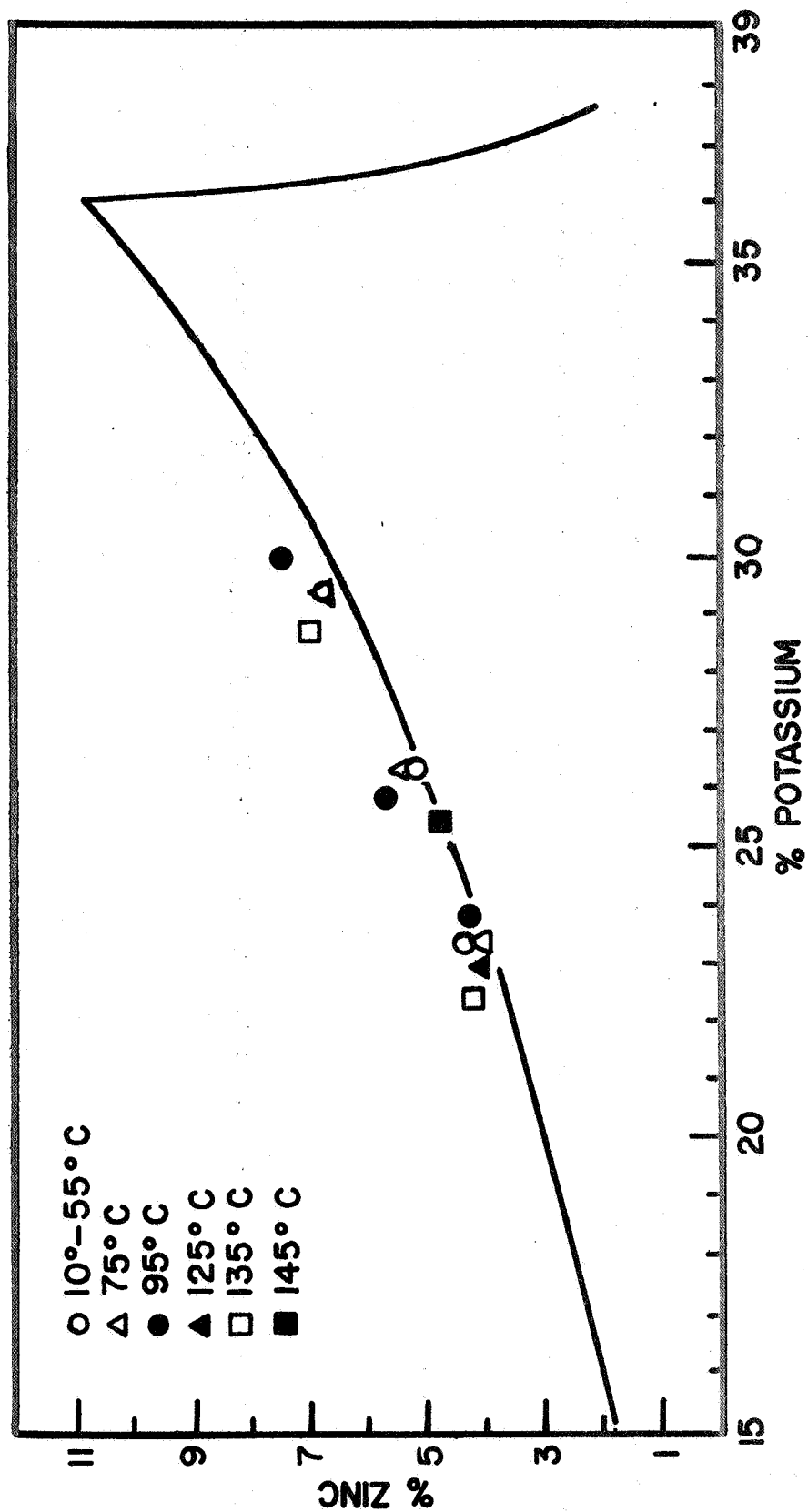
given solubility determination, KOH saturated with ZnO at room temperature was placed with excess ZnO into the solution bomb. The apparatus was then assembled in sealed condition with all valves closed, and brought up to temperature in the oil bath. The solution was stirred at least 48 hours to assure attainment of equilibrium, using a magnetic stirrer suspended by silver wire and activated by a rotating horseshoe magnet external to the bomb. After allowing the excess suspended ZnO to settle for a minimum of 48 hours, valve "A" was opened and a sample of the saturated solution was transferred through the siphon tube; the excess vapor pressure in the solution bomb relative to the empty sample bomb was sufficient to accomplish this transfer. When both bombs reached the same pressure valve "A" was closed; the oil bath was then allowed to cool to room temperature and the sample removed for analysis.

Results of the solubility experiments for all temperatures are given in Table XI and plotted in Figure 8. The 25°C curve from Figure 6 is included in Figure 8 for comparison. The data from this work confirms that there is little or no temperature dependence of ZnO solubility in aqueous KOH over the range 35-46% KOH and 10-145°C.

TABLE XI  
Solubility of ZnO in KOH at Elevated  
Temperatures

Temperature (°C)	Initial % KOH	Final		
		% ZnO	%K	% Zn
10; 25; 55	35.3	5.2	23.3	4.2
	40.4	6.5	26.3	5.2
	46.1	8.3	29.5	6.7
75	35.3	5.1	23.3	4.1
	40.4	6.7	26.2	5.4
	46.1	8.4	29.5	6.7
95	36.2	5.4	23.8	4.3
	40.0	7.1	25.8	5.7
	47.4	9.0	30.0	7.2
125	35.0	5.1	23.0	4.1
135	33.8	5.2	22.3	4.2
	45.1	8.7	28.7	7.0
145	38.9	6.0	25.4	4.8

**FIG. 8**  
 SOLUBILITY OF ZnO IN KOH AT ELEVATED  
 TEMPERATURES



### (3) Solubility of Zn Electrode

A number of solubility experiments were also conducted on electrolytes sterilized in contact with individual cell components and finally complete test cells. The following observations were made:

1. Dissolution rates of ZnO electrodes of various design are approximately the same as for powdered ZnO in equivalent configurations.
2. Upon sterilization of a Ag-Zn cell (with high ZnO/KOH) at any of the specified temperatures and heating times with any practical KOH concentration, the equilibrium ZnO solubility will be reached or closely approached regardless of the type of ZnO electrode used.
3. No evidence of supersaturation of ZnO in KOH or of ZnO recrystallization after sterilization was found; however, surfaces of sterilized electrodes were in some cases roughened somewhat as compared to those soaked at room temperature for an equal time.

#### d. Solubility of AgO ( $\text{Ag}_2\text{O}$ ) in KOH

Work on the AgO ( $\text{Ag}_2\text{O}$ ) system under the present contract was limited to a single study in which it was shown that electrolyte conductivity is not appreciably affected by the presence of dissolved AgO or  $\text{Ag}_2\text{O}$ .

A brief review will be given here, however, of silver oxide solubility investigations made previously in this laboratory and elsewhere.

Kovba and Balashova (Russ. J. Inorg. Chem. 4, 94 (1959) ) measured the solubilities in 1-10N KOH at room temperature using a radioactive tracer technique and obtained the following results:

35% KOH (8.4 N):	0.0087% $\text{Ag}_2\text{O}$ ( $5 \times 10^{-4}$ N)
40% KOH (10 N):	0.0082% $\text{Ag}_2\text{O}$

AgO solubility was the same or slightly lower. No effect of zincate ion on the solubility of either oxide was found. Solubilities of  $\text{Ag}_2\text{O}$  in 40% KOH at higher temperatures were as follows:

50°C:	0.012% $\text{Ag}_2\text{O}$
78°C:	0.032% $\text{Ag}_2\text{O}$

Amlie and Ruetschi (J. Electrochem. Soc. 108, 813 (1961) ) studied the dissolution of  $\text{Ag}_2\text{O}$  and  $\text{AgO}$  powders at room temperature in 1-14 N KOH by a rotating electrode method. Only monovalent species were detected in solution. Quantitative analysis by potentiometric titration gave the following results:

wt. % KOH	wt. % $\text{Ag}_2\text{O}$	N $\text{Ag}_2\text{O}$
35	0.0077	$4.5 \times 10^{-4}$
40	0.0071	$4.3 \times 10^{-4}$
45 (11.7 N)	0.0064	$4.0 \times 10^{-4}$

Addition of zincate affected  $\text{Ag}_2\text{O}$  solubility slightly.

Data of other investigations on silver oxide solubilities at lower KOH concentrations are in substantial agreement with the above findings. The work of Kovba and Balashova indicates a noticeable increase in  $\text{Ag}_2\text{O}$  solubility at higher temperatures. This is immaterial to the present study, however, since cells are in the uncharged state during high temperature sterilization, i.e. the positives are in the form of metallic silver.

#### e. Cell Performance as a Function of Electrolyte Composition

In the case of both unsterilized and sterilized silver-zinc cells, studies were made on the effect of electrolyte variations on cell capacity for concentrations of 35, 38, 40, 43, and 45% KOH, with and without added  $\text{ZnO}$ . The 3-plate cells were silver limiting. ESB standard electrodes of the type described previously were used except that the  $\text{ZnO}$  electrodes contained no additive for gassing protection. The positives were wrapped with one layer of EM 476 absorber and four layers of RAI-116 separator material. Approximately 15 ml of electrolyte were used in each cell; the electrolyte level was adjusted so that it covered the electrodes but did not flood over the separator material. The cells were unsealed, but were covered to prevent excessive electrolyte evaporation and carbonate formation.

On the first cycle the cells were charged at 35 ma constant current for 91 hours and on subsequent cycles at the 40-hour rate based on 120% of the previous cycle. After charge acceptance had been confirmed on each cycle, the cells were discharged at 600 ma until either the Ag vs.  $\text{Hg}/\text{HgO}$  reference voltage reached -0.1 volts or the total cell voltage reached 1.2 volts (for Ag-Zn) or 0.8 volts (for Ag-Cd). Voltages and discharge times were recorded for three cycles and cell capacities calculated in ampere-hours and watt-hours. In general, test cells for each variation were made in triplicate; average values were calculated.

#### (1) Ag-Zn Cells

The cycling data for the three plate silver-zinc cells were examined and tabulated. The steps in the examination of the data were as follows:

- (i) The original data were examined to eliminate cells which never reached the oxygen evolution potential, which were dry (high end-of-charge voltage), or which were shorted (low end-of-charge voltage).
- (ii) Both the original data and notebook tabulations were examined to eliminate the data from those cells in which the end of discharge positive-to-reference (HgO) voltage was higher than -0.075 volts. The specifications of the experiment called for cell cut off at -0.100 volts (Ag vs. reference) or at 1.20 volts across the cell.

In a number of cases, because of the inefficiency of the negative electrode, the cell had to be cut off prior to reaching -0.100 volts (Ag vs. ref.). Those cells which were cut off above -0.075 volts were considered to be incompletely discharged and therefore uncharacteristic of the group. The value -0.075 was chosen because it was observed that in some instances the cells dropped below zero volts and tended to level off at a small negative voltage prior to the final "knee" of the curve; -0.075 was considered to be below the "knee" in all cases. It should be noted that in some instances a cell removed by this criterion had the highest capacity of the group. It was felt that the resulting reduction in average capacity was not as important as the exclusion of an uncharacteristic cell. All data included in the tabulation are, therefore, positive limited capacities.

In several instances the procedure outlined above eliminated the data from all but one cell. This fact is noted in the tables. In one instance, (35% KOH, near-saturated, sterilization temperature 145°C, first cycle) all the cells were eliminated because they had not reached O<sub>2</sub> evolution prior to discharge. The results are given in Table XII. The data indicate that:

- (i) The concentration range 38-40% KOH is preferred; however, acceptable performance may be obtained throughout the entire range 35-45% KOH.
- (ii) Initial ZnO dissolved in the electrolyte has little or no effect on performance.
- (iii) Sterilization temperature has little effect on performance.

## (2) Ag-Cd Cells

Because of energy density considerations mentioned earlier, Ag-Cd cells were tested less extensively than Ag-Zn cells. Table XIII shows the data obtained for these negative limiting Ag-Cd cells. The main conclusions drawn from these data are as follows:



TABLE XII  
Ag-Zn Cell Capacities as a Function of Electrolyte Composition

Sterilization	Electrolyte	amp-hours		watt-hours		
		Cycle 1	Cycle 2	Cycle 1	Cycle 2	
None	35	2.38 + .04	2.14 + .15	3.36 + .03	3.45 + .27	3.10 + .32
	35(S)	2.26 + .09	2.42 + .04	3.22 + .18	3.44 + .10	3.06 + .24
	38	2.12 + .11	2.37 + .42	2.87 + .18	3.12 + .22	3.04 + .08
	40	2.19 + .06	2.36 + .08	3.00 + .12	3.24 + .12	3.05 + .10
	40 (1/2)	2.44 + .10	2.23 + .11	3.40 + .19	3.08 + .25	3.20 + .16
	40(S)	2.23 + .06	2.36 + .01	3.12 + .10	3.28 + .05	3.17 + .33
	43	2.07 + .06	2.33 + .07	2.58 + .08	2.98 + .02	2.68 + .40
	43(S)	1.94 + .04	2.01 + .07	2.57 + .11	2.71 + .06	-
	45	1.81 (A)	1.93 + .16	2.17 (A)	2.49 + .12	2.28 (A)
	45 (1/2)	1.84 + .07	2.18 + .12	2.38 + .13	2.80 + .18	2.28 + .34
	45(S)	1.97 + .06	2.21 + .06	2.59 + .14	2.91 + .26	2.65 + .54
125°C	35(S)	2.32 + .02	2.02 + .03	3.22 + .03	3.08 + .05	3.01 (A)
	38	2.63 + .04	2.30 + .01	3.70 + .02	3.22 + .08	3.14 + .18
	40	1.71 + .63	2.33 (A)	2.34 + .81	3.20 (A)	3.10 (A)
	40(S)	2.23 + .20	2.34 + .09	3.05 + .29	3.22 + .15	3.09 + .06
	43(S)	2.07 + .05	2.19 + .05	2.69 + .05	2.83 + .04	3.01 + .04
	45	2.38 + .04	2.33 + .11	3.05 + .10	2.93 + .11	2.63 + .13
135°C	35(S)	2.32 + .08	2.11 + .04	3.22 + .14	2.93 + .06	2.94 + .00
	38	2.41 + .41	2.20 + .08	3.27 + .27	3.10 + .14	3.26 + .30
	40	2.49 + .02	2.24 + .05	3.46 + .03	3.13 + .09	3.15 + .05
	40(S)	2.35 + .02	2.33 + .19	3.19 + .06	3.20 + .26	3.08 + .12
	43(S)	1.91 + .08	2.07 + .01	2.54 + .13	2.72 + .03	2.95 + .14
	45	2.44 + .04	2.27 + .11	3.24 + .09	3.05 + .15	2.89 + .14

TABLE XII (continued)  
Ag-Zn Cell Capacities as a Function of Electrolyte Composition

Sterilization	Electrolyte	amp-hours			watt-hours		
		Cycle 1	Cycle 2	Cycle 3	Cycle 1	Cycle 2	Cycle 3
145°C	35	2.10 (A)	2.25 (A)	1.56 (A)	2.86 (A)	3.06 (A)	2.12 (A)
	35(S)	-	2.25 ± .12	2.05 ± .18	-	3.06 ± .25	2.86 ± .30
	38	2.07 ± .09	2.29 ± .06	2.21 ± .08	2.77 ± .11	3.07 ± .14	2.95 ± .15
	40	2.38 ± .03	2.37 ± .11	2.36 ± .02	3.36 ± .02	3.32 ± .18	3.29 ± .06
	40 (1/2)	2.34 ± .37	2.32 ± .33	2.10 ± .27	3.14 ± .51	3.13 ± .46	2.78 ± .45
	40(S)	2.06 ± .22	2.13 ± .16	2.23 ± .12	2.92 ± .35	3.01 ± .49	3.16 ± .23
	43(S)	2.19 ± .19	2.44 ± .04	2.42 ± .01	2.95 ± .20	3.26 ± .03	3.22 ± .06
	45	2.30 ± .05	2.43 ± .05	2.42 ± .10	3.01 ± .06	3.19 ± .07	3.16 ± .14
	45 (1/2)	2.03 ± .04	2.14 ± .07	2.25 ± .06	2.61 ± .01	2.78 ± .08	2.92 ± .08
	45(S)	2.18 ± .15	2.29 ± .03	2.31 ± .13	2.81 ± .25	3.00 ± .06	3.05 ± .19

# NOTES

Number alone indicates pure aqueous KOH of given wt. %

(1/2) indicates electrolyte approximately half saturated with ZnO.

S indicates electrolyte saturated with ZnO.

(A) indicates one cell data only.

TABLE XIII  
Ag-Cd Cell Capacities as a Function of Electrolyte Composition

Sterilization	KOH Conc.	amp-hours		watt-hours	
		Cycle 1	Cycle 2	Cycle 1	Cycle 2
None	35%	1.41 ± .06	1.76 ± .19	1.40 ± .04	1.76 ± .17
	40%	1.52 ± .08	1.86 ± .11	1.50 ± .12	1.84 ± .15
	35%	1.38 ± .04	1.67 ± .25	1.33 ± .06	1.61 ± .25
125°C	40%	1.37 ± .03	1.82 ± .02	1.28 ± .05	1.70 ± .03
	45%	1.63 ± .01	1.72 ± .15	1.51 ± .04	1.56 ± .18
	40%	1.62 ± .02	1.71 ± .14	1.56 ± .04	1.64 ± .14
135°C	40%	1.38 ± .28	1.68 ± .19	1.33 ± .29	1.60 ± .19
	45%	1.50 ± .00	1.59 ± .10	1.37 ± .04	1.40 ± .12
145°C					

Cell capacities are 3 cell averages.

- (i) The lowest capacity was generally obtained on the first cycle under all conditions. This is normal for Ag-Cd cells.
- (ii) For unsterilized cells, 40% KOH gives better performance than 35% KOH for all cycles.
- (iii) When cells were sterilized at 125°C and 145°C, 45% KOH gave the best capacity on the first cycle with 40% usually second best. On cycles two and three, however, 40% KOH gave the best performance. Where tested, 35% KOH yielded the lowest capacity of the various concentrations employed on cycles two and three.

#### 4. Separators

At the outset of the present contract, JPL specified that two heat sterilizable separator materials developed by RAI Research Incorporated under JPL Contract No. 951015 were to be used in the cell studies. These separators were designated RAI-110 and RAI-116. Recently, another heat sterilizable membrane, SWRI-GX, obtained from Southwest Research Institute has been included in the cell studies. The following section deals first with the evaluation of the two RAI materials and later with the SWRI separator.

All of these separators are reputed to be cross-linked polyethylene film to which an acrylic acid has been radiationgrafted. There are differences in the method of manufacture, but properties are similar. JPL has supplied all of the separators needed in this program.

Among the first rolls of RAI-116 received, one was found to contain brown areas which had much higher electrical resistance than the clear areas. The results are shown in Table XIV. Such areas did not occur in other rolls, and subsequent work was carried out only with clear material.

TABLE XIV  
Specific Resistance of Clear and Brown Areas  
in RAI-116  
(Soaked 24 hours in 40% KOH)

Sample No.	Brown Areas		Clear Areas	
	$a_r$ ohm-cm <sup>2</sup>	$\rho$ ohm-cm	$a_r$ ohm-cm <sup>2</sup>	$\rho$ ohm-cm
Roll 9 -1	.501	200	.201	72
-2	.550	220	.171	68
-3	.463	160	.215	86
average	.505 $\pm$ .045	190 $\pm$ 30	.196 $\pm$ .025	75 $\pm$ 11

Procedures for characterizing separators have been described in Cooper and Fleischer "Characteristics of Separators for Alkaline AgO/Zn Secondary Batteries. The properties measured in the current work were dimensional stability, electrolyte retention, ion exchange capacity, and electrical resistance. These properties were evaluated before and after sterilization (40% KOH - 7.5% ZnO at 145°C for 108 hours) and in some cases before and after cycling. It was found desirable to soak separator samples for at least 24 hours in 40% KOH in order to assure reproducible values and the ability to survive sterilization; incompletely soaked RAI separators were damaged at sterilization temperatures. The sterilization process generally had a marked effect on most of the properties examined.

Dimensional changes due to sterilization are shown in Table XV. It is seen that the separators swell in thickness but shrink in one linear dimension.

The total amount of electrolyte absorbed was increased by sterilization, but the percent of absorbed electrolyte which was retained was decreased by sterilization as shown in Table XVI. The measurements were made by weighing the separator dry, completely soaked with electrolyte, and after draining for 10 minutes on a non-absorbing surface at a 45° angle.

TABLE XVI  
Electrolyte Retention Before and After Sterilization

Sample Number	When Sampled*	Wt. of Separator, g.	Wt. of Electrolyte Undrained	Wt. of Electrolyte Drained	% Electrolyte Retained
RAI-116-5	Before	0.0602	0.2278	0.1025	45
	After	0.0658	0.6582	0.1642	25
RAI-116-2	Before	0.0653	0.2998	0.0809	27
	After	0.0665	0.8582	0.1934	23
RAI-110-1	Before	0.0681	0.2342	0.1452	62
	After	0.0690	0.9289	0.2124	23
RAI-110-3	Before	0.0698	0.2700	0.1377	51
	After	0.0736	1.1318	0.3099	27

\* Sampled Before or After Sterilization

Ion exchange capacity increases during sterilization and during electrical cycling as shown in Table XVII.

Electrical resistance measurements on RAI-116 and 110 before and after sterilization are given in Tables XVIII and XIX. Measurements on SWRI, which was available later, are given in Table XX.

TABLE XV

Dimensional Changes in RAI Separators Due to Sterilization \*

	Dry - before sterilization			Wet - after sterilization			% Change relative to original dry separator		
	Length cm	Width cm	Thick- ness - cm	Length cm	Width cm	Thick- ness - cm	Length	Width	Thickness
RAI-116 Roll 2	7.62	2.54	.0020	6.85	2.80	.0051	-10	+10	+155
	7.62	2.54	.0020	6.80	2.75	.0051	-11	+ 8.3	+155
RAI-116 Roll 5	7.62	2.54	.0020	7.15	2.75	.0053	- 6.2	+ 8.3	+165
	7.62	2.54	.0020	7.10	2.75	.0053	- 6.8	+ 8.3	+165
	7.62	2.54	.0020	7.10	2.80	.0053	- 6.8	+10	+165
RAI-110 Roll 1	7.58	2.54	.0023	7.75	2.45	.0053	+ 2.2	- 3.5	+130
	7.58	2.54	.0023	7.75	2.40	.0053	+ 2.2	- 5.5	+130
	7.58	2.54	.0023	7.75	2.40	.0053	+ 2.2	- 5.5	+130
RAI-110 Roll 3	7.62	2.54	.0025	7.95	2.60	.0048	+ 4.3	+ 2.4	+ 92
	7.62	2.54	.0026	8.05	2.60	.0048	+ 5.6	+ 2.4	+ 85
	7.62	2.54	.0025	8.00	2.50	.0048	+ 5.0	- 1.6	+ 92

\* 40% KOH - 6.5% ZnO, 145°C, 112 hours.

TABLE XVII  
Ion Exchange Capacity of RAI Separators

<u>Before Sterilization</u>	<u>Capacity calculated to "as received" form</u>	<u>Capacity calculated to "H<sup>+</sup> form"</u>
RAI-116 Roll 2	2.8 meq. /g 0.0074 meq. /cm <sup>2</sup>	3.4 meq. /g
RAI-116 Roll 5	3.5 meq. /g 0.0112 meq. /cm <sup>2</sup>	4.6 meq. /g
RAI-110 Roll 1	2.9 meq. /g 0.0091 meq. /cm <sup>2</sup>	3.5 meq. /g
RAI-110 Roll 3	2.9 meq. /g 0.0098 meq. /cm <sup>2</sup>	3.5 meq. /g
<u>After Sterilization</u>		
RAI-116 Roll 2		4.9 meq. /g 0.0169 meq. /cm <sup>2</sup>
RAI-116 Roll 5		5.0 meq. /g 0.0168 meq. /cm <sup>2</sup>
RAI-110 Roll 1		5.0 meq. /g 0.0173 meq. /cm <sup>2</sup>
RAI-110 Roll 3		6.4 meq. /g 0.0194 meq. /cm <sup>2</sup>
<u>Unsterilized After 4 Electrical Cycles</u>		
RAI-116 Roll 1		
Cell No. 1		5.2 meq. /g
Cell No. 2		6.3 meq. /g
Cell No. 3		4.5 meq. /g
Cell No. 4		6.0 meq. /g

TABLE XVIII  
Electrical Resistance of RAI-116 Before and  
After Sterilization

	Sample	<u>Unsterilized</u>		Sample	<u>Sterilized</u>	
		$a_r$ ohm-cm <sup>2</sup>	$\rho$ ohm-cm		$a_r$ ohm-cm <sup>2</sup>	$\rho$ ohm-cm
Roll 1	1	.151	40			
	2	.167	56			
	3	.128	34			
Roll 2	1	.380	150	4	.0663	14
	2	.372	170	5	.0670	14
	3	.389	180	6	.0613	13
Roll 3	1	.176	49			
	2	.145	38			
	3	.141	37			
Roll 4	1	.183	56	4	.119	23
	2	.188	62	5	.169	35
	3	.222	74	6	.108	21
Roll 5	1	.268	96			
	2	.354	130			
	3	.231	82			
Roll 16	1	0.66		13	.11	
	2	0.93		14	.08	
	3	1.14		15	.31	
	4	0.12		16	.12	
	5	0.72		17	.18	
	6	1.83		18	21.60	
	7	1.55		19	0.64	
	8	1.29		20	.31	
	9	1.54		21	.15	
	10	2.03				
	11	2.64				
	12	0.10				
Roll 20	1	1.83				
	2	0.44				
	3	0.28				
	4	0.39				
	5	0.49				
	6	0.90				
	7	2.93				
	8	0.17				



TABLE XIX  
Electrical Resistance of RAI-110 Before and After  
Sterilization

<u>Sample</u>	<u>Unsterilized</u>		<u>Sample</u>	<u>Sterilized</u>	
	$a_r$ <u>ohm-cm<sup>2</sup></u>	$\rho$ <u>ohm-cm</u>		$a_r$ <u>ohm-cm<sup>2</sup></u>	$\rho$ <u>ohm-cm</u>
Roll 1	1	.128	4	.0813	16
	2	.121	5	.0848	17
	3	.127	6	.0791	16
Roll 2	1	.264			
	2	.236			
	3	.279			
Roll 3	1	.304	4	.0841	16
	2	.194	5	.0877	16
	3	.219	6	.0884	17
Roll 4	1	.670			
	2	.187			
	3	.212			

These data show pronounced variation within samples from the same roll and among rolls of the same separator for RAI-116 and RAI-110. Separator SWRI-GX is much more uniform and is to be preferred. In general, sterilized samples are considerably lower in resistance than unsterilized samples.

Increase in electrical resistance is linear with increasing layers of RAI-116 as shown in Fig. 9. Again, sterilized separator shows lower resistance than unsterilized separator.

Limited cell cycling tests indicated RAI-116 to give somewhat higher capacities than RAI-110 for unsterilized 3-plate cells through four cycles. Formation was at 35 ma for 91 hours. Subsequent charges were 60 ma for 40 hours, while discharges were 600 ma to a cut-off at 1.20 volts. The data are given in Table XXI.

TABLE XX  
Electrical Resistance of SWRI-GX Before and After  
Sterilization

Sterilized 135°C, 120 hrs.

<u>Roll</u>	$a_r$ <u>ohm-cm<sup>2</sup></u>	$a_r$ <u>ohm-cm<sup>2</sup></u>
21	0.22	0.10
	0.15	0.13
	0.13	0.14
	0.12	0.10
22	0.17	0.19
	0.23	0.10
	0.27	0.12
	0.12	0.13
23	0.26	0.18
	0.73	0.18
	0.16	0.13
	0.13	0.13
24	0.36	0.30
	0.15	0.19
	0.17	0.14
	0.13	0.11
25	0.38	0.35
	0.23	0.20
	0.17	0.16
	0.13	0.10
28	0.13	
	0.15	
	0.31	
	0.30	
	0.31	
31	0.42	
	0.48	
	0.28	
	0.12	
	0.10	
34	0.12	
	0.11	
	0.16	
	0.11	
	0.11	

ELECTRICAL RESISTANCE OF RAI-116 AS A  
FUNCTION OF NUMBER OF LAYERS

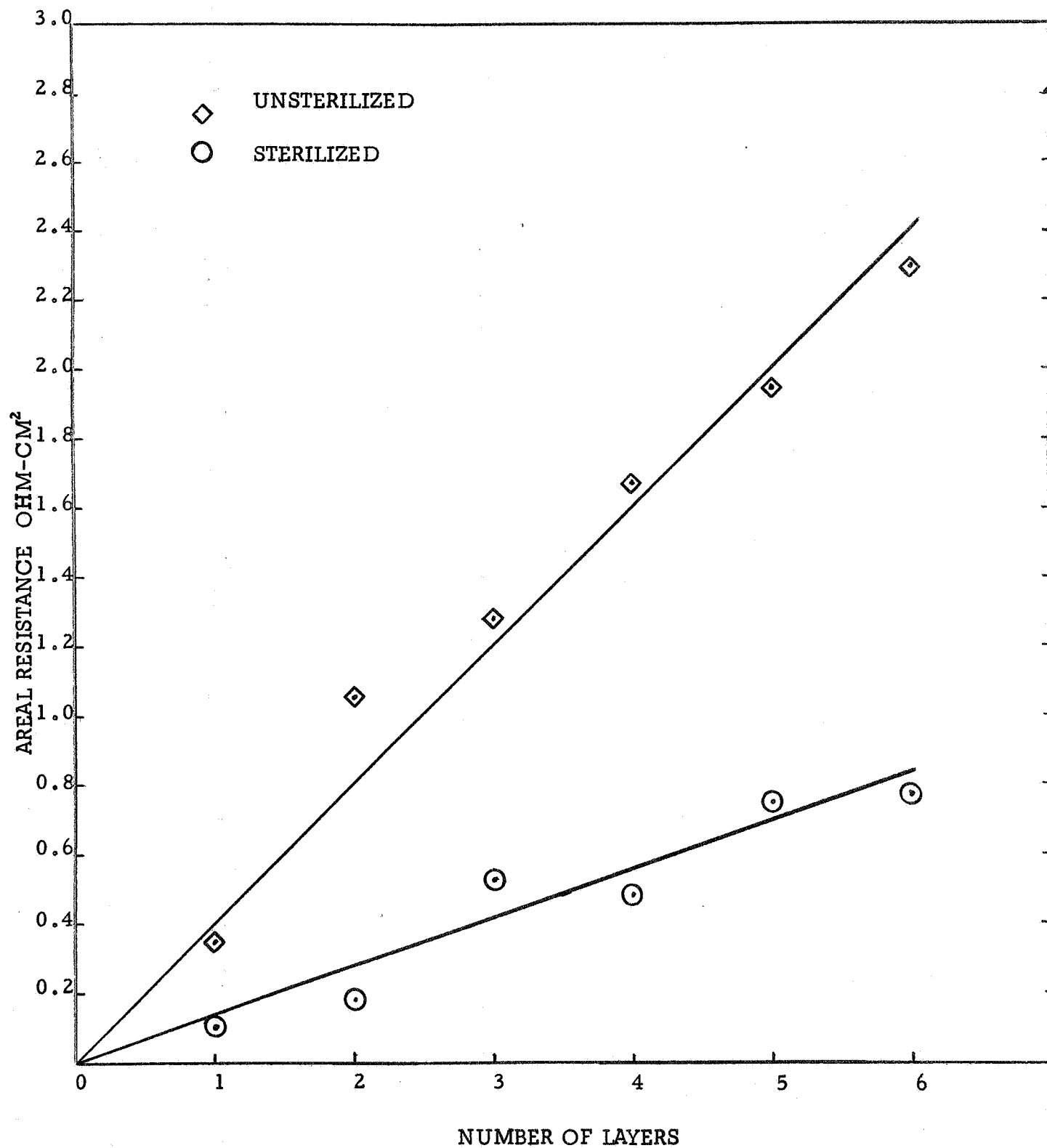


TABLE XXI  
Capacity of Cells with RAI-116 and RAI-110  
During Four Cycles

<u>Cell No.</u>	<u>1</u>	<u>2</u>	<u>3</u>	<u>4</u>
RAI-116-1	.32	.30	.30	.29
RAI-116-2	.32	.31	.30	.29
RAI-116-3	.32	.30	.30	.27
RAI-110-4	.26	.27	.28	.26
RAI-110-5	.29	.29	.29	.26

The separator from one cell containing RAI-116 was unwrapped after four cycles and analyzed for silver in the individual layers. The results are shown in Table XXII.

TABLE XXII  
Silver Content of RAI-116 Layers After Four  
Cycles

<u>Layer of Separator *</u>	<u>Wt. of Ag in mg</u>
1	0.85
1'	0.88
2	0.80
2'	0.78
3	0.26
3'	0.27
4	0.44
4'	0.36

\* The layers closest to the faces of the Ag electrodes are called 1 and 1'.

Unfortunately, the analytical method used would not have distinguished between silver and mercury, which perhaps accounts for the higher values in layers 4 and 4' which were closest to the Zn electrode containing mercury.

In a test using sealed cells (see section B. CELL STUDY, 2. Performance of Sealed Cells, A. Cell Packs Sterilized then Sealed, page 73) ten cells were constructed using separator RAI-116 and a like number with RAI-110. After sterilization in cell packs at 125°C for half of each group and at 135°C for the others they were sealed in plastic cases and life cycled. Cells made with RAI-116 averaged six cycles when sterilized at 135°C and seven cycles at 125°C. In the case of cells made with RAI-110 four cells, two from each sterilization condition, are still cycling after 68 cycles. Of the three cells in each group which failed, those sterilized at 135°C averaged 40 cycles compared to 47 cycles for those at 125°C (see Table XXXVII).

A pressure gage had been added to one cell in each group of five at the time of sealing in the above mentioned experiment. From the results shown in the table on page 74, it was suspected that sealed cells made with RAI-110 might develop lower pressures than those made with RAI-116.

Failure of separator RAI-116 on life cycling has generally been found upon examination to be due to silver penetration or to zinc dendrite growth over the tops of separators which were 1/4" above the plates. However, these results may not be typical for the 116 composition since it has been found that the properties of this separator vary greatly from roll to roll as well as within a roll. How representative our sampling was for the above experiment is not known.

#### a. Separator Screening Tests

In addition to the general tests for separator materials screening tests were conducted on all lots of separator materials used in section V. FABRICATION AND TESTING OF CELLS (page 122). Test methods are detailed in ESB Material Specification 263. Table XXIII is a summary of test data obtained on four lots of RAI-116. Table XXIV is a summary of test data on four lots of SWRI-GX. In the SWRI-GX material, which is similar in composition to RAI-116, lot to lot uniformity was excellent.

#### b. Testing of SWRI-GX in AgO-Cd Cells during Cycling, on Float, and on Charged Stand

##### (1) Test Program

The program embodied in this task resulted from the request by JPL for an electrochemical screening test for SWRI-GX utilizing the silver-cadmium oxide couple in a sealed cell. The separator was to be evaluated before and after sterilization. Three modes of cell operation were required,

TABLE XXIII

## SUMMARY OF RAI 116 MEMBRANE EVALUATION DATA\*

ESB Lot No.	Sample No.	Thickness Mils**		Weight mgm/in <sup>2</sup>		Wet Dimension Changes, %			Electrolyte Absorption gm/gm	Porosity (%)	Pore Diameter $\mu$
		Dry	Wet	Dry	Wet	L (Roll)	W	T			
1116-8 in (31% KOH)	1	1.45	1.98	25	51	13	.6	37	1.3	69	"X" S
	2	1.45	1.98	25	45	14	1.4	37	1.1	56	
	3	1.45	1.98	23	43	11	2.4	37	1.1	54	
	4	1.45	1.98	24	44	12	2.0	37	1.1	55	
	5	1.45	1.98	25	54	9	2.4	37	1.4	74	
1116-8 in (40% KOH)	1	1.45	2.05	24	59	8	-.4	41	1.7	79	5.9
	2	1.45	2.05	22	57	14	-4.0	41	1.9	79	
	3	1.45	2.05	23	53	14	-2.0	41	1.6	68	
	4	1.45	2.05	27	63	14	4.0	41	1.8	86	
	5	1.45	2.05	24	66	7	1.0	41	1.9	92	
1116-10 (40%)	1	1.50	1.81	23	49	3	0	20	1.2	65	2.7
	2	1.38	1.65	21	42	2	-1.0	20	1.0	56	
	3	1.50	1.88	22	53	3	2.0	25	1.5	74	
	4	1.38	1.81	21	48	3	0	31	1.4	67	
1116-11 (40%)	1	1.63	2.20	25	93***	3	2.0	35	2.8	135***	2.9
	2	1.38	1.63	21	81***	4	2.0	18	3.0	162***	
	3	1.75	2.40	25	55	4	1.0	37	1.3	56	
	4	1.28	1.57	21	51	3	0	28	1.5	85	
1116-12	1	1.38	1.93	20	50	2	1	40	1.5	67	3.2
	2	1.50	1.92	20	40	2	1	28	1.1	47	
	3	1.38	1.89	19	47	2	1	37	1.6	66	
	4	1.50	2.05	19	48	2	1	37	1.6	63	
RAI Specification***		1.2-1.6	1.6-1.7			7 $\pm$ 2	7 $\pm$ 2	9-40			

(\*) Tests per ESB MS-263.

(\*\*) Method of measuring thickness improved after lot 116-8.

(\*\*\*) Sample did not shed electrolyte reproducibly in vertical hang method in allotted time of 5 mins.

(\*\*\*\*) Electrical resistance, 40% KOH, 30  $\pm$  5 milliohm-in<sup>2</sup>

Tensile strength, roll direction, 800-1000 psi.

TABLE XLV

ACCEPTANCE TEST RESULTS SWRI-GX  
SEPARATOR MATERIAL\*

Lot No.	Spec. No.	Dry Thickness/ mils	Wet Thickness/ mils	Length Change + % (Roll)	Width Change + %	Thickness Change %	Weight		Porosity %	Pore Size A	Unit Electrolyte Absorption (gms/gms)
							Dry mgm/ in <sup>2</sup>	Wet mgm/ in <sup>2</sup>			
GX 85	1	1.3	2.5	5.0	7.0	100	21	48	50.	2.0	1.5
	2	1.3	2.5	5.0	6.0	100	21	47	50.	1.8	1.5
	3	1.4	2.5	5.0	7.0	79	21	47	49	1.8	1.5
	4	1.8	2.5	5.0	7.0	43	21	48	51	1.8	1.6
	$\bar{X}$	1.4	2.5	5.0	6.8	81	21	48	50	1.8	1.5
GX 86	1	1.4	1.5	6.0	7.0	7	22	46	77	2.0	1.4
	2	1.4	2.0	4.0	6.0	43	22	45	54	1.7	1.2
	3	1.8	2.3	5.0	7.0	29	23	47	50	1.9	1.3
	4	1.3	2.0	4.0	6.0	60	22	47	59	2.0	1.4
	$\bar{X}$	1.5	1.9	4.8	6.5	35	22	46	60	1.9	1.3
GX 87	1	1.5	1.8	8.0	6.0	20	26	52	71	1.7	1.3
	2	1.5	2.0	7.0	6.0	33	24	49	60	1.5	1.3
	3	1.5	2.0	6.0	6.0	33	23	47	58	1.7	1.3
	4	1.5	2.3	5.0	5.0	53	24	48	50	1.5	1.2
	$\bar{X}$	1.5	2.0	6.5	5.8	35	24	49	60	1.6	1.3
GX 88	1	2.0	2.3	7.0	8.0	13	26	53	61	2.0	1.4
	2	2.0	2.3	6.0	7.0	13	25	53	59	2.0	1.4
	3	2.0	2.3	6.0	6.0	13	24	52	58	1.7	1.4
	4	2.0	2.5	4.0	6.0	25	23	52	60	1.2	1.5
	$\bar{X}$	2.0	2.3	4.8	7.0	16	24	53	60	1.7	1.4
All	$\bar{\mu}$	1.6	2.2	5.5	6.4	42	23	49	57	1.8	1.4
	$\sigma$	.12	.30	1.2	0.7	30	1.7	2.7	7.9	0.2	0.12
± 3	Max.	2.0	3.1	9.1	8.5	132	28	57	80	2.5	1.8
	Min.	1.2	1.3	1.9	4.3	0	18	41	34	1.2	1.0

(\*) Tests per ESB MS-263 using 40% KOH.

continuous cycling, float, and charged stand. The time requirements imposed made it imperative that provision be made to accelerate the charged stand. The stand test is designed to accomplish this by comparing capacity losses at room temperature and at 45°C. It is planned to extrapolate the data obtained at 45°C to predict loss figures on room temperature stand. In addition, the batteries from stand are to be cycled so that any deleterious effects of charged stand on cell life can be examined. The test program which evolved is given in Figure 10.

## (2) Cell Construction

The test vehicle consists of two cadmium electrodes, a central silver electrode, and two recombining electrodes attached to the cadmium electrodes. A non-woven polypropylene absorber (EM 476, Kendall Mills) is used in addition to the primary separator material. The three plate assembly is shimmed into a polystyrene container which is then completely encased in an epoxy outer shell. One hundred cells assembled into five cell batteries comprise the test group with one half of the batteries containing cell assemblies which had been exposed to sterilization conditions. The sterilization procedure was carried out in nickel containers which held eight assembled cell stacks. Three nickel containers could be placed one above the other in a stainless steel bomb. The sterilization cycle of 135°C for 120 hours was run in an air circulating oven.

All cells prior to sealing were formed, discharged and cycled twice more. The formation and conditioning cycles were run with the electrolyte level at the plate tops. The level was adjusted to 1/2 of this prior to sealing. The formation charge was sufficient to exceed the theoretical capacity of the positive but provide only 78% of the negative capacity thus providing excess negative capacity to prevent hydrogen formation on overcharge. Silver recombining electrodes were included to protect against pressure build up due to oxygen produced on overcharge. The constructional details are stated in Table XXV.

## (3) Separator Testing

The shipment of separator material (RAI-110, Rolls 14, 15, 16) designated for this test was found to vary widely in electrical resistance across the film width. This variation was far beyond specification limits and the material was rejected. A new lot of RAI-116 material was submitted in March together with several rolls of SWRI-GX. Both materials were spot checked for resistivity and were subsequently put through the sterilization cycle and the resistivity re-determined. The SWRI material was initially more uniform in resistivity and maintained this uniformity better after sterilization. The resistance figures measured on the lots of separator material received are given in Tables XVIII and XX. Samples for



FIGURE 10

SEPARATOR TEST PROGRAM SCHEDULE

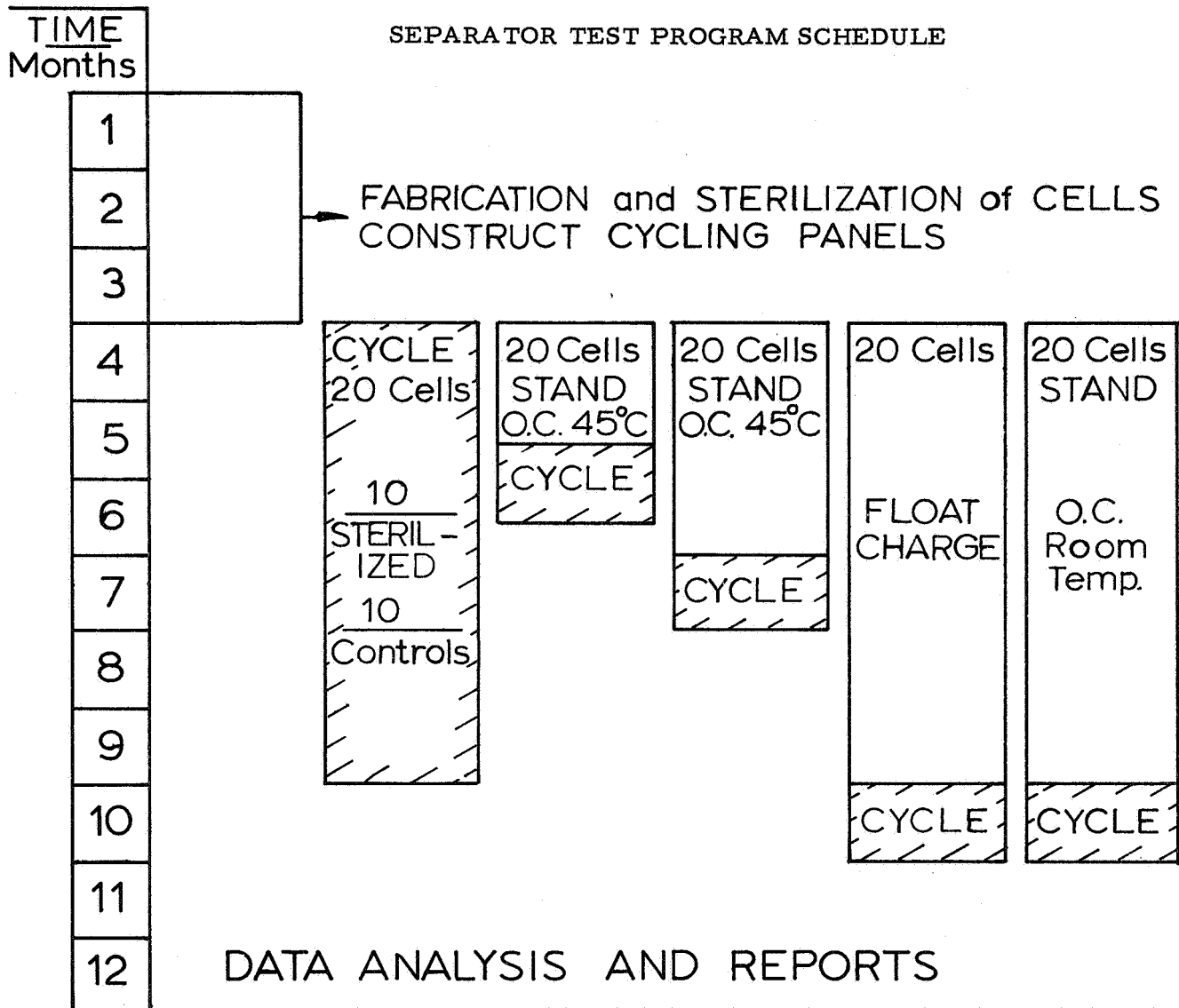


TABLE XXV  
Constructional Details  
Three Plate Silver Cadmium Cells

1. Positive Plate

Grid	2/0 Ag
Active Material wt.	6.25 g
Dimensions, inches	1.75 x 1.875 x .028
No. per cell	1
Retainer	1 EM 476
Membrane	6 SWRI-GX

2. Negative Plate

Grid	2/0 Ag
Active Material wt.	6.3 g CdO (plus 0.70 g Ni powder)
Dimensions, inches	1.75 x 1.875 x 0.050
No. per cell	2
Absorber	1 EM 476

3. Membrane Separator Expansion Factor in 40% KOH

- Sterilized 1.5 - 1.8
- Non-sterilized 1.1 - 1.5

For calculating pack tightness an S.E.F. of 2.5 was used for all cells.

4. Electrolyte - 40% KOH.

5. Recombining Electrodes - Silver Electrodes, 1.75 x 1.875 x .010 inches, placed outside of and connected to negative electrodes.

6. Shim Material - Polysulfone sheet .011 and .091 inch

7. Outside Spacer 20 mesh polypropylene screen  
 Thickness .046 inch  
 Placement Between recombining electrode and shim stock.

measurement were taken across the roll direction at several places along the roll. Each set of values represents edge to edge samples (actually one inch in from edge) at one location along the length.

The decision was then made to build the test cells using the SWRI - GX material and sufficient of this separator was obtained from JPL.

#### (4) Cell Stack Sterilization

The first lot of cell stacks processed through the sterilization cycle were only partially immersed in electrolyte due to leakage of the stainless steel bomb. The leakage was sufficient to expose approximately one-third of the electrode area and to concentrate the electrolyte from 40% to 48% KOH. Randomly sampled cell stacks performed acceptably through formation and two additional cycles; but when all of the cells were similarly assembled and cycled, poor charge acceptance and discharge capacities were found in eighteen of the forty-eight cells. The decision was made to discard the entire lot of forty-eight cells and repeat the experiment maintaining the electrolyte level above the tops of the plates. Greater uniformity in initial performance was found in cells constructed from this lot of sterilized cell stacks, with an average capacity of  $2.02 \pm 0.22$  amp-hr compared to  $1.57 \pm 0.10$  for their unsterilized counterparts. Examination of separator wraps removed from the first lot of sterilized cells showed that partial drying out of the separator had occurred in the poorer cells resulting in adjacent layers sticking tenaciously together. Performance similar to that observed with these cells was obtained with open cells similarly constructed but filled with 50% KOH.

#### (5) Electrochemical Tests

Twenty 5-cell batteries each consisting of either sterilized or non-sterilized cells, were assembled from the three plate cells and two batteries of both sterilized and non-sterilized were assigned to each of the test regimes. A brief resume of the regimes and the status of the cells in each is given below.

(a) Cycling: discharge at a current of 0.50 amp for three hours, recharge c.p. at 1.60 volts with initial current limited to 0.35 amp.

Cells have completed 50 cycles with the sterilized cells exhibiting higher discharge voltages, better charge acceptance and better discharge capacity compared to unsterilized cells.

#### (b) Room Temperature Charged Stand

At the two month mark of a projected six month stand period a marked differentiation has appeared between the sterilized and non-sterilized

batteries. All non-sterilized cells have open circuit voltages characteristic of the divalent silver plateau while 9 of 10 sterilized cells have OCV's attributed to the monovalent silver plateau.

#### (c) Charged Stand at 45°C

Four 5-cell batteries of each type, sterilized and unsterilized, were placed on charged stand to be tested for residual capacity at six and twelve weeks. The six-week cells have been removed from stand and discharged. Five of ten sterilized cells had neither voltage nor capacity. Capacities on the remaining five cells ranged from 0.75 to 1.53 amp-hr which represents retention of from 35 to 72 percent of pre-stand capacity. Only two of the ten sterilized cells scheduled to stand for twelve weeks have an OCV as high as 1.10. It is planned to forego the additional six week stand period, and discharge these cells without completing the scheduled period.

In the non-sterilized group all OCV's (20 cells) are below 1.40v and one cell is below 1.10v. The ten cells scheduled for the six week stand period have been discharged. Capacities are from 0.45 to 1.15 amp-hr which represents capacity retentions of from 33 to 73 percent. The remaining ten cells will also be removed from test and discharged to conform to the test schedules applied to the sterilized batteries. Decay of open circuit voltage below about 1.10v is indicative of internal shorting. These batteries, both sterilized and unsterilized, after discharge will be recharged and the charging curves of each cell monitored. Where normal recharge is found, it is planned to cycle manually to establish a discharge capacity value and then to place the cells on automatic cycle. Shorted cells will be disassembled and examined to determine the cause of failure.

#### (d) Float at 1.60v per Cell

Test cells have been on float for two months. Float current for both sterilized and non-sterilized cells is ten to twenty milliamperes. One cell in each battery is rigged with a pressure gauge and the readings are 95 and 39 psig non-sterilized and 11 and 34 psig for the sterilized cells.

The present schedule calls for completion of this program by May of 1968.

### 5. Absorbers

The successful operation of sealed silver-zinc or silver-cadmium cells depends heavily on the absorber placed around the silver electrode and the retainer enclosing the zinc or cadmium oxide electrodes because of the necessity to use limited electrolyte for good recombination. Thus, the ability of the absorber to wick the electrolyte several inches and its ability to retain the electrolyte are important properties along with electrical

resistivity and resistance to structural and dimensional change during sterilization. Accordingly, this section is divided into two parts. The first deals with the properties of existing materials whereas the second considers materials developed for the present purpose.

#### a. Commercial Materials

A polypropylene base material, designated EM 476 by Kendall Mills, meets all of these requirements to some degree. However, when EM 476 is sterilized by itself it becomes quite stiff, and it was thought that this material could be either improved or replaced with some other product. Consequently, tests have been run on EM 476 modified by oxidation with chromic acid and solvent leaching with methylene chloride. Tests have been run with and without surfactants in an attempt to improve its properties. Properties of other polypropylene base materials and other possible materials have been determined and reported.

##### (1) Structural Stability

The effect on samples of absorbers sterilized in 40% KOH at 145°C for 112 hours are given in Table XXVI.

##### (2) Electrical Resistivity

No systematic study of electrical resistance of absorbers was carried out because absorbers are generally quite porous and have good conductivity. However, a few isolated experiments were run and are described below.

Resistance measurements were made on Kendall EM 476 as received and after treatment with polysulfone dissolved in  $\text{CHCl}_3$ . A non-woven glass fiber mat was also treated with polysulfone in an attempt to make it resistant to KOH. Specific resistances of these materials are shown in Table XXVII. The polysulfone treatment of EM 476 increased the resistance from about 45 to 280 ohm-cm before sterilization and from 42 to 77.1 ohm-cm after sterilization. The treatment offered no advantages. Upon sterilization, the glass fiber fell apart and hence was not acceptable.

Asbestos, while it disintegrated during sterilization, appeared that it might stay in place in a tightly packed cell. Should this be the case, asbestos, which has excellent wicking and electrolyte retention properties, might make a good absorber. Some energy utilization data for unsterilized and sterilized cells using various thicknesses of asbestos are shown in Table XXVIII. Asbestos thus may still be considered as a useful absorber, except that it is somewhat more difficult to handle than EM 476.

TABLE XXVI  
Absorber Composition and Stability

<u>Test</u>	<u>Absorber</u>		<u>Composition</u>	<u>Sterilizable</u>
1	Kendall	EM 476	Polypropylene	yes
2	"	SM 133.3	" and nylon	yes
3	"	SM 134.5	" " "	yes
4	"	SM 135.1	" " "	yes
5	Pellon	20240 B	"	yes
6	"	20240 BK	100% Polypropylene	yes
7	"	FT 2140		yes
8	"	2517		
9	"	20272	100% Polyamide	no
10	"	2504	"	no
11	Kendall	H653	Polypropylene and nylon	no
12	"	H654	" " "	no
13	"	H655	" " "	no
14	"	Asbestos	Inorganic	no

Observations:

No pressure build-up during sterilization of any of the above absorbers.

EM 476 became stiff and apparently less absorbent.

SM series remained pliable and absorbent. (However, see "Wicking Ability" later.)

Products 9 through 13 were degraded and became friable.

Asbestos disintegrated.

TABLE XXVII  
Specific Resistance of EM 476 and Glass Fiber Absorbers

Sample	EM 476				EM 476 treated with Polysulfone				Fiber Glass Treated with Polysulfone	
	Unsterilized		Sterilized		Unsterilized		Sterilized		Ar	$\rho$
	Ar	$\rho$	Ar	$\rho$	Ar	$\rho$	Ar	$\rho$		
A	0.379	47	0.311	32	1.93	270	0.876	84.2	0.0506	2.93
B	0.421	47	0.352	44	1.94	270	0.657	63.1	-	-
C	0.366	41	0.381	50	2.22	300	0.899	84.0	-	-
Ave.	0.389	45	0.348	52	2.03	280	0.811	77.1	-	-
Max. Dev.	+0.032	+4	+0.037	+10	+0.19	+18	+0.154	+14		

All measurements made in 40% KOH - 7.5% ZnO.

Sterilization was at 145°C for 112 hrs. in 40% KOH - 7.5% ZnO.

Ar is in ohm-cm<sup>2</sup> and  $\rho$  is given in ohm-cm.

TABLE XXVIII  
Energy Utilization of  
Cells with Asbestos Absorber  
(watt-hr/gm Silver)

<u>Cell #</u>	<u>Absorber Thickness mils</u>	<u>Sterilized</u>	<u>#1</u>	<u>Cycle</u>		<u>#4</u>
				<u>#2</u>	<u>#3</u>	
7	7.0	no	.427	.518	.488	.476
8	7.0	no	.438	.518	.503	.486
9	7.0	no	.397	.503	.490	.485
10	2.9	no	.460	.512	.521	.501
13	3.5	yes	.443	.391	(.219) *	
14	3.5	yes	.455	.400	-	
15	3.5	yes	.316	.307	(.231) *	
16	3.5	no	.396	.374	(.126) *	
17	3.5	no	.364	.396	(.242) *	
18	3.5	no	.442	.388	(.361) *	

\* Cells #13 through #18 inclusive on Cycle #3 were discharged at 900 ma.

All other discharges were at 300 ma.

NOTE: (1) Four layers of RAI-116 separator material were used for all cells.

(2) Ag electrodes averaged 6.4 grams in weight.



### (3) Wicking Ability

The usefulness of absorbers in sealed cells depends on their ability to soak up electrolyte and hold it adjacent to the positive electrode. In an attempt to measure this property a wicking test was used. This consisted of cutting strips of unsterilized materials six inches long by one inch wide and noting the height to which 40% KOH would rise from reservoirs placed at the lower ends of the strips. In the case of sterilized materials the level to which drying out from the top of the absorber descended was noted. Table XXIX gives some wicking results. It is interesting to note that EM 476, which after sterilization became stiff, still had the ability to wick about as well as the unsterilized material. Also, SM 134.5 which was soft and pliable after sterilization did not wick as well as EM 476. When the EM 476 absorber was treated with methylene chloride, some material, presumably a carding agent, was removed from its surface. Its wicking ability then dropped to zero. However, if a surfactant such as Triton X-100 was added to the electrolyte, wicking ability was partially restored.

The drying-out test used for soaked or sterilized materials left something to be desired. The end point was not sharp and the test was time consuming. For this reason, a second test was used based on the capacity of a cell constructed with the test material and with the electrolyte level only one third up the plate height for plates of 1 3/4 inches. Even though the cells were not sealed, the better the wicking and retention properties the better should be the cell's capacity. Thus, cell capacity on charge and discharge became a measure of the wicking ability of the material. The ratio of capacity of the test cell to that of an unsterilized cell containing EM 476 run in the flooded condition where wicking and retention was not a problem became a wicking efficiency measurement.

Data on wicking efficiency as determined by this capacity test is reported in Table XXX. The test cells were sterilized at 135°C for the usual 112 hours. The electrolyte was 40% KOH - 7.5% ZnO. Cells were charged at 40 ma and discharged at 600 ma. It is notable that EM 476 was the best material tested either sterilized or unsterilized and that the sterilized absorber, with a wicking efficiency of 83% of a flooded cell, was actually superior to the unsterilized absorber which had a wicking efficiency of 78%. The second best absorber tested was 20240 B, a polypropylene base material produced by Pellon.

A weakness in the above test was that the cells were sterilized in a flooded condition in nickel containers whereas they were charged and discharged in polystyrene containers with limited electrolyte. Substances might be removed from the surface of absorbers by hot electrolyte during sterilization and not all of this material would be transferred to the working cell. The test conditions were modified to permit running the cells in the same nickel containers in which they were sterilized. This change in procedure was utilized to evaluate the grafted absorbers in Table XXXII.

TABLE XXIX  
Absorber Wicking Tests on EM 476 and SM 134.5

<u>Absorber</u>	<u>Condition</u>	<u>Sterilization Temperature</u>	<u>Test</u>	<u>Height (inch)</u>			
				<u>0</u>	<u>24 hrs.</u>	<u>72 hrs.</u>	<u>144 hrs.</u>
EM 476	Unsoaked	unsterilized	wicking	0	2	6	6
EM 476	Soaked	unsterilized	drying out	6	6	6	5
EM 476	Soaked	125°C	" "	6	6	6	5
EM 476	Soaked	135°C	" "	6	6	6	6
SM 134.5	Unsoaked	unsterilized	wicking	0	0	0	0
"	Soaked	"	drying out	6	6	4	3
"	Soaked	125°C	" "	6	6	4	4
"	Soaked	135°C	" "	6	6	5	4
EM 476	Carding agent removed	unsterilized	wicking	0	0	0	-
EM 476 (W.G.) <sup>1</sup>	Triton X-100 *	"	"	0	3	4	-
EM 476 (A.G.) <sup>2</sup>	"	"	"	0	2	3	-

1) W. G. = with the grain

2) A. G. = across the grain

\* After removing the original carding agent, Triton X-100 was added to the electrolyte.

TABLE XXX  
Capacity Test for Absorber Wicking Ability

Absorber	Condition (1)	Cycle 1		Cycle 2	
		Discharge amp-hr	Wicking Efficiency (2)	Discharge amp-hr	Wicking Efficiency (2)
EM 476	U	1.86	78	1.88	79
EM 476	S	1.98	83	2.00	83
20240 B (3)	S	1.78	74	1.75	75
20240 BK (3)	S	1.23	51	1.06	44
FT 2140 (3)	S	1.24	51	0.76	32
2517 (3)	S	1.08	46	0.90	38
EM 476 Cr (4)	S	1.60	67	1.32	55
SM 135.1	U	0.74	31	-	-
SM 135.1	S	1.69	70	1.66	69

(1) U = unsterilized. S = sterilized.

(2) Cell discharge amp-hrs.  $\div$  2.4 amp-hr (capacity for flooded cells made with EM 476, unsterilized).

(3) Polypropylene

(4) Chromic acid treated.

## b . Grafted Absorbers

As part of the search for a better absorber material, RAI Research Corporation was subcontracted by ESB to conduct a research and development investigation of grafted polypropylene. The grafted surfaces to be produced were acrylic and methacrylic polymers, three levels of graft being made with each polymer using Kendall EM 476 as the base felt. Two other samples used Pellon FT 2140 as the base polymer, one grafted with acrylic acid and one with methacrylic acid. The monomer selection was based on previous wetting action of acrylic acid grafted felts and improved oxidation resistance of methacrylic acid grafted membrane.

Sample quantities of materials were prepared, some of which showed improved wicking action and electrolyte retention as well as lower electrical resistivity. Measurements of significant properties were made, as reported in RAI Research Corporation Document RAI-373 (February 14, 1967), and the following conclusions reached:

1. Acrylic acid grafts on polypropylene felt result in better electrolyte retention, wicking and lower electrical resistance than control samples or felt samples grafted with methacrylic acid.
2. EM 476 felt grafted with acrylic acid gives better results at an equivalent graft level than Pellon FT-2140.
3. Optimization of the best sample prepared during this program appears to be possible by investigating the graft level of acrylic acid on EM 476.

Samples of the grafted polypropylene absorbers were also provided for ESB Research Center to evaluate. Wicking tests have been run, with the results shown in Table XXXI. Samples 9 and 10 were controls, untreated EM 476 and FT 2140 respectively. Earlier data with EM 476 had shown a wicking height of 5 inches rather than the value of 3 inches shown in the table. This might indicate a difference in starting materials or non-uniformity of the sample. These data suggest that samples 1 and 5 which are acrylic acid grafted EM 476 should give the best results in cells.

There can be little doubt, especially at high charge-discharge rates that absorber wicking ability is very important for good cell performance. By comparing the capacity of the cross-linked radiation treated absorber which had both high retention and wicking with one having about the same high retention but low wicking, it was possible to show that, without high wicking, 25% of the cell capacity was lost. These data shown in Table XXXII were obtained using the capacity test described earlier.

TABLE XXXI  
Wicking Action in 40% KOH of Grafted Absorbers

<u>Absorber</u>	<u>Solution</u>	<u>Treatment</u> <u>% Graft</u>	<u>Wicking Height (inches)</u> <u>After various hours</u>		
			<u>24</u>	<u>72</u>	<u>262</u>
1 - EM 476	25% Acrylic Acid	37.8	0.5	5	5
2 - "	" Methacrylic Acid	12.4	0	0	0
3 - "	" Acrylic Acid	84.6	0	0	0
4 - "	" Methacrylic Acid	29.2	0	0	0
5 - "	" Acrylic Acid	67.5	3	3	5
6 - "	" Methacrylic Acid	21.5	0	0	0
7 - FT 2140	" Acrylic Acid	78.2	3	3	3
8 - "	" Methacrylic Acid	17.7	0	0	0
9 - EM 476	-	-	3	3	3
10 - FT 2140	-	-	0	0	0

TABLE XXXII  
Electrolyte Retention and Wicking Ability vs. Capacity

<u>Sample</u>	<u>Retention * %</u>	<u>Wicking Height * inches</u>	<u>Capacity ** AH</u>
EM 476 37.8% grafted AA Acrylic	250	4	1.48
FT 2140 78.2% grafted AA	241	1/4	1.11

\* RAI data  
\*\* Average of four cells

## 6. Effects of PPO and Epoxy Resin on Ag-Zn Cells

There was some suspicion that the electrochemical system of the Ag-ZnO cells may be impaired by being sterilized in the presence of the PPO material and/or the epoxy sealant. To check this, three tests were run.

Test A - Two 3-plate Ag-Zn cells were sterilized in the presence of each of the following:

1. PPO 531-801 shims.
2. PPO 541-801 shims.
3. DEN438-EK85 with DMP 30 catalyst, coated on polysulfone shims.

Sterilization was at 135°C for 136 hrs. Electrolyte was 40% KOH.

The sterilized cell packs, electrolyte, and shims were placed in open cell cases and formed at 35 ma. Discharge in all instances was at 600 ma to a 1.00 volt cutoff. First recharge was at 100 ma and subsequent recharges were at 70 ma. Results are listed in Table XXXIII.

On first cycle the cells containing epoxy appeared to have been damaged considerably, whereas those containing PPO were only slightly damaged if at all. Subsequent cycles show a recovery, both in ampere-hour capacity and in midvoltage.

Test B - Six more 3-plate Ag-ZnO cells were constructed, and two of these were sterilized in the presence of each of the following:

1. Epoxy DEN438-EK85 with DMP 30 catalyst coated and cured onto a PPO 531-801 shim.
2. PPO 531-801 shim.
3. Control cells not in contact with either PPO material or epoxy.

These cells were sterilized at 135°C for 136 hrs. After sterilization the cell packs and shims were placed in open Plexiglas cases. The cycle data, reported in Table XXXIV, indicates no damage due to epoxy occurred in this test. Since this test was designed to expose approximately the same amount of epoxy sealant that a sealed cell would have, the conclusion is that there should be no trouble from this system in the final cells.

TABLE XXXIII  
Effect of PPO and Epoxy Resin on Cell Performance  
Test A

<u>Cycle</u>	<u>Cell #</u>	<u>Additive</u>	<u>Chg. to Gassing (amp-hr)</u>	<u>Dischg. (amp - hr)</u>	<u>Midvolt</u>
1	1	531-801	2.20	1.92	1.29
	2	"	2.29	2.16	1.32
	3	541-801	1.89	1.95	1.31
	4	"	2.17	1.95	1.33
	5	Epoxy	1.86	1.50	1.23
	6	"	-	0.90	-
2	1	531-801	1.94	1.83	1.32
	2	"	1.94	1.83	1.36
	3	541-801	1.80	1.80	1.33
	4	"	1.87	1.83	1.37
	5	Epoxy	1.48	1.77	1.25
	6	"	1.47	1.53	1.26
3	1	531-801	2.00	1.89	1.32
	2	"	1.87	1.80	1.36
	3	541-801	1.87	1.89	1.37
	4	"	2.06	1.95	1.37
	5	Epoxy	1.85	1.77	1.30
	6	"	1.85	1.47	1.30
4	1	531-801	1.90	1.92	1.33
	2	"	1.91	1.92	1.36
	3	541-801	1.90	1.93	1.36
	4	"	1.93	2.08	1.37
	5	Epoxy	1.95	1.91	1.30
	6	"	1.97	1.86	1.29

TABLE XXIV  
Effect of PPO + Epoxy on Cell Performance  
Test B

<u>Cycle</u>	<u>Cell #</u>	<u>Additive</u>	<u>Chg.</u>	<u>Dischg.</u>	<u>Midvolts</u>
1 (35 ma)	1	Epoxy	2.36	2.27	1.33
	2	"	2.18	2.12	1.33
	3	531-801	2.26	2.13	1.32
	4	"	2.29	2.21	1.34
	5	Control	2.31	2.07	1.31
	6	"	2.35	2.16	1.32
2 (70 ma)	1	Epoxy	2.27	2.04	1.36
	2	"	2.15	2.00	1.36
	3	531-801	2.11	1.96	1.32
	4	"	2.14	2.05	1.37
	5	Control	2.18	1.78	1.30
	6	"	2.27	2.20	1.35
3 (70 ma)	1	Epoxy	2.34	2.03	1.36
	2	"	2.27	1.90	1.34
	3	PPO-531	2.73	1.85	1.33
	4	"	2.73	1.99	1.37
	5	Control	2.27	1.87	1.33
	6	"	2.17	1.94	1.32
4 (70 ma)	1	Epoxy	2.24	2.10	1.38
	2	"	2.14	1.97	1.36
	3	PPO-531	2.24	1.98	1.36
	4	"	2.24	1.99	1.37
	5	Control	2.24	1.93	1.37
	6	"	2.10	1.94	1.37



Test C - Because Test A indicated possible trouble with epoxy and Test B indicated no trouble when epoxy was used in the normal ratio of sealant to case, this test was run to simulate the worst conditions to see how bad epoxy might be. Accordingly, epoxy was ground finely to expose as much area to attack as possible. The following cells were constructed in duplicate:

1. With epoxy DEN438-EK85 + 5 wt. % DMP 30 cured 16 hr. at 25°C, 2 hr. at 50°C, 2 hr. at 75°C and 16 hr. at 100°C (Experiment 76).
  - (a) Sterilized epoxy liquor in a sterilized cell.
  - (b) " " " " an unsterilized cell.
  - (c) Epoxy chips in a sterilized cell.
  - (d) " " " an unsterilized cell.
2. The same experimental scheme was followed using the same epoxy and catalyst with 10 wt. % DER741A and the same curing schedule (Experiment 78).
3. Control - 3 plate Ag-ZnO cell unsterilized. No contact with epoxy.

The sterilized epoxy liquor was prepared by placing 1.5 gms of ground up epoxy in 50 mls of 40% KOH in a Teflon container and sterilizing in a nickel bomb at 135°C for 120 hrs. Upon opening the bombs after sterilization a distinct MEK odor was noticed, but this disappeared after the electrolyte sat overnight in a closed polyethylene container.

The cells were constructed with wrapped negatives using RAI-110. Cycling of these cells was carried out in open cell cases. Charge rate was 35 ma for formation and 50 ma on subsequent recharges. Discharge was at 600 ma to 1.20 v cutoff. Cycle data is given in Table XXXV.

It appears that the epoxy may have caused some damage on the first cycle, but, in all cases except one, the cells have recovered on the second and subsequent cycles. The "78-Liquor-Sterilized" (Experiment 78) cells were most severely damaged on the first cycle and have yielded the poorest capacities on the remaining cycles. These cells, however, have shown some gradual improvement with cycling. Unanswered, however, is the question of whether improvement would occur to the same extent on the second cycle in a sealed cell where possible removal of gaseous products can not occur. Experiments to clarify this point are being run.

TABLE XXXV  
Effect of Epoxy on Cell Performance  
Test C

Cell No.	Description	Cycle #1		Cycle #2		Cycle #3		Cycle #4	
		Cap	Mid Volts	Cap	Mid Volts	Cap	Mid Volts	Cap	Mid Volts
1	76-Liq-Ster	1.92	1.42	2.47	1.41	2.37	1.42	2.28	1.44
2	" "	2.19	1.41	2.37	1.41	2.23	1.41	2.23	1.44
3	76-Chip-Ster	1.56	1.41	2.43	1.39	2.22	1.41	2.09	1.42
4	" "	1.57	1.41	2.49	1.39	2.44	1.42	2.42	1.44
5	78-Liq-Ster	1.38	1.36	1.93	1.38	2.01	1.38	1.95	1.42
6	" "	1.38	1.35	1.44	1.32	1.60	1.33	1.62	1.39
7	78-Chip-Ster	1.39	1.38	2.27	1.38	2.23	1.41	2.10	1.44
8	" "	1.58	1.38	2.13	1.38	2.11	1.40	2.04	1.43
9	76-Liq-Unster	1.86	1.42	2.55	1.32	2.49	1.38	2.36	1.45
10	" "	1.70	1.42	2.51	1.30	2.44	1.36	2.35	1.44
11	76-Chip-Unster	1.59	1.41	2.52	1.40	2.37	1.41	2.14	1.45
12	" "	2.03	1.41	2.18	1.38	2.13	1.40	2.07	1.44
13	78-Liq-Unster	1.71	1.41	2.40	1.28	2.41	1.36	2.10	1.45
14	" "	2.12	1.41	2.21	1.30	2.12	1.36	2.04	1.44
15	78-Chip-Unster	1.86	1.41	2.57	1.40	2.24	1.42	2.04	1.45
16	" "	2.31	1.39	2.30	1.38	2.14	1.38	1.98	1.43
17	Control Unster	1.91	1.40	2.13	1.41	2.08	1.41	1.95	1.44
18	" "	2.04	1.40	2.34	1.30	2.27	1.32	2.22	1.43

\* 76 and 78 refer to Experiments 76 and 78.

## B. Cell Study

This section includes the first work with sealed cells - first sterilized and sealed and later, when case material became available, sealed and sterilized. The main problem, as with any sealed silver-zinc cell, is gas pressure. No one variable seems responsible, but rather it appears to be the result of interaction of a number of them. The effects of these variables are described and finally a recommendation is made for making cells which will lead to the lowest pressures observed to date.

### 1. Cycle Life of Unsealed Three-Plate Silver-Zinc Cells

In order to obtain an idea of possible maximum cycle-life that might be obtained from sterilized silver-zinc cells a series of small three-plate cells was made and cycled automatically.

The unformed zinc oxide negatives contained 7% Compound 323-43. The unformed, sintered silver positives weighed 6g and were the limiting electrodes. The two zinc oxide electrodes were assembled with 5 layers of RAI-110 or RAI-116 using the u-wrap technique, and the silver electrode was inserted in the fold between the two wrapped negatives. Each cell stack was placed between two Teflon plates and tied snugly with nickel wire. The stacks were activated by immersing in 40% potassium hydroxide in a Teflon cup and evacuated to 28 in. Hg to remove trapped gases. Then the electrolyte level was readjusted to a height approximately  $\frac{2}{3}$  that of the electrodes. The cups containing the cell stacks were inserted into stainless steel bombs, which were subsequently sealed, placed in an air circulating, closely temperature regulated oven at 135°C where they remained for 40 hours. After cooling, the stacks were removed from the bombs and inserted into cell jars using appropriate spacers of sufficient thickness to just equal the difference in thickness between that of the cell stack and the width of the bottom of the jar. Tops were installed, electrolyte from the sterilization liquor added to a height  $\frac{2}{3}$  that of the electrodes and the cells charged. Unsterilized cells were run as controls.

After 24 hours stand, the open circuit voltage was measured and the initial capacity determined. Thereafter, the cells were automatically cycled, being charged in parallel by a constant potential device. A 5 ohm resistor in series with each cell served as a current limiter during charge and as the load during discharge. This resistor together with associated circuitry totaled a 6 ohm load. The discharge time was 6 hours and the charge time 18 hours. For a three electrode cell, essentially all the available capacity was removed during each cycle. The potential of the charging device was selected high enough so that all cells reached the potential at which oxygen was liberated at the silver electrode. Catch out cycles were run periodically following an open circuit period of at least 24 hours. The results are shown in Table XXXVI. These results show no essential difference between the capacities of sterilized and unsterilized cells either in the early cycles or in the 60th cycle. It is therefore concluded that

TABLE XXXVI  
Cycling of Unsealed Three-Plate Silver-Zinc Cells  
Capacity in Amp - Hours

Cell Number	RAI Separator (5 layers)	OCV after 24 hour stand	Cycle Number								OCV before Cycle 60	
			1	2	3	4	26	41	51	60		
101 U	110	1.861	1.65	1.74	1.80	1.80	1.80	1.45	1.32	1.12	1.10	1.851
106 S	110	1.862	1.44	1.53	1.75	1.65	1.40	1.32	1.32	1.20	1.00	1.859
107 S	110	1.862	1.44	1.53	1.75	1.70	1.40	1.32	1.32	1.12	1.20	1.850
108 S	110	1.863	1.44	1.53	1.75	1.65	1.40	1.26	1.26	1.12	1.00	1.849
109 U	116	1.864	1.68	1.80	1.80	1.62	1.40	1.26	1.26	0.87	0.95	1.850
114 U	116	1.862	1.50	1.70	1.75	1.60	1.50	1.50	1.50	1.15	1.10	1.853
115 S	116	1.863	1.44	1.70	1.70	1.60	1.50	1.50	1.50	1.05	1.10	1.854
116 S	116	1.861	1.44	1.65	1.50	1.50	1.15	1.05	1.05	1.05	0.78	1.860

U = Unsterilized

S = Sterilized

sterilization of electrodes containing Compound 323-43 is not detrimental to cycle life at least through 60 cycles. The test was terminated after 60 cycles since it became apparent that more was to be learned through the study of sealed, sterilized cells.

## 2. Performance of Sealed Cells

### a. Cell Packs Sterilized Then Sealed

After the work with open cells was completed, sealed cells were made to study the effect of Compound 323-43 on capacity, cycle life, and gas pressure. Other variables studied were the performance of the several sterilizable separators which had been provided, the effect on performance of the two sterilization temperatures, and the effect of high temperature stand on cell capacity.

Because at this stage the final case had not been developed, the work was done in non-sterilizable cases. This meant sterilizing the cell packs by themselves, transferring and sealing them into cases afterwards. The terminology "sterilized then sealed" is used to differentiate these cells from later cells which were "sealed then sterilized".

#### (1) Cells with Sterilized Components (Comparison of RAI-116 and RAI-110)

In order to obtain cycle life data on sterilized then sealed Ag-Zn cells and to compare cells containing RAI-116 and RAI-110 separators, twenty cell packs were constructed, sterilized in nickel bombs, then transferred and sealed in polystyrene cases. Each cell contained two Ag electrodes and three ZnO electrodes having 7% additive 323-43. The electrolyte was 40% KOH, at a level of about one-half the plate height. Two sterilization regimes were used: 75 hrs. at 125°C for 5 cells with each type of separator; and 135 hrs. at 135°C for the remaining 5 cells of each type. Polystyrene cement was used for sealing the SS 7.5 cases, which were then overpotted in S-20 cases with Bisonite epoxy. Each cell contained either a pressure gauge or a relief valve.

Formation was carried out by modified constant potential. The cells were connected in parallel to a power supply set at 1.96 volts, with a 5-ohm current-limiting resistor in series with each cell. Charge currents were approximately 60 ma on the lower plateau (1.65 v) for 25-45 hrs., and 8-16 ma on the 1.88-1.90 v level for 20 days. The cells were then connected in series and discharged at 1 ampere constant current.

On the following four cycles the constant potential charging was terminated when the upper plateau was reached, and at this point the cells were connected in series and topped off at 0.1 amp constant current to a 1.96 v cut-

off. For all cycles after the fifth, the entire charge was done at constant current to a 1.96 v cutoff. Discharge remained at 1 amp constant current to 1.20 v cutoff for all cycles. Cells were scanned every 40 seconds continuously and voltages recorded during both charge and discharge.

A summary of discharge capacities for the twenty cells through 68 cycles to date is given in Table XXXVII. Cells having RAI-116 separators were subject to early failure with only five cells still performing after 4 cycles and none after 21 cycles. Failure generally occurred by shorting, as indicated by low end of charge open circuit voltages (1.5 v or less) and lack of discharge capacity. Four of the cells with RAI-110 separators are still performing after 68 cycles. Of the six with this separation which failed, one was accidentally damaged by overcharging, which resulted in rupture of the cell case by excessive gas build-up and subsequent drying of the cell pack.

Seven cells which were still cycling at the 54th cycle were put on open circuit stand for 17 days because of failure of the automatic equipment. They were then transferred to another apparatus which also malfunctioned by causing the charge to cut off at 1.92 volts instead of 1.96. Therefore, data between cycles 54 and 62 are not given in Table XXXVII except to report failure of cell No. 20 by shorting after the 56th cycle.

The following data on gassing during cycling was obtained on cells equipped with pressure gauges:

Cell #	Separator	Sterilization Temp.	Pressure (psig)					
			Cycle					
			1	5	10	20	30	65
5	RAI-116	135°C	7	8	8	8	-	-
8	"	125	12	16	18	-	-	-
11	RAI-110	135	< 4	< 4	< 4	< 4	< 4	< 4
16	"	125	5	5	5	-	-	-

There was no pressure in cell #11 when the seal was broken after failure during the 66th cycle.

TABLE XXXVII  
Discharge Capacities of Twenty Cells Sealed after  
Sterilization

Cell #	Variable * RAI T°C	Discharge Capacity (amp-hr)										Cycle Life	
		Cycle											
		1	2	3	4	5	10	20	30	40	50	65	
1	116 135	2.4	-										1
2	" "	2.6	4.0	3.6	4.2								4
3	" "	2.4	-										1
4	" "	3.0	4.1	3.8									3
5	" "	3.0	4.3	4.2	4.1	4.7	3.5	3.4	-				21
6	116 125	2.4	2.7	3.0	2.5	1.2	3.0						11
7	" "	2.4	4.0	-									2
8	" "	2.4	3.9	4.0	3.7	4.5	2.7						16
9	" "	2.4	3.0	-									2
10	" "	2.4	4.2	4.0	4.1	4.3							5
11	110 125	3.1	4.3	4.0	4.3	3.0	3.0	4.2	2.9	3.6	3.3	0.6	66
12	" "	3.2	4.5	4.4	4.8	1.2	1.2	-					10
13	" "	3.2	4.5	4.4	4.6	3.0	3.0	4.2	3.0	3.6	3.6	-	65
14	" "	2.9	4.1	4.0	4.2	2.8	2.8	4.2	2.8	3.4	3.5	1.7	-
15	" "	3.0	4.3	4.0	4.6	2.8	2.8	4.3	3.0	3.5	3.5	2.1	-
16	110 135	3.0	3.2	3.6	2.9	3.5	2.1	-					13**
17	" "	3.1	3.5	3.8	3.1	3.7	2.1	3.0	2.2	2.8	3.5	-	52
18	" "	3.2	3.5	3.8	3.1	3.5	2.6	3.2	2.6	2.8	2.6	1.3	-
19	" "	4.2	3.6	3.7	3.1	3.4	2.8	3.0	2.7	2.6	2.6	2.3	-
20	" "	3.5	3.7	3.7	3.4	3.9	2.8	3.6	2.9	3.3	3.3	-	56

\* Type of separation and sterilization temperature.

\*\* Cell burst on accidental overcharge.

Some of the cells which failed were disassembled and examined. Cell #4 had dendrite burned off at the layer adjacent to the silver electrode. Silver penetration through the separator was appreciable in all cells. Cells #5, 8 and 12 showed evidence of shorting by zinc dendrite growth over the tops of the separators (which extended 1/4" above the plates). This zinc growth was believed to be enhanced by excessive tightness of the cell pack caused by failure to allow room for folds present in the absorber wrapped on the positive plate. (This method of wrapping the silver plate has not been included in the PPO sealed cells, to be described in the next section, a simple U-fold being used instead.)

The gases which built up in cells #5, 6, and 8 were collected and analyzed using the Fisher Gas Partitioner with helium as the carrier gas. The presence of hydrogen was confirmed, the amount being small in cells #5 and 8 but quite large in cell #6 for no apparent reason. In all cases the oxygen-nitrogen ratio was less than that present in an ordinary air sample, indicating efficient oxygen recombination during cycling of the sealed cells.

An additional sealed cell was constructed as above with RAI-110 separator and 135° C sterilization to obtain data under the condition of constant current charging. Capacities were comparable to those of similar cells in Table XXVII. Gas pressure after the first cycle was 6 psig. It had risen to 14 psig by the 20th cycle and to 15.5 psig at failure on the 78th cycle when it would not accept charge.

Then the cell was disassembled and examined, and the gas in the cell analyzed using the Fisher Gas Partitioner. Small amounts of hydrogen were detected and practically all of the oxygen was gone. This indicated that the cell was recombining oxygen on the negative plate. Silver metal was found on the first layer of the RAI-110 separator material, with some (although not severe) silver penetration on the subsequent layers. Zinc growth through the separator next to the negative plate was also noted.

Significant loss of negative active material was noted, especially at the top and side of the plate. The remaining active material was hard and appeared like cement. The Ag electrode was partially charged, the discharged portion taking the shape of the active material remaining in the negative electrode facing it. The silver plate was a little deformed being, compressed with the shape of the Zn electrode. Both electrodes and absorbers were sufficiently wetted. Some zinc growth was found in the outside U-fold. This zinc material was very smooth, thin and flat.

This test emphasizes the variability of separator RAI-116. However, considering this, RAI-110 appears to give much longer cycle life. The capacities appear normal for sealed cells and show that the presence of Compound 323-43, which permitted sterilization, did not detract from them.



## (2) Cells on High Temperature Stand

Some of the earlier cells that had been constructed to study various electrochemical properties of the system after sterilization were placed on stand at the elevated temperature of 160°F. This temperature was selected because it would accelerate any capacity robbing reaction and give some indication of what type of stand life on sterilized cells could be expected at ambient temperatures. If it is assumed that increasing the temperature by 18°F doubles the rate of the reaction, a stand period of one month at a temperature of 160°F would be expected to produce a loss similar to that of approximately 16 to 20 months at room temperature. This relationship has not been verified for temperatures of this magnitude, however. The results of this study are given in Table XXXVIII. Generally results indicated a capacity loss of 13-18% during the first 15 days; and 37-40% during the first 30 days. After 45 days two of the four cells had either shorted or had nearly done so, so that shorting occurred during the subsequent recharge. Cells that had been on stand up to 30 days at 160°F had not been damaged, and after recharging gave nearly as much capacity in some cases and more capacity in others than they did before the start of stand. The reason for this is not known.

### b. Cells Sealed in PPO Cases Prior to Sterilization

After a case and sealant had been developed which met all of the necessary requirements, an experiment was set up to demonstrate the capability of carrying a group of Ag-Zn cells through the complete sequence of sealing, sterilization, and electrical performance through four cycles. Six 5-plate cell packs were constructed using RAI-110 separator and fitted dry into JPL cases, Figure 6, molded in PPO 531-801, cut down to a height of 3 inches. Free space within the cell was filled with Teflon shims. The PPO cover was epoxy sealed to the case with DEN438-EK85 (with DMP 30 catalyst) and the seal cured for 24 hours at room temperature. The cells were then flooded with 40% KOH and allowed to soak for 24 hours. Excess electrolyte was then drained off, leaving a level about 3/4" above the bottom of the cell pack, and the fill cap was sealed into place. The cells were then enclosed in a constant humidity chamber containing 40% KOH for heat cure of the seals (6 hrs. at 75°C, 16 hrs. at 100°C). Finally, the terminals were sealed closed with silver solder.

Five of the cells were overpotted into larger PPO cases, using DEN438-EK85 with DMP 30, the sixth cell being left unpotted. All the cells were then supported in steel frames, and sterilization was begun (64 hr. at 135°C). After this first half of the specified sterilization requirement, the epoxy had become severely cracked on all potted cells and there was evidence that all cells had leaked.

TABLE XXXVIII

Capacity Retention After Stand at 160°F

Cell No.	22	25	26	27	28	34	37	38	39	40	44	45	48
Separation	(1)	(1)	(1)	(1)	(1)	(2)	(3)	(2)	(4)	(1)	(1)	(1)	(2)
Capacity in AH before Stand	4.6	4.4	4.6	5.6	4.6	4.5	4.5	5.0	5.0	5.1	4.6	4.8	4.6
Days on Stand	45	45	45	45	70	30	30	30	30	30	15	15	15
Temperature	160°F	160°F	160°F	160°F	RT	160°F	160°F	160°F	160°F	160°F	160°F	160°F	160°F
OCV After Stand	1.57	1.54	1.60	1.60	1.86	1.81	1.84	1.58	1.58	1.57	1.85	1.84	1.84
Capacity in AH After Stand	0.5	shorted	0.7	0.8	4.2	2.4	2.4	3.0	3.2	1.6	4.2	3.8	3.8
Per cent of Capacity retained	11	0	15	14	91	53	53	60	60	31	87	82	82
Capacity in AH following recharge after discharge following stand	shorted	shorted	1.2	1.3	-	5.0	4.4	4.5	6.1	5.6	5.5	4.9	5.2

NOTES:

1. Separator code: (1) 5 layers RAI-116  
(2) 5 layers RAI-110  
(3) 5 layers SWRI-GX  
(4) 5 layers SWRI-G
2. Cell 27 contained ZnO-HgO negatives and was unsterilized; all others contained ZnO-Compound 323-43 and were sterilized.

All the overpotted cells rose rapidly above 2 volts on applying 70 ma formation current, indicating drying out of the cell packs. The remaining cell (unpotted) did not accept charge, but yielded only 1.3 amp-hrs on discharge.

The six cell cases were cut open and inspected. Leakage apparently had occurred primarily via cracks in the area of the terminal insert in the cover. Portions of the epoxy overpot and epoxy seal were discolored. The cell packs, which appeared to be almost completely dried out, were placed in open cases and soaked 16 hrs. in 40% KOH and formation was again tried. All accepted only a small amount of charge and yielded almost zero capacity on discharge. They were then stripped of the RAI-110 separator and rewrapped with fibrous sausage casing, whereupon cycling performance was greatly improved with discharge capacities in the range 2.3 - 3.6 amp-hr. This indicates that damage had been chiefly to the separator material rather than to the electrodes themselves.

Since the first attempt to sterilize cells sealed in PPO cases failed chiefly due to leakage at the terminals, a second set of six Ag-Zn cells was constructed using a different method of bringing electrical contacts through the covers. In this modification, silver wires were sealed into machined covers with epoxy rather than using the molded covers with terminal inserts. Also, the fill hole in the new type cover was fitted with a threaded plug. A 1/2-inch head space between the top of the cell pack and the bottom of the cover was also provided, making the total cell height 3 1/2 inches.

The cell packs (3 ZnO electrodes and 2 Ag electrodes) were constructed in the usual manner, using RAI-110 separator. Silver wires were spot welded to the plate leads and the dry cell packs installed with Teflon shims into the PPO 531-801 cases. Machined covers were sealed to the cases and the silver wires into the covers with DEN438-EK85 epoxy (with DMP 30 catalyst). After a 16-hr cure at room temperature, excess 35% KOH was added by vacuum filling for a 24-hr soak, after which the electrolyte level was lowered to the top of the plates by siphoning. The seals were then heat cured at 100°C for 24 hrs. in a constant humidity chamber containing 35% KOH. The electrolyte level was finally adjusted to 2/3 - 3/4 the plate height and the fill hole was plugged and sealed.

From previous tests it was known that the cell would lose approximately 2.5 g of water during sterilization. Starting with 35% KOH and losing this amount of water would bring the KOH composition to about 40% after sterilization. The electrolyte level would also drop to about 1/2 the plate height.

The cells were clamped between steel plates and sterilized for two cycles of 60 hr. each at 135°C. The cell cases were weighed before sterilization and after each of the sterilization cycles. After the first cycle, 2 of the 6 cells showed excessive weight losses and evidence of electrolyte leakage. Since it appeared that no leaks occurred at the seals or terminals,

electrolyte loss was due to migration through the cell case walls, apparently via stress cracking. These two cells (#5 and #6) did not complete the entire sterilization regime. The four remaining cells did complete both sterilization cycles with only expected weight losses. Seals and terminals appeared in very good condition.

It should be noted that the two cases which leaked during sterilization (as well as three others which did not leak) had been used previously for sterilization and pressure tests. Since they appeared in good condition, they were simply cut down to the desired height for the present experiment. Possibly, however, stresses had been generated in the earlier tests. Another contributing factor may have been the Teflon shims used. Since Teflon expands to a greater extent on heating than PPO, this may have added to the stresses on the case during sterilization.

Since a set of sealed and then sterilized cells had not been completed without mishap, twelve additional 5-plate AgO-Zn cells, sealed in PPO cases, were constructed and sterilized. They were cycled in the same manner as the previous six. Except for the use of new rather than used cases, and PPO rather than Teflon shims construction was the same as described above. All passed the sterilization procedure without leaking.

Cycle data for the cells described above, plus those for two additional cells identical in construction and cycling but not sterilized, are given in Table XXXIX. The first set of sterilized cells are numbered 1 to 6, the second group are 1A to 6A and 7 to 12, and the non-sterilized controls are C-1 and C-2. Sterilization apparently causes capacity loss and probably contributes to scatter of the data. The controls show excellent agreement throughout cycling.

However, if the capacities of unsterilized cells C-1 and C-2 are compared with those of sterilized cells nos. 16-20 in Table XXXVII through the early cycles, there is little or no difference. These five cells, sterilized at 135°C, were also made with RAI-110 separator. The main difference is that these cells were not sterilized in the presence of either epoxy (DEN 438-EK85) or PPO (531-801). Some question still remains concerning the choice of epoxy or possibly the case material, PPO. This can be resolved only by a test of these materials in sealed cells. This test is underway.

#### c. Gas Generation in Sealed Cells

Silver-zinc cells are noted for their tendency to produce gas. Therefore, gauges were added to many of the sealed cells to determine the magnitude of this problem for sterilized cells. From early data it was evident that: (1) a wide variation in pressures occurred, seemingly associated with the separation used in construction, and (2) cells having chemically cross-

TABLE XXXIX  
Cycle Tests - Cells Sealed before Sterilization

Cell #	Discharge Capacity (amp-hr) Cycle)			
	1	2	3	4
	(a)	(b)	(b)	(b)
1	3.0	2.4	2.2	2.5
2	3.2	2.5	2.4	2.5
3	3.0	1.9	1.8	2.0
4	2.9	2.7	2.6	2.7
5	3.5	3.6	3.6	3.3
6	3.2	3.0	2.8	2.9
$\bar{X} \pm \Delta \bar{X}$	$3.1 \pm .2$	$2.7 \pm .4$	$2.6 \pm .4$	$2.7 \pm .3$
	(a)	(c)	(c)	(b)
1A	2.3	2.4	2.7	2.5
2A	2.3	2.5	2.9	2.9
3A	2.7	2.9	3.0	2.7
4A	1.8	2.1	2.4	2.7
5A	2.0	2.2	2.4	2.6
6A	2.9	2.9	3.0	2.8
$\bar{X} \pm \Delta \bar{X}$	$2.3 \pm .3$	$2.5 \pm .3$	$2.7 \pm .3$	$2.7 \pm .1$
	(a)	(b)	(b)	(b)
7	4.2	3.5	3.5	3.1
8	3.2	2.6	2.5	2.5
9	1.7	1.6	2.2	2.2
10	3.8	3.2	3.1	2.7
11	2.7	2.3	2.7	2.5
12	2.8	2.2	2.0	1.8
$\bar{X} \pm \Delta \bar{X}$	$3.1 \pm .7$	$2.6 \pm .5$	$2.7 \pm .4$	$2.5 \pm .3$
	(a)	(b)	(b)	(b)
C-1	3.5	3.8	4.1	4.6
C-2	3.6	3.7	4.4	3.9
$\bar{X} \pm \Delta \bar{X}$	$3.6 \pm .1$	$3.8 \pm .1$	$4.3 \pm .2$	$3.8 \pm .2$

(a) 70 ma charge to 1.96 v.

(b) 100 ma " " " .

(c) Two-step charge: 100 ma to 1.96 v, then 35 ma to 1.96 v.

All discharges were at 1.0 A to 1.2 v.

linked RAI-116 generally developed greater pressures than those having radiation cross-linked RAI-110. Since, however, there was an overlapping of data which suggested that other factors were probably involved, a further study of some of these variables was begun.

#### (1) Cell Pack Tightness

One variable studied was that of cell pack tightness. One of the characteristics of grafted separators is that expansion occurs during equilibration with electrolyte. The amount of expansion is related to the concentration of electrolyte, being greater in dilute electrolyte than in concentrated, and to the temperature during equilibration. Examination of the cell components after sterilization indicated that this expansion would occur, regardless of the expansion space provided, at the expense of other cell components. In this instance the zinc oxide electrode was compacted, it being the most easily compressed element in the cell. Since this variable could be more easily studied in cell stacks being placed in actual cell jars and since sterilizable cell jars were not available at the time, a preliminary study was made using unsterilized cells. These were seven-electrode cells having plate dimensions of 1 3/4 in. by 1 3/4 in. Separation consisted of 5 layers of SWRI-GX. The dry thickness of this material is approximately 0.0013 in. per layer. Proper spacing was selected to allow expansion to 0.0014, 0.0017, and 0.0021 in. per layer in three cells. Data on these cells are found in Table XL. The data suggest that the internal pressure tended to be highest in the more tightly packed cell and lowest in the more loosely packed one. Discharge voltage and capacity tended to diminish as separator expansion allowance increased.

#### (2) Cells with Positives Wrapped

It is well known that changes in electrolyte levels and concentrations occur on charge and discharge in alkaline cells where membranes are present. Thus, the magnitude of these changes should depend on the volume enclosed within the separator placed around the electrode. By wrapping the positives the major volume of the cell is now given over to the zinc electrode and concentration changes should be minimized for whatever effect this might have on gas production from the negative plate. Since all sealed cells made to date were negative wrapped, some data on positive wrapped cells was also desired. Six cells (5-plate Ag-ZnO) were constructed by wrapping the positive plates with separator to test the effect of this assembly on the amount of gas produced. Three cells were made using RAI-116 and three using RAI-110. They were then sterilized at 135°C for 120 hrs. The cell packs were sealed into polystyrene cases, fitted with pressure gauges and overpotted with epoxy.

One of the RAI-116 wrapped cells developed excessively high pressure on formation and was removed before the cycling tests. When the cell was

TABLE XL  
Internal Pressure as a Function of Cell Pack Tightness

Cell No.	68	69	70
Separator thickness allowance per layer	0.0014	0.0017	0.0021
Formation charge acceptance at 60 ma per sq. in; AH per gm Ag	0.37	0.37	0.36
Pressure change during formation, in. Hg g	63	13.6	13.0
First discharge capacity; AH per gm Ag at 100 ma per sq. in.	0.28	0.28	0.26
Median voltage	1.43	1.40	1.38
Recharge mode, CP 1.96 v for X hrs	90	90	73
final current; ma	<1	<1	1
final pressure; in. Hg g	83.2	20	15
Pressure after 72 hrs. OC; in. Hg	79.2	13.6	9.8
Second discharge capacity; AH at 100 ma per sq. in.	5.85	5.22	5.50
continued at 20 ma per sq. in.	0.75	0.59	0.68
Total capacity; AH	6.60	5.81	6.18
Capacity, AH per gm Ag	0.36	0.32	0.34

removed from the charger, pressure was at 120 psig. The cell maintained a 1.87 v open circuit voltage, but within 3 hours the pressure had risen to 129 psig. The cell was disassembled and a sample of the gas collected. Analysis showed only traces of hydrogen present; however, since an unknown quantity of air was inadvertently mixed with the gas sample, the actual level of hydrogen in the cell was not determined. Neither the positive nor the negative plates were completely charged. Some Zn dendrite growth was noticed at the bottom of the cell case which may have contributed to the gassing. Dendrite growth appears to be much greater in these positive-wrapped cells; however, excessive pressures were not attained during formation of the remaining five cells.

The remaining cells after completing four cycles were placed on float or stand. Cycle and pressure data are given in Table XLI. Float and stand data are given in Table XLII. Comparing pressure change during cycling of these positive wrapped cells (Table XLI) with similar negative wrapped cells (cells with sterilized components), no appreciable difference in pressure generation between positive and negative wrapped cells is noted.

For the cells shown in Table XLII there has been some pressure increase for both the cells on 1.96 volts constant potential float and those on stand, and the float cells have increased in pressure at a greater rate than the cells on stand. However, it is of interest to note that most of the pressure increase occurred during the first 30 days of testing. Cell 6-116-S has shown an increase in pressure after approximately 90 days of stand. This cell established a gas pressure during formation and retained it for 13 days, after which time the pressure decreased and remained at the diminished pressure for nearly 3 months before increasing again. Cell 3-110-F was taken out of the float circuit after 88 days because the cell potential was 1.70 volts while under a 1.96 volt constant potential charge, and had no capacity on discharge. This cell will be examined to determine the cause of failure.

Gas pressure in these cells which had the separator wrapped on the positives was no less than that in those with wrapped negatives (see Cells with Sterilized Components). Obviously, possible changes in electrolyte level within the separator did not contribute to gas production during the early cycles. However, considering dendrite growth and the amount of dendrite debris at the bottom of these cells, it is possible that this is a cause of gas build-up with time. Dendrites are relatively pure zinc and contain nothing to inhibit gassing. Thus, it is concluded from the standpoint of possible gas generation that it is better technique to wrap negatives than positives in this cell system.

### (3) Teflon

Previously, it appeared from the data that the quantity of gases evolved during formation and early cycling was related to the cell pack tightness



TABLE XLI  
Cycle and Pressure Data - Positive Wrapped Cells

Cycle	Cell	Chg. Cap.	Dischg.	Pressures (psig)	
		AH	AH	After Chg.	After Dischg.
1 Chg. 70 ma Dischg. 1.0 A	1-110	5.02	3.55	7.0	7.0
	2-110	4.14	2.80	0.0	0.0
	3-110	4.65	3.40	3.0	3.5
	5-116	5.22	3.75	9.0	9.5
	6-116	4.56	3.10	3.0	3.0
2	1-110	3.32	3.18	8.0	8.5
	2-110	3.68	3.46	3.0	3.0
	3-110	4.04	3.93	5.0	5.5
	5-116	3.36	3.33	14.0	14.5
	6-116	2.95	2.87	4.0	5.0
3	1-110	- *	3.55	10.0	8.5
	2-110	- *	3.30	3.0	3.0
	3-110	2.73	2.60	6.0	7.0
	5-116	- *	3.25	15.0	15.0
	6-116	- *	3.00	6.5	7.0
4	1-110	3.35	3.28	9.0	9.0
	2-110	3.49	3.50	5.0	5.0
	3-110	3.47	3.38	8.0	8.0
	5-116	3.21	3.10	16.5	16.5
	6-116	2.93	2.83	7.0	7.0
5	1-110	3.60	Stand	9.0	
	2-110	3.22	Float	5.0	
	3-110	3.38	Float	8.0	
	5-116	2.97	Float	16.5	
	6-116	2.87	Stand	7.0	

\* Insufficient charge data

Chg. at 100 ma

Dischg. at 1.0 A

TABLE XLII  
Pressures and Voltages of Positive-Wrapped Sealed Ag-Zn  
Cells

<u>Cell No.</u>	<u>1st day</u>	<u>30th day</u>	<u>60th day</u>	<u>90th day</u>
1-110-S	9.5 psi    1.86 v	11.0 psi   1.85 v	11.0 psi   1.84 v	12.0 psi   1.84 v
2-110-F	5.0 "    1.87 v	9.0 "    1.90 v	9.0 "    1.85 v	-    -
3-110-F	7.5 "    1.87 v	13.0 "   1.91 v	15.0 "   1.86 v	-    -
5-116-F	16.5 "   1.87 v	20.5 "   1.92 v	23.0 "   1.88 v	28.0 "   1.95 v
6-116-S	6.0 "    1.86 v	on pin   1.85 v	on pin   1.84 v	2    "   1.84 v

during sterilization and also to the presence of Teflon powder in the active material mix used for fabrication of the negative electrodes. While considerable variations in pressures were observed, there were generally higher pressures in cells containing negatives having Teflon powder than in those that did not.

This can be observed for cells containing negatives with no Teflon in Table XLIII as compared with those containing Teflon in Table XLIV.

Since Teflon is sometimes added to negative electrodes to increase the recombination of oxygen, the question arose as to whether omitting Teflon would have an adverse effect. This can be determined also from Tables XLIII and XLIV. All cells were floated in parallel at 1.96 volts. Current to each cell was determined by clip-on ammeter with a maximum inaccuracy of 3% and with ranges of 1 ma, 3 ma... Cells having no Teflon in the negative electrodes had pressures generally lower than their counterparts having Teflon after 11 days of float. After 23 days, the differences were greater, the cells without Teflon having decreased in pressure, while the others in most cases increased. Cell 112 was disconnected after 15 days when its pressure reached 28.3 psig which approached the maximum value for which the gauge was calibrated. After four days the pressure had decreased to 14 psig. Either the cells without Teflon recombined oxygen better than did those with it, or as is more unlikely, the latter produced gases other than oxygen.

#### (4) Amalgamated Grids

As a result of the study of the "Couple Effect" described on page 18 it seemed reasonable that amalgamating the grids of the negative electrode might help to alleviate gas evolution during the early stage of formation. Preliminary tests showed that the addition of Compound 323-50 to the negative mix used with amalgamated grids could improve cell capacity and when used without amalgamated grids did not detract from it. It was, therefore, added to the mix used in a factorial experiment designed to determine the significance of grid amalgamation, cell pack tightness, and the presence of Teflon on gas pressure and cell capacity in sealed cells. Unfortunately, the presence of Compound 323-50 caused excessive gassing in all cells and cast doubt on the validity of the experiment.

However, four cells had been made like the ones in the factorial experiment but without Compound 323-50. These results are shown in Table XLV and show that Compound 323-43 with no Teflon in the negative mix is conducive to low pressure.

A summary of the conclusions on the gassing problems are:

TABLE XLIII  
Pressure Data on Ag-Zn Cells Floating at Constant  
Potential - No Teflon in Negative

Cell No.	93	98	103	104	105	110	111
Pressure (in. Hg g) at end of third charge cc to 2.02 v	-2.0	14.2	0	0	4.2	2.0	2.0
<u>After Float, c.p. 1.96 v</u>							
X days on float	14	11	11	11	11	8	8
current, ma	2.3	1.4	0.8	0.9	0.6	0.9	0.8
Pressure, in. Hg g	0	9.6	5.0	3.2	5.6	4.0	7.8
X days on float	23	23	23	23	23	20	20
current, ma	0.9	1.3	1.0	1.0	0.6	0.6	0.7
Pressure, in. Hg g	0	4.0	4.5	3.0	5.0	2.5	4.0

TABLE XLIV  
Pressure Data on Ag-Zn Cells Floating at Constant  
Potential - 2% Teflon in  
Negative

Cell No.	95	106	108	109	112
Pressure (in. Hg g) at end of third charge cc to 2.02 v	1.0	5.0	3.8	10.0	9.0
After CP charge and float, CP 1.96 v					
X days on float	14	11	11	11	8
current, ma	2.7	0.5	0.6	1.4	1.8
Pressure, in. Hg g	13.0	6.2	14.8	16.0	34.8
X days on float	23	23	23	23	*
current, ma	0.7	0.6	0.8	1.1	
Pressure, in. Hg g	8.0	5.0	10.0	22.0	

\* At end of 12 days, pressure was 56.6 in. Hg g and cell charging was discontinued.  
After 4 days, pressure had decreased to 28 in. Hg g.

TABLE XLV  
Pressure (psig) and Discharge Capacity (amp-hr) of  
7-Plate Sterilized Then Sealed Ag-Zn Cells

<u>Cell No.</u>	<u>Composition *</u>	<u>Cycle</u>	<u>Capacity</u>	<u>Pressure</u>
17	To, PT1.5, Ao	1	5.48	11.0
18	To, PT1.5, A1		5.88	5.0
19	To, PT3.5, Ao		5.76	on pin
20	To, PT3.5, A1		4.60	0
17		2	5.35	10.0
18			4.75	on pin
19			4.60	on pin
20			5.18	2.0
17		3	6.26	10.0
18			5.46	5.0
19			5.31	5.0
20			4.52	2.0
17		4	6.02	10.0
18			5.54	5.0
19			5.12	5.0
20			3.85	4.0

\* To - 0% Teflon

PT1.5 - Tight Cell Pack

Ao 0% Grid Amalgamation

PT3.5 - Loose Cell Pack

A1 1% Grid Amalgamation

- (1) Excessive pack tightness is to be avoided.
- (2) Grid amalgamation appears to have little effect under the conditions of the experiment.
- (3) Omission of Teflon is preferred for small plates and short cycle life.
- (4) The negatives should be wrapped.
- (5) Compound 323-50 should not be used.

Cells incorporating these recommendations are being made to test the reproducibility of sealed cells.

#### IV. CASE MATERIALS AND SEALING TECHNIQUES

There were three principal objectives in this phase of the work.

- (1) The establishment of one or more plastic materials capable of withstanding heat sterilization in the presence of high concentrations of aqueous KOH without physical or chemical deterioration.
- (2) Demonstration of the feasibility of molding suitable cell cases and covers of these materials.
- (3) Development of techniques suitable for sealing terminals to covers and covers to cases such that the final assembly would withstand specified internal pressures and the action of KOH during sterilization.

##### A. Material Qualifying Studies

The only plastic materials which appeared capable of meeting the requirements were polysulfone (PS) Grade P-1700, Union Carbide Corporation, and several grades of polyphenylene oxide (PPO, registered trademark), General Electric Company. These materials were selected for their chemical stability and high temperature mechanical properties. In the course of this work, modified types of PPO became available and were included in the program. Polysulfone P-1700, and polyphenylene oxide grades PPO 533-111 and 681-111 were clear, unfilled plastics; PPO 531-801, PPO 541-801 and GFP3-111 were opaque, filled materials.

The mechanical properties of PS P-1700 and PPO 531-801 and 681-111 were evaluated in molded tensile bars following ASTM D 638. The materials as received and after annealing had the values shown in Table XLVI. The conclusion from this evaluation was that the values obtained were in satisfactory agreement with the data published by the supplier. Additional properties on these and the other plastics examined are available from the manufacturers.

The comparative physical properties of the glass filled (30 wt. %) GFP3-111 relative to PPO 531-801 and PPO 541-801 are given in Table XLVII. The significant properties of GFP3-111 are: the specific gravity (1.27), tensile strength at 257°F (15,500 psi), and coefficient of linear expansion ( $1.5 \times 10^{-5}$  in./in./°F). These properties are advantageous with respect to PPO 531-801 or PPO 541-801 and justified preliminary screening evaluations on the glass-filled materials.

##### 1. Stability Under Sterilization Conditions

For preliminary evaluations of the four grades of PPO and for P-1700 PS, experiments were conducted in 2-liter Parr bombs (AA 229HC6) of



TABLE XLVI  
Mechanical Properties of PS P-1700 and PPO 531-801 and 681-111:  
Determined at 72°F Using ASTM D638 Molded Tensile Bars

<u>PS P-1700</u>			
Tensile Strength (Yield) psi	As Received	Annealed 4 hr. 325° + 3°F (1)	Annealed then Equilibrated at 72.4°F, 50% R. H.
	10,300 ± 190 SD	12,200 ± 790 SD	12,200 ± 110 SD
Tensile Modulus psi	-	$3.5 \times 10^5 \pm .85 \times 10^5$	$3.5 \times 10^5 \pm 0.13 \times 10^5$
<u>PPO 531-801</u>			
Tensile strength - yield point (psi)	As Received	Annealed 4 hr. 356° + 3°F (1)	Annealed then Equilibrated at 72.4°F, 50% R. H.
	10,000 ± 140 SD	11,100 ± 100 SD	10,900 ± 190 SD
Tensile Modulus (psi)	$2.66 \times 10^5 \pm$ $0.13 \times 10^5$ SD	$3.12 \times 10^5 \pm$ $0.17 \times 10^5$ SD	$3.24 \times 10^5 \pm$ $0.62 \times 10^5$ SD
<u>PPO 681-111</u>			
Tensile Strength (Yield) (psi)	As Received	Annealed 4 hr. 329° + 3°F (1)	
	10,000 ± 60 SD	11,200 ± 50 SD	
Tensile Modulus (psi)	$2.7 \times 10^5 \pm$ $0.1 \times 10^5$ SD	$3.3 \times 10^5 \pm$ $0.3 \times 10^5$ SD	

(1) Specimens pulled without equilibrating with 50% relative humidity.

S.D. = Standard deviation 5 samples

R.H. = Relative humidity

TABLE XLVII  
Properties of Polyphenylene  
Oxides

	ASTM			
	Method	PPO 531-801	PPO 541-801	GFP3-111
Specific Gravity	D792	1.06	1.43	1.27
Water Absorption Equilibrium				
72°F (wt. %)		0.10	0.12	0.10
212°F "		-	0.31	-
Tensile Strength Yield	D638			
73°F (psi)		10,000-11,000	12,500	18,000
257°F "		5,500- 6,500	-	15,500
Tensile Modulus	D638			
73°F (psi)		$3.7 \times 10^5$	$7.4 \times 10^5$	$1.24 \times 10^6$
257°F "		$3.3 \times 10^5$	-	$1.20 \times 10^6$
Heat Deflection at	D648	375-380	337	360
264 psi (°F)				
Coefficient of Linear	D696	$2.9 \times 10^{-5}$	-	$1.5 \times 10^{-5}$
Expansion (in./in./°F)				
Mold Shrinkage in./in.	D955	0.007	0.003	0.001

Data from General Electric Company literature.

316 stainless steel using ASTM tensile bars of the plastics. The tensile bars were drilled with 1/4 inch holes and were supported on 1/8 inch nickel rod with 50% immersion of the tensile bars in electrolyte. After the bombs were loaded and sealed, they were evacuated to  $20 \pm 2$  mm of mercury and then charged with  $N_2$  to atmospheric pressure. The purging operation was carried out twice. The total weights of the charged bombs were unchanged between start and end of three sterilization routines within an error of  $\pm 2$  g.

The results of the sterilization tests on PPO and PS in the presence of 40% KOH, ZnO, HgO, and silver powder are given in Table XLVIII which lists average changes in hardness, weight, and dimensions. During these experiments a slight pressure increase was due to corrosion of the bomb. The important result of these experiments was the absence of significant changes in tensile strengths of P-1700, PPO 531-801 and PPO 681-111.

ASTM tensile bars were used in preliminary steam crazing and sterilization evaluations of GFP3-111. The initial tensile strength was 16,500 psi. After 35 hours in saturated steam at 135°C, tensile strength of bent tensile bars (1/4 inch deflection between 5 3/4 inch centers) decreased to 10,200 psi although there were no craze cracks visible at magnifications of 14 to 60. The specimens had an average weight increase of 0.32%, and had no significant dimensional or hardness change in this steam crazing test. For the sterilization test, the tensile bars were partially immersed in 40 wt. % KOH and held at 135°C for 35 hours. The sterilized specimens had an average weight loss of 0.38 wt. % and a white matte surface of raised glass fibers. The tensile strength decreased to 12,400 psi.

Based on the measured properties, both PPO 531-801 and PS P-1700 appeared to have adequate stability for cell cases of a silver-zinc system undergoing sterilization. PPO 533-111 displayed crazing which eliminated it from further consideration. In later tests, PS P-1700 and PPO 681-111 also crazed and were eliminated. Although PPO 541-801 showed a loss in tensile strength, its weldability kept it under consideration.

## 2. Stability Under Decontamination Procedures

Decontamination procedures (JPL Spec. GMO 50198-ETS-A) were carried out on tensile bars in stainless steel bombs. The bombs were attached to a vacuum line manifold along with a mercury manometer, cylinders of ethylene oxide (Matheson, purity 99.7% minimum) and dichlorodifluoromethane (Freon-12 or F-12, Matheson purity 99.7% minimum), and a bulb containing water. An oil pump (minimum pressure  $2 \times 10^{-3}$  mm mercury) was used to evacuate the system. The water was degassed by boiling initially then freezing and melting under vacuum. The gas phase was synthesized in the bombs using the manometer to determine the partial pressure of each component.

TABLE XLVIII

Stability of P-1700 and PPO 531-801, 533-111, 541-801, and 681-111  
Under Sterilization Conditions  
3 cycles, 36 hr. each, at 145  $\pm$  2°C

	<u>PS P-1700</u>	<u>PPO 531-801</u>	<u>PPO 533-111</u>	<u>PPO 541-801</u>	<u>PPO 681-111</u>
Surface Appearance	no change	no change	crazed	no change	no change
Average weight change wt. %	+0.27	+0.08	+0.22	-0.004	+0.16
Average hardness change (Shore D)	2	0	0	0	0
Average dimensional change					
length in./in.	-0.0012	-0.0004	-0.002	-0.001	NS
width "	NS	NS	-0.001	NS	0.001
thickness "	NS	NS	NS	NS	-.003
Tensile Strength					
yield point (psi)	12,000 $\pm$ SD 55	10,700 $\pm$ SD 280	6,900 $\pm$ SD 400	7,600 $\pm$ SD 250	11,300 $\pm$ SD 100
control yield point (psi)	12,200	10,900	10,900	10,700	10,000

Specimens: 5 ASTM Tensile bars  
50% immersion

Bomb Charge:

H<sub>2</sub>O 672. g Atmosphere N<sub>2</sub>  
KOH 448.  
ZnO 80.  
HgO 11.3  
Ag powder 0.2

Bomb: 200 ml Parr AA229HC6 316 SS

NS = Not significant

SD = Standard deviation on 5 specimens

The results of the decontamination procedures and the conditions employed are given in Table XLIX. The tensile bars sustained Procedure I (24 hours at  $24.5 \pm 0.2^\circ\text{C}$ ) with no change in surface appearance and hardness. The only significant change was the pressure decrease in each bomb which was 30 mm mercury for PPO 531-801 and 14 mm mercury for PS. This pressure decrease is presumed to arise from the absorption of F-12 by the two resins. After Procedure II the pressure decrease was 10 mm mercury for PPO 531-801 and 16 mm mercury for PS. The average weight increases for the resins did not agree with the pressure drops (PPO 531-801 0.40 wt. % and PS 0.12 wt. %). This effect may arise from differences in the rates of evolution of absorbed gas during the final evacuation specified. After Procedure II there was no change in surface appearance, hardness and average dimensions in PS specimens, while PPO specimens gave measureable changes in length and width. The tensile properties were: PPO 531-801 9,800 and PS 10,400 psi; the initial tensile properties were: PPO 10,000 and PS 11,100 psi.

In order to observe the absorption of Freon-12 under intensified conditions a simpler apparatus was set up. The PPO 531-801 sample was reduced to a powder (50-60 mesh); dried for 4 hours at  $120^\circ\text{C}$  under nitrogen; then pumped ( $10^{-2}$  mm Hg) at room temperature for 4 hours. Freon-12 was admitted to the system and the pressure observed as a function of time. In spite of the large surface area of the sample the F-12 was taken up very slowly at room temperature; in 140 hours only 11.4 ml F-12 (STP) were absorbed per gram of PPO 531-801. Absorption of F-12 does not appear to be a problem.

#### B. Molded Cell Cases and Covers

The experimental qualification of materials for the sterilizable battery containers used several different lots of molded cases and covers. The choice of cases was dictated largely by availability of case molds of a suitable size.

The initial lot of cell cases and covers obtained from existing molds (SC-6 (ESB) ) are shown in Figures 11 and 12 (Drawing No. 1-062 and Drawing No. 1-070). The silver terminal molded in the cover is shown in Figure 13 (Drawing No. 1-069).

A lot of cases and covers were molded in PPO 531-801 and PS P-1700. Subsequent tests with PPO 531-801 cases from this mold showed failures due to cracks in the bottom of the cases. This observation led to the conclusion that the mold design was not satisfactory for these plastic materials.

A second lot of cell cases, Figure 14 (Drawing No. 1-074 Rev. A) and covers, Figure 15 (Drawing No. 1-089) were molded in PS P-1700 and PPO 681-111 with silver inserts for terminals. The quality of the

TABLE XLIX  
Stability of PPO 531-801 and PS P-1700 in Ethylene Oxide.  
Decontamination Procedure JPL Spec. GMO 50198-ETS-A

<u>Procedure I</u> Gas Phase	H <sub>2</sub> O	8 mm Hg	24.5 ± 0.2°
	C <sub>2</sub> H <sub>4</sub> O	207	
	CF <sub>2</sub> Cl <sub>2</sub>	<u>551</u>	
		766	
After 24 hr.	<u>PPO 531-801</u>		<u>PS P-1700</u>
Pressure change	-30 mm Hg		-14 mm Hg
Surface appearance	NC		NC
Hardness (Shore D)	NC		NC
<u>Procedure II</u> Gas Phase	H <sub>2</sub> O	19 mm Hg	40 ± 0.5°C
	C <sub>2</sub> H <sub>4</sub> O	205	
	CF <sub>2</sub> Cl <sub>2</sub>	<u>548</u>	
		772	
After 24 hr.			
Pressure change	-10 mm Hg		-16 mm Hg
Surface Appearance	NC		NC
Hardness (Shore D)	NC		NC
Average Weight Change	0.40 wt. %		0.12 wt. %
Average Dimensional Change			
Length	0.0003 in. /in.		NS
Width	0.0009 "		NS
Thickness	NS		NS
Tensile Strength			
Yield Point	9,800 ± S.D. 50 psi		10,400 ± S. D. 160 psi
Specimens:	5 ASTM Tensile Bars as molded		

Pressure measurements ± 0.5 mm Hg

Dimensional measurements ± 0.001 in.

SD = Standard Deviation on 5 specimens

NC = No change

NS = Not significant

10-22-65

444 1-4-65

## CARL F. MORBERG RESEARCH CENTER

DWG No 1-062

.062 R.

031 R.  
MAX.

SECT. A-A

125 R.

SECT. B-B

-140 R.

SECT. C-C

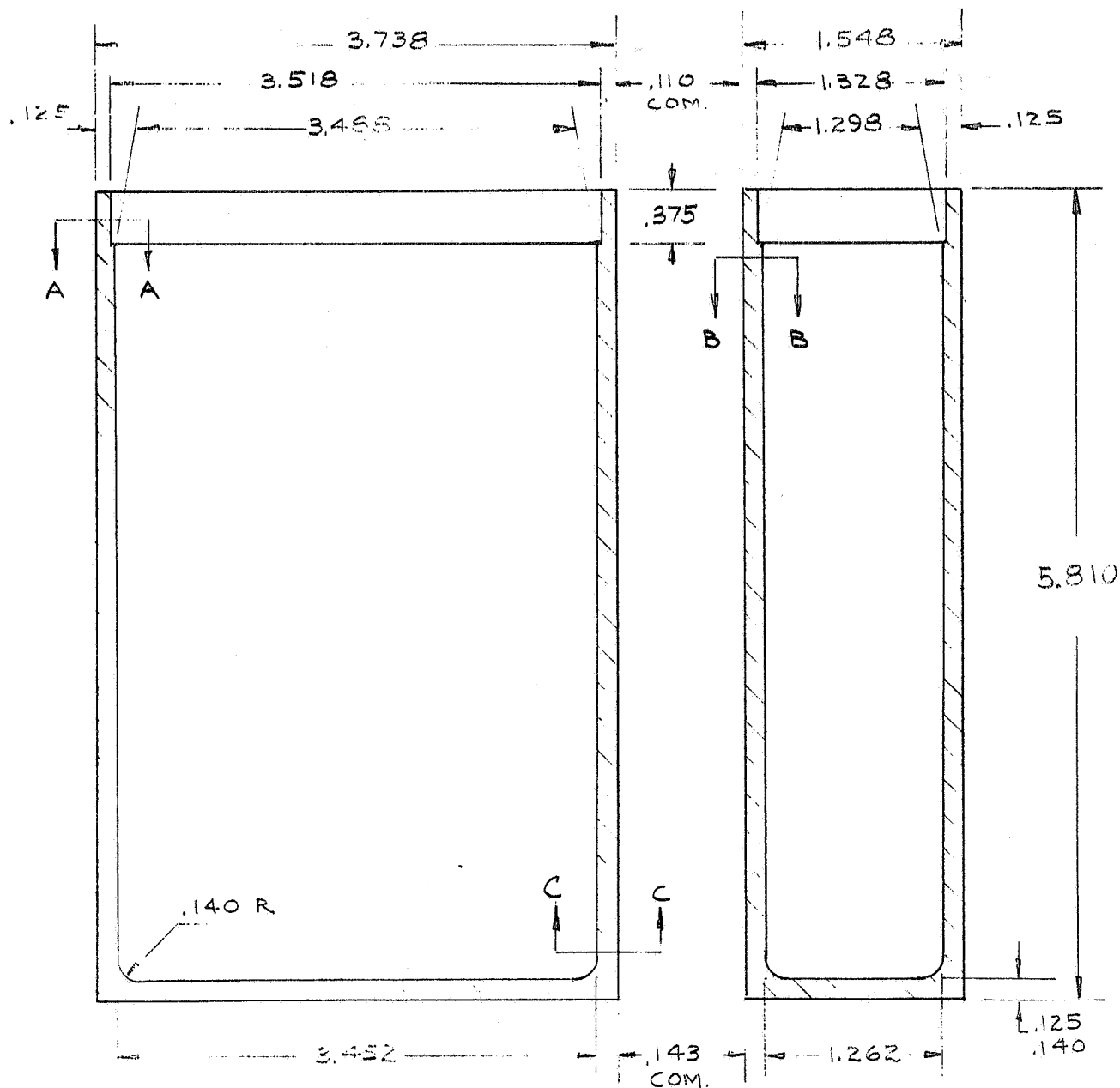


FIGURE 11  
CONTAINER 1-062

DATE	BY	REVISION	RECORD	AUTH.	DR.	CHK.

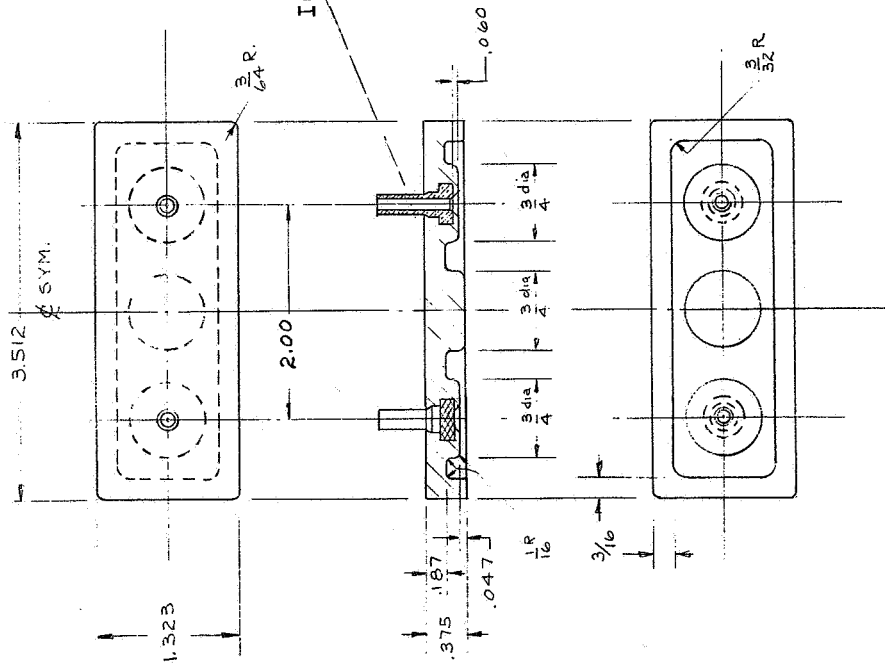


FIGURE 12

TOLERANCES (EXCEPT AS NOTED)		THE ELECTRIC STORAGE BATTERY CO. THE CARL F. MOORE RESEARCH CENTER HARDLET, PA.	
DECIMAL	± .003	SCALE	DRAWN BY J.W.C. APPROVED BY
FRACTIONAL	± .010	TITLE COVER 1-070	
ANGULAR	±	DATE	DRAWING NUMBER
		11-17-65	1-070

ENG. APPROVAL DATE

RELIABILITY DATE

12/4/65



MED. DIAMOND KNURL



MATERIAL.

FINE SILVER - HARD AS DRAWN

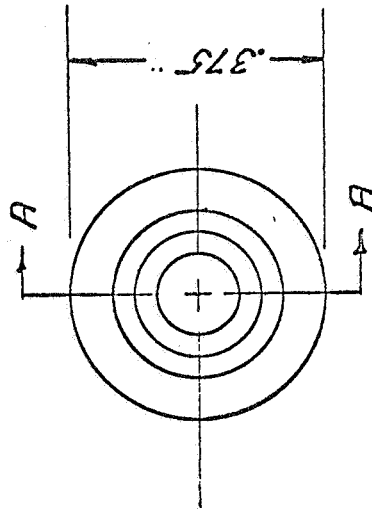
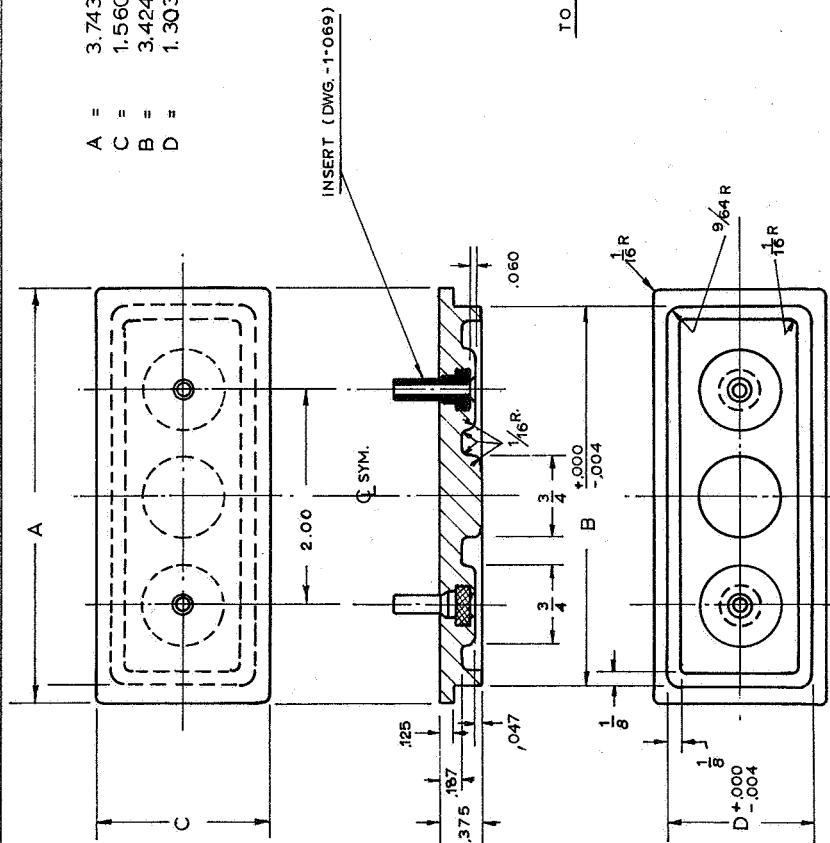


FIGURE 13  
TERMINAL 1-069



DATE	BY	REVISION	RECORD	AUTH.	DR.	CK.

A = 3.743"  
 C = 1.560"  
 B = 3.424"  
 D = 1.303"



MOLDED COVER  
 TO FIT CONTAINER DWG'S 1,074 REV. "A" and 1-075

TOLERANCES (EXCEPT AS NOTED)	THE ELECTRIC STORAGE BATTERY CO. THE CARL F. NORBERG RESEARCH CENTER YARDLEY, PA.			
DECIMAL	± .003	SCALE	B FULL	DRAWN BY J.W.C. APPROVED BY
FRACTIONAL	± .010	TITLE	COVER 1-089	
ANGULAR	±	DATE	3-24-66	DRAWING NUMBER 1-089
ENG. APPROVAL	RELIABILITY			

FIGURE 15

moldings in this lot of case assemblies and recommendations from General Electric Company representatives led to the selection of yet another mold design and a different molding machine for subsequent lots of case assemblies.

The third lot of case assemblies were molded in PPO 681-111 in a JPL-owned mold developed by Delco Division of General Motors under Study Contract 950364. In this report items molded in this equipment are referred to as JPL cases and covers. These are shown in Figures 16 and 17.

The resin beneath the terminal bases in the cover for the JPL case in PPO 531-801 occurred frequently due to stress cracks at the junction of the metal terminal and the resin. The terminal insert Figure 18 (Drawing No. 1-096) was prepared based upon recommendations of General Electric Company representatives. This design eliminated knurled surfaces and square corners, and allowed the insert to project through both top and bottom surfaces of the cover.

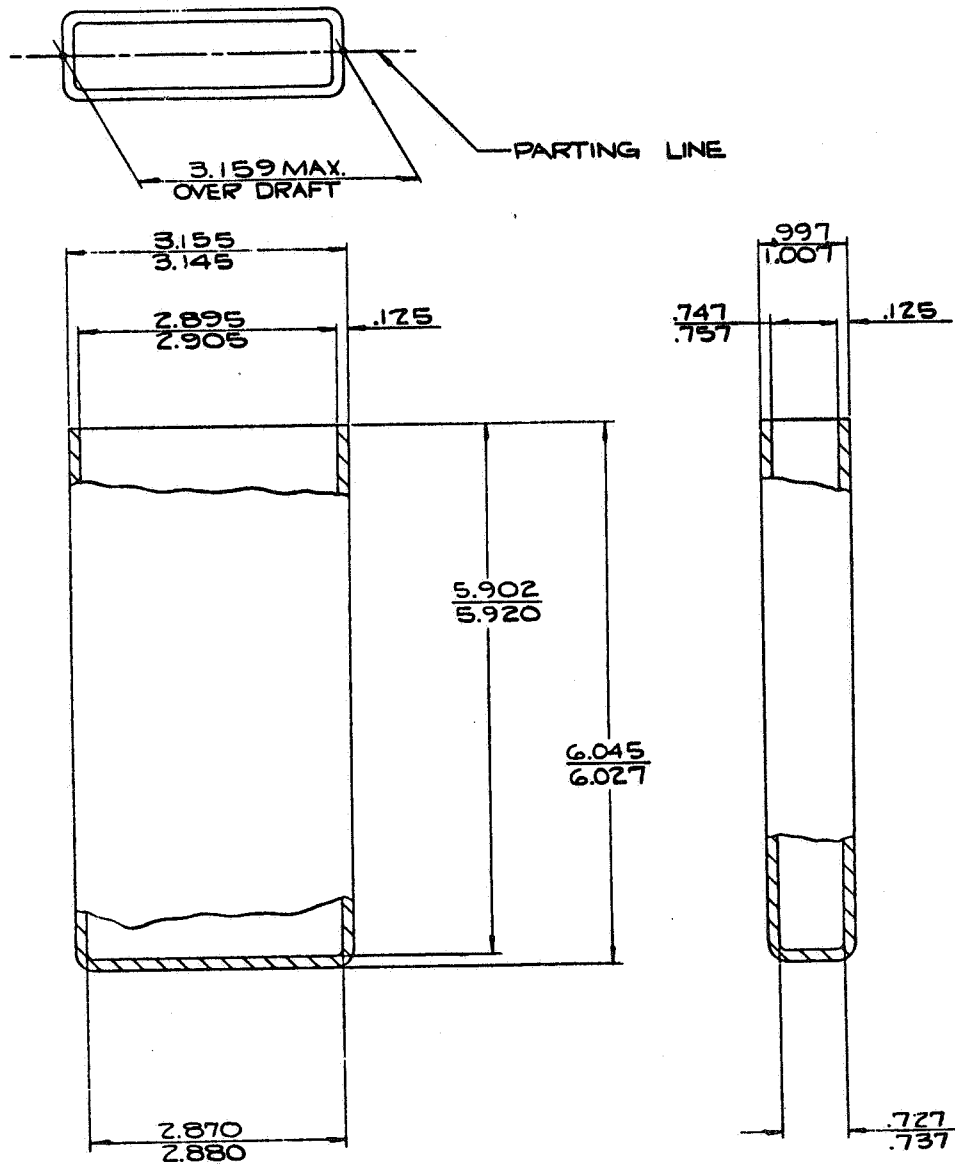
JPL case assemblies with the terminal Drawing No. 1-096 were molded in PPO 531-801 and PPO 541-801 with JPL source inspection. The molding conditions are given in Table L. The dimensional and weight variations in molded cases and covers in PPO 531-801 and PPO 541-801 represented the normal spread.

Twenty covers for the JPL case in PPO 531-801 with silver terminal were observed for stress cracks at the junction of terminal and resin. After six weeks, all covers showed some stress cracks usually 1-2 mils long. There has been no significant crack propagation, however, since that time. The new terminal design has reduced crack propagation but has not eliminated the problem. Coating of the resin-terminal junction on both the top and bottom of the cover with an epoxy resin appears to be required for this filled resin.

### C. Cell Case Seals

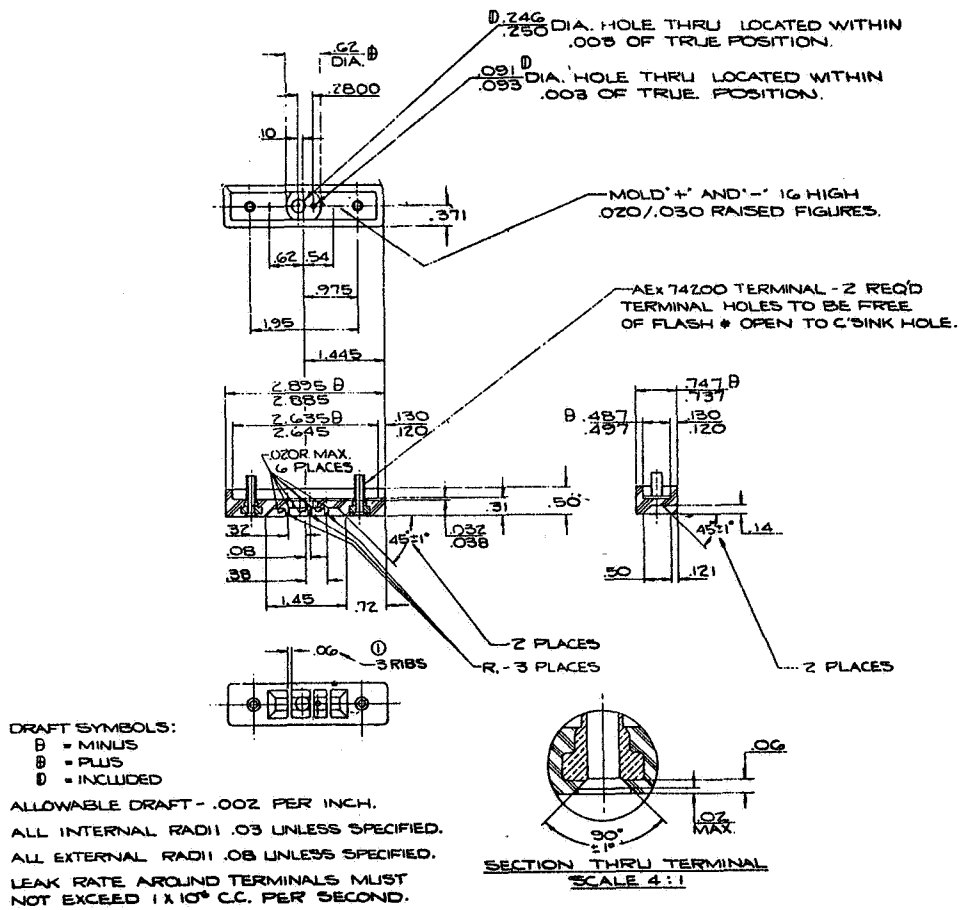
Three general sealing techniques were evaluated for the cell cases; (1) welding by hot gas or by heating, (2) solvent or cement sealing, and (3) adhesives. The General Electric Company reported that PPO 531-801 cannot be hot gas welded and recommended solvent, cement (2 wt. % PPO in solvent), or adhesive seals. Hot gas and ultrasonic welding were recommended by Union Carbide Corporation for PSP-1700 which yielded 90-100% of the bulk mechanical properties on gas welds. Solvent or cement seals on PS were not possible due to solvent crazing.

FIGURE 16  
JPL CASE

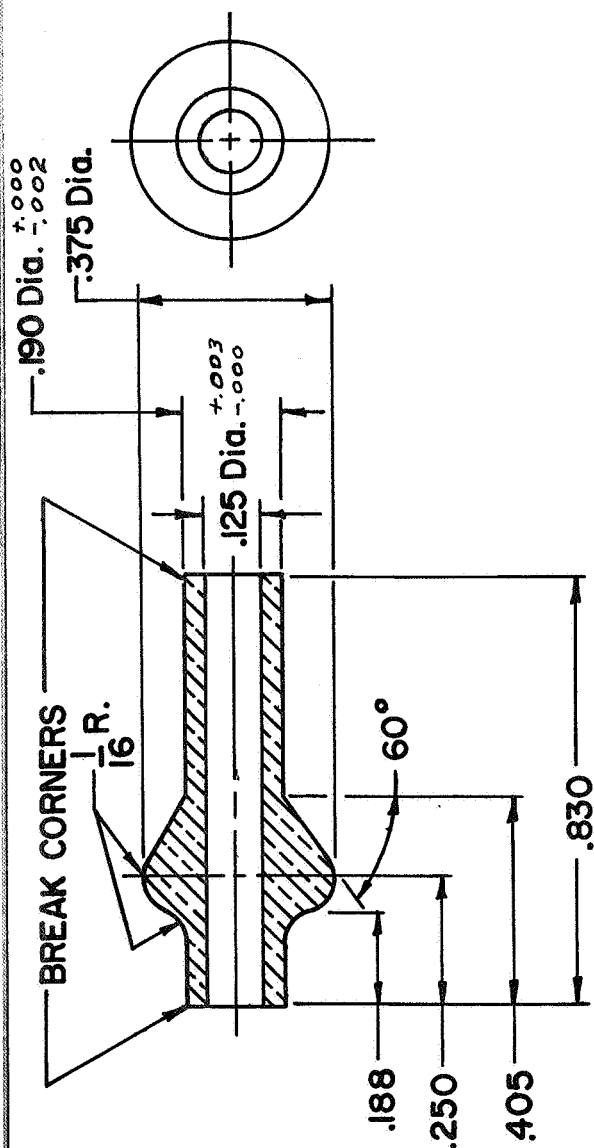


ALL INTERNAL RADI .08 UNLESS OTHERWISE SPECIFIED.  
ALL EXTERNAL RADI .20 UNLESS OTHERWISE SPECIFIED.

FIGURE 17  
JPL COVER



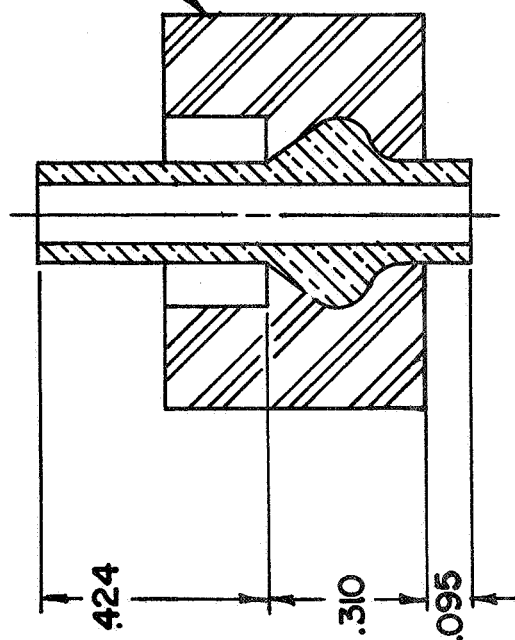
DATE	SYM	REVISION RECORD	AUTH.	DR.	CK.



**MATERIAL**  
FINE SILVER HARD  
AS DRAWN

J.P.L. COVER

FIGURE 18



TOLERANCES (EXCEPT AS NOTED)	THE ELECTRIC STORAGE BATTERY CO. The Carl F. Norberg Research Center Yardley, Pennsylvania		
DECIMAL	SCALE	DRAWN BY	APPROVED BY
± .003	3:1	B. PAUL	
FRACTIONAL	TITLE		
± .010	INSERT FOR CELL COVER J.P.L. CASE ASSEMBLY		
ANGULAR	DATE	DRAWING NUMBER	
± 1°	3/27/67	I-096	

TABLE L  
Molding Conditions for JPL Cell Case Assemblies with Silver  
Terminals (Drawing No. 1-096)

<u>Molder</u>	S & T Tool & Die Co., 125 E. Railroad Ave., Monrovia, Calif.			
<u>Machine</u>	Reed Prentice, Model 200 TD, 9 oz, 200 ton clamp			
<u>Material</u>	<u>PPO 531-801</u> <u>Lot 0093</u>		<u>PPO 541-801</u> <u>Blend 007</u>	
	Case	Cover	Case	Cover
<u>Cylinder Temperatures (°F)</u>				
Feed	560	540	568	540
Center	580	560	605	580
Nozzle	605	595	600	590
Melt	625	610	610	610
Front	580	575	615	590
<u>Mold Temperatures (°F)</u>				
Core	290-330	-	310-340	-
Mold	280	270	285	270
<u>Pressure (psig)</u>				
Inject	1800	1600	1300	2000
Hold	1200	1200	1200	1900
<u>Cycle (sec)</u>				
Fill	4-5	1	3	2
Inject	30	30	30	30
Cool	50	15	40	15
Total	90	58	95	58
	(approximate)			
<u>Molding Date</u>	5/17/67	5/17/67	5/17/67	5/17/67

JPL Source Inspection



## 1. Heat Sealing

### a. Hot Gas Welded Polysulfone Cases

Five cases (Drawing No. 1-062) and covers (Drawing No. 1-070) in PS P-1700 were chamfered on inside edges of case and top edge of covers to form a 60° "V" for the molding bead. Case walls were cut in each corner at the ends of each chamfer so that each weld started and stopped on the outside edge of the case. The cases, covers and 5/32 inch welding rod were dried 4 hours at  $120 \pm 2^\circ\text{C}$  ( $248 \pm 4^\circ\text{F}$ ). Welding conditions were:  $\text{N}_2$  8 psig, 115 V on 920 W heater. The equipment was Kamweld Products Company welding gun Model 10 HS, round tip KR and speed tip KRS-2C. The speed tip yielded better fusion in the joint than the round tip. The five cases were annealed (4 hours at  $162 \pm 2^\circ\text{C}$ ,  $324 \pm 4^\circ\text{F}$ ) about 72 hours after the welding operation. Stress cracks formed in the corners of every case during annealing, indicating the necessity of immediate annealing after welding.

Polysulfone cases (Drawing No. 1-062) and covers (Drawing No. 1-070) were prepared as previously described, then welded with the Kamweld gun with speed tip KRS-2C,  $\text{N}_2$   $7 \pm 1$  psig and  $110 \pm 2$  V on 920 W heater. The welds were annealed with the welding gun immediately and then annealed 4 hours at  $162 \pm 2^\circ\text{C}$ . These cases sustained  $90 \pm 2$  psig pressure test with a rectangular clamp around the top of the case. Without the clamp support joints failed at 20 psig due to the bowing of the larger faces of the case which created sufficient moment to rupture the side wall near or at the seal.

Parallel plate supports were made with 0.010 inch clearance between the plates and large faces of the cell. This support held only the large vertical faces of the case, while the top, bottom, and smaller side faces of the case had no support. With this support all welded PS cases sustained the 90 psig test at room temperature and 65 psig at  $145 \pm 2^\circ\text{C}$  ( $293 \pm 4^\circ\text{F}$ ) without failures in the seals. After the  $145^\circ\text{C}$  pressure test, stress cracks frequently were found in the boss surrounding the base of the terminal.

### b. Sterilization of Polysulfone Cases

Welded cases in PS which sustained the pressure tests were charged with 40 wt. % KOH 140 g, ZnO 11.2 g, HgO 1.1 g and silver powder 0.1 g. One silver terminal was sealed by welding and the other connected to a pressure gauge through Swagelok fittings (Crawford Fitting Co.) and 1/8 inch 304 stainless steel tubing. The cases, with supports, were held in a gas-tight steel box in which a  $\text{N}_2$  atmosphere was maintained by a slow  $\text{N}_2$  stream from a cylinder. All cases failed in the first 2 to 15 hours of the first sterilization cycle at  $145^\circ\text{C}$ , due to stress crazing, principally upon the larger faces of the case.

To demonstrate the mechanism of the crazing effect, three cases were assembled in the sterilization set-up and exposed only to steam at a pressure of 28-30 psig. About 1 ml of water was added to each case before connecting to system; at 145°C after a few hours, all cases failed. Again all cases had cracks on the sides and ends. This experiment shows that the crazing effect is due to steam.

#### c. Heat Sealing of PPO 531-801

Heat sealing of PPO 531-801 was evaluated in lap joints (1/2 inch x 1 inch) in sheet 0.080 inch thick. The mating surfaces were sanded with 240 emery cloth then held in a Carver press with a heated platen at 450-475  $\pm$  5°F (232-246  $\pm$  3°C) for 3-15 minutes at pressures from 10,000 to 40,000 psig. The minimum bond strength was 1,500 psi with a high deviation. The most serious defect was the formation of a honeycomb structure in the heated area due to polymer decomposition which made this sealing technique unsatisfactory for PPO 531-801.

#### d. Hot Gas Welding of PPO 541-801

The weldability of PPO 541-801 was evaluated on 1/8 inch stock in butt joints. The first attempt was on undried stock at a relatively high temperature setting on the nitrogen stream in the welding torch. This was a poor choice since the welding rod flowed too fast. The average tensile strength however was 1,700 psi. The next two welds were made on dried stock with N<sub>2</sub> at 6 psig, 115 V and 7.4 amps and yielded average tensile strengths of 5,200 and 5,900 psi respectively. These results indicated that PPO 541-801 might be welded satisfactorily for case sealing.

#### e. Hot Gas Welding of PPO 681-111

Hot gas welding of thin sections of PPO 681-111 (0.060 inches) might be useful in electrode reinforcement in the final cell design, so 1/16 inch stock of "Z Tron" was gas welded to demonstrate feasibility. The stock was cut into strips 4 inches x 16 inches, beveled, and dried at 120  $\pm$  2°C (248  $\pm$  4°F) for three hours. The beveled edges were butted and clamped on transite board by metal bars three inches from the weld line. This butt weld was made with N<sub>2</sub> at 6 psig and 115 V on the Kamweld gun. The clamping permitted some buckling of the stock during the welding so that plane specimens were not obtained. The weld was annealed for three hours at 170  $\pm$  2°C, then cut into one inch strips. The average tensile strength on this joint based on 10 specimens was 3,800 psi with a maximum of 4,400 psi and a minimum of 3,100 psi. A second butt weld was made under the same conditions but with better clamping to avoid buckling. After annealing, this joint had an average tensile strength of 7,900 psi with a maximum of 9,400 psi and a minimum of 6,600 psi in 10 specimens of the weld. It can be concluded that satisfactory welds can be obtained on the PPO 681-111 even on 0.060 inch stock.

f. Sterilization of Hot Gas Welded JPL Cases  
in PPO 541-801

The initial JPL cases in PPO 541-801 were prepared with a 1/16 inch chamfer on the inside of the top edge of the case. The cover was allowed to project 1/8 inch above the top of the case. The case, cover and welding rod were dried at  $120 \pm 2^\circ\text{C}$  for two hours and then welded with a Kamweld gun using  $\text{N}_2$  6 psig, 120 V and 7.6 amp. The cases were tested at 90 psig and only one out of ten cases sustained the test. The failures were in the weld area indicating inadequate fusion of the bead with the cases or cover.

Ten JPL cases in PPO 541-801 had covers machined to fit; the top of the case and cover were chamfered to yield a  $60^\circ$  groove 1/8 inch wide across the base. Welding was carried out with two guns - one preheating immediately in front of the weld bead. The welding conditions were: preheating gun  $\text{N}_2$  6 psig, 110 V, welding gun  $\text{N}_2$  6 psig, 119 V, 7.4 amps. Only three cases sustained 90 psig pressure test; after repair two more cases sustained this test; however, on sterilization four out of four cases failed. Leaks were in the weld areas.

Welded JPL cases in PPO 541-801 with the silver terminal (Drawing No. 1-096) were welded with 1/8 inch round welding rod obtained by cutting sections from a molded case of the same material. The welding conditions were:  $\text{N}_2$  6 psig on both guns, preheating 114 V and welding gun 120 V and 7.6 amp. The preheating was continued until the bottom of the V's began to fuse, then welding rod was applied. Only two welds out of ten passed the 90 psig test. Leaks in welds were repaired by milling a slot and re-welding. This operation was a failure since 8 out of 8 welds still leaked. These results indicate that a feasible welding operation has not been demonstrated, and a welded seal on PPO 541-801 cases can not be recommended.

g. Sterilization of Welded PPO 681-111 JPL  
Cases

Three cases with projecting covers at the welded seal were charged with:

KOH 40 wt. %	50 ml
ZnO	5.6 g
HgO	0.5 g
Ag powder	0.1 g

and run through 3 sterilization cycles at  $145 \pm 2^\circ\text{C}$  for 36 hours each cycle. One case leaked during the first cycle; had a slow leak rate during the third cycle. Penetrating cracks were found on all cases in the upper quarter of the broad faces of all specimens. These experiments indicate that the stress level in cases under sterilization conditions exceeds the permissible level in the presence of steam.

Since the temperature in the sterilization procedure was reduced from 145°C to 135°C, a series of welded JPL cases in PPO 681-111 were prepared for evaluation at the lower sterilization temperature. The result was essentially the same as in previous work with this material; namely stress cracking in the body of the case although the crazing was less extensive. The conclusion is that PPO 681-111 is also not a satisfactory case material.

## 2. Solvent Sealing

### a. Crazing of Polysulfone

Cell case sealing with epoxy adhesives or solvents necessitated evaluation of the effects of such agents on case materials. The central portion of ASTM tensile bars, 1 inch long, molded from PS P-1700 was painted with adhesives or 5 wt. % PS in  $\text{CH}_2\text{Cl}_2$ . The adhesives were Dow (DEN 438 and DEN 438-EK85), Rohm and Haas (DMP 30), ESB Atlas Minerals and Chemicals Division (XBS-68). Control samples were carried through the same temperature schedule to eliminate any temperature effect on tensile properties. Epoxy resins and solvents reduced the tensile strength of PS 19 to 30% which supported the manufacturer's statement that solvent or adhesive seals were unsatisfactory on polysulfone P-1700.

### b. Solvent Seals on PPO 531-801

Solvent and cement seals on PPO 531-801 were evaluated in lap joints (1/4 inch x 1/2 inch) by tensile shear tests. Preliminary experiments with cements (2 wt. % PPO in solvent) showed that  $\text{CHCl}_3$  alone was superior to resin solutions in both bond strength and reproducibility. The best procedure was to sand mating surfaces, paint, dry for 5 seconds, join under 12 psi for 30 minutes at  $25 \pm 2^\circ\text{C}$ , then cure at  $150 \pm 2^\circ\text{C}$  under 4000 psi in a Carver press. The bond strengths of these joints were: average 2100 psi, maximum 2,900 psi and minimum 1,700 psi before and after sterilization. Failures were in the substrate of the joint area.

### c. Pressure Tests and Sterilization of Solvent Sealed PPO 531-801 Cases

Chloroform seals were made on 13 PPO 531-801 cases (1-062) reduced 3/8 inch in height and covers (1-070) machined to fit. The mating surfaces were sanded with No. 240 emery paper, painted with  $\text{CHCl}_3$ , immediately assembled, clamped on all 4 sides, and cured for 30 minutes at 30°C, 3 hours at 75°C, 2 hours at 100°C and 3 hours at 150°C. Nine of these cases sustained 90 psig at room temperature and 6 cases sustained 65 psig at  $145 \pm 2^\circ\text{C}$ . The surviving cases failed on sterilization. Most failures were due to cracks in corners of cases. These results indicated that solvent seals on PPO 531-801 cases were unsatisfactory.

#### d. Solvent Seals on PPO 681-111 JPL Cases

Three PPO 681-111 JPL cases with covers individually machined to fit and fill tab, were sanded with 240 emery cloth on all mating surfaces. The mating surfaces were painted with  $\text{CHCl}_3$ , immediately assembled and clamped with a rectangular clamp around the top of the case and a "C" clamp between the cover and bottom of the case to prevent movement of the cover. The clamped assembly was cured for 4 hours at  $64 \pm 2^\circ\text{C}$  and finally 3 hours at  $150 \pm 2^\circ\text{C}$ . After this curing cycle, severe solvent crazing was found in the seal areas of every case with large cracks parallel to the seals. All seals failed in pressure tests at room temperature. These results indicate that a  $\text{CHCl}_3$  seal is not acceptable on the PPO 681-111 case.

### 3. Adhesive Seals

#### a. Adhesive Seals on PPO 531-801

A series of epoxy resins were evaluated in lap joints on PPO 531-801 to develop technique and find suitable adhesives for cell case seals. The epoxy resins were: XBS-67, XBS-68, Epocast 220, Epocast 211, and Dow DEN-438-EK85. The Dow resin DEN-438-EK85 was found to yield the highest bond strength in lap joints, and study was concentrated upon it. Lap joints on PPO 531-801 were prepared by cutting ASTM tensile bars at the center then forming the joint by painting sanded surfaces and curing the clamped joints 4 hours at  $25^\circ\text{C}$ , 1 hour at  $74^\circ\text{C}$  and 1 hour at  $165^\circ\text{C}$ . The bond strength of the epoxy DEN-438-EK85 decreased from an average of 2,000 psi to 1,300 psi after sterilization. Subsequent studies on case sealing have shown that the bond strengths were decreased by the clamping pressure applied during formation. The best bond strengths were obtained on cell cases with no clamping during the resin curing cycle.

#### b. Sterilization of Adhesive Epocast 221 on PPO 531-801

Joints were prepared on PPO 531-801, ASTM tensile bars to evaluate the stability of this adhesive under sterilization conditions. The tensile bars were cut in the center of the neck area, sanded and painted with the adhesive. The cure cycle was 16 hours at  $25^\circ\text{C}$  under 4 psi pressure, 2 hours at  $75^\circ\text{C}$  and 3 hours at  $145^\circ\text{C}$ . The bond strength decreased from 1050 psi to 850 psi after sterilization. All failures were of the adhesive type - the epoxy separated cleanly from the surface of PPO 531-801. This adhesive is not recommended for sealing cell cases in PPO 531-801.

#### c. Solvent Loss and Cure Rates for Epoxy Resin DEN-438-EK85

The rate of solvent loss from the Dow resin DEN-438-EK85 and its rate of cure are required to establish optimum heating periods on assembled

cells. The samples (10g in 2 inch aluminum dish) were maintained at constant temperature  $\pm 2^{\circ}\text{C}$  in a Blue M circulating air oven. The rate of cure was indicated by the acetone soluble content of the sample. The solvent loss (based upon solvent content) from DEN-438-EK85 with 5 wt. % DMP 30 was 2 wt. % after 20 hours at  $25^{\circ}\text{C}$ , 2.7 wt. % after 15 hours at  $50^{\circ}\text{C}$ , and 12 wt. % after 26 hours at  $75^{\circ}\text{C}$ . The acetone soluble content of this system was zero at the following times:

Temperature $^{\circ}\text{C}$	Cure Time (hr)		
	Catalyst Concentration wt. %		
	5	3	1
25	>100	>100	>1000
45	50	60	> 100
75	3	5	80
100	1	1.5	10

A flexibilizing modifier for DEN-438-EK85 is DER 741A which is recommended by Dow at 10 wt. % level. This system, cured with 5 wt. % DMP 30 at 16 hours at  $25^{\circ}\text{C}$ , 1 hour at  $75^{\circ}\text{C}$ , 1 hour at  $125^{\circ}\text{C}$  and 2 hours at  $160^{\circ}\text{C}$  was evaluated in lap joints in the sterilization procedure. The bond strength 3000 psi was unchanged after sterilization of joints made on PPO 531-801 tensile bars.

#### d. Sterilization of Epoxy-Sealed PPO 531-801 Cases (1-062)

Pressure tests and sterilization were applied to 3 PPO 531-801 cases which were sealed with the Dow epoxy resin DEN438-EK85 catalyzed by 5 wt. % DMP 30 (Rohm and Haas). The cases (Drawing No. 1-062) were reduced 1 inch in height to remove the internal ledge. The covers (Drawing No. 1-070) were individually fitted to each case. The mating surfaces of the case and cover were sanded with 240 emery paper then coated with DEN438-EK85 + 5 wt. % DMP 30 and set 3 hours at  $25^{\circ}\text{C}$ . Covers and cases were assembled with the joint clamp on all sides; a large C clamp on cover and bottom of the case prevented upward movement of the cover. The adhesive was cured following the schedule: 3 hours at  $25^{\circ}\text{C}$ , 1 hour at  $75^{\circ}\text{C}$  and 2 hours at  $162^{\circ}\text{C}$ . All 3 cases passed pressure tests (90 psig at  $25^{\circ}\text{C}$  and 65 psig at  $145^{\circ}\text{C}$ ) but failed on sterilization due to cracks in bottom of case. The seals were intact. These results prompted the abandonment of this case (Drawing No. 1-062).

#### e. Epoxy Seals on PPO 531-801 JPL Cases

Twenty-five JPL case assemblies in PPO 531-801 were supplied by JPL. The covers contained silver plated brass terminals. These cases were molded by S & T Tool & Die Company and provided an independent check on the effects of molding upon the capabilities of the material to meet

case specifications. Inspection of the covers on a low power microscope (10-30 power) found cracks in resin beneath all terminal bases. The thermal stability of these cases and covers was given a preliminary check by heating 2 cases and 2 covers in nitrogen for 64 hours at  $145 \pm 2^\circ\text{C}$ . No distortion was found in the cases, but the cracks in the resin beneath the terminal base increased in length. To minimize crack propagation, the resin beneath the terminal bases was milled out on all covers. The covers were then machined to fit the cases.

Variations in epoxy seals were evaluated on these case assemblies and are summarized in Table LI. This study demonstrated that the resin Dow DEN-438 could meet design requirements for a satisfactory seal. The covers were not of optimum design, since leaks developed in the highly stressed areas under the terminal base, even when the resin was removed by milling. A fillet of epoxy resin at the junction of the terminal with the cover helped to reduce leakage in this area, but was not an adequate solution to the problem. The results show that clamping during the cure of the resin gave dry joints. Moreover, a fillet at the top and bottom of the cover was advantageous in forming a well of resin which filled the glue line during cure. The terminals in these covers were silver-plated hard brass. The solid silver terminals have performed more satisfactorily. It is concluded that the epoxy resin was chemically satisfactory.

Additional work was carried out to evaluate the additive DER 741 A, recommended by Dow as a plasticizer, in DEN438-EK85 at two levels, 5 and 10 wt. %. A maximum cure temperature of  $100 \pm 2^\circ\text{C}$  was selected for the curing since the dry separator materials were believed to be stable at this temperature.

The first series of 10 JPL cases in PPO 531-801 involving DER 741 A was prepared with a groove in the side of the cover to serve as a well for resin. The top and bottom edges of the cover were chamfered to form beads of the adhesive. Seven of 10 cases sustained 90 psig at room temperature, but after this qualification only 1 case out of 4 had reasonable pressure and weight losses during sterilization. It was concluded that the groove on the side of the cover was contributing no added strength to the seal and therefore was dropped from further study. The epoxy system in this series used 10 wt. % addition of Dow DER 741 A based on the resin content of DEN438-EK85.

The second series of JPL cell cases used 5 wt. % addition of DER741A and the cure used a short time at  $160^\circ\text{C}$ . One case had a leak around the terminal which was found prior to the sterilization cycle. The 4 cases had pressure drops of 4 to 37 psig during the sterilization and weight losses of 4.0 to 5.5 g in the same time period. The helium leak rates after sterilization were between  $6.6 \times 10^{-5}$  to  $> 1.7 \times 10^{-4}$  which were not acceptable.

TABLE LI

Epoxy Seals on JPL Cases in PPO 531-801

(Epoxy - DEN438-EK85 + 5 wt. % DMP 30. Cure: 16 hr. at 25°C,  
2 hr. at 75°C, 2 hr. at 160°C)

Exp. No.	378-8	378-11	378-13	378-16	378-24
Cases	5	4	4	5	5
Cover Seal Design	Plane	Plane	Chamfer (1) Cover top	Chamfer (1) Cover top and bottom groove at center	Chamfer (2) Top and bottom of cover
Joint Clamping	Yes	None	None	None	None
<u>Pressure Test</u> 90 psig 25°C	3 Pass	4 Pass	4 Pass	3 Pass 2 leak around terminal	4 Pass 1 terminal leak
<u>Sterilization</u> Conditions	1 Pass	3 Pass 1 Failure	3 Pass 1 Failure	3 Pass 1 Failure	1 Pass 3 Coupling leaks (3)
Temperature (°C)	145	145	145	145	135
Pressure (psig)	65	65	65	65	65
Helium leak rate (ml/sec)		3 cases < 7 x 10 <sup>-7</sup>	1 case 8.1 x 10 <sup>-7</sup> 1 " 8.4 x 10 <sup>-8</sup>	1 case 2.0 x 10 <sup>-7</sup> 1 " 5.4 x 10 <sup>-7</sup>	
Remarks	Dry joint	Leakage around terminals		Leakage at terminal	
(1)	Fillet of epoxy resin around terminal - top of cover.				
(2)	" " "	" "	" "	" "	" - top and bottom of cover.
(3)	Resin fillet interfered with Swagelok coupling.				



The third series of JPL cases in PPO 531-801 had the same seal design and preparation. The adhesive used 10 wt. % addition of DER 741 A and the cure had a maximum temperature of  $100 \pm 2^\circ\text{C}$ . The results are summarized in Table LII. During the sterilization cycle, case No. 4 lost 48 psig which must represent a leak in the system since the weight loss was only 3.27 g and final helium leak rate was  $5.1 \times 10^{-8}$  ml/sec. All cases in this series had acceptable helium leak rates ( $10^{-8}$  ml/sec. It is believed that the difference between cases in series 2 and series 3 may involve the support around the seal. In the latter series the seal area had added support supplied by shims between the case and the parallel plate clamp.

Additional adhesive seals on 5 JPL cases were prepared and put through specification tests. The important result was the finding of leaks at terminals molded in the covers which developed during the sterilization procedure (Table LIII). A lot of 8 JPL cases (with silver terminal 1-096) in PPO 531-801 were prepared to show reproducibility of the epoxy seal through pressure tests, sterilization procedure and final helium leak rate. The total results are given in Table LIV which show 7 out of 8 cases passing required tests. The pressure loss during sterilization was 9 to 11 psig; the weight loss was 2.5 to 3.4 g. The final helium leak rate was  $7.5 \times 10^{-9}$  to  $1.2 \times 10^{-6}$  ml/sec with one case at  $8.7 \times 10^{-6}$  ml/sec. These results demonstrate feasibility of the epoxy seal on JPL cases, although it was necessary to paint the top and bottom of the covers around the terminal inserts with epoxy to insure against possible bad effects due to the stress cracks in the covers.

#### f. PPO 531-801 Cases and PPO 541-801 Covers

PPO 541-801 covers have never shown any stress cracks at the molded insert terminal which is an advantage over PPO 531-801. An attempt was made to seal a cover of PPO 541-801 into a case of PPO 531-801. All 12 cases sealed with the epoxy resin (Dow DEN-438-EK85) passed 90 psig test at room temperature but only 2 out of 7 cases sustained 65 psig at  $135^\circ\text{C}$ . The differential thermal expansion along the longer dimension of the top amounted to 0.007 inch. This added stress was probably responsible for the seal failures. The thermal effect alone was evaluated by heating the remaining 5 cases to  $135^\circ\text{C}$  for 16 hours; after this thermal cycle all 5 cases sustained 90 psig at room temperature. Based on these results the combination of a cover in PPO 541-801 sealed into a PPO 531-801 case by an epoxy resin, does not appear feasible.

#### g. Adhesive Seal on JPL Cases in PPO 541-801

JPL cases were sealed with the epoxy resin DEN438-EK85 and subjected to specification tests. The case preparation and test results are given in Tables LV and LVI. The pressure losses and weight losses particularly were very low. There was no correlation between total pressure loss in the sterilization cycles, the weight loss, and the helium leak rates. The

TABLE LII  
Adhesive Seal on JPL Cases in PPO 531-801

<u>Cases</u>	5				
<u>Cover Seal Design</u>	1/16 in. chamfer on top and bottom edges of cover and on inside of case top. Top and bottom junction of terminal and cover coated with resin. All mating surfaces sanded with 240 emery cloth.				
<u>Resin</u>	DEN 438-EK85	10.0 g			
	DER 741A	0.85			
	DMP 30	0.45			
<u>Cure</u>	40 hr. at $25 \pm 2^\circ\text{C}$ (inverted)				
	7.5 " " 75 "				
	16 " " 100 "				
<u>Pressure Test</u>	5 Pass				
	(90 psig $25^\circ\text{C}$ )				
<u>Sterilization</u>	(65 psig 120 hr. $135^\circ\text{C}$ )				
Case No.	1	2	3	4	
Pressure loss (psig)	9	9	8	48	
Weight loss (g)	2.95	3.00	3.35	3.27	
Helium leak rate (ml/sec) (1)	$3.4 \times 10^{-8}$	$1.7 \times 10^{-8}$	$1.7 \times 10^{-8}$	$5.1 \times 10^{-8}$	
<u>Electrolyte Slurry</u>	Each case				
	KOH 40 wt. %	50 ml			
	ZnO	5.6 g			
	HgO	0.2			
	Ag Powder	0.1			

(1) ESB-EMED Standard Inspection Specification 2.3.3.3 Figure 2, 10

TABLE LIII  
Adhesive Seal on JPL Cases in PPO 531-801

<u>Cases</u>	5			
<u>Cover Seal Design</u>	1/16 in. chamfer on top and bottom edges of cover and on inside of case top. Top and bottom junction of terminals and cover coated with resin. All mating surfaces sanded with 240 emery cloth.			
<u>Resin</u>	DEN 438-EK85	10.0 g		
	DMP 30	0.42		
<u>Cure</u>	46 hr. at $25 \pm 2^\circ\text{C}$ (inverted case) 20 " " 100 "			
<u>Pressure Test</u>	4 Pass			
(90 psig $25^\circ\text{C}$ )	1 leak at terminal			
<u>Sterilization</u>	(65 psig 120 hr., $135^\circ\text{C}$ )			
Case	1	3	4	5
Pressure loss (psig)	7	11	8	9
Weight loss (g)	3.20	3.24	3.47	3.20
Helium leak rate (ml/sec)	$3.6 \times 10^{-8}$	$4.4 \times 10^{-8}$	$3.6 \times 10^{-8}$	$2.9 \times 10^{-9}$
<u>Electrolyte Slurry</u>				
Each case				
KOH 40 wt. %	50 ml			
ZnO	5.6 g			
HgO	0.2			
Ag Powder	0.1			

TABLE LIV  
Adhesive Seals on JPL Cases in PPO 531-801

Cases	8
Seal Design	Top and bottom edges of cover 1/32 in. chamfer, inside top edge of case 1/32 in. chamfer. All mating surfaces sanded 240 emery cloth. Mating surfaces and top and bottom junctions terminal with resin painted with resin.
Resin	Dow DEN 438-EK85 10.0 g Rohm & Haas DMP 30 0.42
Cure	64 hr. at 25 ± 2°C 4 " " 50 " 4 " " 75 "
Pressure Test	(90 psig 25°C) 8 Pass
Sterilization	(65 psig 120 hr. 135°C)
Case No.	1 2 3 4 5 6 7 8
Total pressure loss (psig)	10 11 10 10 9 9 10 11
Weight loss (g)	3.4 3.3 3.2 3.0 2.5 2.5 2.6 2.6
Helium leak rate (ml/sec) *	1.2 x 10 <sup>-6</sup> 1.7 x 10 <sup>-6</sup> 3.4 x 10 <sup>-6</sup> 1.0 x 10 <sup>-6</sup> 8.7 x 10 <sup>-6</sup> < 7.5 x 10 <sup>-9</sup> 7.5 x 10 <sup>-7</sup> 3.0 x 10 <sup>-8</sup>
Electrolyte Slurry	
Each case	
KOH 40 wt. %	50 ml
ZnO	5.6 g
Ag Powder	0.1

\* USB-EMED Inspection Specification 2.3.3.3 Fig. 2.10.

TABLE LV  
Adhesive Seal on JPL Case in PPO 541-801

<u>Cases</u>	5			
<u>Cover Seal</u>	1/16 in. chamfer on top and bottom edges of cover and inside of case top. Top and bottom junction of terminals with cover coated with resin. All mating surfaces sanded with 240 emery cloth.			
<u>Resin</u>	DEN438-EK85	10.0 g		
	DMP 30	0.42		
<u>Cure</u>	16 hr. at 25 ± 2°C			
	3 "	"	50 "	"
	3 "	"	75 "	"
	16 "	"	100 "	"
<u>Pressure Test</u>	5 Passed			
	(90 psig at 25°C)			
<u>Sterilization</u>	(2 cycles 60 hr. at 135°C 65 psig)			
Case No.	1	3	4	5
Pressure loss (psig)	3	5	20	4
Weight loss (g)	1.53	1.77	1.57	1.80
Helium leak rate *				
(ml/sec)	3.6 x 10 <sup>-8</sup>	1.7 x 10 <sup>-8</sup>	6.1 x 10 <sup>-8</sup>	7.2 x 10 <sup>-8</sup>
<u>Electrolyte Slurry</u>				
Each case				
KOH 40 wt. %	50 ml			
ZnO	5.6 g			
HgO	0.2			
Silver Powder	0.1			

\* ESB-EMED Inspection Specification 2.2.3.3 Figure 2.10

Temperatures  $\pm 2^\circ\text{C}$

Pressures  $\pm 2$  psig

TABLE LVI  
Adhesive Seals on JPL Cases in PPO 541-801 with  
Terminal 1-096

Cases	7
Seal Design	Top and bottom edges of cover 1/32 in. chamfer inside top edge of case 1/32 in. chamfer. All mating surfaces sanded, 240 emery cloth. Mating surfaces top and bottom junctions of terminal with resin painted with epoxy resin.
Resin	Dow DEN 438-EK85 10.0 g Rohm & Haas DMP 30 0.42
Cure	2 hr. at 25 ± 2°C 2.5 " " 50 " 4 " " 75 "
Pressure Test	(90 psig at 25°C) 7 Passed
Sterilization	(65 psig, 2 cycles 60 hr, 135°C) Case No. 1 2 3 5 6 7 10 Total pressure loss (psig) 12 37 4 5 8 10 27 Weight loss (g) 1.57 1.39 1.55 1.52 1.60 1.55 1.41 Helium leak rate 7.7 x 10 <sup>-8</sup> < 4.8 x 10 <sup>-9</sup> 1.9 x 10 <sup>-8</sup> < 4.8 x 10 <sup>-8</sup> 3.5 x 10 <sup>-8</sup> 3.5 x 10 <sup>-8</sup> 9.6 x 10 <sup>-7</sup> (ml/sec) *
Electrolyte Slurry	
Each case	KOH 40 wt. % 50 ml ZnO 5.6 g Ag Powder 0.1 g

\* ESB-EMED Inspection Specification 2.3.3.3 Figure 2.10.

Temperatures + 2°C

Pressures + 2 psig

weight losses on 11 PPO 541-801 cases had an average value of  $1.58 \pm 0.11$  g (standard deviation). Four of 11 cases had helium leak rates greater than  $1 \times 10^{-8}$  ml/sec. The reproducibility of the weight losses casts some doubt on the leak rate results. The other results indicated a satisfactory seal on the JPL cases in PPO 541-801.

#### 4. Ultrasonic Sealing

Ultrasonic techniques have two possible applications in the fabrication of the cell case: (1) sealing cover to case, and (2) driving terminals into the cover. Branson Instrument Company, Danbury, Conn. and Cavitron Ultrasonics, Inc. Long Island City, N. Y. were consulted for designs on case seals and terminal driving respectively. Cases and covers in PPO 531-801 and PS P-1700 were machined to the design specifications and sealed by Branson. All seals leaked at 15-20 psig at room temperature. Silver and titanium terminals were driven into specimens of PPO 531-801 and PS P-1700 by Cavitron. All terminals leaked at 10 psig. Further work with this technique was abandoned because a major development effort would be required to prove or disprove the feasibility of a sealing technique based on ultrasonics.

### V. FABRICATION AND TESTING OF CELLS

#### A. Twenty-Five Ampere-Hour Sealed Cell

##### 1. Objectives

- An analysis of cell components for design values involved in high level shock survival.
- Development and fabrication of non-magnetic 25 and 50 AH sealed cells (Ag-Zn or Ag-Cd) capable of surviving high level shock using heat sterilizable components where possible.
- Test cells at impact shock levels of 5,000 g peak from a velocity of 110 ft/sec and 10,000 g peak from a velocity of 180 ft/sec.
- Development of high impact resistant and heat sterilizable cells and tests to determine failure modes and designs leading to survival of both environmental requirements.

##### 2. Cell Components Stress Analysis Under Shock

Initial design concepts for a prismatic 50 AH sealed cell capable of surviving 5,000 g and 10,000 g impacts called for reinforcement of positive

and negative plates to improve tensile and buckling strength, porous membranes with high tensile strength, and heavily supported cell case walls and seals. Quantitative values of mechanical design parameters were not available for compressive and shear strength of plates or friction forces between cell pack components.

A brief investigation of the mechanical characteristics of typical low rate, high energy density sealed silver-zinc cell plates was undertaken. The tests revealed that:

- Flat compression of a wet charged 160 AH cell pack was 0.065 inch at 4 tons giving a spring rate of 100,000 pounds per inch in a cell pack 1.25 inches in depth along the axis perpendicular to the plane of the plates.
- Edgewise compression of a single wet, charged positive plate from this pack would give a crushing stress of 810 psi.
- Diagonal shear strength of a wet, charged positive plate reinforced with 35 x 40 mesh Ag screen and supported at two corners would be 272 psi shear.
- The coefficient of friction of metallic zinc, charged wet negative plates against a plastic jar wall (Union Carbide polysulfone) decreased from 0.5 at 0.3 psi to 0.3 at 3 psi plate pack pressure.
- Negative plates, even when framed by heat pressing polysulfone plastic onto the grid structure, would fail in tensile shear at 8,900 psi.

### 3. First Generation Cells - Model 325 Family

Three cell types differing in the number of plates, plate thickness, and weight were designed to experimentally determine the variation of shock damage with increasing cell energy density. Table LVII summarizes cell components, weights, and the relative electrochemical performance predicted for each design type: A, high rate-low energy density; B, medium rate - medium energy density; and C, low rate-high energy density. Figure 19 is a schematic showing a cut-away of a Type A cell.

#### a. Structural Design Features

Positive and negative plates were reinforced by polysulfone frames milled from sheet stock and heat pressed onto the negative grids or onto embossed areas of the positive plate as shown in Figures 20 and 21.



TABLE LVII

WEIGHT ANALYSIS OF MODEL 325 CELLS  
TYPES A, B, AND C

A. <u>Physical Characteristic</u>	<u>Cell A</u>	<u>Cell B</u>	<u>Cell C</u>
1. Cell Case (PS), g	69.5	69.5	69.5
2. Cell Covers & Sealing Plugs (PS), g	10.1	10.1	10.5
3. Epoxy Sealant, g	41.5	41.5	41.5
4. Terminals, Hex Nuts & Flat Washer, g	21.6	21.6	21.6
5. Inside Shims (PS), g	12.8	12.8	12.8
6. Positive Plates, g and Number	165. (11)	219. (7)	237. (5)
6.1 Active Ag, g	103.0	180.0	216.
6.2 Positive Plate, g	15.0	31.3	47.4
7. Negative Full Plates, g and Number	127.5 (10)	150.9 (6)	159.4 (4)
7.1 Active ZnO	62.6	97.7	108.7
7.2 Plate Weight	12.8	25.2	39.8
8. Negative Half Plates and Number	18.5 (2)	29.6 (2)	44.1 (2)
8.1 Active ZnO, g	6.3	16.3	30.2
8.2 Plate Weight, g	9.3	14.8	22.1
9. Separator System			
9.1 Positive Absorber (EM-476), g	4.7	3.0	2.2
9.2 Membrane (FSC-3L), g	39.6	26.7	20.4
10. Electrolyte (45%), g	<u>105</u>	<u>100</u>	<u>95</u>
11. Total Weight: gms	615.8	684.7	714
lbs.	1.36	1.51	1.57
B. <u>Electrochemical Characteristic</u>			
1. Theoretical Positive Capacity, AH	51.3	89.6	108
2. Theoretical Negative Capacity, AH	45.4	75.0	91.5
3. Expected Positive Capacity on Chg., AH	30.8	53.9	65.0
4. Expected Negative Capacity on Chg., AH	43.1	71.3	87.0
5. Ratio: C+/C-	.715	.755	.746
6. Expected Output, Watt-Hours	47.7	83.1	99.4
7. Expected Output, WH/lb.	35	55	63

**FIGURE 19**

MODEL 325-X CELL ASSEMBLY

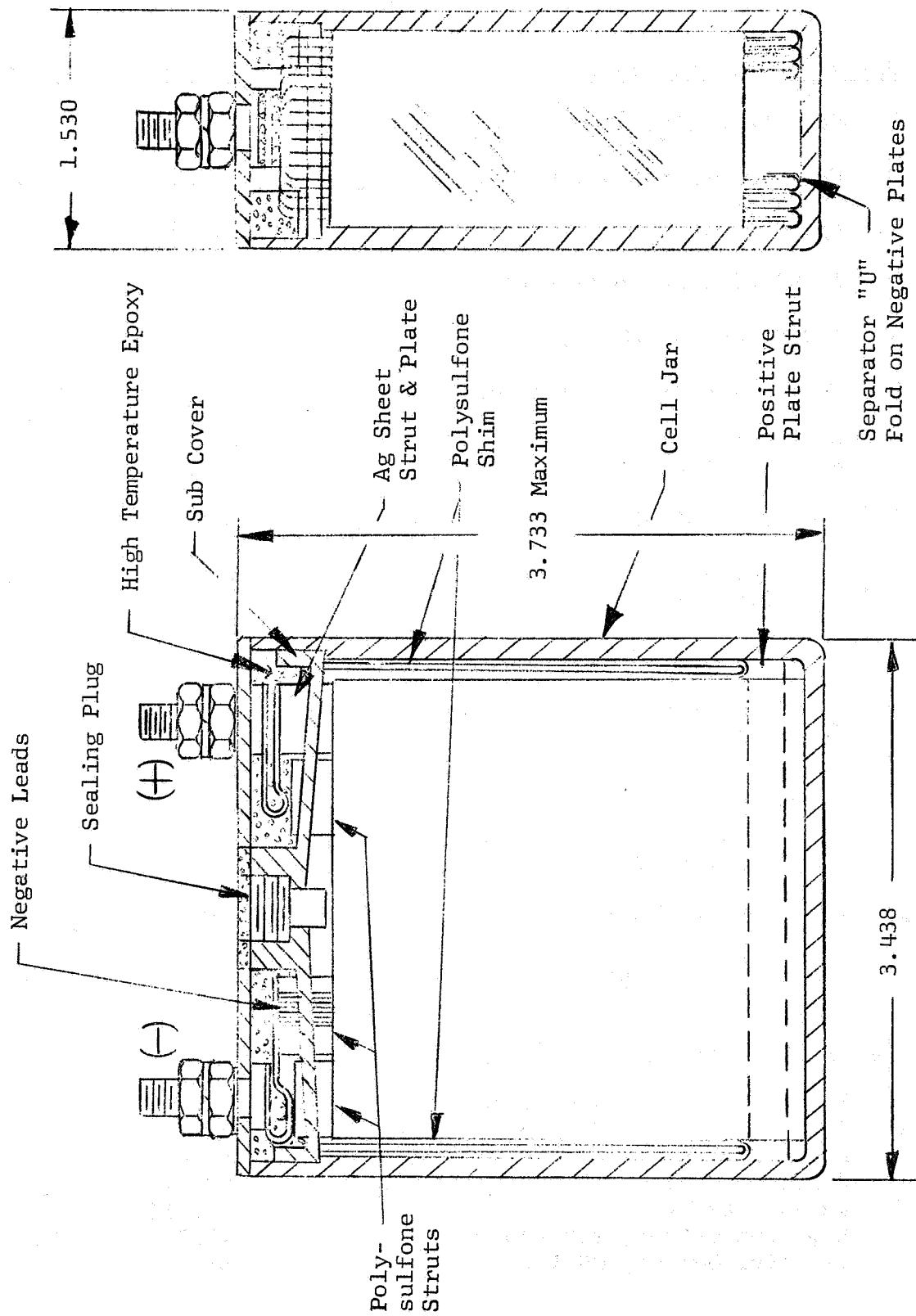


FIGURE 20

MODEL 325-X NEGATIVE PLATE GRID ASSEMBLY

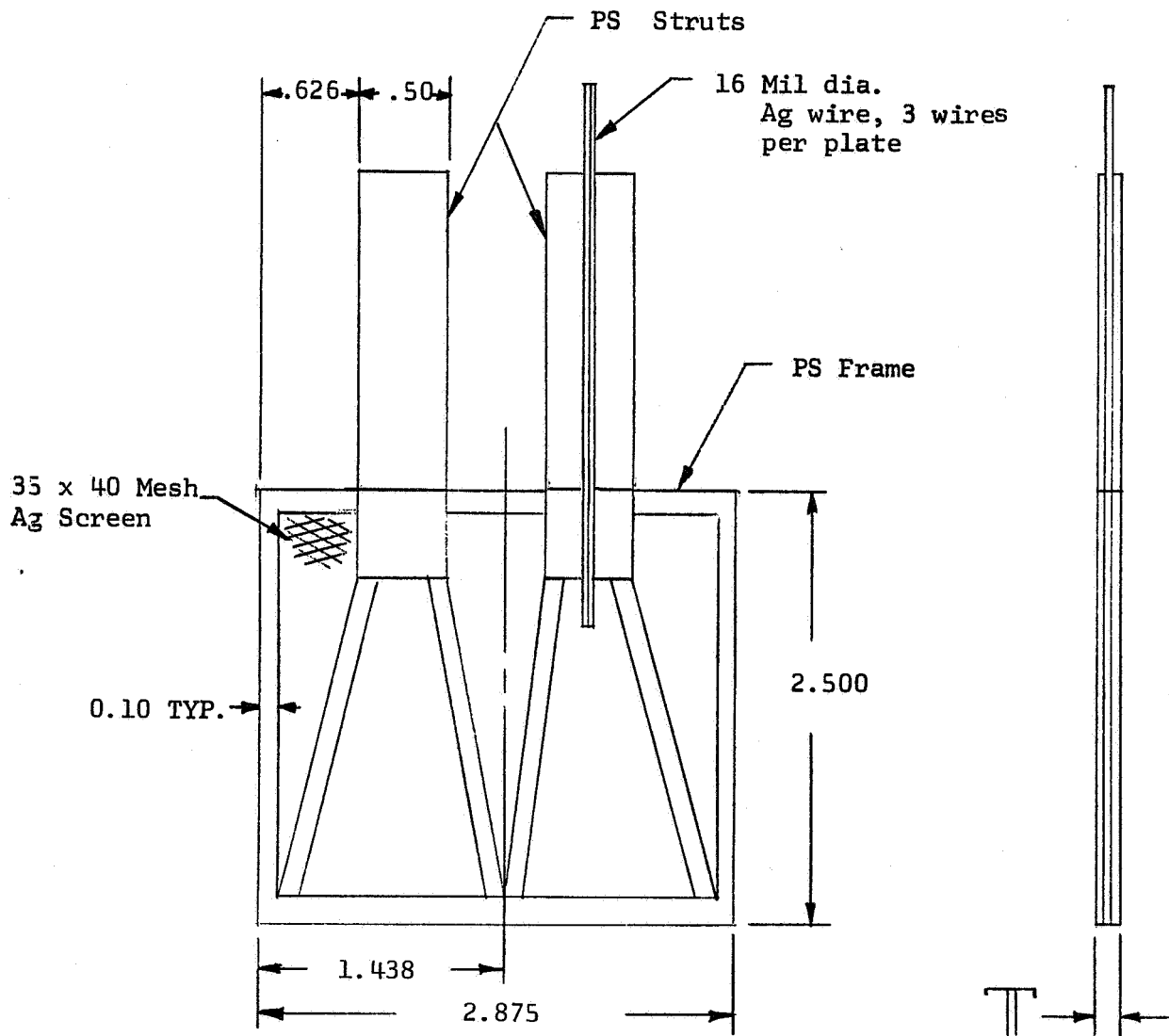
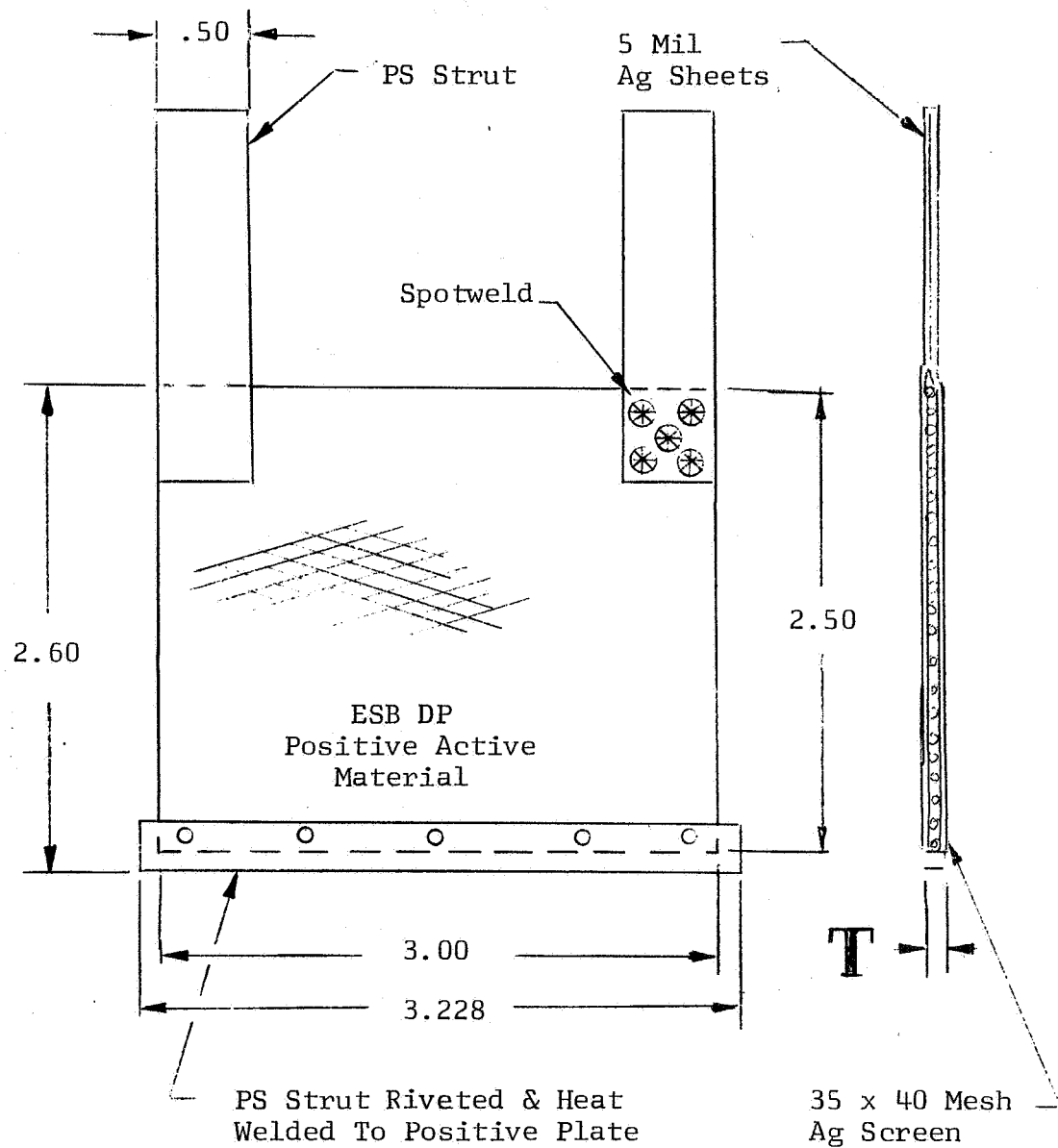


FIGURE 21

MODEL 325-X POSITIVE PLATE ASSEMBLY



Positive plates had load bearing struts at each of 4 corners. One upper strut was an assembly of two 5-mil Ag sheets spotwelded on each side of the active material and then to each other. The other three supports were polysulfone.

Negative plates used 35 x 40 mesh screen as the grid matrix and were placed inside the separator "U" fold suspended by two upper polysulfone struts from the cell cover seal. The heavier positive plates were outside the "U" fold to permit anchoring their bottom corners beneath side shims wedged below the cell seal and above the corner lugs of each plate.

Cell jars were either Union Carbide P-1700 polysulfone or General Electric Polyphenylene oxide 531-801. Each contained a subcover slotted to receive positive and negative plate struts. Electrical connections to cell terminals were made above the subcover and below the top cover. Intervening void was filled with an epoxy encapsulant. This massive subcover assembly anchored the heavy plate pack and prevented concentrated stresses on the cell terminals during shock.

Cells were activated under vacuum and sealed with a threaded sealing plug wetted with epoxy.

#### b. Materials and Process Development

Cell cases, subcovers, and sealing plugs were molded in two heat sterilizable materials: Polysulfone P-1700 and polyphenylene oxide 531-801. PPO was considered a back-up to PS. Neither material molded well in wall thicknesses of 90 mils and flow distances of 2-3 inches. Many surface blemishes, flow lines, and char spots were obtained. Only the best cases were selected for use in the Model 325 cells.

A major problem was encountered in developing an epoxy seal around the polysulfone struts projecting into the subcover-seal. Optimum properties were achieved finally using Furane Epocast 221-927 cured progressively for 2 hours at 70°C, 1 hour at 90°C, and 1 hour at 150°C.

Heat pressing of polysulfone reinforcing struts and frames onto plate structures required extensive process development. Final conditions chosen were:

- Negative grid framing - heat for 4 minutes at 232°C to drive off water, then press between teflon sheets for 1.0 minute at  $232 \pm 2^\circ\text{C}$ .
- Positive plate struts - dry sheet at 288°C for 4 minutes, then heat press for 5.0 minutes at  $288 \pm 3^\circ\text{C}$ . Hot pressed assemblies were cooled between ceramic plates to eliminate

warpage and annealed flat for 4 hours at  $162 \pm 2^\circ\text{C}$  after all machining to drawing tolerances. Detailed procedures are given in Reference (1).

#### c. Stress Analysis of Model 325 Plate Structures

A stress analysis of plate structures was performed to predict the outcome of shock tests on the Model 325 cells at JPL and point out the most likely failure modes. Shock requirements used for this analysis were 10,000 g for 0.1 msec and 5,000 g for 3 msec. As indicated by Crede, the 5,000 g shock for 3 msec is more severe than the 10,000 g shock for 0.1 msec. Dynamic response of a cell structure can amplify the actual shock input by a factor of 2 for long impulses (2).

Calculated stresses at 5,000 g loading for plate stress points in cells Types A, B, and C (plate weight increases from A to B to C) are summarized in Table LVIII. The calculated stresses must be doubled if dynamic response does amplify by a factor of 2:1. Damage factors listed in the table are the ratio of the calculated stress during the 5,000 g shock to the mean strength of the material. Damage was predicted at sites where damage factors exceed the value of 1.0.

#### d. Shock Tests of Model 325 Cells

##### (1) Shock Test Method

Ten cells of each Type A, B, and C were shocked on the JPL sling shot impact tester described by Lonberg (3). No single cell was subjected to more than a single shock to simplify diagnosis of shock damage mechanisms accurately.

Shock levels by cell type and serial number were calculated from measured cell velocities "V" and stopping distances "s" determined by penetration of the impact carriage nose into a metal target, using the equation

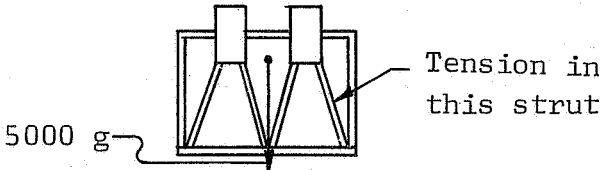
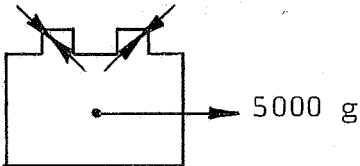
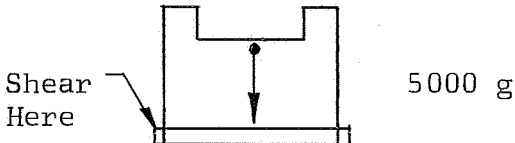
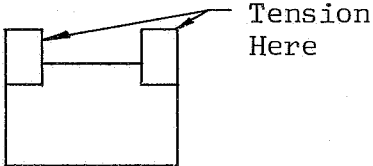
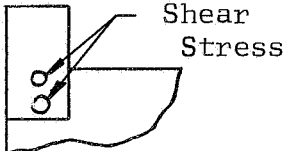
$$\text{mean "g" level} = V^2 / 2s$$

Peak "g" levels were measured in some tests by accelerometers monitored on an oscilloscope. Shock directions and levels are given in Table LIX.

The deterioration of loaded voltage was the primary criteria for internal damage. Breakage of plate tab wires, isolation of plates, and decrease

- 
- (1) First Annual Report, Contract 951296, September 24, 1966 to December 31, 1966, p. 95.
  - (2) C. E. Crede - Specification of Shock Tests, National Aerospace Engineering and Manufacturing Meeting, Los Angeles, California, October 8-12, 1962 (SAE Preprint 585B).
  - (3) J. O. Lonberg - High Impact Survival, JPL TR32-647, September 30, 1964, Figures 6, 7, 8, 9 - 129 - and Table 2.

TABLE LVIII  
STRESSES AT 5000 "G" FOR SELECTED POINTS  
ON THE MODEL 325 CELL PACK

Item	Cell Type	Stress (psi)	Material	Damage Factor
1. Stress in angle struts of negative grid	A	26,800	Silver	1.22
	B	17,500	PS	1.75
	C	14,500	PS	1.45
				
2. Stress in support tabs of negative plates	A	36,000	Silver	1.63
	B	15,000	PS	1.50
	C	12,500	PS	1.25
				
3. Stress in lower support of positive plates	A	11,400	Silver	0.52
	B	6,400	PS	0.64
	C	10,380	PS	1.03
				
4. Stress current tabs positives	A	7,400	Silver	0.34
	B	16,600	Silver	0.75
	C	26,200	Silver	1.19
				
5. Stress in PS rivets in positive tabs	A	2,350	PS	0.11
	B	5,280	PS	0.53
	C	8,340	PS	0.83
				
6. Bearing stress in silver plage at PS rivet	A	6,600	Silver Oxide	
	B	7,400		
	C	7,600		
7. Bond stress in potting at support tabs, negatives	A	880	PS to Potting	
	B	2,400	PS to Potting	
	C	4,000	PS to Potting	
8. Bond of potting to top wall of cell jar	A	1,620	PS to Potting	
	B	1,800	PS to Potting	
	C	1,875	PS to Potting	

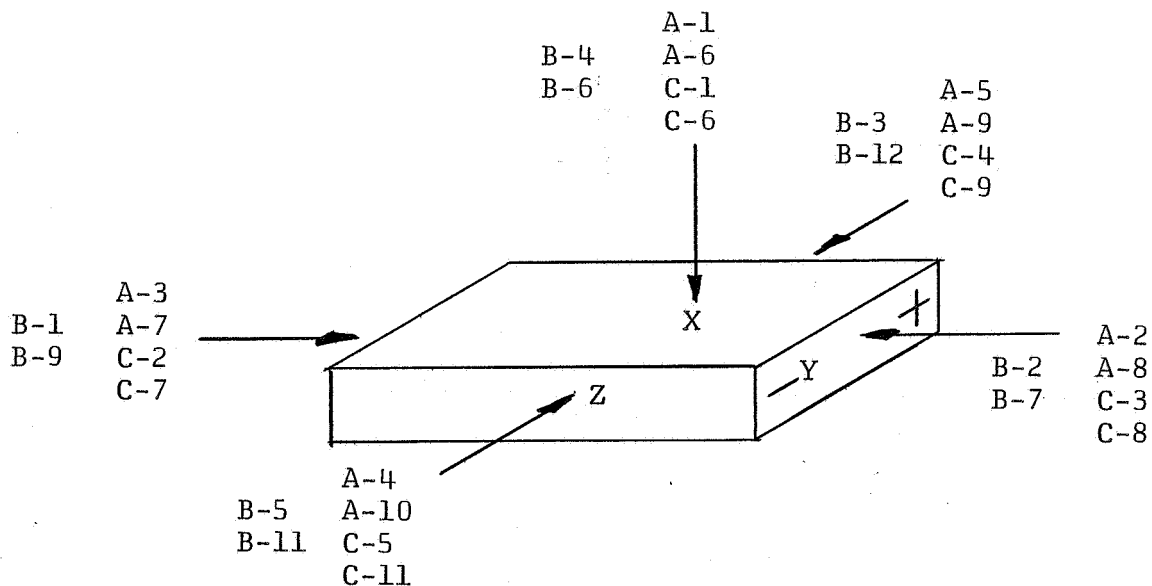
PS = Union Carbide P-1700 Polysulfone.

TABLE LIX

## MODEL 325 SEALED Ag-Zn CELL IMPACT SHOCK LEVELS

## Cell Type

A (High Rate)			B (Intermediate Rate)		C (Low Rate)		
S/N	<u>"g" Level</u>		S/N	<u>"g" Level</u> <u>Mean</u>	S/N	<u>"g" Level</u>	
	<u>Mean*</u>	<u>Peak**</u>				<u>Mean</u>	<u>Peak</u>
1	3200	4500	1	6610	1	4700	5500
2	2880	4000	2	6460	2	4740	5500
3	3080	4500	3	6560	3	4740	6000
4	3200	5000	4	6170	4	4850	5800
5	3300	4000	5	6620	5	4720	5500
6	6620	--	6	4380	6	6450	8000
7	6600	--	7	4380	7	6500	8000
8	6600	--	9	4680	8	6480	8000
9	6620	--	11	4400	9	6520	8000
10	6520	8000	12	4370	11	6630	9000



(\*)  $g = V^2/2s$  where V and s are measured.

(\*\*) Observed with accelerometer.



in active surface area should give lower closed circuit voltages. Tables LX to LXII summarize loaded voltage data obtained before and after the shock tests.

## (2) Relative Damage and Failure Mechanisms

Relative damage and failure modes are given in Table LXIII for the three cell types with brief recommendations for design improvements. Some failure modes were common to all three cell designs:

- Cell case walls failed in corners. Cell wall thicknesses and internal corner radii need to be increased.
- Epoxy bonds between subcovers and jar walls (Epocast 221/927) sheared in the vertical "y" velocity vector permitting the entire subcover assembly to settle into the jar and then spring back. The subcover should be pinned to the case.
- Polysulfone positive and negative plate struts broke in tension at the epoxy to subcover interface with increasing frequency at higher "g" levels and plate weights.
- Fibrous sausage casing (3L FSC) separators were creased and cut slightly at bottom of "U" folds at the higher shock loadings.
- No cells shorted.
- Compression failure of silver sheet positive tabs. Tabs must be reinforced with a stiffer material to prevent buckling.

Positive active material was damaged differently in the three cell designs. In the thin plate high rate cells (Type A) the plate wrinkled with little, if any, loss of active material. In the intermediate rate cells (Type B) active material failed in lateral compression and material flaked off at the juncture of plate and strut. Lower polysulfone anchors buckled in compression and were ripped off downward when shocked in the vertical velocity vector. The heaviest plates of low rate cells, Type C, were severely damaged around the strut to active material interface. Substantial active material flaked off. Thus, increasingly thick plates, which are necessary to obtain high energy densities or watt-hours per pound and watt-hours per in<sup>3</sup> of cell, lead to greater stiffness of plate structure, severe fractures, and dangerous flaking off of active material.

Stiffness of plates is directly proportional to the moment of inertia which is proportional to the cube of the plate thickness. Type B positive plates

TABLE LX

LOADED VOLTAGES OF TYPE "A" CELLS BEFORE AND  
AFTER SINGLE SHOCKS

Cell S/N	Voltages After 5 Second Current Pulses At														"g" Level
	0 Amps		2 Amps		10 Amps		20 Amps		30 Amps		40 Amps				
	Before	After	Before	After	Before	After	Before	After	Before	After	Before	After			
1	1.858	1.853	1.707	1.684	1.496	1.482	1.411	1.411	1.411	1.342	1.340	1.278	1.280		
2	1.857	1.850	1.685	1.664	1.485	1.477	1.406	1.408	1.344	1.340	1.286	1.283		3	
3	1.857	1.849	1.675	1.638	1.482	1.489	1.403	1.427	1.342	1.355	1.280	1.302		0	
4	1.857	1.850	1.686	1.656	1.497	1.497	1.418	1.436	1.350	1.377	1.291	1.324		0	
5	1.858	1.852	1.684	1.615	1.491	1.484	1.412	1.427	1.354	1.369	1.294	1.317			
6	1.856	1.854	1.635	1.636	1.472	1.502	1.389	1.441	1.336	1.380	1.274	1.322			
7	1.856	1.854	1.689	1.681	1.491	1.514	1.407	1.456	1.355	1.397	1.295	1.343		6	
8	1.856	0.734	1.672	**	1.483	**	1.401	**	1.347	**	1.285	**		6	
														0	
9	1.856	1.853	1.713	1.697	1.497	1.513	1.409	1.454	1.350	1.390	1.285	1.338			
10	1.856	1.853	1.713	1.681	1.500	1.504	1.409	1.437	1.355	1.360	1.292	1.300			

(\*) Model 325 cell Type "A".

(\*\*) Broken plate leads.

TABLE LXI

LOADED VOLTAGES OF TYPE "B" CELLS BEFORE  
AND AFTER SINGLE SHOCKS

Cell S/N	Voltages After 5 Second Current Pulses At										"g" Level
	0 Amps		2 Amps		10 Amps		20 Amps		30 Amps		
	Before	After	Before	After	Before	After	Before	After	Before	After	
1*	1.860	1.857	--	1.706	--	1.418	--	1.236	1.233	1.094	6 5 0 0
2*	1.860	1.857	--	1.731	--	1.469	--	1.310	1.243	1.181	
3*	1.859	1.843	--	1.700	--	1.443	--	1.312	1.225	1.170	
4	1.860	1.855	--	1.723	--	1.471	--	1.322	1.226	1.222	
5	1.861	1.856	--	1.740	--	1.495	--	1.370	1.230	1.244	
6	1.855	1.854	--	1.764	--	1.572	--	1.439	--	1.353	4 4 0 0
7	1.858	1.855	--	1.764	--	1.563	--	1.411	--	1.300	
9*	1.858	1.855	--	1.784	--	1.619	--	1.474	--	1.359	
11	1.857	1.855	--	1.756	--	1.551	--	1.431	--	1.333	
12	1.858	1.853	--	1.760	--	1.563	--	1.441	--	1.342	

(\*) Polysulfone cell case cracks.

TABLE LXII  
LOADED VOLTAGES OF TYPE "C" CELLS BEFORE AND  
AFTER SINGLE SHOCKS

Cell S/N	Voltages After 5 Second Current Pulses At														"g" Level
	0 Amps		2 Amps		10 Amps		20 Amps		30 Amps		40 Amps				
	Before	After	Before	After	Before	After	Before	After	Before	After	Before	After			
1	1.861	1.850	1.690	1.661	1.471	1.448	1.339	1.322	1.249	1.284	1.150	1.196	4 7 0 0		
2	1.857	1.851	1.632	1.645	1.423	1.431	1.285	1.298	1.199	1.176	1.092	1.065			
3	1.862	1.856	1.679	1.677	1.456	1.443	1.318	1.294	1.234	1.132	1.130	1.000			
4	1.856	1.851	1.628	1.645	1.431	1.463	1.299	1.355	1.210	1.248	1.100	1.155			
5	1.859	1.854	1.667	1.679	1.453	1.475	1.319	1.362	1.232	1.244	1.120	1.147			
6	1.858	1.854	1.612	1.635	1.440	1.481	1.318	1.386	1.230	1.290	1.125	1.201	6 5 0 0		
7	1.860	1.853	1.604	1.609	1.438	1.398	1.309	1.238	1.215	1.074	1.105	0.933			
8	1.863	1.849	1.692	**	1.471	**	1.333	**	1.240	**	1.140	**			
9	1.856	1.850	1.629	1.631	1.446	1.453	1.320	1.337	1.230	1.220	1.120	1.119			
11	1.865	1.840	1.696	1.616	1.480	1.371	1.350	1.187	1.250	1.003	1.150	0.840			

(\*) Model 325 cell Type "C".

(\*\*) Broken plate leads.

TABLE LXIII

COMPARISON OF IMPACT TEST DAMAGE  
MODEL 325 TYPE A, B, AND C CELLS

Item	Type "A"	Type "B"	Type "C"	Recommendation
Jar	2 PPO jars failed in corners. Jars appeared to be poorly molded.	4 PS jars cracked in corners.	2 PPO jars cracked severely in corners	An alternately designed case should be strengthened by thicker walls.
Subcover-Epoxy Assembly	Two broken subcovers. Several cases had broken bond between jar and subcover.	No broken PS subcovers. General breakage of epoxy bond.	Two broken PPO subcovers with general breakage of epoxy bond.	Increase support of subcover and increase bond area.
Polysulfone (PS) Struts	Nearly all struts broke, usually at the subcover junction.		→	Increase cross-sectional area and use stronger PPO mat'l.
Silver Lugs	No silver lugs broke but most lugs wrinkled severely.		→	Support positive lead in compression with heat pressed PPO supports.
PS Bottom Supports	Moderate damage due to crushing against jar wall.	Moderate damage due to crushing and tensile force.	Severe damage due to heavy plate design.	Support ends of bottom supports against buckling with heat welds or epoxy.
Positive Plate Damage Around structural Supports	Light to moderate damage around silver lugs and PS struts.	Moderate damage to plate material and grid.	Severe damage to both plate mat'l. and grid.	Use relatively light plate design and possibly strengthen area with silver screen.
Positive Plate Material	Heavy wrinkling due to low buckling strength of thin plates.	Light wrinkling and little compression of plate material.	Large cracks across plate with flaking off of active mat'l.	Use medium to light weight plates.
Negative Plate Material	Light wrinkling of plate and frame.	Light wrinkling of plate and frame.	No damage to plate or frame.	Increase thickness of frame to add strength to plate.
Negative Plate Leads	Most of leads intact.	Most of leads intact.	Large portion of leads broken.	Use silver screen thru PPO supports.
FSC Separator (3L)	No damage.	No damage.	No damage.	Use RAI separator for heat sterilization

were 8 x stiffer than Type A positive plates. Plate thicknesses intermediate to Type A and B plates thus appear attractive for reducing active material failure in compression.

e. Electrical Characteristics of Model 325 Type  
A, B, and C Cells

Five cells of each type were charge/discharge cycled to determine voltage and capacity characteristics through the flight temperature range of 0°C to 65°C specified in Paragraph 3.4.6.2 of JPL Design Specifications GMP-50436-DSN-A and GMP-50437-DSN-A, dated 23 August 1965. The discharge and charge profiles were as follows:

- Discharge profile
  - Pulse loads -
    - One pulse load of 2, 10, 20, 30 and 40 amperes for 5 seconds duration at each current at start of test and at steady voltage state.
  - Continuous loads -
    - 10 amperes current to end voltage of 1.30 volt/cell, then reduce current to 2 amperes and discharge to end voltage of 1.30 volt/cell.
  - Discharge temperature -
    - For cycles 1 through 7 the sequence 27°C, 10°C, 65°C, 0°C, 49°C, 27°C.
- Tapered constant current charge profile at room ambient:
  - 1.0 ampere to 1.95 v/cell, then
  - 0.5 ampere to 1.95 v/cell, then
  - 0.1 ampere to 1.95 v/cell.

(1) Cycle Test Results

The effect of temperature from 0°C to 65°C on cell voltages of cells Type A, B and C is shown in Figures 22, 23 and 24, respectively. The discharge capacity and energy characteristics of the three cell types are shown in Table LXIV. The energy density in WH/lb of cell weight and WH/in<sup>3</sup> of cell volume increases from Type A to Type C. All cell types had a common separator system (3L FSC) and were activated with 40% KOH electrolyte. Figures 22, 23 and 24 show that discharge currents cannot exceed 10 amperes to obtain cell voltages greater than 1.30 V at 0°C on any one of the three types of cells.

(2) Charged Stand Tests

One cell of each type was stored for 31 days at 49°C (120°F) and then discharged through the test profile at 27°C. Table LXV summarizes test data and the calculated capacity losses, which averaged 7.0% per month for the three cells.

FIGURE 22

VOLTAGE CHARACTERISTICS MODEL 325 TYPE "A" CELLS

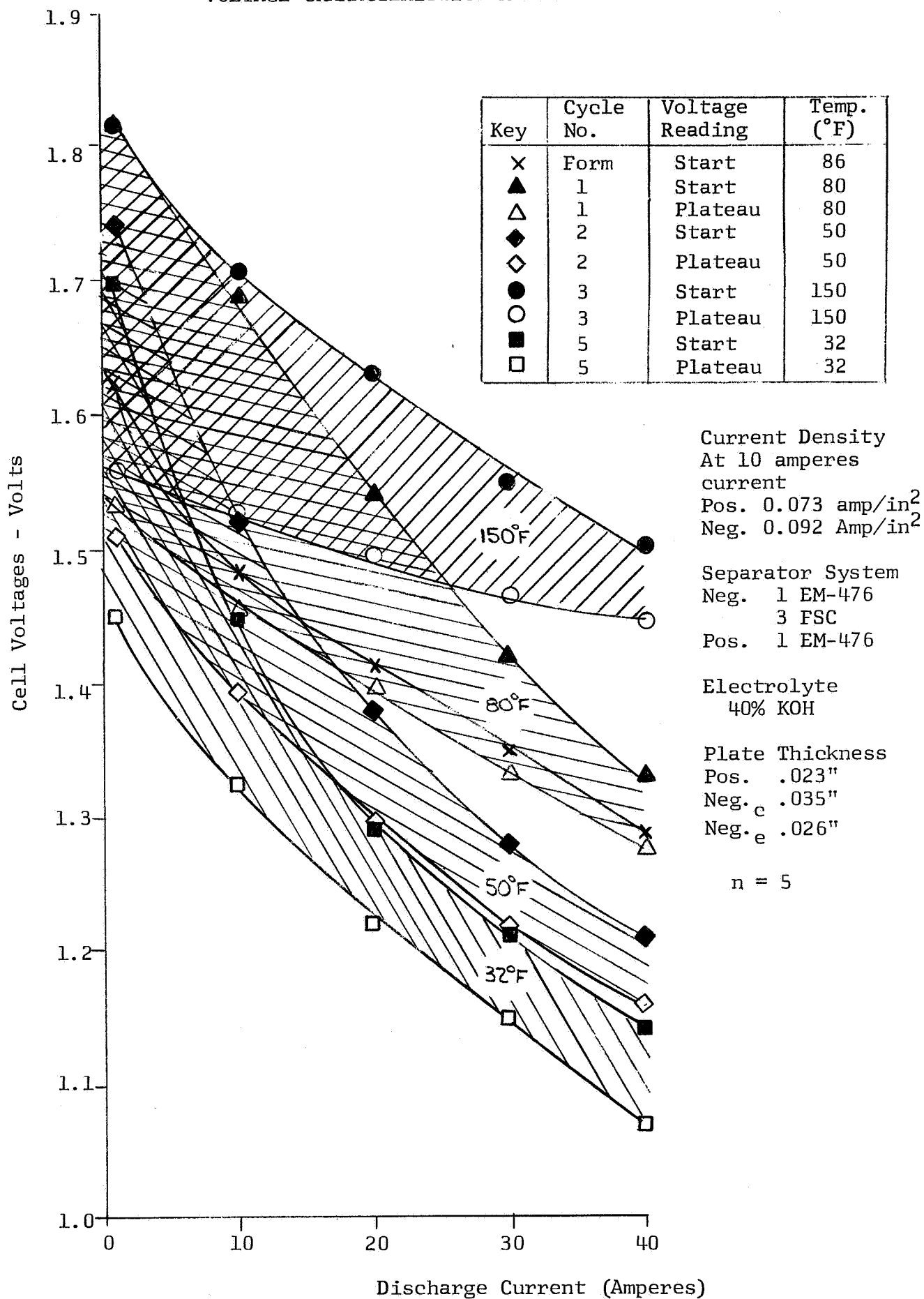


FIGURE 23

VOLTAGE CHARACTERISTICS MODEL 325 TYPE "B" CELLS

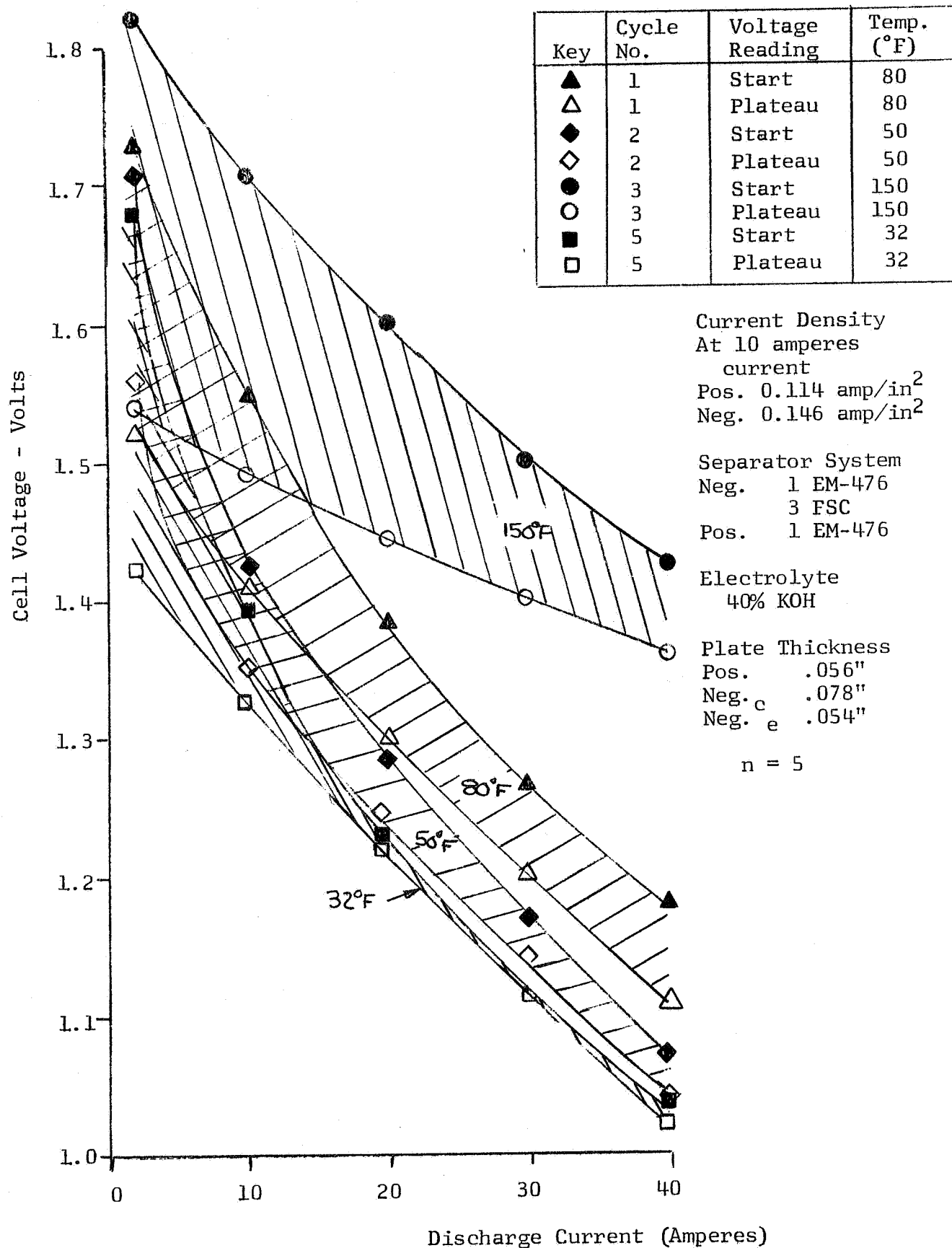




FIGURE 24

VOLTAGE CHARACTERISTICS  
MODEL 325 TYPE "C" CELLS

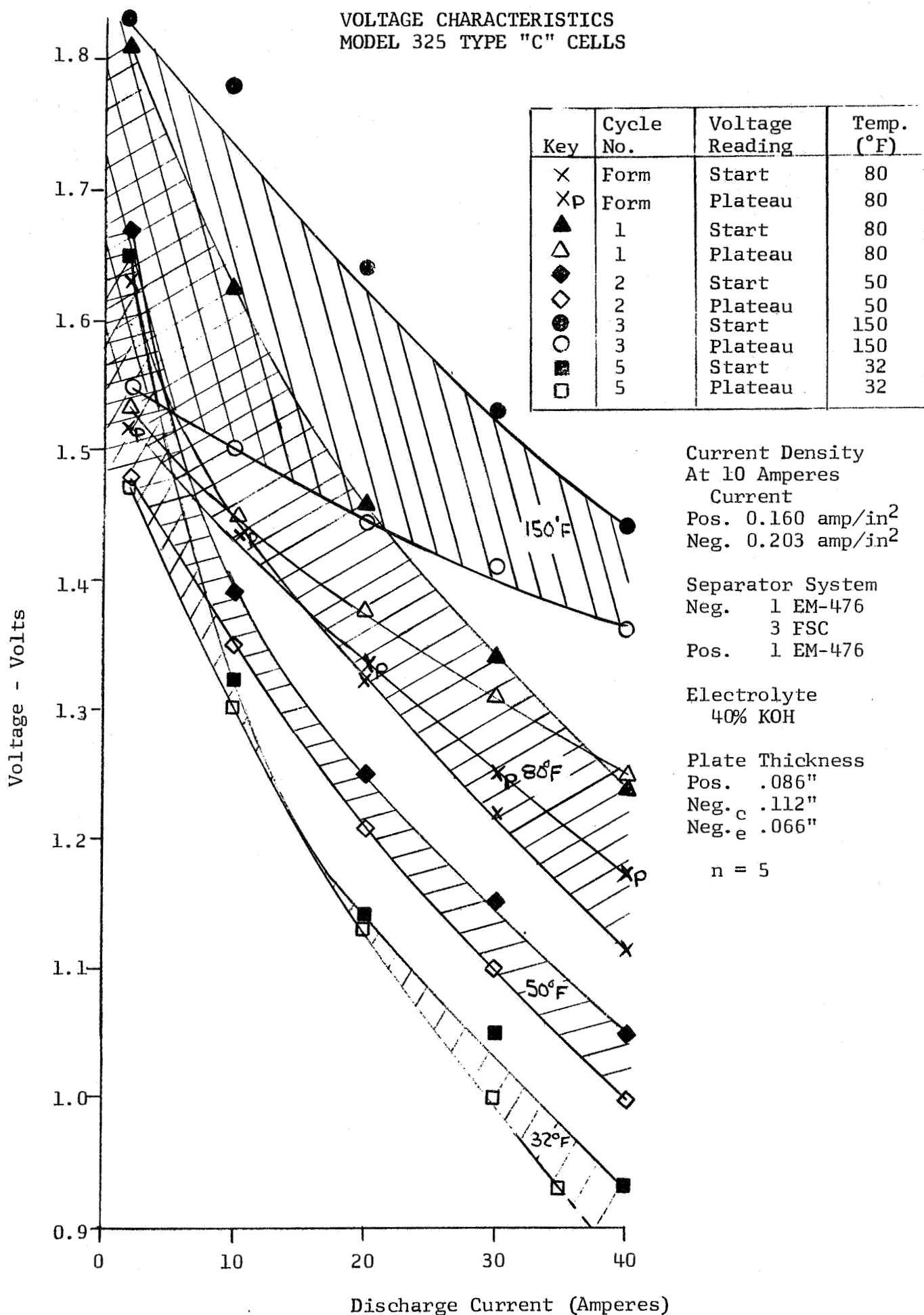


TABLE LXIV

DISCHARGE CAPACITY AND ENERGY  
MODEL 325 CELLS, TYPE A, B AND C

Cell Type	Cycle No.	Temp. (°F)	Average Voltage		Capacity		Total AH	Energy (WH)	Energy Density (WH/lb)
			V@ I=10A	V@ I=2A	AH@ I=10A	AH@ I=2A			
A	Formation	86	1.407	1.431	19.2	6.2	25.4	35.8	25.6
	1	80	1.419	1.383	24.6	3.4	28.0	39.6	28.2
	2	50	1.373	1.412	18.3	4.1	22.4	31.0	22.1
	3	150	1.505	1.441	29.5	5.9	35.4	52.9	37.8
	4	80	1.464	1.459	20.2	12.0	32.2	47.8	34.1
	5	32	1.323	1.367	14.6	6.9	21.5	28.9	20.6
	6	120	1.495	1.414	30.2	1.9	32.1	47.8	34.5
	7	80	1.447	1.426	21.8	5.8	27.6	39.8	28.4
B	Formation	86	1.388	1.431	24.1	8.8	32.9	46.0	29.2
	1	80	1.436	1.439	29.0	15.8	44.8	64.4	40.8
	2	50	1.373	1.452	12.0	31.6	43.6	62.2	39.5
	3	150	1.493	1.408	46.6	14.2	60.8	89.7	56.8
	4	32	1.239	1.226	22.9	10.0	32.9	40.6	25.7
	5	120	1.475	1.420	47.4	3.9	51.3	75.5	47.8
	6	80	1.443	1.451	43.4	5.9	48.3	69.8	44.1
C	Formation	80	1.408	1.412	47.8	12.6	60.4	85.0	53.8
	1	80	1.453	1.437	51.8	12.5	64.3	92.9	58.7
	2	50	1.356	1.426	26.7	30.5	57.2	79.6	50.2
	3	150	1.495	1.410	61.0	3.3	64.3	95.8	60.6
	4	80	1.456	1.407	56.3	5.7	62.0	90.0	56.9
	5	32	1.237	1.205	43.4	14.3	57.7	70.8	44.7
	6	120	1.480	1.418	53.8	6.6	60.4	88.8	56.1
	7	80	1.439	1.430	52.8	7.8	60.6	86.9	54.9
Design Parameters				Unit		Cell Characteristic			
						A	B	C	
Mean Capacity				AH		29.2	46.6	62.3	
Mean Energy				WH		42.4	67.1	89.9	
Weight Cell				Lb.		1.40	1.58	1.58	
Energy Density				WH/lb.		30.3	42.5	56.8	
				WH/in <sup>3</sup>		2.2	3.5	4.6	

Cell volume = 19.4 in<sup>3</sup>. (1.52 x 3.40 x 3.75)

TABLE LXV

WET CHARGED STAND CAPACITY LOSSES MODEL 325 CELLS  
30 DAYS AT 49°C

Cell Type & S/N	Wet Charged Stand		Discharge Characteristics					Capacity Loss	
			Mean Voltage		Capacity				
	Time Days	Temp. °C	10A	2A	10A	2A	Total		
			Volts	Volts	AH	AH		AH	
325 A (13)	3	25	1.437	1.410	26.6	3.3	29.9	1.3	4.3
	31	49	1.436	1.438	20.2	8.4	28.6		
325 B (15)	2	25	1.436	1.395	57.2	1.6	58.8	1.5	2.6
	31	49	1.434	1.433	48.4	8.9	57.3		
325 C (13)	5	25	1.439	1.430	52.8	7.8	60.6	9.1	15.0
	31	49	1.389	1.435	42.5	9.0	57.5		
All									7.3

Separator system: (+) to (-)

1L EM-476

3L FSC

1L EM-476

Electrolyte: 40% KOH

#### 4. Second Generation Cells - Model 334 Design

##### a. Objectives

The Model 334 cell design combined in theory for the first time both a capability for heat sterilization and an improved capability for the high impact test. Major design changes incorporated:

- Heat sterilizable RAI 116 separator membrane (5L) to replace non-heat sterilizable 3L - FSC.
- PPO 681-111 heat pressed plate reinforcements to replace polysulfone stress crazed by epoxies.
- Strengthened negative plate framing and positive plate struts.
- Higher shear strength epoxy seals and a subcover to cell jar seal combining shear and butt joints for improved impact strength.
- PPO 531-801 cell jars replacing polysulfone P-1700 jars.

##### b. Cell Design and Process Development

A list of components for the Model 334 heat sterilizable high impact cell is presented with dimensions, weights, and material composition in Table LXVI. An assembly sketch is given as Figure 25.

Cell jars and top cover were PPO 531-801 sealed to the impact load bearing PPO 681-111 subcover with Dow epoxy DEN 438-EK85 (5%<sub>w</sub> DMP 30 catalyst). Outer sealing rims were also PPO 681-111 cemented with the same epoxy. A basic improvement in impact resistance was achieved by the overlap of the subcover on the jar wall which anchored the subcover to the jar substantially for both vertical shock directions. The outer sealing rim was a vital reinforcement to the cell seal and its structure.

Nine positive plates were reinforced with heat pressed sheet PPO 681-111 as shown in Figure 26 and anchored by both top struts and the bottom support lugs. One "U" fold layer of EM-476 served as a positive plate absorber. Ten negative plates were inserted in the open ends of five closed "U" folds of 5L RAI-116 membrane. Each negative grid was reinforced with sheet PPO 681-111 heat pressed onto 35 x 40 mesh Ag screen. A new "M" design relocated the supporting struts from inboard to the upper plate corners increased active plate area and strut tensile strengths.

Plate struts protruded into windows in the subcover and were sealed with a thixotropic epoxy to the subcover. Lead connections to terminals were made before the final epoxy potting operation.

TABLE LXVI  
MODEL 334 CELL DESIGN

Cell Component	No. In Cell	Material	Dimensions, Inches				Wt. Gms.
			L(in.)	W(in.)	H(in.)	T(in.)	
1. Cell Case	1	PPO 531-801	1.52	3.44	3.66	0.10	64.0
2. Subcover	1	PPO 681-111	1.50	3.42	0.38	--	16.0
3. Top Cover	1	PPO-531-801	1.52	3.44	0.50	0.10	15.0
4. Cover Plate	1	PPO-681-111	1.72	3.62	0.13	--	12.5
5. Sealing Shims							
(a) End	2	PPO 681-111	3.58	1.00	--	0.09	11.2
(b) Side	2	PPO 681-111	1.50	1.00	--	0.09	4.9
6. Side Shims	2	PPO 681-111	1.29	--	3.25	0.09	11.8
7. Adhesive	bulk	Epoxy					35.0
8. Sealant	bulk	Epoxy					8.0
9. Cell Pack							
(a) Positive Blanks	9	Porous Ag	--	3.00	2.50	0.045	228.6
(b) Positive Supports							
Top	18	PPO 681-111	--	1.50	1.33	0.045	28.8
Bottom	9	PPO 681-111		3.20	0.31	0.045	7.8
(c) Positive Absorber	9	EM-476	--	3.13	6.06	0.003	4.0
(d) Negative Membrane	5	RAI-116	--	31.80	6.30	0.0014	22.0
(e) Negative Retainer	9	EM-476	--	7.00	5.12	0.003	5.8
(f) Center Negatives	8	AnO-"X"	--	2.89	2.50	0.065	117.6
(g) Center Negative							
Supports	8	PPO 681-111	--	2.85	3.56	0.040	52.0
(h) End Negatives	1	ZnO-"X"	--	2.89	2.50	0.038	7.4
(i) End Negative							
Supports	1	PPO 681-111	--	2.85	3.56	0.026	4.1
10. Electrolyte, 88 ml/cell	bulk	40% KOH	--	--	--	--	123.0
11. Hardware (Terminals, nuts, washers)							24.0
12. Cell Dimensions							
(a) Overall		--	1.73	3.63	4.80	--	--
(b) Case Only		--	1.52	3.44	4.42	--	--
13. Cell Weight, Total		--	--	--	--	--	803

FIGURE 25

ASSEMBLY SKETCH OF EPOXY-SEALED  
MODEL 334

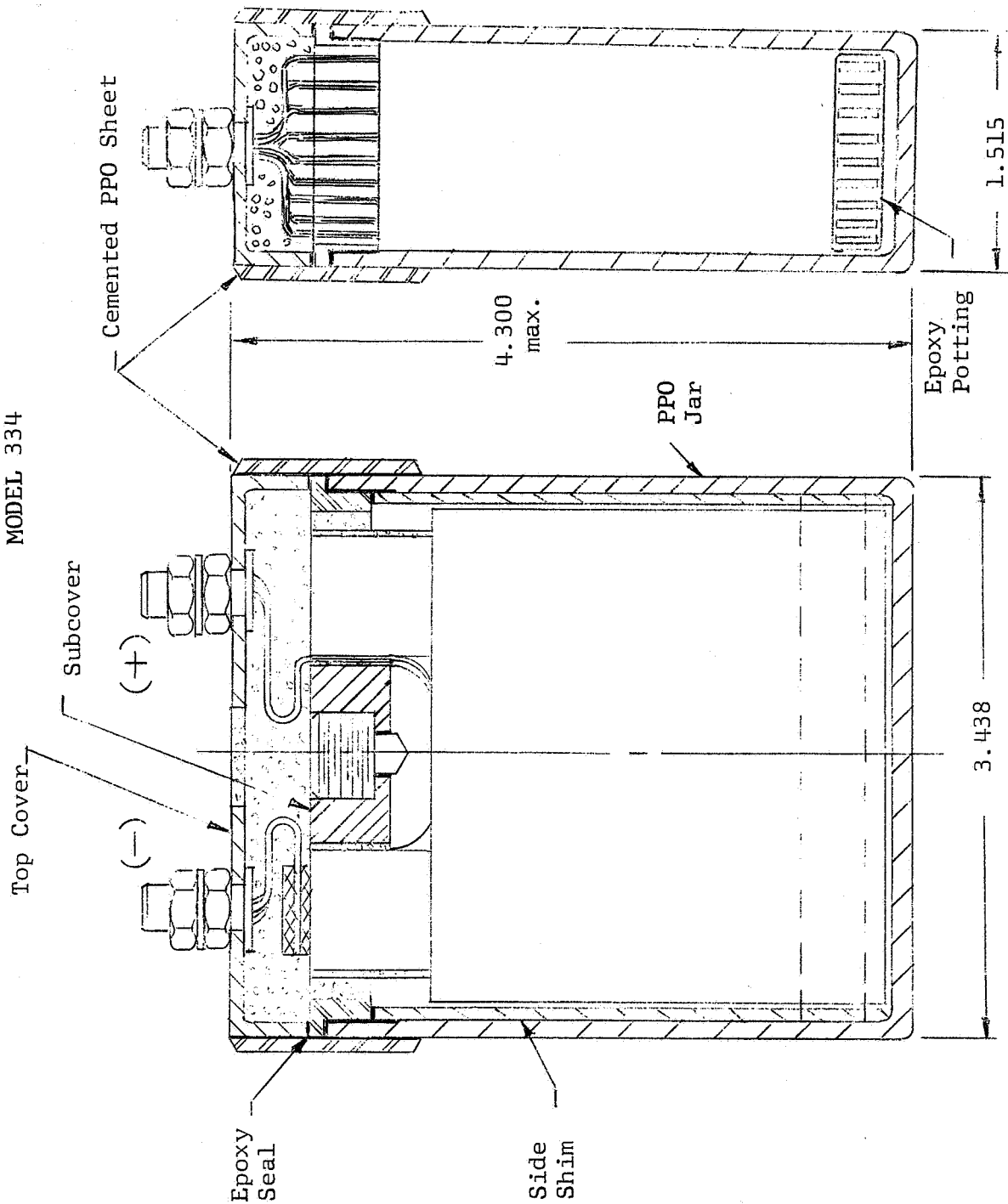
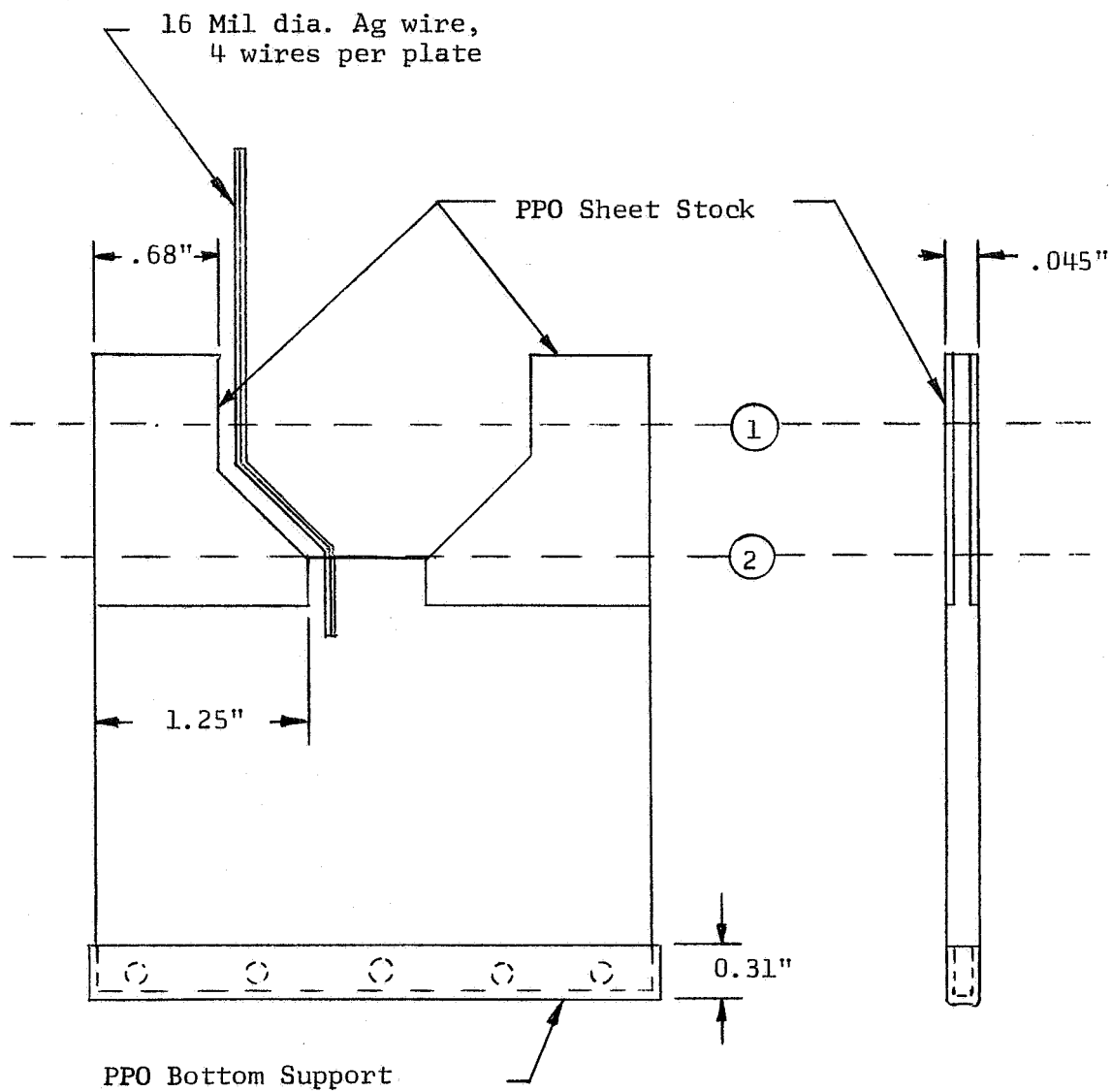


FIGURE 26

STRUCTURAL DESIGN OF POSITIVE PLATE  
FOR MODEL 334 SECOND GENERATION CELL DESIGN



A considerable effort was spent in the development of a heat pressing process for PPO 681-111 sheet. Bubbling of "Z-Tron" \* sheet was observed in the temperature range  $249 \pm 5^{\circ}\text{C}$ . Framing was heat pressed onto negative screens at  $310^{\circ}\text{C}$  after a preheat for 30 minutes at  $225\text{--}238^{\circ}\text{C}$ . Positive plate struts were heat pressed at  $235 \pm 2^{\circ}\text{C}$ . The resulting plate frames and struts were then relatively bubble free. Tensile tests on the above materials indicated a marked reduction in reported strengths:

G.E. Physical Property	10,000 psi
------------------------	------------

ESB Test Data:

.090 - .125" sheet	9,800 psi
.020 unpressed sheet	7,125
.040 heat pressed sandwich	7,060

It would appear from the above data that rolling processes performed by the supplier (Polymer Corporation) on .020 sheet stock are responsible for a 28% reduction in tensile strength. Tensile tests on plates also demonstrated the presence of Ag grid in the heat pressed sandwich contributed little to the tensile strength. Break forces could be explained by the plastic cross-section alone. This reduction in anticipated strength all but eliminated any design safety factor for the 5,000 g 3 msec shock load.

#### c. Heat Sterilization Tests

Twelve Model 334 cells were manufactured and tested as follows: 2 cells for electrical tests only, 3 cells for high impact plus electrical, and 7 cells for heat sterilization, high impact, and electrical tests. Performance is summarized in Table LXVII for control cells S/N 9 and 13 having neither heat sterilization nor shock and equipped with pressure-vacuum gauges. Table LXVIII gives similar performance for cells S/N 2, 3, 4, 5, 10, 11, and 12 after heat sterilization but before JPL high impact tests. For heat sterilization each cell was potted in a close fitting stainless steel box with a silicone potting compound to reproduce anticipated support of a battery chassis. Each cell was then exposed in air for 120 hours at  $135 \pm 3^{\circ}\text{C}$ . Temperature rise to and fall from  $135^{\circ}\text{C}$  was manually controlled at a rate of  $19^{\circ}\text{C/hr}$ . in stair step increments. After sterilization each cell was inspected visually for leakage and case distortion or swelling. Of seven cells sterilized three leaked at 16, 34, and 100 hours elapsed time at  $135^{\circ}\text{C}$ . Each was repaired by replacing electrolyte lost (by weight measure) and resealing. On formation charge the same 3 cells leaked again plus 2 more. The lost electrolyte was replaced again and each cell sealed. Table LXVII shows that the control cells developed more pressure on the formation charge than at any other time in their history to date. Investigation of this gas pressure is described under Electrochemistry.

#### d. Shock Tests at JPL and Failure Modes

\* PPO 681-111 sheet manufactured by Polymer Corp., Reading, Pa.



TABLE LXVII

## MODEL 334 CONTROL CELL CYCLING TESTS

Test Parameter	Cycling Characteristics											
	S/N 13				S/N 9							Mean
	1	2	3	4	1	2	3	4	5	6	7	All
1.0 Charge Profile	(1)	(2)	(6)	(6)	(2)	(2)	(2)	(2)	(2)	(2)	(6)	
1.1 Acceptance (AH)	47.9	40.0	50.0	30.6	51.7	48.6	44.9	38.1	41.6	38.3	31.3	
1.2 Efficiency (%)	(4) 55	122.	137.	111	(4) 59	110	93	101	101	88	89	
1.3 AC Impedance (mohm)												
Before Charge	4.4	44	26	30	150	8	0.2	1.8	2.6	13	--	
After Charge	8.2	43	40	NR	18	2	3	1.7	6.3	32	19	
1.4 Cell Pressure (psig)												
Start Charge	-5.5	0	7	6	-12.5	1.5	-2.5	-3	-2	-3.2	-2.5	
End Charge	-30	7	15.5	8	7.5	3	5.5	2.5	5	2.5	3.0	
2.0 Days Charged Stand	(7) 2	11	25	26	1	1	5	2	8	8	33	
2.1 Discharge Temp. °C												
Profile (3)	25	25	25	25	25	25	0	25	65	25	25	
2.2 Capacity (AH)							(5)					
@10 Amp to 1.30V	10.7	17.5	8.2	13.2	35.0	35.0	28.3	32.7	39.3	28.3	27.5	28.3
@ 2 amp to 1.30V	22.1	18.9	19.2	8.8	9.3	13.2	9.3	8.6	4.1	6.6	9.0	11.2
Total	32.8	36.4	27.4	22.0	44.3	48.2	37.6	41.3	43.4	34.9	38.5	39.5
2.3 Efficiency (% Pre- vious Charge)	73	91	54	72	85	99	84	107	104	91	116	94
2.4 Voltage (Volts)												
10 amp plateau	1.30	1.32	1.32	1.305	1.39	1.405	1.275	1.38	1.46	1.42	1.40	1.37
average	1.358	1.397	1.356	1.335	1.413	1.425	1.275	1.399	1.462	1.42	1.38	1.40
2 amp peak	1.46	1.45	1.44	1.47	1.48	1.48	1.43	1.50	1.44	1.46	1.44	1.46
average	1.413	1.414	1.414	1.419	1.429	1.413	1.309	1.418	1.402	1.420	1.403	1.40
2.5 Energy (WH)	45.7	50.3	38.2	30.1	62.7	68.5	48.2	58.0	63.2	49.6	50.6	55.8
2.6 Energy Density (WH/lb.)	26.3	28.9	22.0	17.3	36.5	39.8	28.0	33.7	36.8	28.8	29.4	32.4
2.7 AC Impedance (mohm)												
Before Discharge	8.2	--	90	190	18	3	--	5	1.9	27	210	
After Discharge	22	--	40	NR	8.4	1	--	2.5	5.8	15	180	
2.8 Cell Pressure (psig)												
Start Discharge	2	10	5.5	NR	1.5	0	--	-1.2	7	-2	-1.7	
Peak Discharge	21	7.5	6.5	NR	3	0	--	-2	10	-2	0	
3.0 Net Input (AH)	--	55.1	68.7		--	56.0	52.0	53.2	53.5	48.4	44.8	54.0

- (1) Charge Profile (cc) I = 0.5A to lower plateau V; I = 1A to 1.97; I = 0.5A to 1.97V.
- (2) Charge Profile (cc) I = 1A to 1.97 V; I = 0.5A to 1.97 V at 25°C.
- (3) Discharge Profile: I = 10A to 1.30V; I = 2A to 1.30 V (5 sec. pulses at 2, 10, 20, 30 & 40 amp at start & 90 minutes discharge time).
- (4) Formation Charge Efficiency = % of theoretical Ag capacity.
- (5) Capacity to 1.20 V.
- (6) CP Charge 1.95 ± .01 V; I = 1.5A maximum; T = 72 hrs. maximum.
- (7) Charged wet stand at 25°C.

TABLE LXVIII

## ELECTRICAL TESTS ON MODEL 334 CELLS BEFORE AND AFTER HEAT STERILIZATION

Test Parameter	Unit	S/N 2	3	4	5	10	11	12	Mean	Notes
1. A.C. Impedance at Seal	mohm	--	40	--	40	47	130	40	59	
2. Heat Sterilization Time	hrs.	34L	120	120	120	120	16L	100L		(5)
3. A.C. Impedance After HS	mohm	8.8	16.5	5.9	16.5	25	40	44	23	
4. Formation Charge Input	AH	61.3L	51.5L	51.5L	57.7	52.2	51.8L	52.1L	54.0	(1), (2), (3)
5. Formation Discharge Output	AH	49.2	42.7	36.5	39.7	35.8	34.4	42.1	40.1	(4), at R.T.
6. A.C. Impedance Before Charge	mohm	22	16	13	2	2	21	1	12	
7. Cycle 1 Input 1.95V CP	AH	55.7	--	47.4	48.7	54.4	55.8	54.9	52.8	(3)
8. Cycle 1 Output, Total	AH	33.0	40.7	42.5	39.9	40.5	39.7	47.5	40.5	(4) at R.T.
At 10A to 1.30V/C		30.5	34.2	37.8	36.9	13.5	30.2	40.8	32.0	
At 2A to 1.30V/C		2.5	6.5	4.7	3.0	27.0	9.5	6.7	8.6	
9. Cycle 1 Plateau Voltage	volts									
At 10A		1.42	1.43	1.42	1.42	1.37	1.39	1.43	1.41	
At 2A		1.51	1.52	1.56	1.42	1.45	1.47	1.46	1.48	
10. Cycle 1 Energy Output	WHr	46.3	59.9	--	58.3	56.6	55.8	68.7	57.6	
11. Cycle 1 Energy Density	WH/lb	26.8	33.8	--	33.1	32.3	30.7	39.0	32.6	
12. A.C. Impedance After Cycle 1	mohm	23	13	18	16	24	12	13	17	
13. Cycle 2 Input 1.95V CP	AH	76.2	39.6	40.8	43.7	40.8	41.1	47.0	47.0	
14. A.C. Impedance After Charge	mohm	38	24	15	5	90	17	25	31	
15. Net Input	AH	111.0	--	60.7	70.5	71.1	74.6	64.4	75.3	(6)

- Notes: (1) Constant current: 0.5A to lower plateau; 1.0A to 1.97;  
0.5A to 1.97A at 25°C.  
(2) Constant current: 1.0A to 1.97V; 0.5A to 1.97V at 25°C.  
(3) CP (modified): initial current limited to 1.5A; voltage at 1.95  
±.01V.  
(4) Constant current: 10A to 1.30V; 2A to 1.30V.  
(5) L=KOH leaks at seal  
(6) Cell S/N 2 went into full float on CP charge.

Table LXIX summarizes cell weights, impact velocities, and stopping distances observed during impact testing at the Jet Propulsion Laboratory, Pasadena, California. Peak "g" levels were measured with accelerometers mounted on the cell shock fixture. The calculated "g" levels for cells S/N 5, 10, and 12 all of which were heat sterilized 120 hours were 4,020 to 4,180 "g". Cells S/N 2, 3, and 4 also heat sterilized were shocked at higher velocities and reached calculated "g" levels from 7,420 to 7,500 "g". Cells S/N 6, 7, and 8, the controls with no heat sterilization, were given the maximum shock reaching 7,900 to 8,200 mean "g" for 0.4 msec. and 10,000 peak "g".

Table LXX summarizes loaded voltage tests performed at discharge rates of 2, 10, 20, 30, and 40 amps before and after high impact with the calculated voltage decreases. Figure 27 shows that the decrease in loaded voltage was greater at increasing "g" values of shock and increasing currents of discharge.

Cells 5, 10, and 12 shocked at 4,100 "g" after 120 hours heat sterilization maintained good loaded voltage and only one of three - S/N 12- suffered a seal failure.

All six cells shocked at 7,420 - 8,200 "g" had cell jar failure ranging from corner hairline cracks in one cell to complete wall fracture in the worst case. Failure of jar walls in two cells - S/N 3 and 4 - during terminals forward shocks left the subcovers inadequately supported which also failed. Flexing of jar walls in four cells damaged the epoxy seal which failed in peel.

Plate strut damage was severe. One shocked cell - S/N 7, an unsterilized cell - showed 60% undamaged plates. In the other five cells which were dissected all struts were broken or damaged. Terminal forward shock damaged plates not adequately supported in buckling despite the use of epoxy shims designed to perform this function. The tensile modulus of PPO 681-111 after heat pressing operations is too low to prevent buckling when case walls bulge outward during impact.

Extensive wrinkling and breakage of charged positive active material (AgO) indicated that greater support from grid structures in the plate are needed to survive the maximum shock loading.

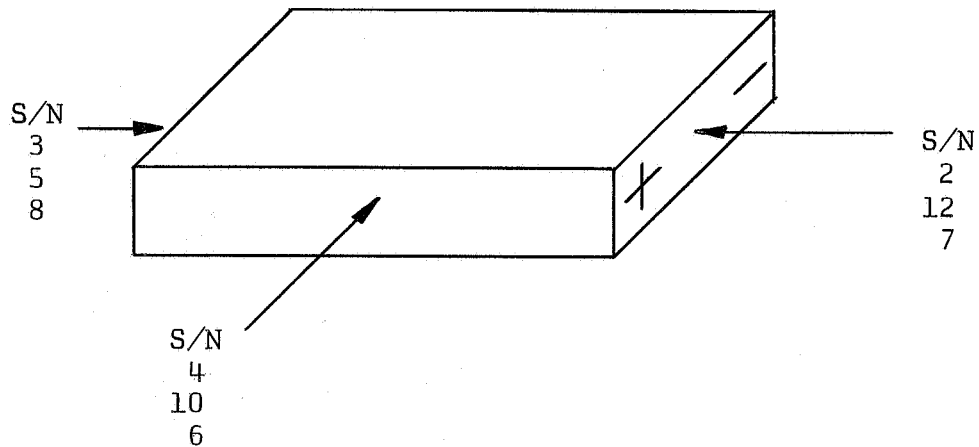
As in the Model 325 cell tests plastic strut projections at each bottom corner of the positive plates failed in shear during terminals-forward shocks. Buckling of the struts at the top of each plate shifted too large a shear force to the bottom supports.

Negative plate "M" frames delaminated from the inner 35 x 40 mesh Ag screen. PPO 681-111 is the only grade PPO which can be heat pressed and even this grade gives inadequate heat bond strength. The bond between zinc active material and Ag screens in the negatives generally was not broken by the shock.

TABLE LXIX  
SHOCK DATA FOR MODEL 334 CELLS

S/N	Weight (gms)	Impact Velocity (Ft/Sec)	Tool Diameter (in.)	Stopping Distance (in.)	Pulse Duration (Msec.)	Calculated Avg. "G"	Measured Peak "G"	HS* Hrs.
5	788	109	3/4	0.530	0.8	4020	6000	120
10	775	110	3/4	0.543	--	4140	--	120
12	788	110	3/4	0.538	0.8	4180	5000	100
2	784	173	1	0.751	0.5	7420	9000	30
3	795	172	1	0.737	0.5	7500	9500	120
4	820	173	1	0.751	0.5	7420	9000	120
6	805	150	1-1/8	0.515	0.4	8150	10000	0
7	790	150	1-1/8	0.532	0.4	7900	10000	0
8	800	150	1-1/8	0.511	0.4	8200	10000	0

VELOCITY VECTORS AT SHOCK



Heat sterilization hours at 135°C before formation charge and high impact.

TABLE LXX

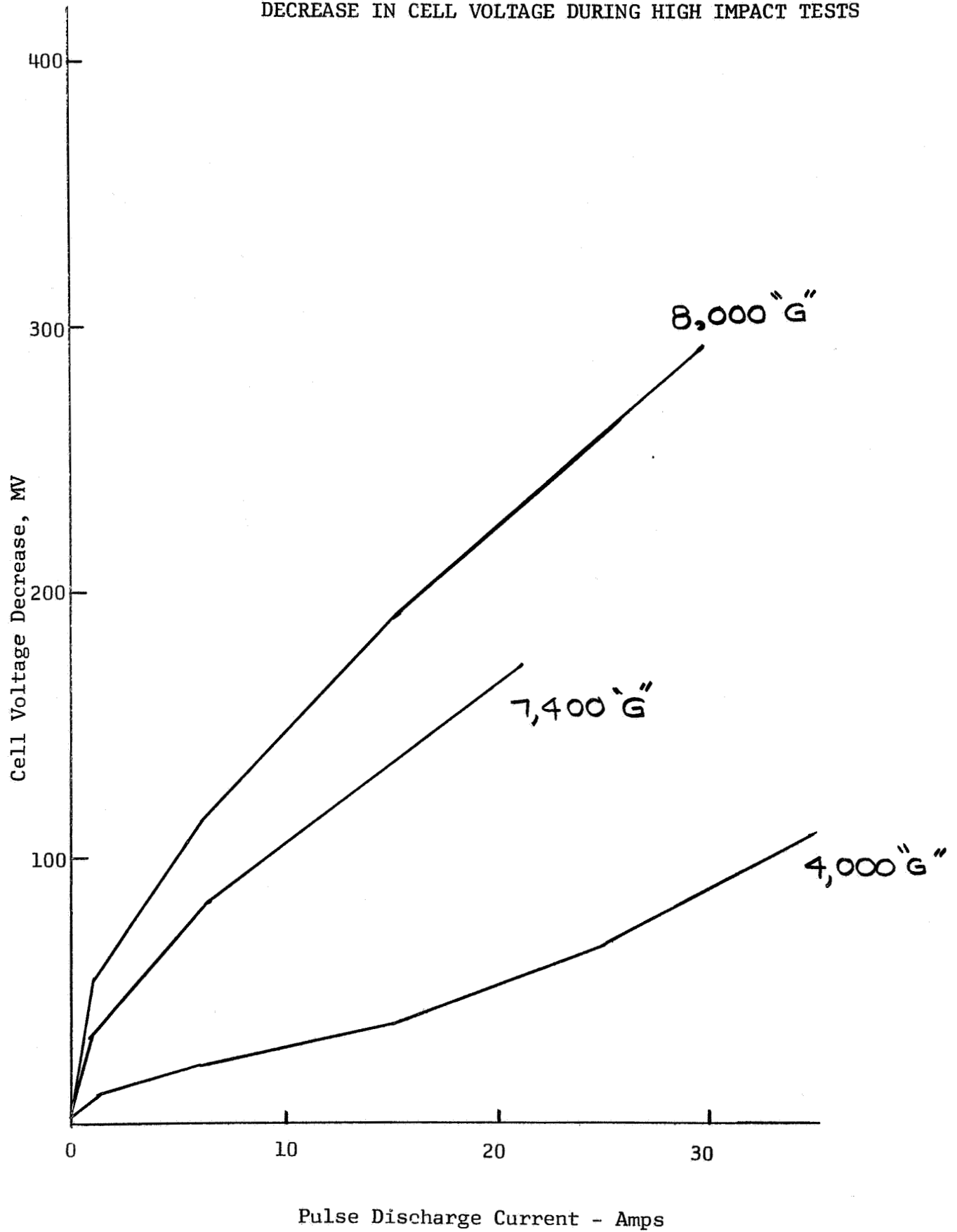
## DECREASE IN CELL VOLTAGES FROM HIGH IMPACT

Discharge Rate, Amps	Time	4,000 "g"			7,400 "g"			8,000 "g"		
		5*	10	12	2	3	4	6	7	8
0	Before	1.859	1.859	1.863	1.857	1.860	1.858	1.572	1.860	1.603
	After	1.857	1.855	1.860	1.853	1.855	1.854	1.569	1.859	1.592
	Decrease, MV	2	4	3	4	5	4	3	1	11
2	Before	1.823	1.652	1.831	1.737	1.827	1.825	1.505	1.744	1.482
	After	1.820	1.618	1.820	1.575	1.826	1.821	1.472	1.695	1.288
	Decrease, MV	3	34	11	162	1	4	33	49	
10	Before	1.738	1.401	1.747	1.574	1.750	1.751	1.280	1.530	1.145
	After	1.719	1.380	1.701	1.273	1.749	1.740	--	1.379	1.028
	Decrease, MV	19	21	46	301	1	9	--	151	117
20	Before	1.639	1.200	1.652	1.464	1.667	1.671	.820	1.347	1.028
	After	1.618	1.210	1.585	.998	1.662	1.649	--	1.120	.770
	Decrease, MV	21	-10	67	466	5	22	--	227	258
30	Before	1.478	.998	1.490	1.248	1.480	1.503	--	1.149	--
	After	1.396	.960	1.344	--	1.433	1.438	--	.870	--
	Decrease, MV	82	38	146	--	47	65	--	279	--
40	Before	1.356	--	1.382	1.150	1.397	1.394	--	1.003	--
	After	1.306	--	1.187	--	1.320	1.309	--	--	--
	Decrease, MV	50	--	195	--	77	85	--	--	--

(\*) Serial number of cell tested.

FIGURE 27

DECREASE IN CELL VOLTAGE DURING HIGH IMPACT TESTS



Polypropylene plate absorbers were not damaged structurally by heat sterilization or shock.

RAI-116 semipermeable membranes were damaged by heat sterilization and by shock. Large splits in single layers were found in sterilized cells--some splits extending from the top of the separator to the bottom of the "U" fold in the center of some plates. In the Model 334 cell design inadequate allowance was made for membrane shrinkage. Shrinkage allowance was increased in later cells to 8.7% of plate width. During terminal--aft shocks the rounded bottom edges of positive plates resting on the "U" fold cut into the membrane at points of greatest impact.

Electrochemical performance of the Model 334 cell was below expectations in voltage and capacity and very variable from cell to cell. A prime reason was accumulation of plate thickness tolerances which gave a tight cell pack.

Relative performance on the two rate discharge during two cycles may be summarized as follows:

Test Parameter		Unit	Non-Sterilized Cells n = 2	Wet Heat Sterilized Cells n = 7
Formation	Charge Input	AH	49	54
	Discharge Output	AH	38	40
Cycle 1	Input	AH	44	53
1	Output	AH	42	41
1	Energy	WH	59	58
1	Energy	WH	34	33
	Density	lb.		

The differences in the above means are well within the variability of the individual cells in either group. A. C. impedances measured between individual cell terminals with a Keithley Milliohmmeter at 90 Hz revealed another cause of variability:

Time of Measurement	A. C. Impedance-mohms			
	X	n	Min.	Max.
At seal before formation charge	59	5	40	130
After heat sterilization	23	7	6	44
After formation discharge	12	7	1	22
After Cycle 1 discharge	17	7	12	24
After Cycle 2 charge	31	7	5	90

## 5. Third Generation Cells - Model 343 - Metal Supports

### a. Design Development

Design objectives for the Model 343 cell were:

- Cell jar walls and cover of increased thickness and strength to eliminate jar failure during shock.
- Plate structures reinforced with non-magnetic metal struts rather than plastic to prevent fracture of plates during shock.
- Use of SWRI-GX to decrease performance variability at no sacrifice in heat sterilizability.
- Nominal capacity of 25 AH and performance per JPL Specification GMP-50437-DSN-C.

Table LXXI summarizes the materials, weights, and major dimensions for the cell components. For a projected output of 25 AH at the 2 hour rate at an operating voltage of 1.39 volts per cell and a cell weight of 1.26 pounds the design energy density is 27 WH/lb. and 2.1 WH/in<sup>3</sup>. Figure 28 is an assembly sketch of the Model 343 cell.

Four 55-mil positive plates were each supported for the high impact by an inner perforated titanium sheet and two upper titanium struts sealed with epoxy into cavities on the underside of the subcover. An independent silver lead wire system connected the positive active material to the positive cell terminal so that capacity would not be lost even if the struts broke during shock.

Three full and two half negative plates (79 and 53 mils thick, respectively), were each supported at three places in the cell jar; at two bottom corners and by one strut projecting from the top center of each plate into a cavity in the subcover.

The cell separator system consisted of a closed "U" fold on the positive plates having (+) to (-) one layer EM-476 polypropylene absorber and five layers Southwest Research Institute GX membrane.

Optimum tensile and compressive strength was needed for plate reinforcements. Light weight metals were highly desirable to decrease shock loads at 10,000 g impact. Physical characteristics of metals considered are given below:

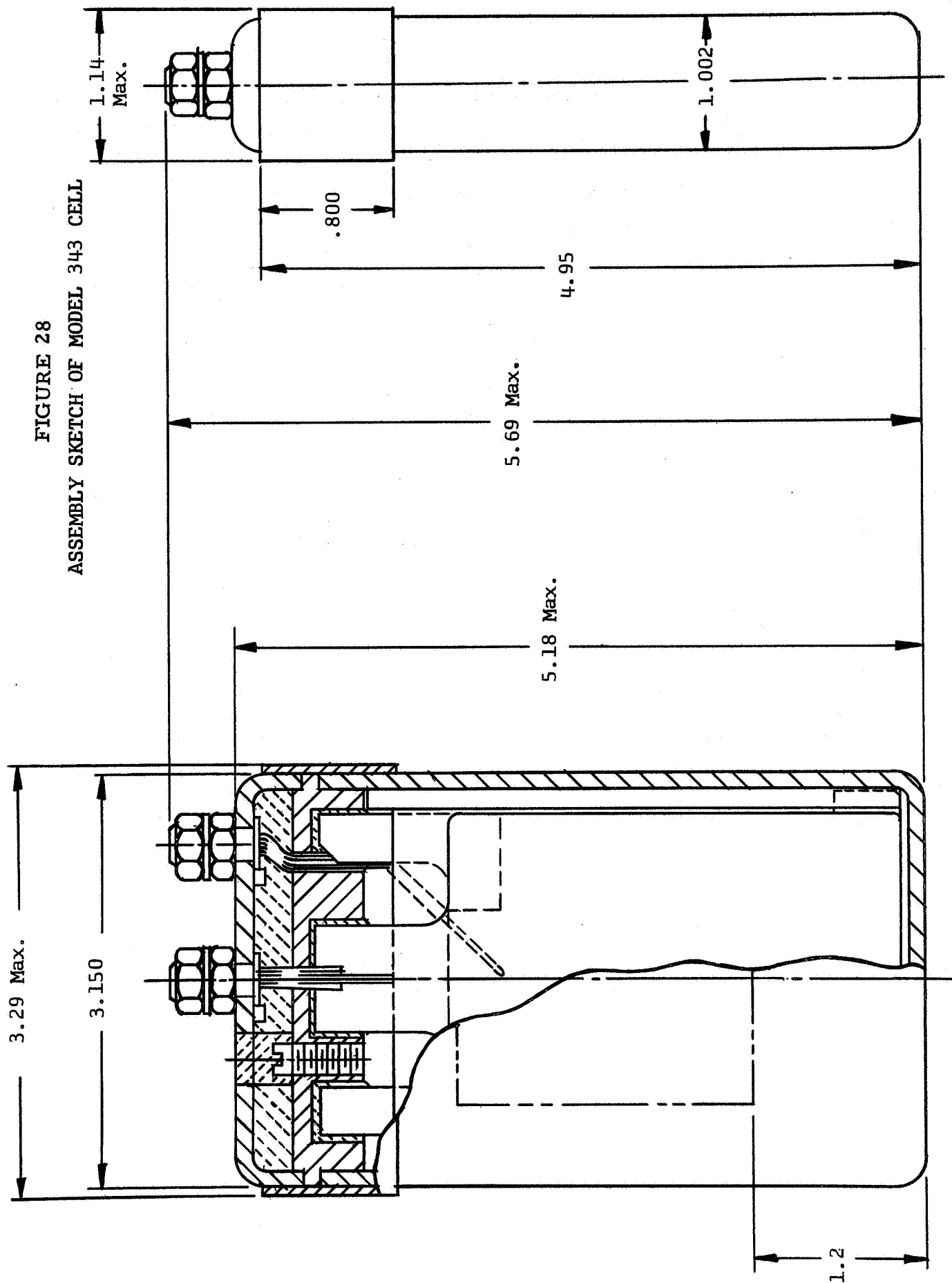


TABLE LXXI

MODEL 343 25 AH  
HEAT STERILIZABLE HIGH IMPACT CELL DESIGN

CELL COMPONENT	NO IN CELL	MATERIAL	DIMENSIONS, INCHES				WT. PER CELL, gms
			L	W	H	T	
Cell Case	1	PPO-531-801	1.00	3.15	4.52	.125	83.3
Subcover	1	PPO-531-801	2.88	.74	.50	.125	13.6
Top Cover	1	PPO-531-801	3.15	1.00	.50	.125	11.8
Side Shims	2	PPO-531-801	4.03	.72		.100	12.6
Sealing Tape	1	Epoxy-glass		.50		.00	10.
Cement	2	Epoxy					15.
Sealant	bulk						
	2	Epoxy					20.
	bulk						
Cell Pack							
Positive Blanks	4	Porous Ag	3.40	2.45		.055	89.2
Positive Grids	4	Titanium	3.40	2.45		.008	28.4
Positive Absorber	4	EM-476 (IL)	8.06	4.96		.003	3.6
Positive Membrane	4	SWRI-GX	28.0	8.00		.003	20.5
		(5L)					
Negative Retainer	5	EM-476 (IL)				.003	3.0
Center Negative Active	3	ZnO	3.42	2.55		.079	59.8
Material							
Center Grids	3	Ag	3.40	2.53		.008	41.4
End Negative Active	2	ZnO	3.42	2.55		.053	19.8
Material							
End Negative Grids							
Electrolyte, 68 cc	bulk	40% KOH					95.
Hardware (Terminals, hex nuts, and washers)							16.
Cell Dimensions							
Overall			1.14	3.29	5.69	-	
Case Only			1.00	3.15	5.18	.125	
Cell Weight, Wet, Sealed							<u>570.</u>
Cell Volume, in <sup>3</sup> (16.3)							( <u>1.26 lbs</u> )

FIGURE 28  
ASSEMBLY SKETCH OF MODEL 343 CELL



<u>Metal</u>	<u>Density gm/cc</u>	<u>Tensile Strength psi X10<sup>3</sup></u>	<u>Modulus of Elasticity psi x 10<sup>6</sup></u>	<u>Other</u>
Ag, annealed	10.5	22	11	Non-magnetic
Ag, unannealed		54		
Titanium, (98.6-99.3%)	4.5	60 - 110	15 - 16	Non-magnetic
Nickel 200 (99.5%)	8.9	55 - 75	30	Magnetic
Copper (99.95%)	8.9	32 - 35 (soft) 50 - 55 (hard)	17	Must be Ag plated
Beryllium Copper 172	8.2	60 - 80 (soft) 165 - 185 (hard)	19	"
Stainless Steel 316	8.0	80 - 84 (annealed)	28	Magnetic
Monel K-500	8.5	130 - 170	26	Non-magnetic

Magnetic requirements of JPL Specification GMP-50437-DSN-C eliminated those metals containing nickel except Monel. Copper was eliminated because of the demonstrated production of blue cupric ion during heat sterilization tests at EMED. Titanium was attractive because of its low density and high stiffness factor (modulus per unit density) and was considered corrosion resistant, especially when used as a positive plate support sheathed in AgO/Ag<sub>2</sub>O. Unfortunately, its corrosion rate in 40% KOH at 135°C during heat sterilization was later discovered to be too great.

Titanium positive plate reinforcements were designed to withstand an allowable tensile force of 1080 pounds per plate for an estimated 650 pound force during the 10,000 "g" shock, or a safety factor of 66%. The tensile modulus for titanium (15 x 10<sup>6</sup> psi), approximately 40 times greater than PPO 681-111 which failed in buckling in the Model 334 cell, predicted on allowable buckling load for each positive plate of 2050 pounds and a safety factor of 3:1.

Ag has met the non-magnetic requirement of one gamma at six times the average 18-cell battery dimension. On a full negative plate having a silver sheet support structure the design load of 875 pounds was greater than the estimated load at 10,000 "g" of 740 pounds by an 18% safety factor. This marginal safety factor predicted a negative plate tensile failure mode during shock.

Thirteen Model 343 cells were fabricated in the Engineering Pilot Plant. Adhesion between Ti positive plate reinforcements and sintered Ag was

improved by serrating the outer edges of the Ti sheet and by sintering the Ag active material through the perforations in the Ti sheet.

A wet slurry of negative active material was used to paste the Ag sheet - 2/0 grid assembly in the negative plates. Plates were wrapped in an EM 476 retainer and wet pressed to drawing dimensions and densities.

All mating PPO sealing surfaces cemented in the final assembly were both sanded and etched in hot chromic acid. Dow DEN438-EK-85/DMP-30 was used as the epoxy adhesive for close fitting parts and Epocast 221/927 was used to seal voids around struts and cell terminals.

#### b. Heat Sterilization

Two control cells were equipped with pressure gauges. The remaining eleven cells were torqued hard finger tight in wooden clamps coated with a thin film of well cured RTV-11 silicone to distribute the clamping pressure over as large a surface as possible up to the edge of seal area. Oven temperature was raised at 19°C per hour to 135°C. Ten of the eleven cells developed leaks within the first eight hours of sterilization between the jar wall and the subcover. Weight measurements showed electrolyte losses of 15-20 cc from the leaking cells. Two of the leakers were resealed with pressure gauges after adjusting electrolyte weights to normal values, and the sterilization continued. After 4 hours at 135°C, cell pressures were 17 psig and 28 psig and climbing. Corrosion tests of samples of the .010" sheet titanium used in the positive plates immersed in boiling 40% KOH gave 8% weight loss in 6 hours. This experiment conclusively demonstrated that titanium cannot be used in heat sterilizable cells without generation of high pressures sufficient to break epoxy seals.

All leaks in the above cells occurred at points where insertion of negative plate struts into the subcover cavity had bowed the subcover 10-20 mils. When the subcover was installed in the cell jar, epoxy cement was wiped from the mating surfaces in the bowed area and gas pressures forced bond failure in peel.

#### c. Shock Tests at JPL

In spite of the failures in heat sterilization an evaluation of the all metal plate support structures was considered vital to future design improvements. Ten of the eleven cells were reworked. Nine were given formation charges vented to air. Charge acceptance shown in Table LXXII was a nominal 30.4 AH, 72% of theoretical AgO input; charge rate was 10 milliamperes/in<sup>2</sup> plate area to 1.97 volt/cell then continued at 5 milliamperes/in<sup>2</sup> to 2.05 ± .05 volt per cell or 30 AH total acceptance. Eight of the cells were then sealed and shipped to JPL for shock tests.

Shock environment test data is summarized in Table LXXIII. Decrease in cell loaded voltages resulting from the shock damage is given for each cell in Table LXXIV. Figure 29 shows greater discharge voltage drop

TABLE LXXII

FORMATION CHARGE ACCEPTANCE  
MODEL 343 CELLS

Cell No. (S/N)	Acceptance**		Efficiency Pos. (AH/g Ag)	Voltage		AC Impedance		Weight Sealed (grams)
	I = 0.6 amp (AH)	I = 0.3 amp (AH)		End Charge CCV	After Seal OCV	Before Charge (ohm)	After Charge (ohm)	
3	10.75	20.32	31.07	2.10	1.86	0.15	0.052	568
4	21.90	14.41	36.31	1.955	1.86	0.11	0.022	567
5	21.90	8.15	30.05	1.92 NR	1.86	0.086	0.016	574
6	21.90	8.40	30.30	2.10	1.86	0.084	0.018	568
7*	21.90	6.40	28.30	2.04	1.86	0.076	0.017	--
9	21.90	8.15	30.05	2.045	1.86	0.082	0.013	571
10	21.90	6.40	28.30	2.08	1.86	0.078	0.024	574
11	10.75	18.70	29.45	2.10	1.86	0.175	0.057	567
12	21.90	8.15	30.05	1.92 NR	1.86	0.12	0.016	567
Mean	19.42	11.01	30.43		1.86	0.103	0.031	569

(\*) Cell S/N 7 assembled with pressure gage sealed for EMED testing, all other cells shipped to JPL for shock test.

(\*\*) Cells reworked after leak occurred within 8 hours of heat sterilization and in vented state.

TABLE LXXIII  
SHOCK ENVIRONMENT DATA  
MODEL 343 CELLS, SEALED, NON-STERILE

Cell S/N	Velocity Vector	Velocity (ft/sec)	Impact		Pulse Duration (msec.)	Shock Level		Effect of Shock on Cell
			Tool Diameter (in.)	Penetration (in.)		Peak (G)	Avg. (G)	
4	Toward bottom of cell	180	1.25	--	--	23,000	--	4) Test error; plastic guide broke; impact off steel frame of targets. Negative plates compressed approx. 0.67" & positives 0.1" in height. Cell jar cracked along bottom and one end. Cell pack shorted.
6	Toward top of cell	182	1.25	--	0.8	14,000	--	6) Test error; plastic guide failed; impact off center of target. Plate lugs and structure buckled. Cell pack moved approx. 0.5" off bottom of cell cavity. Cell pack shorted.
3	Toward pos. terminal edge of cell	182	1.25	.589	0.6	12,000	10,460	3) Pos. & neg. plates buckled. Pos. plate active material shattered. Separators torn. Cell pack shorted. Cell jar cracked on one side.
5	Toward top of cell	112	.876	.384	0.8	7,000	6,000	5) Survived impact with cracked side wall of jar. X-ray showed plates buckled. Cell supported 2 to 40 ampere current 22 hrs. after shock before shorting.
12	Toward pos. terminal edge of cell	118	.75	.525	0.8	6,000	4,940	12) Survived impact. X-ray showed bottom tabs of neg. plate moved out of slots pos. terminal end and cell pack shifted toward opposite end of cell. Cell supported 2 to 40 amp current 2 hours after shock. Capacity 20.16 AH @6.4 amp and 2.67 AH @1.3 amp to 1.30V. Total capacity 22.83 AH. Plateau voltage 1.42 and 1.45 V at 6.4 and 1.3 ampere.
9	Toward bottom of cell	113	.75	.505	0.8	6,000	4,700	9) Survived impact. X-ray showed neg. plate lugs moved downward out of sub cover. Possible broken wires. Cell supported 2 to 30 amp current with low voltage 3 hrs after shock. Supported full discharge profile 3 days after shock. Capacity 8.32 AH @6.4 amp & 1.95 AH @1.3 amp to 1.30V. Total capacity 10.27 AH. Plateau voltage 1.38V & 1.48V @6.4 & 1.3 amp.

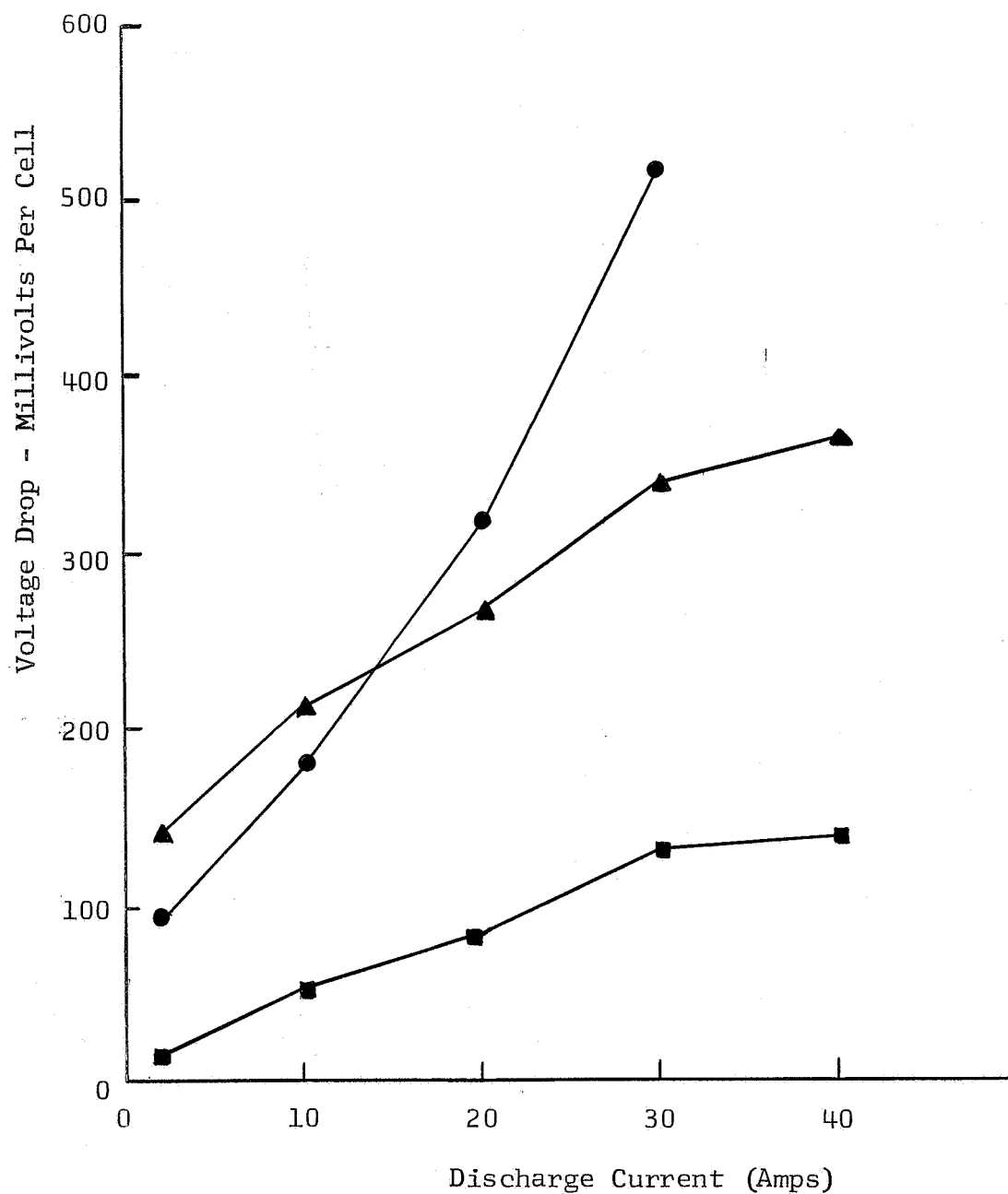
TABLE LXXIV

DECREASE IN CELL VOLTAGE FROM HIGH IMPACT  
MODEL 343 SEALED NON-STERILE CELLS

Discharge Current (Amp)	Discharge Time	S/N 4 23000 (V)	S/N 6 14000 (V)	S/N 3 *12000 (V)	S/N 5 7000 (V)	S/N 9 6000 (V)	S/N 12 6000 (V)
0	Before After Decrease	1.863 <u>1.843</u> 0.020	1.864 <u>1.439</u> 0.425	1.860 <u>1.449</u> 0.411	1.864 <u>1.747</u> 0.117	1.863 <u>1.852</u> 0.011	1.863 <u>1.856</u> 0.007
2	Before After Decrease	1.826 --	1.825 --	1.769 --	1.830 <u>1.691</u> 0.139	1.831 <u>1.779</u> 0.052	1.829 <u>1.811</u> 0.018
5**	Before After Decrease	1.627 <u>1.276</u> 0.351	1.594 -- --	1.497 <u>0.5</u> 0.997	1.623 <u>1.604</u> 0.019	1.683 <u>1.589</u> 0.094	1.628 <u>1.613</u> 0.15
10	Before After Decrease	1.741 --	1.724 --	1.495 --	1.746 <u>1.533</u> 0.213	1.758 <u>1.580</u> 0.178	1.755 <u>1.701</u> 0.054
20	Before After Decrease	1.646 --	1.610 --	1.173 --	1.654 <u>1.387</u> 0.267	1.677 <u>1.363</u> 0.314	1.670 <u>1.589</u> 0.081
30	Before After Decrease	1.557 --	1.502 --	0.869 --	1.567 <u>1.227</u> 0.340	1.598 <u>1.080</u> 0.518	1.588 <u>1.457</u> 0.131
40	Before After Decrease	1.484 --	1.415 --	-- --	1.500 <u>1.135</u> 0.365	1.535 --	1.514 <u>1.378</u> 0.136

(\*) Shock, peak "g" level environment.

(\*\*) 5 amp current applied prior to, during, and after shock.



- ▲ S/N 5 7000 "g" peak, velocity vector → pos. terminal end.
- S/N 9 6000 "g" peak, velocity vector → bottom of cell.
- S/N 12 6000 "g" peak, velocity vector → top of cell.

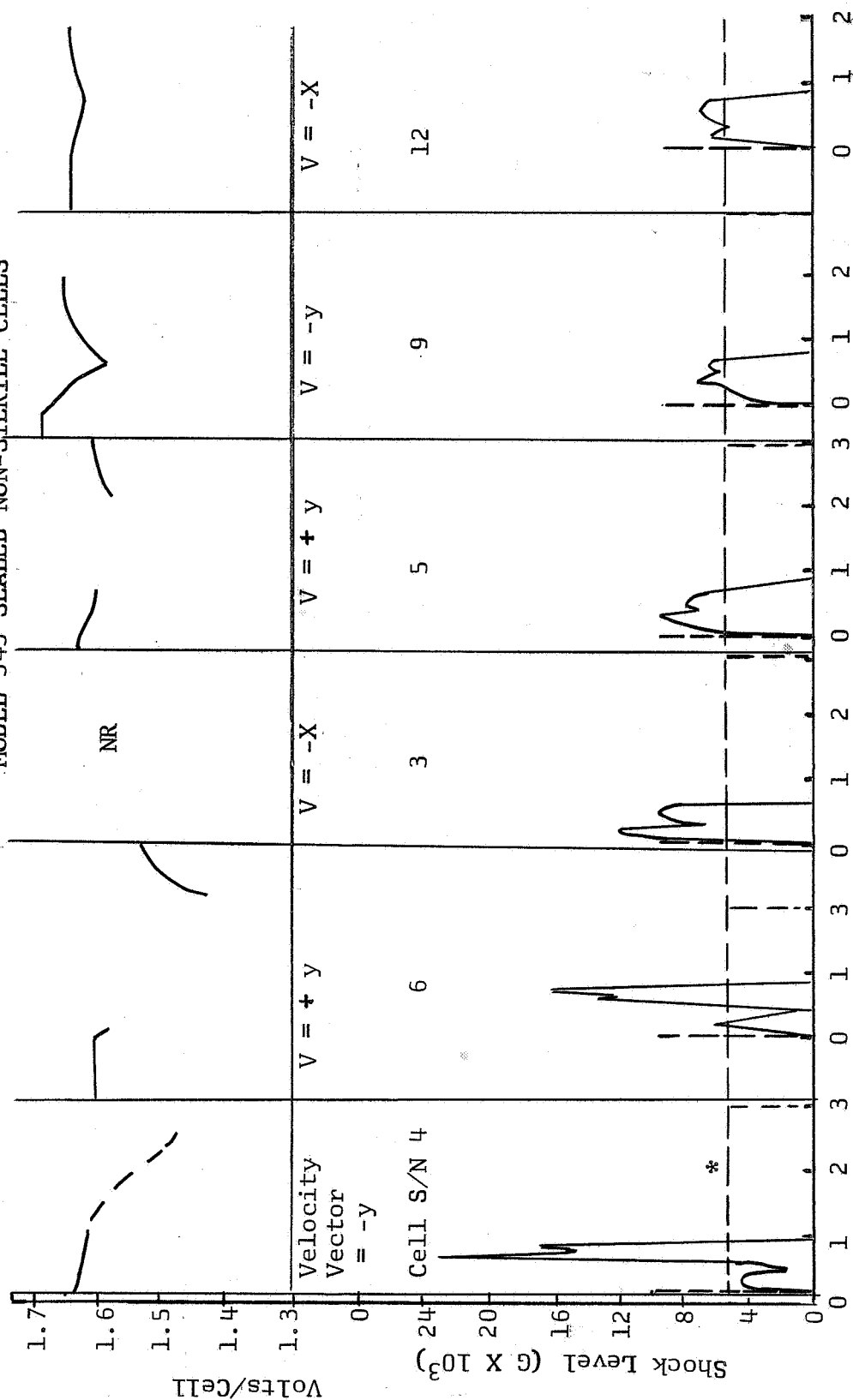
FIGURE 29

CELL VOLTAGE DROP  
AFTER HIGH IMPACT SHOCK  
MODEL 343 SEALED NON-STERILE CELLS



FIGURE 30

SHOCK LEVEL AND CELL VOLTAGE TRACES  
MODEL 343 SEALED NON-STERILE CELLS



(\*) Specification requirement 10,000 "g" for 0.1 msec plus 5,000 "g" for 3 msec.

of cells that survived 6,000 to 7,000 "g" peak shock level in the vertical (-Y) axis with velocity vector toward bottom of cell.

Actual instrumentation shock "g" level traces and cell voltage drop during the shock under a 5 amp load are sketched in Figure 30.

#### d. Shock Damage - Individual Cells

The first two cells tested failed catastrophically when their mounting guides broke prior to impact diverting the projectile from the soft copper target to its steel frame. Cell S/N 4 reached 23,000 "g" peak force with the velocity vector toward bottom of cell. Negative plate lugs sheared their epoxy seal to the subcover. Negative plates were compressed downward 0.67 inch in height and the positive plates compressed 0.10 inch in height. Plate damage is shown in Figure 31. (In Figures 31, 33, and 33, the darker-colored plates with two struts are positives while the lighter-colored plates with one strut are negatives.) The cell jar cracked across the bottom and one end. Buckling plates tore the membrane and the cell shorted.

Cell S/N 6 reached 14,000 peak "g" with velocity vector toward top of the cell. The cell case broke across the bottom and one side. Plate struts buckled and collapsed allowing cell pack to move upward 0.5 inch off jar bottom. Plate damage is shown in Figure 32. The cell shorted through torn separators.

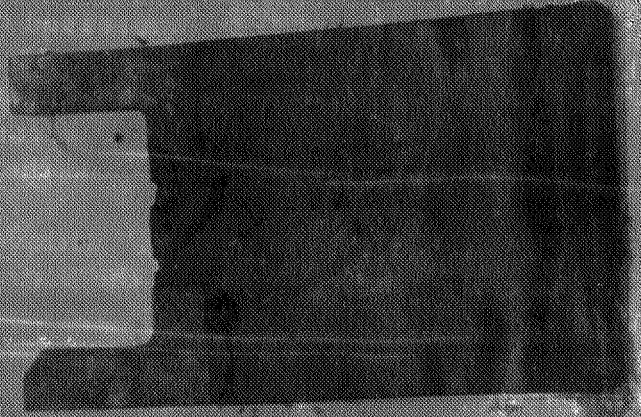
The third test cell impacted properly on the target, reaching 10,460 mean "g" for 0.8 msec with the velocity vector toward the positive terminal edge of cell. The pack shifted laterally buckling the struts nearest the impact point and shattering positive active material from the Ti sheet reinforcement. Separation tore and the cell shorted.

Fourth cell, S/N 5, survived 7,000 "g" peak and 6,000 "g" calculated average force of 0.8 msec duration with velocity vector toward top of cell. One side wall of the case was cracked approximately 2.3 inches along the end wall radii. After shock test the cell was sealed with tape. X-ray showed buckled plate lugs. The cell shorted after supporting discharge currents of 2 to 40 amperes 22 hours after shock test. Figure 33 shows the buckled titanium struts on the positives (black plates) and Ag struts on the negatives.

Fifth cell, S/N 9, survived 4700 "g" calculated average force of 0.8 msec duration with velocity vector toward the bottom of the cell. No visible damage could be seen, and the cell supported discharge currents of 2 to 30 amperes 3 hours after shock environment. The voltage drop in Table LXXIV and Figure 30 plus x-ray pictures which showed that the negative plate lugs moved downward out of the subcover indicated that some negative plate lead wires were broken. The cell was left at JPL for post-shock discharge profile tests.

FIGURE 31

PLATE DAMAGE, CELLS/N 4, -Y VELOCITY  
VECTOR, 23K "g"

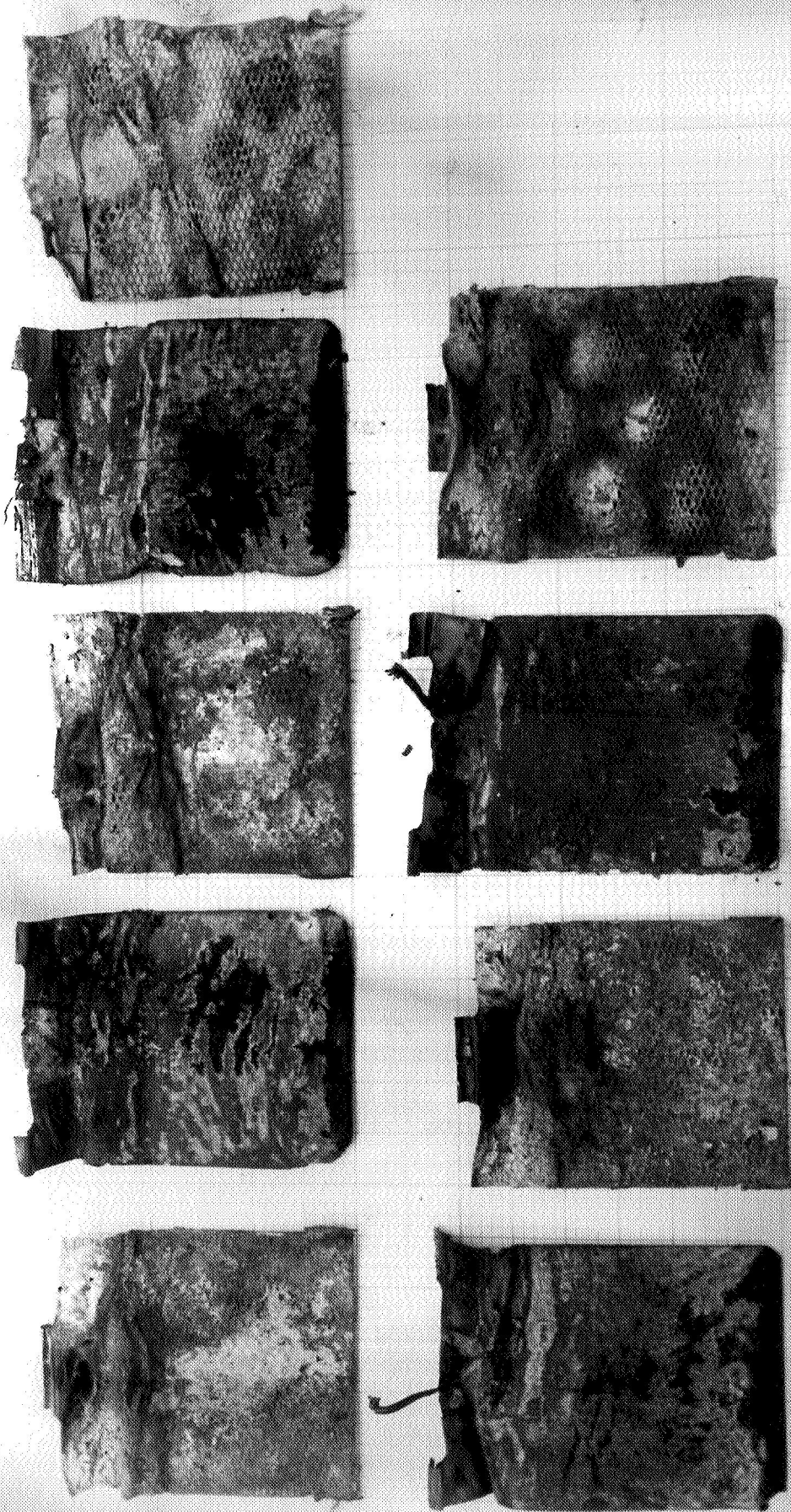


ESK Model 343  
SIN 4  
9-13-67



FIGURE 32

PLATE DAMAGE, CELL S/N 6, +Y VELOCITY  
VECTOR, 14 K "g"



ESB Model 343

S/N 6

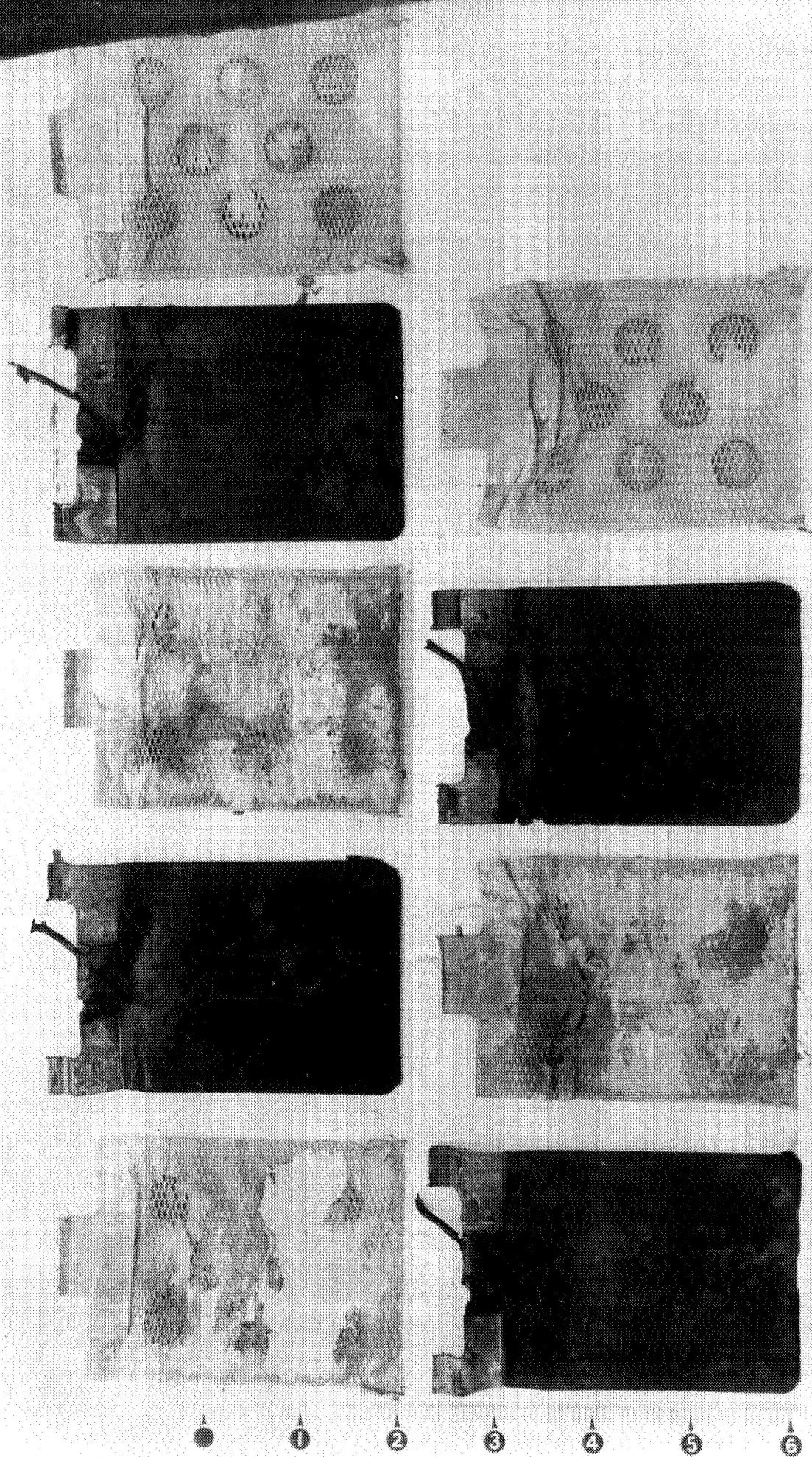
9-13-67

Post shock



FIGURE 33

PLATE DAMAGE, CELL S/N, +Y VELOCITY  
VECTOR, 7K "g"



Model 343 S/N 5 9-15-67

The sixth cell, S/N 12, survived 4940 "g" calculated average force of 0.8 msec duration with velocity vector toward the positive terminal edge of cell with no visible damage. The cell supported discharge currents of 2 to 40 amperes 2 hours after shock test. X-ray showed that the bottom tabs of the negative plates had moved out of the shim slots of the positive terminal edge of the cell and that the cell pack had shifted toward the opposite end of the cell. The cell was left at JPL for post-shock discharge profile tests.

#### e. Discussion of Shock Damage

At impact the projectile kinetic energy is transformed into damage or absorption of energy by plate movement without damage, or both. The potential energy at impact is a function of the product

$$M \bar{V} \bar{g} t$$

where M = projectile mass,  $\bar{V}$  the mean velocity during time t and mean deceleration  $\bar{g}$ . EMED has estimated that to obtain the JPL specification shock of 5,000 g's for 3 msec the initial velocity would have to be 460 ft/sec. for Model 343 cells in their aluminum fixture (6 lbs. total weight). Shock test results to date indicate in such a test cell damage would be catastrophic, and that no simple structural design changes or material design changes are evident which could permit a cell to survive such conditions.

It is recommended that this high impact requirement be reviewed to determine if a more realistic requirement is possible. A reduction of shock loads by 50% would seem at this time to be an attainable goal for a heat sterilizable 25 ampere-hour cell.

#### B. 7.5 Amp-Hr Design Parameter Cell Tests

From time to time during the design and fabrication of cells it was desirable to study certain parameters in direct comparison with a well-known cell system. For this purpose, the S 7.5 cell size was chosen. Altogether fifty-four 7.5 AH cells (vented, sealed and sterilized-sealed) were tested to determine the relative effects on cell operating voltage of:

- ESB compound 323-43 in negative plate. (1)
- Negative plate wrap of 6 layer RAI-116 membrane with 1 layer EM-476 negative plate retainer and positive plate absorber. (2)
- No zinc metal grid in the negative plate. (3)
- Combined use of 1, 2 and 3.
- Negative plate wrap of 4 layer 193-PUDO membrane with 1 layer EM-476 negative plate retainer and positive plate absorber. (5)

- Combined use of 1, 3 and 5.
- Titanium grid in positive plate combined with 1, 2, and 3. (7)
- Positive plate density reduction combined with 7.
- Pb plate Ti grid in positive plate combined with 1, 2, and 3.
- Negative grid assembly of 2/0 expanded Ag on each side of a 0.005" Ag sheet, combined with 1 and 2.

The various cell pack designs are shown in Table LXXV. Charge acceptance, discharge voltage, capacity, capacity retention and cell pressure were compared with ESB standard S7.5 unsealed non-heat sterilizable non-high impact resistant cells containing HgO negative plate additive, Ag and Zn negative grid and positive plate wrap of FSC membrane. Test results and post-mortem of cells contributed the following conclusions:

#### 1. Silver Penetration of Separator

Good Ag stopping capability was shown by the combination of RAI-116 and Compound 323-43. A heavy Ag deposit was observed on the layer of RAI adjacent the positive plates, approximately 20% coverage of the next layer, and no coverage on layers closest to the negative plate.

#### 2. Loss of Cell Voltage

Plateau voltage changes in Table LXXVI were calculated from observed voltage characteristics summarized in Figure 34. Compound 323-43 has negligible effect on cell voltage at discharge current densities less than 0.25 amp/in<sup>2</sup> (C<sub>1</sub> rate). The cause of the greatest loss in cell voltage is shared equally by incorporation of 6L RAI-116 and the omission of zinc negative grids and the addition of EM-476 absorbers and retainers. Decreased positive plate density increased cell voltage.

#### 3. Connection of Lead Wires

Titanium perforated sheet and 2/0 expanded silver positive plate grid showed low discharge voltage and capacity caused by the attachment of current carrying leads to one side of the positive plate only. Wires secured to the expanded Ag grid on both sides of the titanium sheet in Model 343 cells have good voltage.

#### 4. Positive Active Material Density vs. Electrical Characteristics

Cells with 69 g Ag/in<sup>3</sup> positive active material density exhibited higher voltage, greater discharge capacity and energy at lower cell pressure than cells with 78 g Ag/in<sup>3</sup> positive active material density.

TABLE LXXV

## 7.5 AH CELL DESIGN SETS

Cell Construction	△	△	△	(3) △	△	△	△	△	△	△	△
Neg. plate, grid mix retainer membrane	(6) Ag/Zn ZnO-HgO Viskon --	Ag/Zn ZnO-X Viskon 6 RAI (5)	Ag/Zn ZnO-HgO Viskon 6 RAI	Ag 1/0 ZnO-X EM-476 6 RAI	Ag 1/0 ZnO-X EM-476 4-193 PUDO	Ag 1/0 ZnO-HgO EM-476 4-193 PUDO	Ag 1/0 ZnO-X EM-476 6 RAI	Ag 1/0 ZnO-X EM-476 6 RAI	Ag 1/0 ZnO-X EM-476 6 RAI	(2) Ag ZnO-X EM-476 6 RAI	Ag 1/0 ZnO-X EM-476 6 RAI
Pos. plate, grid support	Ag 1/0 None	Ag 1/0 None	Ag 1/0 None	Ag 1/0 None	Ag 1/0 None	Ag 1/0 None	Ag 1/0 None	Ag 2/0 Ti.010"	Ag 1/0 None	Ag 1/0 None	Ag 1/0 None
density g/in <sup>3</sup> absorber membrane	78 None 2 FSC(4)	78 1EM476 None	78 1EM476 None	78 1EM476 None	78 1EM476 None	78 1EM476 None	69 1EM476 None	(8) 69 1EM476 None	78 1EM476 None	78 1EM476 None	None Ti2/0 Pb 69 1EM476 None

(1) X = ESB compound 323-43.

(2) Ag 2/0 - Ag .005" sheet - Ag 2/0.

(3) Set No. 7 same design as set 4.

(4) FSC = Fibrous sausage casing.

(5) 6 RAI = RAI-116 membrane, 6 layers.

(6) Ag/Zn = 1/0 Ag and 3/0 Zn grids.

(7) 2/0 expanded titanium grid plated from acid solution of lead fluoborate.

(8) Ag 2/0 - Ti .010 sheet - Ag 2/0.



TABLE LXXXVI  
EFFECT OF CELL PACK DESIGN  
ON SEALED 7.5 AH CELL PERFORMANCE

Cell Pack Design Change	Reference Cells Set No.* (n vs n)	Change In Plateau Voltage		Capacity at C <sub>1</sub> Rate (%)	Change In Loss Rate on 80°F Charged Stand (%)		Energy WH @C <sub>1</sub> % Change
		0.5 C <sub>1</sub> ** (Volts)	1C <sub>1</sub> (Volts)				
1) Replacement of 2% HgO by 7% Compound 323-43	5 vs 6	-0.01	-0.01	-6	+18	-5	
2) 6 layer RAI-116 negative wrap vs 2 layer FSC positive wrap	1 vs 3	-0.05	-0.08	-9	+4	-14	
3) Omission of zinc negative grid, replacement of Viskon negative retainer by EM-476 and addition of EM-476 as positive absorber	2 vs 4	-0.025	-0.08	-22	+6	-24	
4) Decrease positive density from 78 to 69 gm/in <sup>3</sup>	4 vs 8	+0.01	+0.05	+9	-7	+9	
5) Combined effect of 1, 2 and 3, 4	1 vs 4	-0.08	-0.17	-22	+6	-29	
6) Heat sterilization on best head	8 vs 8 SS	--	+0.02	-3	+13	-2	

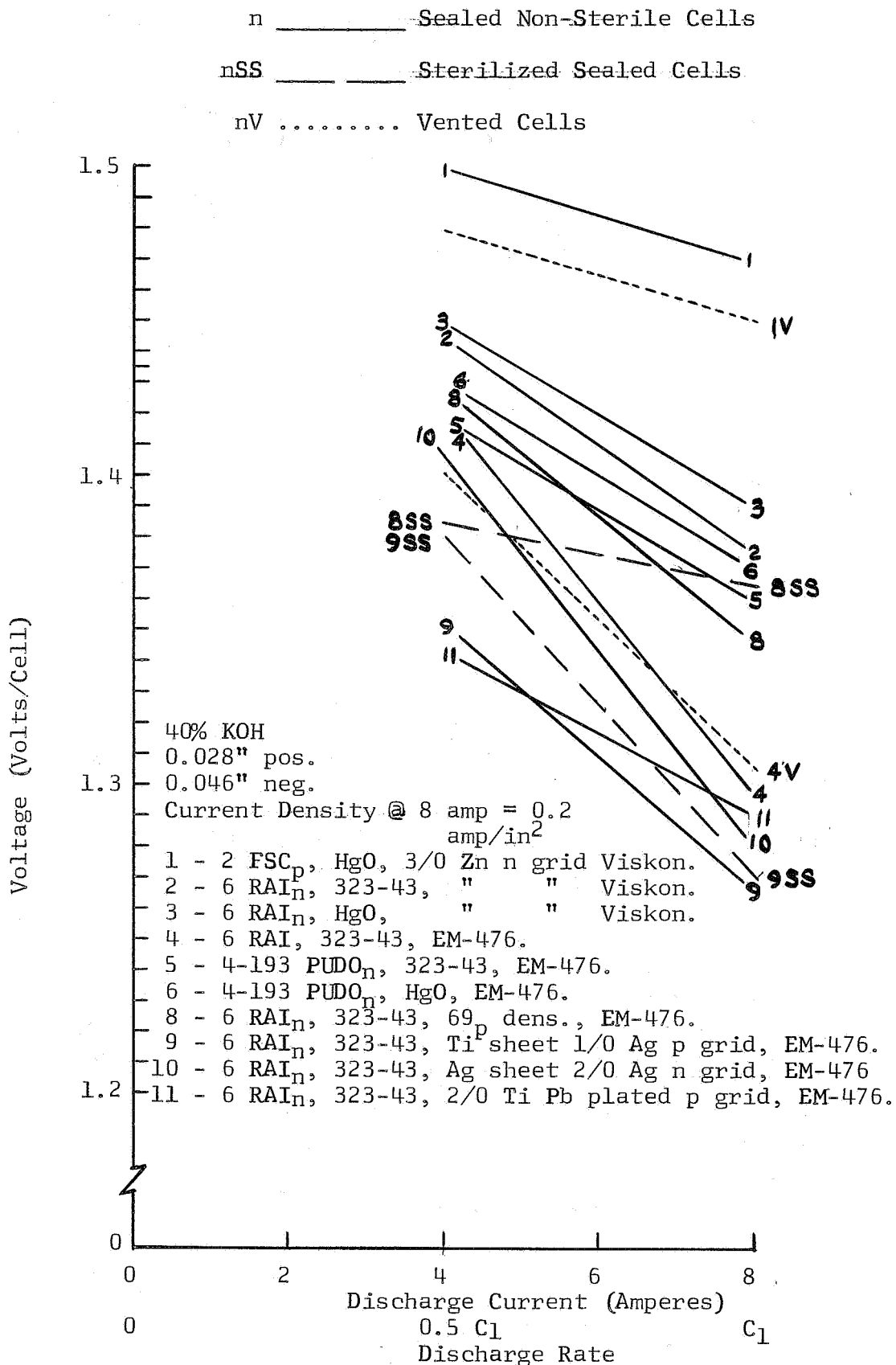
(\*) Refer to Figure 1 and Table III. Sample size minimum 2 cells.

(\*\*) 0.5 C<sub>1</sub> = Discharge rate of 0.125 amp/in<sup>2</sup> current density.

1 C<sub>1</sub> = Discharge rate of 0.25 amp/in<sup>2</sup> current density.

FIGURE 34

VOLTAGE CHARACTERISTICS  
VARIOUS CELL PACK DESIGNS  
7.5 AH CELL TEST



## 5. Effect of Components on Charge Acceptance

Negative plate Compound 323-43 increased charge acceptance (sets, 2, 3, 5, 6) by approximately 9% over cells containing HgO. Cells containing 6 layers of RAI-116 had charge acceptance of 75% compared with 69% for the cell containing FSC or cellophane (sets 1, 3, 4, 5). A Omission of the zinc negative grids and addition of EM-476 negative retainer and positive absorber reduced charge acceptance 17% compared with cells containing zinc negative grid, Viskon negative retainer and no positive plate absorber (sets 2 and 4). Decrease in positive plate active material density from 78% to 69 g/in<sup>3</sup> increased charge acceptance by 10%. Formation charge acceptance at 4 ma/in<sup>2</sup> is shown in Figure 35 as a % theoretical positive plate capacity.

## 6. Stand Losses

Capacity and energy losses of the 35 day charge stand cells were as great as 47 and 54% per month, respectively, for vented cells, 25 and 29% per month, for sealed cells, and 53 and 57% per month, respectively, for sterilized-sealed cells. See sets 8 and 9 of Table LXXVII which ranks 10 test cell designs in order of increasing energy loss in the sealed state. These are extremely high loss rates compared to the 5% capacity and 7% energy loss/month of sealed cells containing the 4 layer cellophane membrane wrap. See set 6 of Table LXXVII. The addition of Compound 323-43 to the negative plate increased the cell capacity loss rate by 18% per month (see Table LXXVI). The omission of the zinc negative grid and addition of EM-476 negative retainer and positive absorber decreased cell capacity and energy by 22 and 2%, respectively.

## 7. Effect of Components on Cell Pressure

Cell pressure readings plotted in Figure 36 show that Compound 323-43 in negative plates of non-sterilizable sealed cells containing cellophane barrier (cell 5b) gave lower cell pressures than cells containing HgO negative additive. The omission of the zinc negative grid also decreased cell pressure. Cell pressure during tests was less than 20 psig except for:

- Sterilized cell S/N 11a with Pb plated Ti positive grid. High charge voltage and 100 psig pressure probably was caused by reaction of electrolyte with the Ti grid during heat sterilization with a reduction of free electrolyte in the cell.
- Sterilized cell S/N 8 g which had 48 psig pressure after approximately 50% of formation charge acceptance. This cell was intentionally vented and cycled as a vented cell.

FIGURE 35  
FORMATION CHARGE ACCEPTANCE  
7.5 AH CELL TESTS

FORMATION CHARGE ACCEPTANCE  
% THEORETICAL POSITIVE PLATE CAPACITY

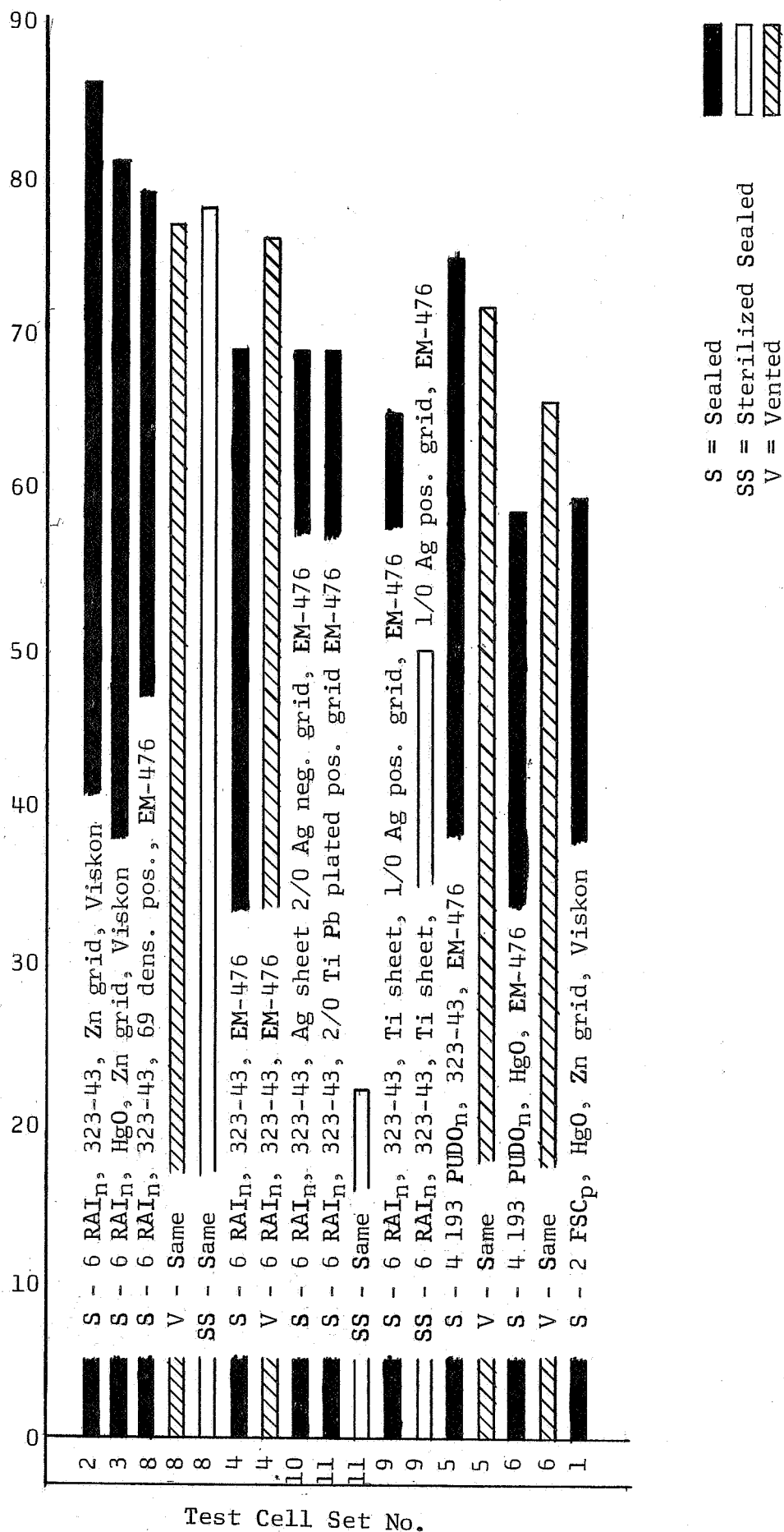


TABLE LXXVII

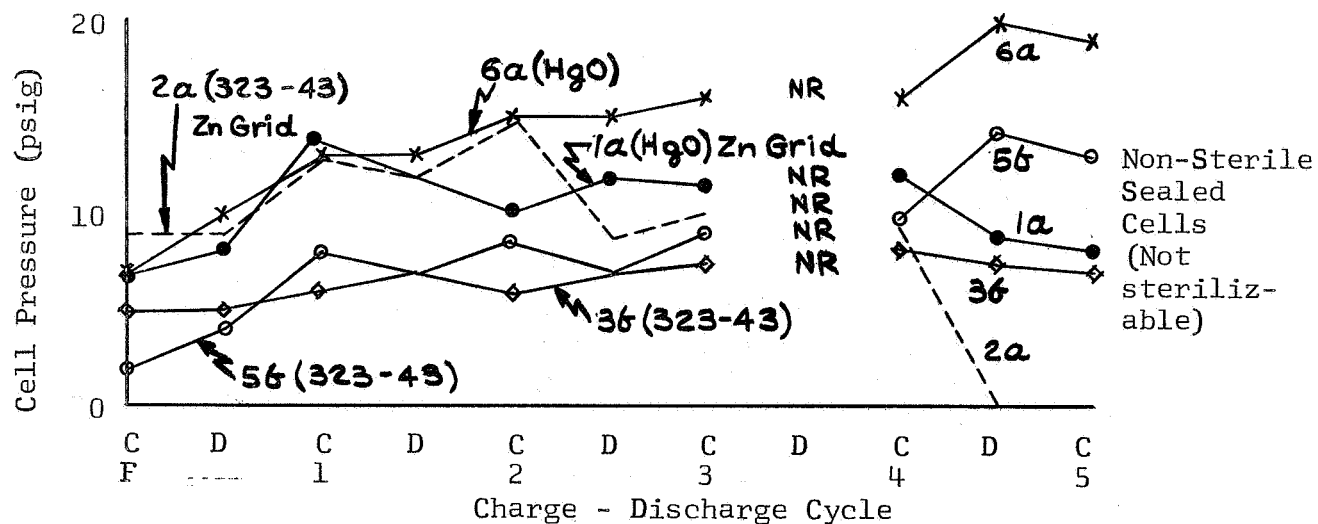
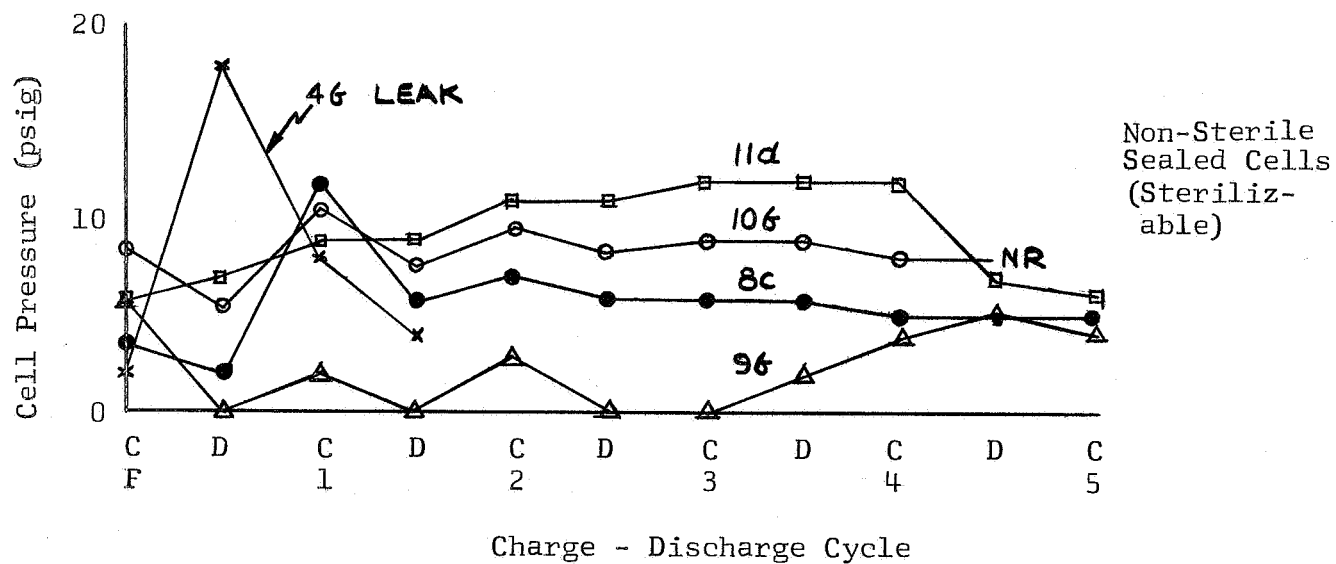
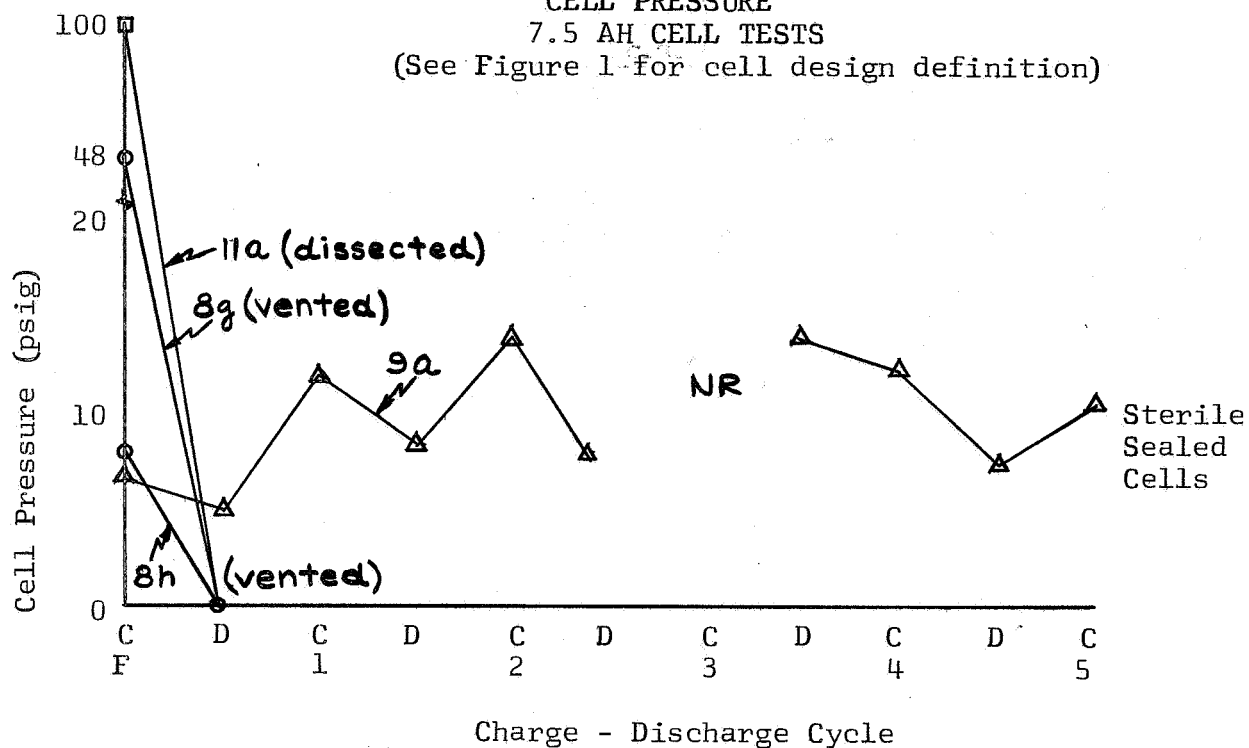
CAPACITY ENERGY STAND LOSS, 7.5 AH CELLS  
 35 DAY CHARGED STAND @77 ±8°F  
 DISCHARGE CURRENT 8 AMPERE TO 1.00V

Set No.	Cell Design		Capacity			Energy		
	Type	Description*	1 day stand (AH)	35 day stand (AH)	Loss (%)	1 day stand (WH)	35 day stand (WH)	Loss %/Month
6	S V	4-193 PUDOn, HgO, EM476 Same	10.40 9.44	9.84 7.36	5.5 22	14.10 12.40	13.13 9.34	7 25
1	S	2 FSCp, HgO, Zn grid, Viskon	10.61	9.04	15	15.20	12.75	16
8	S V SS	6 RAI <sub>n</sub> , 323-43, 69p, EM476 Same Same	9.40 8.00 9.15	8.08 4.24 6.67	14 47 27	12.60 10.50 12.40	10.47 4.78 7.84	17 54.5 37
2	S	6 RAI, 323-43, Zn grid,Viskon	10.72	9.20	14.5	14.55	11.91	18
3	S	6 RAI, HgO, Zn grid,Viskon	9.68	7.84	19	13.00	10.34	20.5
5	S V	4-193 PUDOn, 323-43, EM476 Same	9.66 8.94	7.36 6.40	24 28.5	12.70 12.40	9.67 8.54	23 31
11	S SS	6 RAI <sub>n</sub> , 323-43, 2/0 Ti, Pb plate pos, EM476 Same (1)	7.27 --	5.94 --	18 --	8.84 --	6.76 --	23 --
10	S	6 RAI <sub>n</sub> , 323-43, Ag sheet, 2/0 Ag neg, EM476	7.80	6.24	20	9.92	7.52	23.5
4	S V	6 RAI <sub>n</sub> , 323-43, EM476 Same	8.60 8.06	6.80 4.24	21 47.5	11.05 10.55	8.42 4.81	24 54.5
9	S SS	6 RAI <sub>n</sub> , 323-43 Ti sheet Pb EM476 Same	7.27 4.26	5.45 2.00	25 53	9.03 5.44	6.37 2.31	29.5 57.5

(\*) Seal; membrane; negative additive; grid stype; retainer. See Table I.  
 S = Sealed Cell; V = Vented Cell; SS = Sterile Sealed Cell.

(1) Cells did not accept formation charge after heat sterilization because of corrosion of Ti grid and loss of conductivity.

FIGURE 36  
CELL PRESSURE  
7.5 AH CELL TESTS  
(See Figure 1 for cell design definition)



## C. Heat Sterilizable-High Impact 5.0 AH Cell

### 1. Objectives

Objectives require the design and development of a heat sterilizable-high impact resistant 5 AH cell in accord with JPL Specification GMP-50437-DSN-C (28 November 1966) and the delivery of two-hundred (200) production type cells on or before 1 December 1967.

### 2. Cell Design and Prototype Fabrication

Design objectives for the cell included capability for:

- Activation, seal, heat sterilization for 120 hours at 135°C.
- Formation charge as an 18-cell battery, check out, flight of 8 months duration on float (or on full charged stand).
- Withstanding landing impact 10,000 "g" peak 0.1 msec followed by a 5,000 "g" peak square pulse of 3 msec duration.
- Delivery of 5.0 AH at rates as high as 300 watts at a minimum voltage of 22.5 volts (18 cells) over the temperature range 10° to 55°C.

Figure 37 is an assembly sketch of the 5.0 AH cell. Allotted volume for a six cell group, including shock honeycomb supports, has been designated to be a rectangular block 4.00" x 3.50" x 3.75". Table LXXVIII lists components with materials and dimensions. The overlapping top cover, the subcover, and the cell jar shown in Figure 37 are intended to perform a reliable seal function during the 10,000 "g" shock after heat sterilization and will all be molded to close tolerances in polyphenylene oxide 531-801 material. The epoxy seal between these components and around the plate struts will consist of DOW DEN438-EK85 with catalyst DMP-30 adhesive plus a sealant to be selected by tests in progress. This sealant has the function of sealing around silver sheet struts and to PPO 531-801 over the 255°F thermal shock from the low storage temperature minimum of 20° F to the heat sterilization maximum of 275° F.

Figure 38 provides sketches of positive and negative plate reinforcements. Effective plate area will be 33.8 in<sup>2</sup> giving a maximum current density at 300 watts per battery of 0.37 amp/in<sup>2</sup>.

The ratio of active mass to total mass in this cell design is very low because of structural requirements and accounts for the low estimated energy densities of 18 WH/lb and 1.7 WH/in<sup>3</sup> for a discharge capacity of 6.8 AH at a mean voltage of 1.33 volts.

FIGURE 37  
ASSEMBLY SKETCH OF PROPOSED 5 AH CELL

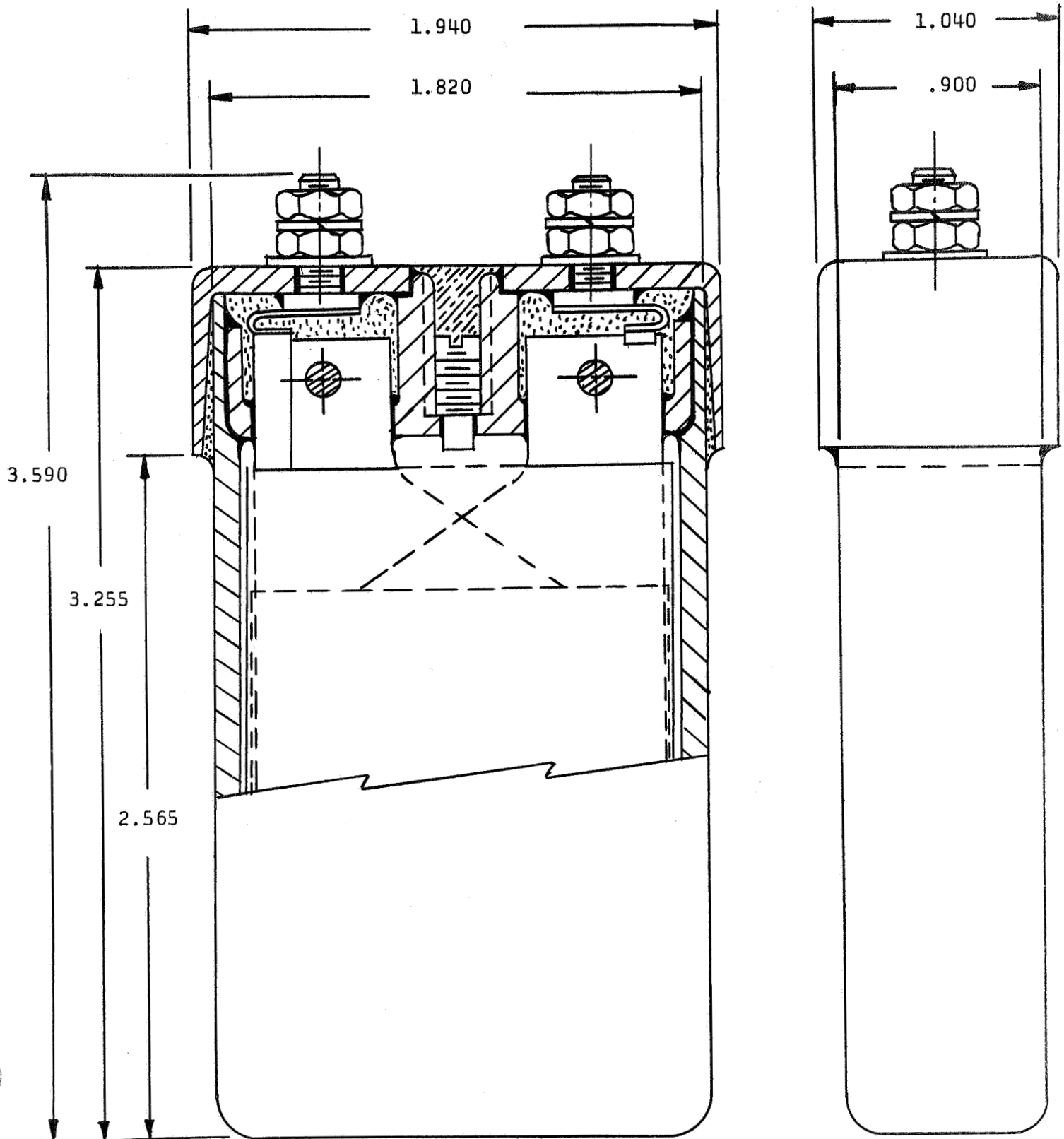




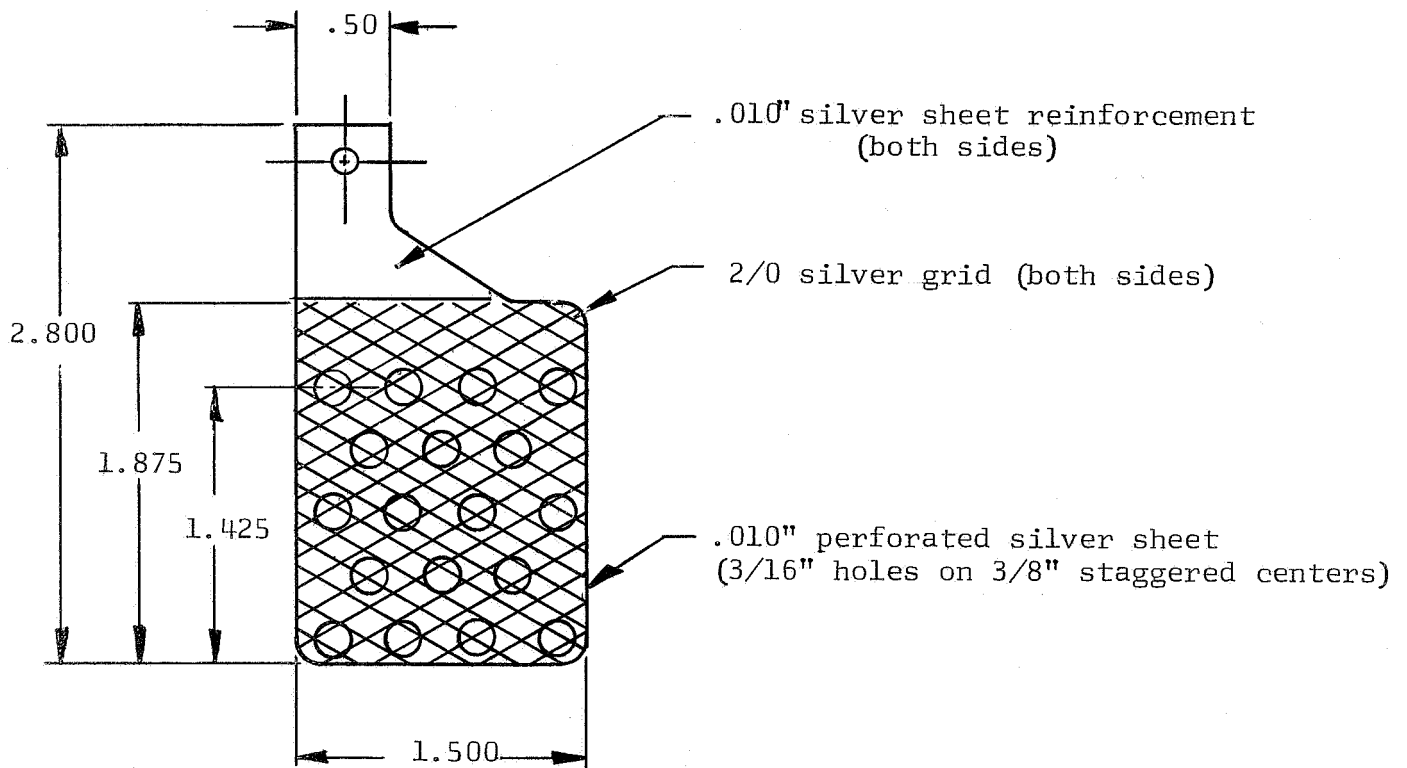
TABLE LXXVIII

MODEL 344 5 AH HIGH RATE  
HEAT STERILIZABLE, HIGH IMPACT CELL DESIGN

Cell Component	No. In Cell	Material	Dimension, Inches				Weight Per Cell gms
			L	W	H	T	
Cell Case		PPO 531-801	.90	1.80	3.14	.12	32.1
Subcover		PPO 531-801	.78	1.68	.58	.10	8.0
Top Cover & Plug		PPO 531-801	1.04	1.94	.69	.10	7.7
Cement		Epoxy					5.0
Sealant		Epoxy					10.0
Cell Pack							
Positive Blanks	6	Porous Ag		1.50	1.88	.020	23.4
Positive Grids	6	Ag Sheet		1.50	2.80	.031	14.1
Positive Absorber	3	EM-476 (1 L)	5.00	3.07		.003	1.1
Positive Membrane	3	SWRI-GX(4 L)	12.8	4.90		.003	4.5
Negative Retainer	7	EM-476 (1 L)	3.9	3.4		.003	1.4
Negative Active Material	7	ZnO, "X"		1.50	1.88	.023	22.1
Negative Grids	7	Ag Sheet & Grid		1.50	1.88	.013	47.6
Electrolyte, 27.5 cc		40% KOH					38.6
Hardware (Terminals, hex nuts, washers)	--						10.0
Cell Dimensions							
Overall			1.04	1.94	3.59		
Case Only			.90	1.82	3.26		
Volume, in <sup>3</sup>	5.3						
Cell Weight, Wet							<u>225.6gms</u> (0.5 lb <sub>max</sub> )
Capacity, Expected, AH	6.8						
Energy, Expected, WH	9.0						
Energy Density, WH/lb	18.0						
WH/in <sup>3</sup>	1.7						

FIGURE 38

5 AH CELL PLATE SUPPORT STRUCTURE  
FOR 10,000 "G" IMPACTS  
(POSITIVE PLATE AND NEGATIVE PLATE)



To improve cell voltages the engineering cells will have only four layers of Southwest Research Institute film GX as the semi-permeable membrane. From positive plate to negative plate the total wet thickness will thus be:

1L EM-476 Absorber	.003
4L SWRI-GX	<u>.012</u>
Total Wet Thickness:	.015 inch

This design choice may compromise cell total life for high rate performance; however, this choice appears necessary to achieve the 300 watt discharge rate at no sacrifice in impact resistance.

Molded parts were obtained and are now undergoing acceptance and sealing tests. On the first test, 6 cell cases were sealed with dummy plates and electrolyte containing ZnO and Ag powder and supported only across the sealing flange broad sides during heat sterilization. After 16 hours of sterilization all but one cell case exhibited leakage through the walls of the case; 4 through vertical cracks located at the point of maximum bulge and one along a vertical edge. No leaks occurred through the epoxy seal or adjacent to it.

Additional tests are in progress to establish reasons for this failure mode. Current opinion is that the case side walls should have been supported during sterilization and that a nitrogen atmosphere instead of air would have been preferable in the sterilization chamber.

## VI. CONCLUSIONS

### Electrodes

1. Standard ESB silver electrodes, uncharged, survive heat sterilization and deliver rated performance if mercury contamination is avoided.
2. Mercury contamination of the silver electrode, resulting in low capacity, can occur during heat sterilization as a result of the solubility of HgO normally used in the negative electrodes.
3. Substitution of Compound 323-43 for HgO in the ZnO electrode avoids mercury contamination of the silver electrode. Cell packs made with this combination, sterilized, then placed in styrene cases, sealed, and formed show expected capacities.
4. Unpredictably, sealed cells often show pressures higher than anticipated during formation. The elimination of Teflon powder from the negative mix, the amalgamation of the silver negative grid, and looser

cell packs show some improvement in this respect, but consistent reproducibility of low pressures can not yet be claimed.

5. Cadmium oxide electrodes have too low energy density for high shock-resistant cells when the excess weight of strengthening members is taken into account.

#### Electrolyte

6. Potassium hydroxide concentrations from 35 to 45% are satisfactory; the range 38-40% may be optimum. The solutions should be saturated with respect to zincate ion.

#### Separators

7. RAI-110, RAI-116, and SWRI-GX when they are kept wet with electrolyte all survive heat sterilization satisfactorily.

8. Separators wrapped around negative electrodes help to keep active material in place and thereby appear to minimize gassing.

9. The available samples of RAI-110 gave cells with longer cycle lives than comparable cells made with RAI-116.

10. Samples of SWRI-GX received to date have been more uniform in conductivity than the chemically similar RAI-116.

#### Absorbers

11. Kendall Mills' EM476 shows the best all around performance of the absorbers investigated.

12. Wicking ability as well as electrolyte retention is important in a good absorber.

#### Case Material

13. General Electric polyphenylene oxide grades PPO 531-801 and 541-801 chemically and physically resist heat sterilization in the presence of concentrated KOH.

14. Molding conditions for these materials are more critical than for better-known plastics, and proper mold design is a very important factor.

#### Sealing Techniques

15. Epoxy resin adhesives, preferably Dow DEN438-EK85 cured with 5% Rohm and Haas DMP 30, have given case-to-cover seals in

both laboratory and pilot-plant which pass all requirements including heat sterilization when properly supported during the latter process.

16. Attempts at hot gas welding PPO 541-801 have not been successful.

#### Cell Design and Fabrication

17. A cover-to-case construction has been devised which, when supported externally, does not leak during or after sterilization.

18. Supported PPO 531-801 cases appear capable of withstanding shock peaks of 10,000 g.

19. Impacts on the flat sides of cells caused little or no damage. Shocks on the narrow sides of cells caused twisting of electrodes which was minimized by design changes. Shocks on the terminal end or bottom of the cells caused buckling of electrodes, some loss of active material, and some shearing of connections. However, in recent designs, cells have still delivered current after such shocks at an average level of about 5,000 g.

20. The cells referred to in the last sentence above had reinforcing metal sheets - silver or titanium - within the electrode.

#### VII FUTURE WORK

1. Greater reproducibility of cells showing only small pressure increase during formation and minimal loss of capacity must be attained. Some steps in this direction are indicated in Conclusion 4.

2. It is not yet clear whether exposure to epoxy resins or PPO during sterilization may reduce capacity. This must be determined.

3. A newly added requirement calls for development of a cell capable of 400 cycles with 50% depth of discharge. This will require considerable research, particularly on the zinc electrode.

4. Stronger metals such as zirconium and Inconel will be used as reinforcing members in cells to be shocked.